Universität Rostock

Traditio et Innovatio

Synthese und Charakterisierung von niedrig-koordinierten Stickstoff-Pniktogen-Verbindungen

Kumulative Dissertation

zur

Erlangung des akademischen Grades

doctor rerum naturalium (Dr. rer. nat.)

der Mathematisch-Naturwissenschaftlichen Fakultät

der Universität Rostock

vorgelegt von **Christian Hering**, geb. am 15.03.1986 in Güstrow

Rostock, 21.03.2014

Datum des Promotionskolloquiums: 24.06.2014

Die vorliegende Arbeit wurde am Lehrstuhl für Anorganische und Elementorganische Chemie der Universität Rostock von Oktober 2011 bis März 2014 unter der Betreuung von Professor Dr. Axel Schulz angefertigt.

1. Gutachter: Prof. Dr. Axel Schulz (Universität Rostock)
2. Gutachter: Prof. Dr. Frank Breher (Universität Karlsruhe)
3. Gutachter: Prof. Dr. Stephan Schulz (Universität Duisburg-Essen)

Erklärung

Hiermit versichere ich an Eides statt, dass ich die vorliegende Arbeit selbständig angefertigt und ohne fremde Hilfe verfasst habe. Dazu habe ich keine außer den von mir angegebenen Hilfsmitteln und Quellen verwendet. Die aus den benutzten Werken inhaltlich und wörtlich entnommenen Stellen sind als solche kenntlich gemacht.

Rostock, den 21.03.2014

Christian Hering

Zusammenfassung

In der vorliegenden Dissertation werden ausgewählte Reaktionen von silylierten Amino(dichlor)pniktanen $RN(SiMe_3)PnCl_2$ (R = $SiMe_3$, Mes*, Ter; Pn = P, As, Sb) mit verschiedenen Lewis-Säuren präsentiert. Es konnte gezeigt werden, dass die $GaCl_3$-assistierte Me_3SiCl-Eliminerung ausgehend von $(Me_3Si)_2NPCl_2$ zu isolierbaren Phosphenium-Salzen führt. Die Reaktivität dieser Salze wurde umfassend studiert und bisher unbekannte Bindungssituationen und Reaktionskanäle aufgedeckt. So konnten neuartige niedrig-koordinierte PN-Verbindungen dargestellt und charakterisiert werden. Neben der $GaCl_3$-assistierten Me_3SiCl-Eliminierung wurde die thermische Eliminierung ausgehend von $(Me_3Si)_2NPCl_2$ untersucht, und es gelang die formale Übertragung von molekularem Phosphornitrid unter Bildung eines *cyclo*-Tetraphosphazans, welches einen multidentaten Liganden darstellt.

Ausgehend von Bisaminochlorarsanen und $GaCl_3$ konnte ein acyclisches Arsenium-Kation dargestellt werden. Außerdem wurde die Reaktion mit AgOTf näher untersucht und das Reaktionsverhalten mit dem analogen Bisaminochlorstiban verglichen. Des Weiteren wurde die Reaktivität der Antimonverbindung $(Me_3Si)_2NSbCl_2$ gegenüber $GaCl_3$ untersucht und es gelang die Isolation eines Chlorstibenium-Kations, welches in der Folge weiter zu definierten Stibino-Stibonium-Salzen reagiert. Es zeigte sich, dass die Antimonverbindungen bevorzugt unter einem Chlor/Methylaustausch reagieren, wodurch verschieden substituierte Chlorstibane hergestellt werden konnten.

Summary

This thesis reports on selected reactions of silylated amino(dichloro)pnictanes $RN(SiMe_3)PnCl_2$ (R = $SiMe_3$, Mes*, Ter; Pn = P, As, Sb) with different Lewis acids. It could be demonstrated that the $GaCl_3$ assissted Me_3SiCl elimination starting from $(Me_3Si)_2NPCl_2$ results in the formation of isolable phosphenium salts. The reactivity of these salts was comprehensively studied and new bonding motifs and reaction channels have been uncovered. New low-coordinated PN compounds could be synthesized and characterized. Furthermore, the thermal Me_3SiCl elimination from $(Me_3Si)_2NPCl_2$ was investigated and molecular phosphorus nitride could be formally transferred, whereby a *cyclo*-tetraphosphazane was formed which is a multidentate ligand.

Starting from bisaminochloroarsanes and $GaCl_3$, the synthesis of an acyclic arsenium cation was achieved. Furthermore, the reactivity towards AgOTf was studied and the reactivity was compared to that of the analogous bisaminochlorostibane. Moreover, the reactivity of the antimony compound $(Me_3Si)_2NSbCl_2$ towards $GaCl_3$ was studied and a chlorostibenium cation could be isolated, which further reacts to yield defined stibinostibonium salts. The antimony compounds were shown to react in chlorine/methyl-exchange reactions resulting in the isolation of differently substituted chlorostibanes.

Danksagungen

Ich danke in besonderem Maße Herrn **Professor Dr. Axel Schulz** für das in mich gesetzte Vertrauen, die mir eingeräumte wissenschaftliche Freiheit, das interessante Thema, die vielen hilf- und lehrreichen Gespräche, die Bereitstellung des Laborplatzes, das Interesse an meiner Arbeit und vor allem für die Unterstützung in allen Situationen.

Ein besonderer Dank gilt Herrn **Dr. Alexander Villinger** für die Einarbeitung in die Röntgenkristallstrukturanalyse und die zeitraubende Unterstützung beim Lösen vieler Strukturen und deren Verfeinerung. Seine Hilfsbereitschaft und Unterstützung bei der Arbeit im Labor war von größter Bedeutung für das Gelingen dieser Arbeit. Außerdem trug er entscheidend dazu bei, dass die Arbeit stets abwechslungsreich war und ein sehr gutes Arbeitsklima im Labor herrschte.

Herrn **Dr. Mathias Rapphahn** möchte ich für die Einführung in die SCHLENK-Arbeitstechnik und die Betreuung während der Diplomphase danken.

Bei **Julia Rothe**, **Max Thomas** und **Maximilian Hertrich** bedanke ich mich für die geleistete Arbeit im Rahmen ihrer jeweiligen Bachelorarbeit, für das mir entgegengebrachte Vertrauen und die Entschlossenheit, mit welcher auch noch so schwierige Themen angegangen wurden.

Jonas Bresien danke ich für die gute Zusammenarbeit im Labor, die Hilfe beim quantenchemischen Rechnen, die Unterstützung bei Computerfragen und die Weiterführung des Phosphorprojektes, welches nicht Teil dieser Arbeit ist.

Ebenso möchte ich mich bei **Kati Rosenstengel**, **Denise Heyl**, **Fabian Reiß**, **Rene Labbow**, **Alexander Hinz** und **Marcus Kuprat** bedanken, die immer für ein angenehmes Arbeitsklima im Labor sorgten, und mir bei Problemen jederzeit mit Rat und Tat zur Seite standen.

Natürlich gilt mein Dank auch allen anderen Mitarbeitern im Arbeitskreis Schulz für die freundliche Aufnahme, die gute Zusammenarbeit sowie die unzähligen kleinen und großen Hilfen im Laboralltag.

Weiterhin möchte ich mich bei der analytischen Abteilung des Hauses und des LIKATs bedanken. Bei Herrn **Dr. Dirk Michalik**, Frau **Brigitte Goronzi** und Frau **Heike Borgwaldt** für die Anfertigung der NMR-Spektren, bei Frau **Angela Weihs** für die Anfertigung der IR-

Spektren und DSC-Messungen, bei Frau **Sigrun Roßmeisl** für die Durchführung diverser MS-Messungen, bei Frau **Petra Duncker** sowie bei Frau **Sieglinde Pries** und für die Durchführung der Elementaranalysen.

Ich danke dem ***Fond der chemischen Industrie*** für die finanzielle Unterstützung während des Promotionsstudiums. Des Weiteren bedanke ich mich bei der ***Studienstiftung des deutschen Volkes*** für die finanzielle und ideelle Förderung während meines Chemiestudiums.

Herrn **Prof. Dr. Andreas Gansäuer** danke ich für die Leitung des wissenschaftlichen Kollegs III der *Studienstiftung des deutschen Volkes*, die vielen wissenschaftlichen und privaten Diskussionen und vor allem für die Übernahme eines Gutachtens für die Stipendienbewerbung.

Ich danke Herrn **Prof. Christopher C. Cummins** dafür, dass er mir ermöglichte, ein dreimonatiges Forschungspraktikum in seiner Gruppe in Boston durchzuführen und für das mir entgegengebrachte Vertrauen und das interessante Thema während des Aufenthalts.

Ich bedanke mich bei den „Mensa-Allstars“ **Peter Sponholz**, **Hendrik Büttner**, **Johannes Diebler**, **Christopher Passow**, **Johannes Schranck**, **Marco Rosenfeldt**, **Norman Kühl** und **Christoph Kulmey** für die unzähligen, unvergesslichen Momente in der Mensa und während meiner gesamten Zeit an der Universität Rostock.

Ich möchte mich ganz besonders bei meiner Familie, insbesondere bei meinen **Eltern** und **Großeltern** für ihre finanzielle und ideelle Unterstützung und ihr Verständnis bedanken, mit welchem sie mir das Studium und die anschließende Promotion überhaupt erst ermöglicht haben.

Ein besonderer Dank gebührt hier meinem Großvater Herrn **Prof. Dr. Rudolf Hering**, der schon im frühen Kindesalter versuchte, mich für die Wissenschaft und insbesondere die Chemie zu begeistern.

Christine, dir danke ich für die Geduld und die Entbehrungen, die du während des Studiums und der Promotion auf dich genommen hast. All die schönen Momente mit dir und die liebevolle Unterstützung haben mir immer wieder neue Kraft und Motivation gegeben und so entscheidend zum Gelingen dieser Arbeit beigetragen.

Herzlichen Dank!

Für Christine

Inhaltsverzeichnis

Abkürzungsverzeichnis

AO	Atomorbital	**kov**	Kovalenz
ATR	*Attenuated Total Reflection* (abgeschwächte Totalreflexion)	**m**	*medium* (IR), *meta* (NMR), Multiplett (NMR)
bipy	2,2'-Bipyridyl	**Mes***	2,4,6-Tri-*tert*-butylphenyl = Supermesityl
chd	*cyclo*-Hexadien	**MO**	Molekülorbital
δ	Chemische Verschiebung (NMR)	**MS**	Massenspektrometrie
DFT	Dichtefunktionaltheorie	$\tilde{\nu}$	Wellenzahl
dmap	*N,N*-Dimethylaminopyridin	**NBO**	*Natural Bond Analysis*
dmb	2,3-Dimethyl-1,3-butadien	**NMR**	*Nuclear Magnetic Resonance* (Kernspinresonanzspektroskopie)
DSC	*Differential Scanning Calometry* (Dynamische Differenzkalorimetrie)	**ORTEP**	*Oak Ridge Thermal Ellipsoid Plot* (Kernspinresonanzspektroskopie)
Et	Ethyl	**OTf**	Triflat = Trifluormethansulfonat
et al.	und andere (lat. *et alii/aliae*)	**p**	para
ex.	im Überschuss (engl. *excess*)	**Ph**	Phenyl
fac	*facial*	**Pn**	Pniktogen
GIAO	*Gauge Invariant Atomic Orbitals*	**ppm**	*parts per million*
HOMO	*Highest Occupied Molecular Orbital*	**RT**	Raumtemperatur
INEPT	*Insensitive Nuclei Enhanced by Polarizaition Transfer*	**s**	*strong* (IR), Singulett (NMR)
IR	Infrarotspektroskopie	***t*Bu**	*tert*-Butyl
***i*Pr**	*iso*-Propyl	**Ter**	2,6-Dimesitylphenyl = Terphenyl
J	Kopplungskonstante	**theor**	theoretisch
LA	Lewis-Säure	**thf**	Tetrahydrofuran
LUMO	*Lowest Unoccupied Molecular Orbital*	**vdW**	*van der Waals*

Vom SI-System abweichende Einheiten

In dieser Arbeit werden die im Internationalen Einheitensystem (SI) gültigen Maßeinheiten verwendet. Alle davon abweichenden Einheiten und deren Umrechnung in SI-Einheiten sind im Folgenden aufgeführt.

Größe	**Symbol**	**Bezeichnung**	**Umrechnung in SI-Einheit**
Frequenz	MHz Hz	Megahertz Hertz	$1\ MHz = 10^6\ s^{-1}$ $1\ Hz = 1s^{-1}$
Länge	Å	Ångström	$1\ Å = 10^{-10}\ m$
Leistung	mW	Milliwatt	$1\ mW = 10^{-3}\ kg \cdot m^2 \cdot s^{-3}$
Temperatur	°C	Grad Celsius	x°C = (x + 273.15) K
Volumen	ml	Milliliter	$1\ ml = 1cm^3 = 10^{-6}\ m^3$
Wärmemenge	kJ	Kilojoule	$1\ kJ = 10^3 m^2 \cdot kg \cdot s^{-2}$
Wellenzahl	cm^{-1}	reziproke Zentimeter	$1cm^{-1} = 100\ m^{-1}$
Zeit	h min	Stunde Minute	1 h = 3600 s 1 min = 60 s

1 Aufgabenstellung

Ausgangspunkt dieser Arbeit war die Frage, ob es möglich ist, ausgehend von $(Me_3Si)_2NPCl_2$ ein Polymer herzustellen, welches nur aus P und N aufgebaut ist. Hierzu sollte zunächst die $GaCl_3$-unterstützte Me_3SiCl-Eliminierung untersucht werden. In diesem Zusammenhang sollten zunächst reaktive Intermediate, wie zum Beispiel Phosphenium-Kationen isoliert und charakterisiert werden. In einem weiteren Schritt sollte dann in Gegenwart von Me_3SiN_3 versucht werden, neuartige fünfgliedrige PN-Heterocyclen darzustellen. Dabei sollte getestet werden, ob $(Me_3Si)_2NPCl_2$ als „verstecktes Dipolarophil“ anzusehen ist. Darüber hinaus sollten auch die thermische Stabilität dieses einfachsten silylierten Aminodichlorphosphans untersucht und mit Hilfe geeigneter Reagenzien reaktive Zwischenstufen abgefangen werden.

In einem weiteren Themenkomplex sollte der Vergleich zu den schwereren Homologen des Phosphors $RN(SiMe_3)PnCl_2$ (Pn = As, Sb) gezogen und verschiedene Vorstufenmoleküle für die Synthese von Pniktadiazonium-Kationen synthetisiert werden, welche wiederum für die Synthese binärer Pniktogen-Stickstoff-Heterocyclen eingesetzt werden können. In diesem Zusammenhang sollte wiederum das Reaktionsverhalten in Abhängigkeit verschiedener sterisch anspruchsvoller Gruppen R ($R = Me_3Si$, Mes*, Ter) und der eingesetzten Lewis-Säuren LA ($LA = GaCl_3$, AgOTf) näher untersucht werden.

Mit Hilfe der Röntgendiffraktometrie an geeigneten Einkristallen sollte die Struktur der synthetisierten Verbindungen im Festkörper untersucht werden. Darüber hinaus sollte die Struktur und das chemische Verhalten durch schwingungsspektroskopische Methoden (IR- und Raman-Spektroskopie) und multinukleare Kernspinresonanzspektroskopie (^{31}P-, ^{29}Si-INEPT-, ^{14}N-, ^{13}C- und ^{1}H-NMR) in Lösung und Festkörper aufgeklärt werden. In Kombination mit den Ergebnissen von *ab-initio*- und DFT-Rechnungen sollten so die Bindungsverhältnisse in den Molekülen charakterisiert werden, um einen konkreten Zusammenhang zwischen Struktur und Reaktivität herzustellen. Zur Interpretation experimenteller Daten sollten zudem berechnete ^{31}P-NMR-Verschiebungen herangezogen werden.

2 Einleitung

2.1 Iminophosphane

Bereits 1894 berichteten Michaelis und Schröter von der Bildung eines Iminophosphans, welches in der Reaktion von salzsaurem Anilin mit einem Überschuss PCl_3 erhalten wurde. Auf der Basis von Elementaranalysen identifizierten sie das Produkt als "Phosphazobenzolchlorid" PhN=PCl mit einer Stickstoff-Phosphor-Doppelbindung.[1] In einer Fußnote bemerkten sie: „Unter der unwahrscheinlichen Annahme der doppelten Molekülgröße würde die Verbindung einen viergliedrigen Ring $[PhNPCl]_2$ bilden." Erst 90 Jahre später konnte zweifelsfrei durch eine Röntgenkristallstrukturanalyse belegt werden, dass die dimere Form, das *cyclo*-1,3-Dichlordiphospha-2,4-diphenyldiazan $[ClP(\mu\text{-}NPh)]_2$, das Hauptprodukt der Reaktion ist (Schema 1).[2]

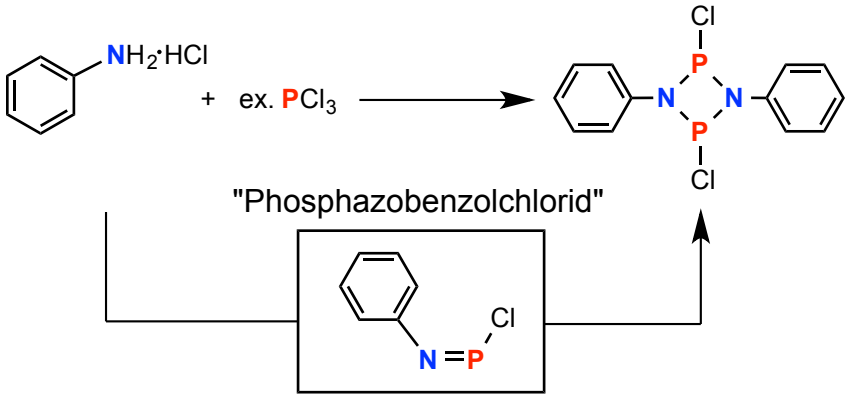

Schema 1. Darstellung von „Phosphazobenzolchlorids" aus salzsaurem Anilin und PCl_3.

1973 gelang Niecke und Flick die Synthese des ersten monomeren, isolierbaren Iminophosphans. Die Umsetzung von $(Me_3Si)_2NPF_2$ mit $Li[N(SiMe_3)_2]$ verläuft unter Me_3SiF-Eliminierung und $(Me_3Si)_2N{-}P{=}N(SiMe_3)$ wurde als gelb-grüne, extrem lichtempfindliche Flüssigkeit isoliert.[3,4] Bei Raumtemperatur dimerisiert dieses langsam zum korrespondierenden *cyclo*-1,3-Diphospha-2,4-diazan. Verbindungen mit zweifach koordinierten Phosphoratomen sind im Vergleich zu ihren Vorstufenmolekülen mit drei Substituenten am Phosphor im ^{31}P-NMR-Spektrum immer zu tiefem Feld verschoben, da das Phosphoratom durch das Entfernen eines Substituenten wesentlich entschirmt wird

(Schema 2). Dies wird durch die charakteristische chemische Verschiebung von $(Me_3Si)_2N{-}P{=}N(SiMe_3)$ von 325 ppm verdeutlicht.

Schema 2. Darstellung von $(Me_3Si)_2N{-}P{=}N(SiMe_3)$ nach *Niecke* und *Flick*.[3]

In der Folgezeit wurden verschiedenste Iminophosphane dargestellt und es haben sich vier Hauptsyntheserouten etabliert (Schema 3):

(i) 1,2-Eliminierungsreaktionen ausgehend von geeigneten Aminophosphanen des Typs R(X)P−N(Y)R. Die Doppelbindung wird durch die Eliminierung eines Moleküls XY gebildet und kann sowohl thermisch als auch basenassistiert erfolgen.[5]

(ii) Iminophosphane mit einer nukleofugen Gruppe am Phosphor können mit Nukleophilen eine Liganden-Austausch-Reaktion eingehen.[6,7]

(iii) Umlagerungsreaktionen stellen eine weitere, jedoch wenig verbreitete, Variante der Iminophosphandarstellung dar. [1,3]-Silyl- oder [1,3]-Dialkylamino-Gruppenwanderungen führen ausgehend von geeigneten Substraten ebenfalls zu Verbindungen mit PN-Doppelbindungen.[8]

(iv) Es ist des Weiteren möglich, ausgehend von Azadiphosphiridinen[9] oder Diphosphadiazanen[10] Iminophosphane in einer thermischen oder photochemischen Cyclo-Reversionsreaktion darzustellen.

Jedoch sind die dargestellten Iminophosphane in Bezug auf eine Dimerisierung der PN-Doppelbindung thermodynamisch nicht stabil, was eine der folgenden Stabilisierungsmethoden erfordert: (a) Die Doppelbindung kann durch den Einbau in ein delokalisiertes π-System stabilisiert werden; (b) In geladenen Systemen sind solche Doppelbindungen ebenfalls stabilisiert; (c) Die Reaktivität der PN-Mehrfachbindung kann ebenfalls durch die Koordination an ein Übergangsmetall inhibiert werden.[11] Im Gegensatz dazu steht die Stabilisierung durch sterisch anspruchsvolle Gruppen, welche eine Form der kinetischen Stabilisierung gegenüber einer Dimerisierung darstellt. Erst kürzlich untersuchte unsere Gruppe mit Hilfe von quantenchemischen Studien das Monomer/Dimer-Gleichgewicht zwischen Iminophosphanen und *cyclo*-Diphosphadiazanen (Schema 4).[12]

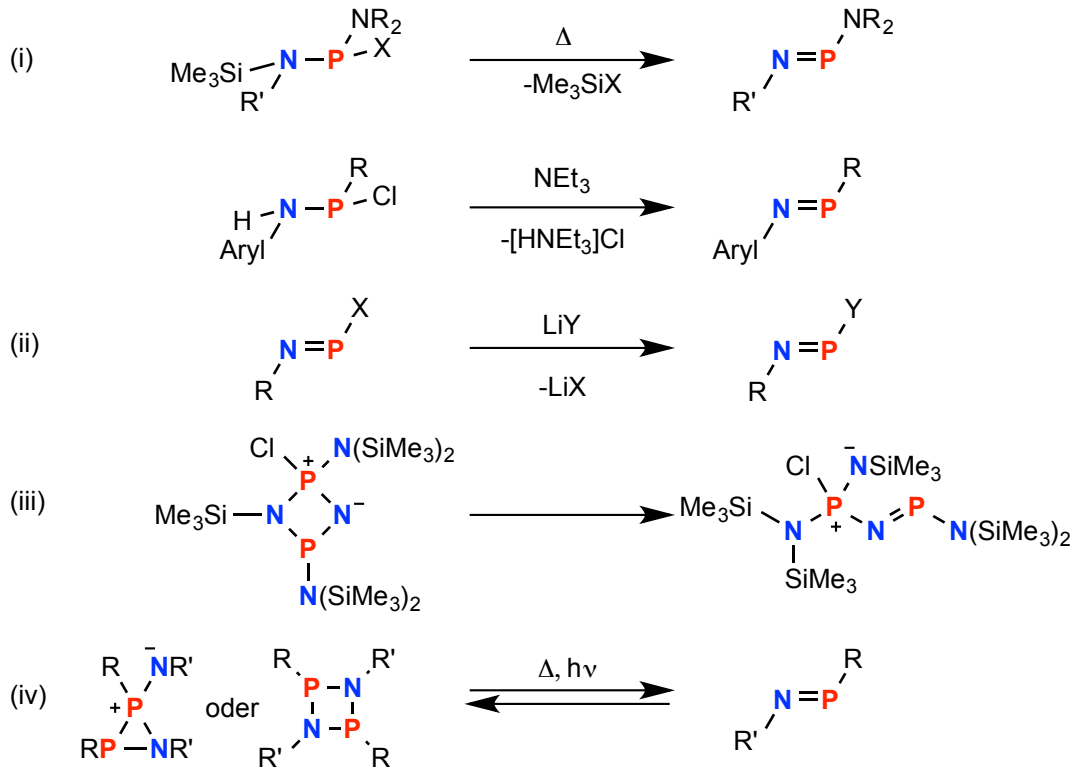

Schema 3. Verschiedene Möglichkeiten der Darstellung von Iminophosphanen.

Das Monomer ist demnach stabiler, wenn sterisch anspruchsvolle, elektronenschiebende Substituenten an das Stickstoffatom gebunden sind. Diese Ergebnisse stimmen sehr gut mit den experimentellen Befunden überein, wobei Mes*N=PCl das einzige Iminochlorphosphan ist, welches sowohl im Festkörper als auch in Lösung als Monomer vorliegt.[13]

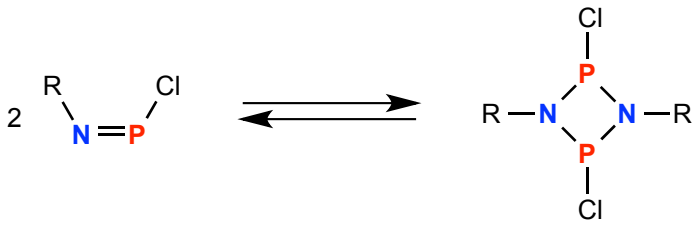

Schema 4. Monomer-Dimer-Gleichgewicht zwischen Iminochlorphosphanen und *cyclo*-1,3-Dichlor-diphospha-2,4-diazanen.

Ausgehend von Mes*N=PCl gelang es, durch Chloridabstraktion mit $AlCl_3$ erstmals ein Iminophosphenium-Kation mit einer Phosphor-Stickstoff-Dreifachbindung darzustellen (Schema 5).[13] Dieses Phosphadiazonium-Salz ($\delta[^{31}P] = 79.6$ ppm) zeigt im Gegensatz zum

Iminophosphan ($\delta[^{31}P]$ = 138.6 ppm) eine signifikante Hochfeldverschiebung im ^{31}P-NMR-Spektrum; auch im isovalenzelektronischen, aber neutralen Phosphalkin Mes*C≡P ($\delta[^{31}P]$ = 34.4 ppm) ist das Phosphoratom vergleichbar stark abgeschirmt.[14]

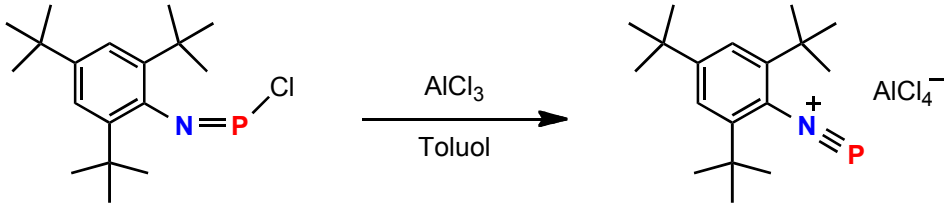

Schema 5. Synthese des ersten Phosphadiazonium-Kations mit einer PN-Dreifachbindung.

2.2 Binäre, stickstoffreiche, fünfgliedrige Ringsysteme

Ausgehend von Iminophosphenium-Salzen, welche als 1,2-Dipolarophil angesehen werden können, ist es möglich, in $GaCl_3$-assistierten [3+2]-Cycloadditionen mit 1,3-Dipolmolekülen wie Me_3SiN_3 binäre, stickstoffreiche, fünfgliedrige Ringsysteme herzustellen, z.B. Tetrazaphosphole RN_4P (R = Mes*[15], Ter[16]) und Triazadiphosphole RN_3P_2 (R = $N(SiMe_3)_2$,[17] Mes*[18]). Dabei kann vom isolierbaren Chloriminophosphan Mes*N=PCl und $GaCl_3$ ausgegangen werden (Schema 6). Diese Syntheseroute ist für andere Systeme nicht zugänglich, da z.B. für R = Ter nur das dimere *cyclo*-1,3-Diphospha-2,4-diazan $[ClP(\mu\text{-NTer})]_2$ darstellbar ist.[16] Bereits in früheren Arbeiten konnte die Arbeitsgruppe Schulz zeigen, dass silylierte Aminodichlorphosphane $RN(SiMe_3)PCl_2$ (R = Mes*, Ter) ideale Ausgangsverbindungen für die intermediäre Generierung der hoch reaktiven Iminophosphenium-Kationen des Typs $[RN{\equiv}P]^+$ darstellen, wobei $GaCl_3$ die intramolekulare Me_3SiCl-Eliminierung unterstützt und als Chlorid-Abstraktionsreagenz fungiert.[15,16,18] In einem zweiten Reaktionsschritt reagiert das 1,2-Dipolarophil $[RN{\equiv}P]^+$ dann mit einem 1,3-Dipolmolekül wie Me_3SiN_3 in einer formalen [3+2]-Cycloaddition zum $GaCl_3$-Addukt des Tetrazaphosphols unter Eliminierung eines weiteren Äquivalents Me_3SiCl. Jedoch war zu Beginn dieser Arbeit noch nicht geklärt, ob nach der Zugabe von $GaCl_3$ ein Aminochlorphosphenium-Kation gebildet wird und ob ausgehend von diesem ein acyclisches Azidophosphenium-Kation eine mögliche Zwischenstufe auf dem Weg zum Tetrazaphosphol darstellt (Schema 6).

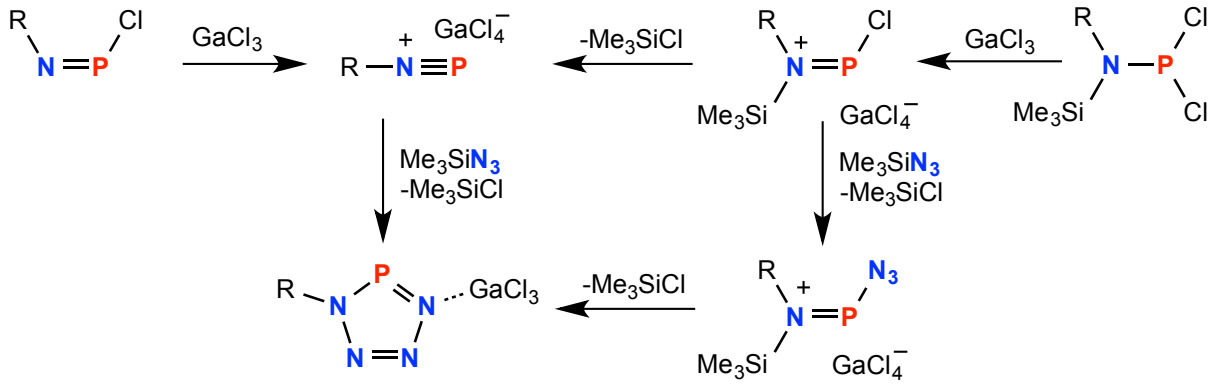

Schema 6. Darstellung eines Tetrazaphosphols in einer $GaCl_3$-assistierten [3+2]-Cycloaddition ausgehend von einem Iminophosphan RN=PCl oder einem „versteckten Dipolarophil“ $RN(SiMe_3)PCl_2$ (R = Mes*, Ter).

Darüber hinaus gelang es, für das analoge Arsensystem $[ClAs(\mu\text{-}NMes^*)]_2$ in einer $GaCl_3$-assistierten Cyclo-Reversion das Arsadiazonium-Salz $[Mes^*N{\equiv}As][GaCl_4]$ mit einer Stickstoff-Arsen-Dreifachbindung freizusetzen und strukturell zu charakterisieren (Schema 7).[19]

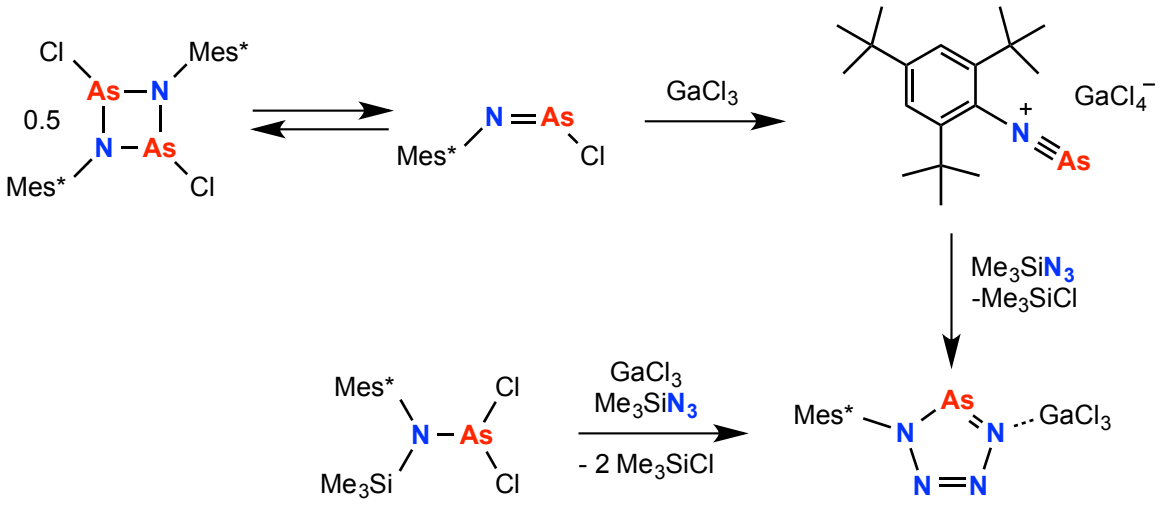

Schema 7. Darstellung von $[Mes^*AsN_4 \cdot GaCl_4]$ ausgehend von $[ClAs(\mu\text{-}NMes^*)]_2$ oder vom „versteckten Dipolarophil“ $Mes^*N(SiMe_3)AsCl_2$.

Bereits 2008 gelang im Arbeitskreis Schulz die Synthese des ersten Tetrazarsols $[Mes^*AsN_4 \cdot GaCl_3]$ ausgehend vom „versteckten Dipolarphil“ $Mes^*N(SiMe_3)AsCl_2$ in der Umsetzung mit $GaCl_3$ und Me_3SiN_3.[20] Alternativ kann auch das Arsadiazonium-Ion $[Mes^*N{\equiv}As]^+$ als 1,2-Dipolarophil eingesetzt werden.[19] Diese Syntheseroute war für das

analoge Antimonsystem nicht erfolgreich, jedoch konnte ein Tetrazastibol [Mes*SbN$_4$ · B(C$_6$F$_5$)$_3$] durch eine ungewöhnliche Isomerisierung von [N$_3$Sb(μ-NMes*)]$_2$ mit Hilfe der Lewis-Säure B(C$_6$F$_5$)$_3$ erhalten werden (Schema 8).[21]

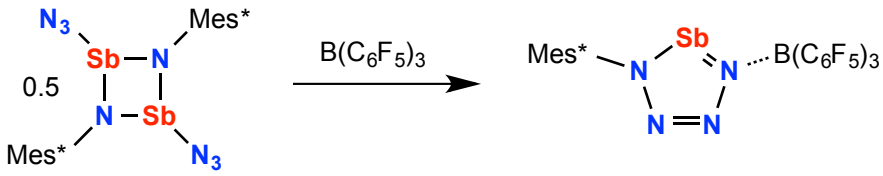

Schema 8. Darstellung von [Mes*SbN$_4$ · B(C$_6$F$_5$)$_3$] in einer B(C$_6$F$_5$)$_3$-assistierten Isomerisierungsreaktion.

2.3 Pniktenium-Kationen

Phosphenium-Kationen stellen das Phosphor-Analogon der Carbene dar. Sie besitzen ein zweifach koordiniertes, formal positiv geladenes Phosphoratom und sollten nach dem Isolobal-Konzept in ihrer Reaktivität und Eigenschaften den Carbenen ähneln.[22] Phosphenium-Kationen des Typs [X–P–Y]$^+$ werden am besten stabilisiert, wenn die beiden Substituenten X und Y π-Donatoren wie z.B. Aminogruppen sind, welche das Elektronendefizit am Phosphoratom absättigen können und so zur Stabilität des Kations beitragen.[23] Schmidpeter schlug vor, Phosphenium-Kationen nach der Ladungsverteilung im π-Elektronensystem zu kategorisieren (Schema 9).[24] Zum einen kann die Ladung vollständig auf die Substituenten delokalisiert sein. Das Phosphoratom besitzt dann ausschließlich nukleophile Eigenschaften (Typ A). Zum anderen kann die positive Ladung auch am Phosphoratom konzentriert sein. Das Phosphoratom reagiert dann als ambiphiles Zentrum, sowohl als Lewis-Säure als auch -Base (Typ B).

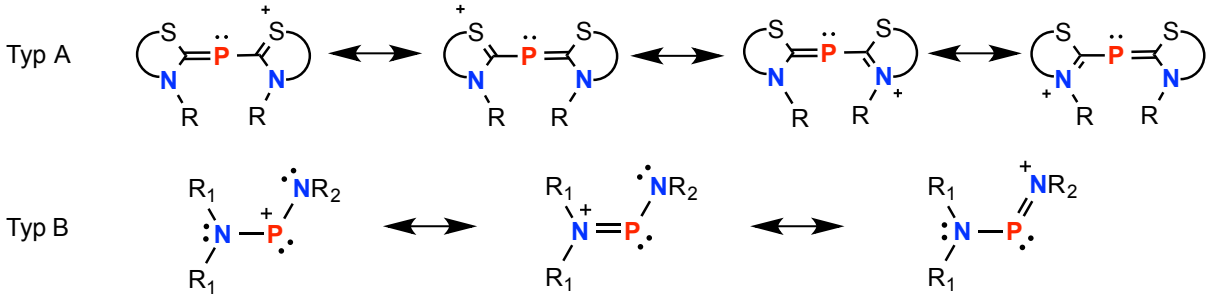

Schema 9. Kategorisierung von Phosphenium-Kationen in Typ A und Typ B nach Schmidpeter.

Die ersten Phosphenium-Spezies wurden 1964 von Dimroth und Mitarbeitern in der Synthese von Phosphamethincyaninen beschrieben, welche dem Typ A zuzuordnen sind (A, Schema 10).[25] 1975 berichteten Parry et al. von der Synthese der ersten Amino-substituierten, acyclischen Phosphenium-Kationen. $[(Me_2N)_2P]^+$ und $[Me_2NPCl]^+$ wurden durch Halogenid-Abstraktion ausgehend von Aminohalogenphosphanen und $AlCl_3$ hergestellt (B, Schema 10). Aminophosphenium-Ionen sind im Gegensatz zu den Phosphamethincyaninen Vertreter des Typs B (Schema 9). Die Umsetzung von Halogenphosphanen mit Halogenabstraktions-reagenzien wie z.B. $AlCl_3$, $GaCl_3$ oder Me_3SiOTf stellt den besten Zugang zu Phosphenium-Salzen dar. Die bereits erwähnten Aminoiminophosphane bilden in der Reaktion mit $AlCl_3$ oder $GaCl_3$ acyclische Zwitterionen, die durch Eliminierung von Me_3SiCl zu viergliedrigen ylidischen Ringen cyclisieren, welche ein lokalisiertes Phosphenium-Zentrum aufweisen (C, Schema 10).[26] Ebenso werden Phosphenium-Ionen ausgehend von $[Mes^*N{\equiv}P]^+$ erhalten, wenn diese z.B. mit Aminen oder Alkoholen reagieren.[27] Im Fall der Aminolyse entstehen acyclische Diaminophosphenium-Spezies (D, Schema 10). Diese wurden erst kürzlich von unserer Gruppe als Sonde für Kation-Anion-Wechselwirkungen eingesetzt.[28] Cyclische Phosphenium-Kationen sind im Gegensatz zu den acyclischen Derivaten zahlreich und ihre Eigenschaften wurden systematisch, insbesondere als Liganden in der Übergangsmetall-chemie, untersucht und in verschiedenen Übersichtsartikeln zusammengefasst.[29-31]

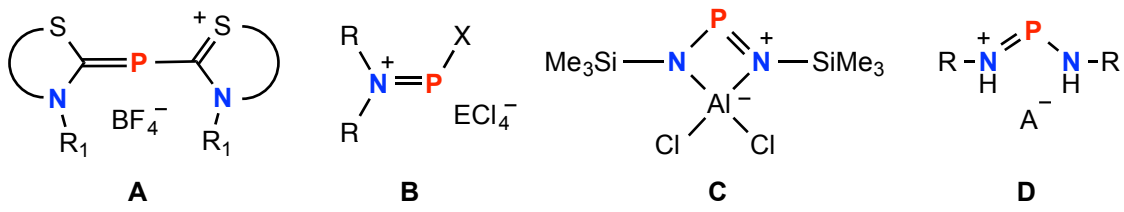

Schema 10. Verschiedene Phosphenium-Spezies: Phosphamethincyanin (**A**), Aminochlorphos-phenium-Salze (R = Me, Et, *i*Pr; X = Cl, NR_2) (**B**), cyclisches Zwitterion 1,3,2λ^2,4-Diazaphosphaaluminata-*cyclo*-butan (**C**) und Diaminophosphenium-Salze (R = Mes*, Ter; A = F, Cl, $GaCl_4$, CF_3SO_3, $B(C_6F_5)_4$, $CB_{11}H_5Br_6$) (**D**).

Im Gegensatz dazu konnten nur wenige acyclische Aminophosphenium-Spezies isoliert und strukturell charakterisiert werden. Insbesondere die bereits zuvor diskutierten Aminochlor-phosphenium-Kationen konnten bisher nur in ^{31}P-NMR-Experimenten beobachtet werden.[32-34] Ausgehend von $[R_2NPCl][AlCl_4]$ (R = Me, *i*Pr) untersuchten Wolf und Mitarbeiter 1984 die Reaktion mit Me_3SiN_3. In diesem Zusammenhang detektierten sie in ^{31}P-NMR-Experi-menten die intermediäre Bildung eines Aminoazidophosphenium-Kations $[R_2NPN_3]^+$.[35]

Strukturdaten von acyclischen Aminophosphenium-Salzen sind limitiert und beschränken sich auf wenige Bisaminophosphenium-Spezies[36] und Aminophosphenium-Ionen mit einer Arylgruppe am zweifach koordinierten P-Atom.[37,38] Das erste vollständig charakterisierte kationische Phosphorazid, ein 1-Azido-*cyclo*-1,3-diphospha-2,4-diazenium-Ion, $[Ter_2N_2P_2(N_3)]^+$ mit einem komplexen Gegenion $[N_3(GaCl_3)_2]^-$, wurde 2008 beschrieben (Schema 11).[16] Ausgehend von $[ClP(\mu\text{-}NTer)]_2$ wird in einem ersten Reaktionsschritt zunächst das cyclische Phosphenium-Kation $[Ter_2N_2P_2(Cl)]^+$ gebildet, welches dann mit zwei Äquivalenten Me_3SiN_3 weiter zur Azid-substituierten Spezies reagiert, die wiederum ein Konstitutionsisomer des Tetrazaphosphols $[TerPN_4 \cdot GaCl_3]$ darstellt. Darüber hinaus konnten die analogen Arsen-Spezies ausgehend von $[ClAs(\mu\text{-}NTer)]_2$ dargestellt werden. Erst kürzlich gelang auch die Synthese der analogen Antimonspezies $[Ter_2N_2Sb_2(Cl)]^+$.[39,40]

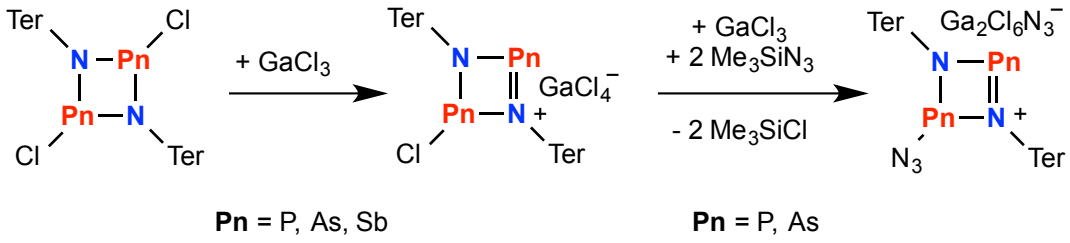

Schema 11. Darstellung verschiedener *cyclo*-1,3-Dipnikta- 2,4-diazenium-Salze.

Aufgrund ihres ambiphilen Charakters spiegeln Phosphenium-Kationen die Reaktivität der elektrophilen Carbenoide wider. Kationen des Typs B (Schema 9) sollten in der Reaktion mit σ-Donatoren wie z. B. 4-Dimethylaminopyridin (dmap) Addukt-Kationen bilden, so wie Carbene mit Pyridinen echte Ylide bilden (Schema 12).[41] Wird dieses Konzept noch erweitert, so ist anzunehmen, dass Phosphenium-Kationen des Typs B auch mit konjugierten Dienen wie 2,3-Dimethyl-1,3-butadien in chelotropen [4+1]-Cycloadditionsreaktionen reagieren. Bereits 1983 zeigten die Arbeitsgruppen von Baxter und Cowley unabhängig voneinander,[42,43] dass solche Reaktionen möglich sind und zu der Bildung von fünfgliedrigen Phospholen führen, so dass die Reaktion von Phosphenium-Kationen mit Dienen als Erweiterung der McCormack-Reaktionen anzusehen ist (Schema 12).

Im Gegensatz zu den Phosphenium-Kationen ist die Chemie der schweren homologen Arsenium-, Stibenium- und Bismutenium-Kationen bisher wenig untersucht. Cyclische

Arsenium-Kationen wurden erstmals von Burford Ende der 80er Jahre beschrieben und deren Reaktivität aufgeklärt.[44]

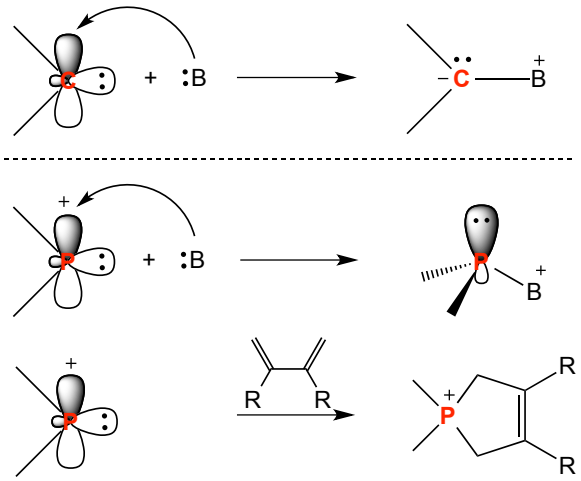

Schema 12. Ambiphiles Reaktionsverhalten von Phosphenium-Spezies in der Reaktion mit Lewis-Basen (B) und konjugierten Dienen.

Im Gegensatz zu den analogen Phosphenium-Systemen wird im Fall von Arsenium-Ionen ein Monomer-Dimer-Gleichgewicht beobachtet, wobei die Reaktivität der monomeren Einheit erhalten bleibt (Schema 13).[45] Mit konjugierten Dienen reagieren diese Arsenium-Spezies in [4+2]-Cycloadditionen, die zu der Isolation von Molekülen mit $AsNC_4$-Ringen führten. Pniktenium-Kationen werden ebenfalls am effektivsten durch die Kombination eines Halogenpniktans mit einem Halogenabstraktionsreagenz ($AlCl_3$, $GaCl_3$, Me_3SiOTf) erhalten.[46] Auf diese Weise konnte eine Vielzahl cyclischer Arsenium-Kationen präpariert und röntgenografisch charakterisiert werden.

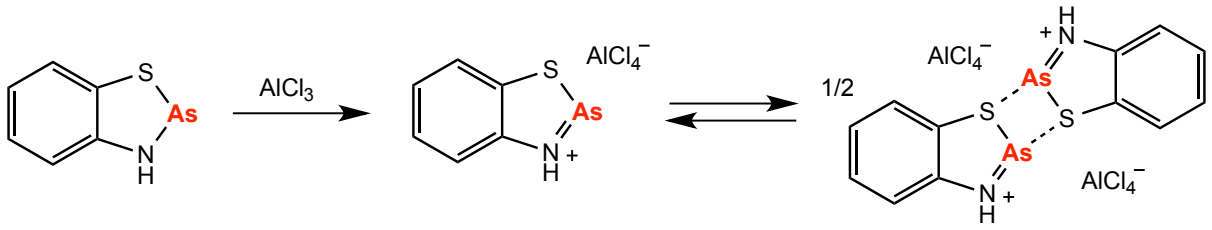

Schema 13. Synthese des ersten Arsenium-Salzes, welches im Gleichgewicht mit dem Dimer vorliegt.

Strukturparameter von acyclischen Pniktenium-Spezies $[R_2Pn]^+$ (Pn = As, Sb, Bi) sind jedoch rar. Zu Beginn der 90er Jahre berichteten Wolf und Mitarbeiter, dass ausgehend von Amino-substituierten Dichlorarsanen R_2NAsCl_2 in der Reaktion mit AgOTf acyclische Aminochlorarsenium-Salze des Typs $[R_2NAsCl]^+[OTf]^-$ synthetisiert werden können.[47] Acyclische Pniktenium-Ionen wurden in der Folge zumeist *in situ* erzeugt und mit geeigneten Pniktanbasen abgefangen. Über diesen synthetischen Ansatz konnte eine Vielzahl von Pniktino-Pniktonium-Salzen dargestellt werden, welche in der Literatur auch als Interpniktogen-Koordinationsverbindungen bezeichnet werden (Schema 14).[48-51]

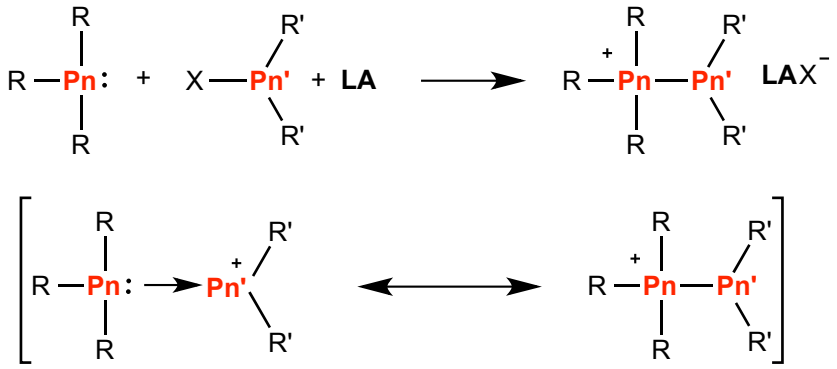

Schema 14. Oben: Darstellung von Pniktino-Pniktonium-Salzen, durch die *in situ* Generierung eines Pniktenium-Ions $[Pn'R'_2]^+$ in Gegenwart geeigneter Pniktanbasen $[PR_3]$ (Pn = P, As, Sb, Bi; LA = $AlCl_3$, $GaCl_4$, Me_3SiOTf; R, R' = Alkyl, Aryl). Unten: Interpniktogen-Koordinationsverbindung mit einer dativen Pn−Pn'-Bindung (links) und Pniktino-Pniktonium-Formulierung mit einer kovalenten Pn−Pn'-Bindung (rechts).

Des Weiteren sind in der Literatur nur wenige isolierbare Stibenium- und Bismutenium-Salze erwähnt. So gelang 2008 erstmals die Isolation eines blauen, homoleptischen Bismutenium-Kations ausgehend von $[(Me_3Si)_2NN(SiMe_3)]_2BiCl$ (Schema 15). Metallocen-artige Kationen des Typs $[Cp^*_2Sb]^+$ wurden erstmalig 1983 von Jutzi und Mitarbeitern synthetisiert und strukturell charakterisiert.[52]

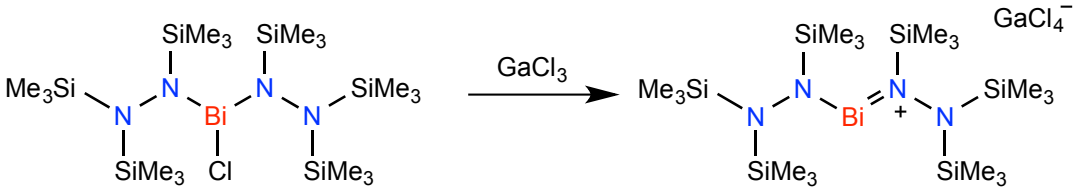

Schema 15. Darstellung des ersten acyclischen Bishydrazinobismutenium-Kations.

3 Ergebnisse und Diskussion

3.1 Übersicht

Zu Beginn der Promotionsarbeit lag der Fokus der Untersuchungen auf der $GaCl_3$-assistierten Me_3SiCl-Eliminierung. Ausgehend von $(Me_3Si)_2NPCl_2$ konnte gezeigt werden, dass die Abspaltung eines Moleküls Me_3SiCl in Gegenwart von $GaCl_3$ gelingt, wobei im ersten Schritt ein Aminochlorphosphenium-Salz gebildet wird. Die Bildung eines binären PN-Polymers konnte nicht beobachtet werden, da es auf diese Weise nicht möglich war, die Eliminierung des zweiten Äquivalents Me_3SiCl zu initiieren. Im Rahmen dieses Projektes gelang es erstmals, acyclische Pseudoholgen-substituierte Phosphenium-Kationen darzustellen und deren Reaktivität systematisch zu untersuchen (Kapitel 3.1 und 3.2).

Darüber hinaus sollte der Fokus auf die thermische Me_3SiCl-Eliminerung ausgehend von $(Me_3Si)_2NPCl_2$ gelegt werden. Auch in diesem Fall gelang die Eliminierung eines Äquivalents Me_3SiCl. Die reaktiven Intermediate bilden jedoch undefinierte Oligo- und Polymere, welche noch Chloratome und Me_3Si-Gruppen enthalten. In Gegenwart konjugierter Diene gelang es, diese Intermediate abzufangen und formal zweiatomiges Phosphornitrid ausgehend von $(Me_3Si)_2NPCl_2$ zu übertragen. Des Weiteren sollte die thermische Labilität durch die Substitution der Chloratome durch CF_3SO_3-Gruppen erhöht werden. Die Ergebnisse dieser Studie sind in Kapitel 3.3 zusammengefasst.

In einer weiterführenden Studie wurde die Reaktivität der silylierten Bisaminopniktane $[(Me_3Si)_2N]_2PnCl$ (Pn = As, Sb) gegenüber $GaCl_3$ und AgOTf genauer betrachtet. Im Rahmen dieser Studie konnten erstmals acyclische Arsenium-Salze isoliert werden und es wurde die unterschiedliche Reaktivität von Arsanen und Stibanen verdeutlicht (Kapitel 3.4).

Abschließend sollten verschiedene „versteckte Dipolarophile“ des Antimons in $GaCl_3$-assistierten Me_3SiCl-Eliminierungsreaktionen getestet werden. Dabei galt es zunächst, die Reaktivität von $(Me_3Si)_2NSbCl_2$ gegenüber $GaCl_3$ näher zu untersuchen. Es konnte gezeigt werden, dass in Abhängigkeit des Lösemittels verschiedene Stibino-Stibonium-Salze gebildet werden, welche das Produkt von Methyl/Chloraustauschreaktionen sind. Weitere silylierte Stibane des Typs $RN(SiMe_3)SbCl_2$ (R = Mes*, Ter) wurden mit $GaCl_3/Me_3SiN_3$ und AgOTf umgesetzt und die Produkte verschiedener Methylaustauschreaktionen konnten isoliert werden (Kapitel 3.5).

3.2 Azidophosphenium-Salze und Untersuchungen zu deren Stabilität

Ausgangspunkt dieser Untersuchung war die Frage, ob $(Me_3Si)_2NPCl_2$ als „verstecktes Dipolarophil“ in Gegenwart von Me_3SiN_3 in formalen $GaCl_3$-assistierten [3+2]-Cycloadditionsreaktionen eingesetzt und so neuartige Tetrazaphosphole des Typs $[(Me_3Si)PN_4 \cdot GaCl_3]$ synthetisiert werden können oder ob eine weitere Me_3SiCl-Eliminierung zur Bildung eines binären PN-Polymers führt.

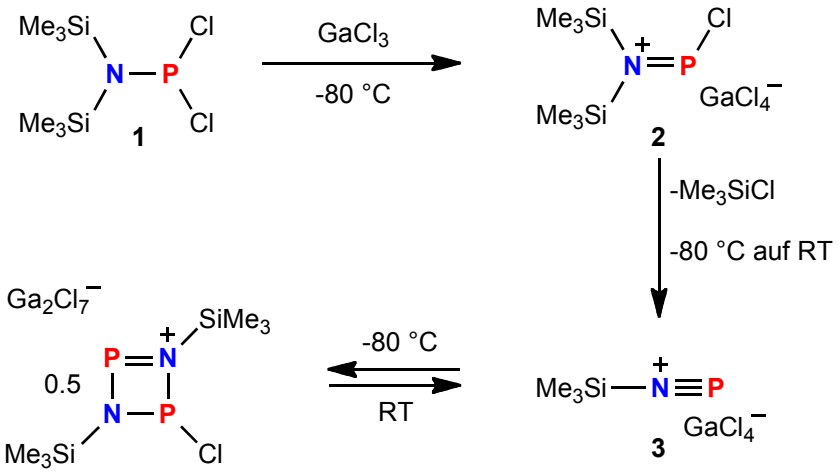

Schema 16. Synthese des Aminochlorphosphenium-Salzes **2** und dessen thermische Me_3SiCl-Eliminierung unter Bildung des Phosphadiazonium-Salzes **3**.

$(Me_3Si)_2NPCl_2$ (**1**) ist über eine einfache Salzmetathese zugänglich, wobei $Li[N(SiMe_3)_2]$ in *n*-Hexan bei −60 °C zu PCl_3 zugetropft wurde. Das Rohprodukt konnte nach Abtrennen des LiCl durch Destillation im Vakuum gereinigt werden. **1** wurde als farblose, lichtempfindliche Flüssigkeit erhalten. Bei der Umsetzung von **1** mit $GaCl_3$ bei −80 °C wurde die sofortige Bildung eines farblosen kristallinen Niederschlags beobachtet, der kristallografisch als das neuartige Aminochlorphosphenium-Salz $[(Me_3Si)_2NPCl][GaCl_4]$ (**2**) identifiziert wurde (Schema 16; Abbildung 1, rechts). Analog wurden bei der Umsetzung mit $AlCl_3$ und mit zwei Äquivalenten $GaCl_3$ das Tetrachloroaluminat- bzw. das Hepatachlorodigallat-Salz erhalten. Diese Verbindungen stellen die ersten strukturell charakterisierten acyclischen Chlorphosphenium-Spezies dar. Annähernd zeitgleich berichteten Weigand und Mitarbeiter über die strukturelle Charakterisierung von $[c\text{Hex}_2NPCl][GaCl_4]$.[53] In **1** wird eine durch Hyperkonjugation zwischen einem besetzten p-Atomorbital (AO) am Aminostickstoff und dem σ*-Orbital einer P−Cl-Bindung verkürzte $P-N_{Amin}$-Bindung mit 1.6468(8) Å gefunden,

wobei sich das dreifach koordinierte P-Atom in einer trigonal pyramidalen Umgebung befindet (Abbildung 1, links). Die Salzbildung mit $GaCl_3$ wird durch eine signifikante Kontraktion der P−N-Bindung auf 1.595(2) Å angezeigt (vgl. Σr_{kov}(P=N) = 1.60; (P−N) = 1.82 Å),[54] welche auf der Basis von NBO-Rechnungen als lokalisierte N−P-$p_\pi p_\pi$-Doppelbindung charakterisiert werden konnte. Der kürzeste Anion-Kation-Abstand P−Cl_{Anion} ist mit 2.871(4) Å deutlich innerhalb der Summe der Van-der-Waals-Radien für Phosphor und Chlor (vgl. Σr_{vdW}(P=N) = 3.55 Å).[55] **2** ist nur im Festkörper bei tiefen Temperaturen stabil. In Lösung wird beim Erwärmen auf Raumtemperatur die Bildung des Iminophosphenium-Salzes $[Me_3SiN{\equiv}P][GaCl_4]$ (**3**) beobachtet, welches im ^{31}P-NMR Spektrum bei einer chemischen Verschiebung von 89 ppm detektiert wird (Schema 16).

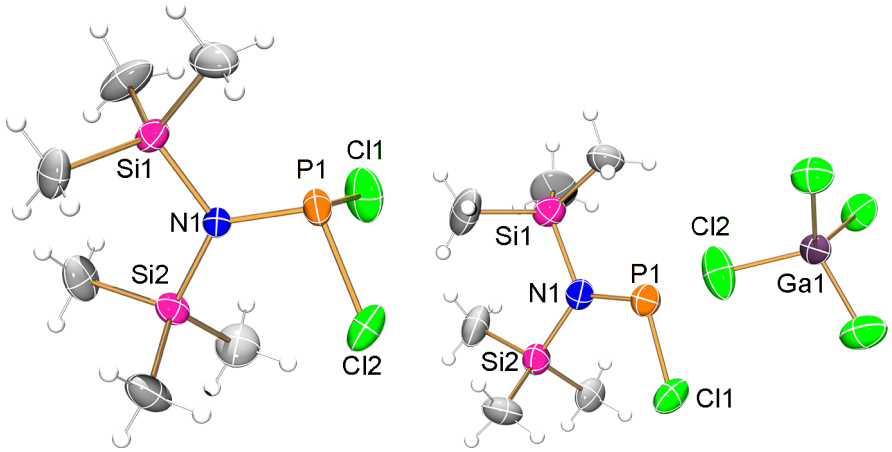

Abbildung 1. ORTEP-Darstellung der Molekülstruktur von $(Me_3Si)_2NPCl_2$ (**1**) (links) und $[(Me_3Si)_2NPCl][GaCl_4]$ (**2**) (rechts). Thermische Ellipsoide entsprechen 50 % Wahrscheinlichkeit bei 173 K.

Dieser Wert ist in guter Übereinstimmung mit dem theoretischen Wert, welcher mit Hilfe einer GIAO-Rechnung[56] erhalten wurde, und suggeriert, dass die Bildung von **3** als $GaCl_3$-assistierte Me_3SiCl-Eliminierung zu verstehen ist. Diese Eliminierungs-Reaktion wurde mit ^{31}P-NMR-Experimenten bei verschiedenen Temperaturen zwischen −80 °C und 25 °C visualisiert. Das Aminochlorphosphenium-Ion $[(Me_3Si)_2NPCl]^+$ ist demnach bis ca. −25 °C stabil und wird bei tiefem Feld detektiert ($\delta[^{31}P]$ = 285 ppm bei −25 °C). Im Folgenden wird intermediär ein Addukt $[(Me_3Si)_2NP(Cl)PN(SiMe_3)_2]^+$ zwischen dem Chlorphosphenium-Kation und **1** gebildet ($^1J_{P,P}$ = 669 Hz). Die große $^1J_{P,P}$-Kopplungskonstante ist charakteristisch für Donor-Akzeptor-Verbindungen mit einer P−P-Bindung.[57]

Bei Raumtemperatur verbleibt nur eine breite Resonanz bei 89 ppm, welche dem Phosphadiazonium-Ion $[Me_3SiN{\equiv}P]^+$ mit einer PN-Dreifachbindung zuzuordnen ist. Dessen Existenz wurde wiederum durch ^{31}P-NMR-Experimente bei tiefen Temperaturen bewiesen; bei −80 °C wird die Bildung des zyklischen Dimers, eines *cyclo*-1,3-Dichlordiphospha-2,4-diazenium-Kations beobachtet (Schema 16).

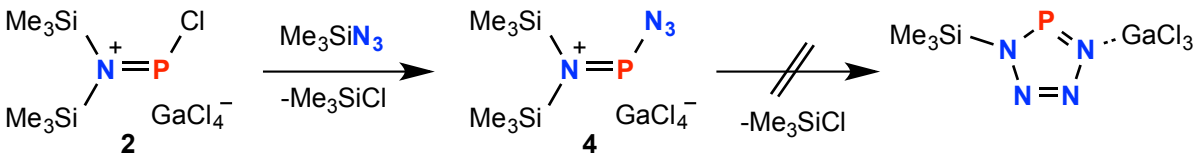

Schema 17. Darstellung des ersten isolierbaren Azidophosphenium-Salzes.

Bei der Umsetzung von $[(Me_3Si)_2NPCl][GaCl_4]$ mit Me_3SiN_3 bei −50 °C in CH_2Cl_2 fällt ein farbloser kristalliner Niederschlag aus (Schema 17), welcher kristallografisch bei tiefen Temperaturen (T < −50 °C) und durch ^{31}P-NMR-Experimente bei −65 °C ($\delta_{exp.}$ = 368 ppm, vgl. $\delta_{theor.}$ = 354 ppm) eindeutig als das hoch labile Azidophosphenium-Salz $[(Me_3Si)_2NPN_3][GaCl_4]$ (**4**) charakterisiert wurde (Abbildung 2, links). Das Kation stellt ein Konstitutionsisomer des cyclischen Tetrazaphospholium-Kations $[(Me_3Si)_2PN_4]^+$ dar. In Form isolierter Kristalle ist **4** erstaunlich stabil und kann bei −30 °C für wenigstens ein Jahr gelagert werden. Zu dieser Stabilität im Festkörper tragen schwache Wechselwirkungen zwischen Anion und Kation bei (P−Cl_{Anion} 3.3932(6) Å; Abbildung 2, rechts). Das gesamte Si_2NPN_3-Gerüst im Kation ist planar, und es findet eine effektive Delokalisation von π-Elektronen in dieser Ebene und senkrecht dazu statt. Daraus resultiert ein kurzer P−N_{Azid}-Abstand von 1.673(2) Å, was auf einen partiellen Doppelbindungscharakter hindeutet. Außerdem wird ein kurzer N_{Amin}−P-Abstand von 1.597(2) Å gefunden, was in guter Übereinstimmung mit einer NBO-Rechnung auf eine stark polarisierte PN-Doppelbindung hindeutet. Dieses π-Bindungssystem im Kation kann als einer der Gründe dafür angesehen werden, dass eine Zersetzung in Lösung erst ab −30 °C einsetzt. Oberhalb dieser Temperatur ist **4** nicht stabil und zersetzt sich unter Gasentwicklung in einer Staudinger-Reaktion zu Kationen des Typs $[(Me_3Si)_2NPNP(Cl)_2N(SiMe_3)_2]^+$. Die Cyclisierung zu einem Tetrazaphosphol wurde nicht beobachtet (Schema 17).

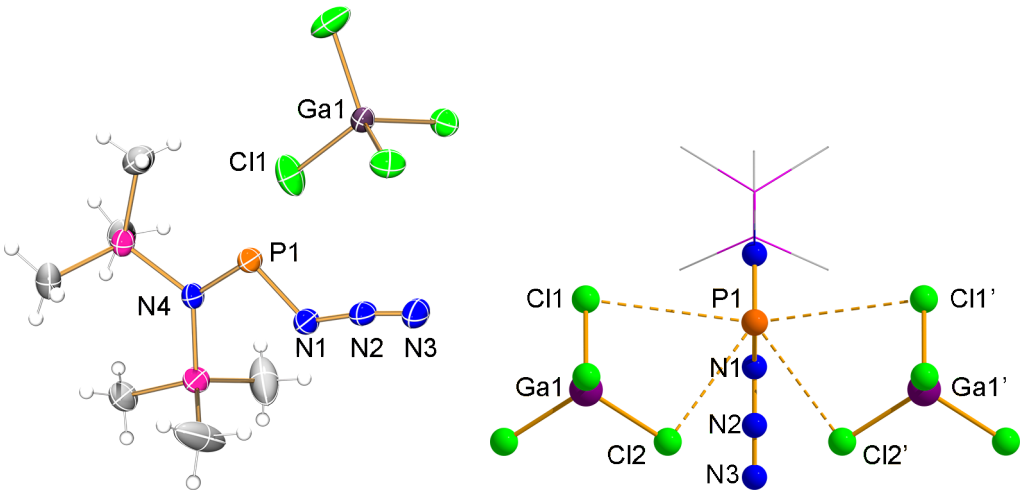

Abbildung 2. Links: ORTEP-Darstellung der Molekülstruktur von $[(Me_3Si)_2NPN_3][GaCl_4]$ (**4**). Thermische Ellipsoide entsprechen 50 % Wahrscheinlichkeit bei 173 K. Rechts: *Ball-and-Stick*-Darstellung der Anion-Kation-Wechselwirkung im Festkörper.

Bereits im Jahre 1984 berichtete Wolf,[35] dass $[i\mathrm{Pr}_2NPN_3][AlCl_4]$ in einer Staudinger-Reaktion mit $[i\mathrm{Pr}_2NPCl][AlCl_4]$ reagiert.[58] Die Autoren postulierten auf der Basis von ^{31}P-NMR-Daten die Bildung eines Phosphor-Biskations des Typs $[i\mathrm{Pr}_2NPNP(Cl)Ni\mathrm{Pr}_2]^{2+}$. Jedoch ist die Bildung von Kationen mit einem trigonal planarem P-Atom sehr unwahrscheinlich,[59] und daher wurde die von Wolf beschriebene Synthese als Ausgangspunkt für die systematische Untersuchung der Zersetzungsreaktion von **4** gewählt.

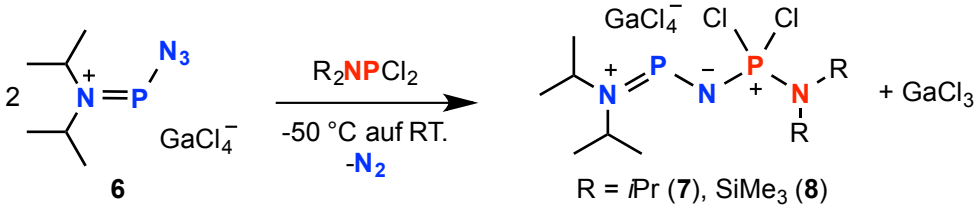

Schema 18. Reaktion des Azidophosphenium-Salz $[i\mathrm{Pr}_2NPN_3][GaCl_4]$ (**6**) mit Dichlorphosphanen.

In Analogie zur Darstellung der Me_3Si-Derivate gelang die Darstellung der Phosphenium-Salze $[i\mathrm{Pr}_2NPCl][GaCl_4]$ (**5**) und $[i\mathrm{Pr}_2NPN_3][GaCl_4]$ (**6**), wobei die Molekülstruktur beider Salze erstmals bestimmt werden konnte (Tabelle 1), im Gegensatz zu den Trimethylsilyl-substituierten Spezies sind diese Salze thermisch stabil und können auch bei Raumtemperatur gehandhabt werden. Daraus ergeben sich zwei entscheidende Vorteile gegenüber den Me_3Si-Verbindungen: (i) Sie können kein Me_3SiCl eliminieren. (ii) $GaCl_3$-assistierte Methyl/

Chloraustauschreaktionen zwischen Phosphor und den Silylgruppen sind nicht möglich.[60] Zunächst wurde die Reaktion äquimolarer Mengen von **5** und **6** in CH_2Cl_2 untersucht, wobei die Mischung schnell von −50 °C auf Raumtemperatur aufgetaut wurde. ^{31}P-NMR-Experimente zeigten in guter Übereinstimmung mit kristallografischen Methoden die Bildung eines Iminophosphoran-substituierten Phosphenium-Salzes des Typs [*i*Pr$_2$NPNP(Cl)$_2$NiPr$_2$][GaCl$_4$] (**7**) mit einem Phosphenium-Phosphoratom (δ[^{31}P] = 311.2 ppm) und einem vierfach koordinierten Phosphoniumzentrum (δ[^{31}P] =27.4 ppm; $^2J_{P,P}$ = 111.5 Hz) (Abbildung 3, links), wobei ein Äquivalent $GaCl_3$ in Lösung verbleibt. Wird **6** mit *i*Pr$_2$NPCl$_2$ umgesetzt, wird die quantitative Bildung des Staudinger-Produktes beobachtet. Salze mit gemischten Kationen des Typs [*i*Pr$_2$NPNP(Cl)$_2$N(SiMe$_3$)$_2$][GaCl$_4$] (**8**) wurden erhalten (Abbildung 3, rechts), wenn **6** mit **1** umgesetzt wurde (Schema 18). Die dargestellten Salze weisen kurze PN-Bindungen entlang des N_3P_2-Gerüstes auf, und es werden nur lose Kontakte zwischen Anion und Kation detektiert. Die Bindungsparameter der Salze sind in Tabelle 1 zusammengefasst.

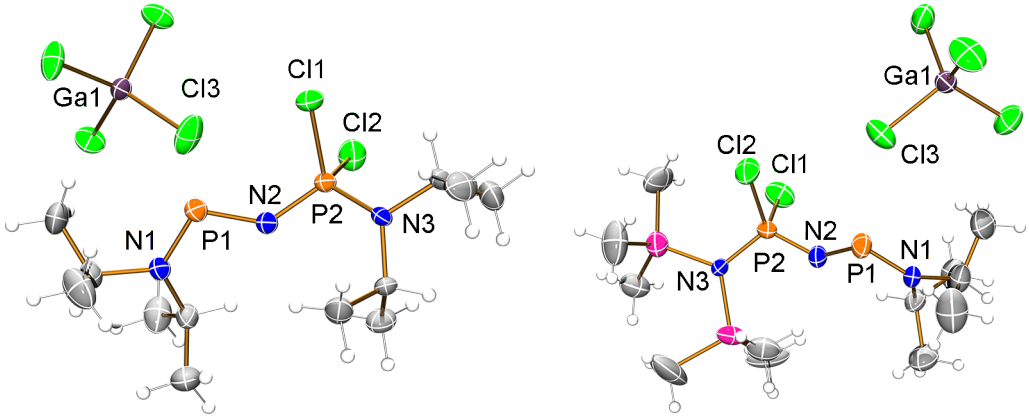

Abbildung 3. ORTEP-Darstellung der Molekülstruktur von [*i*Pr$_2$NPNP(Cl)$_2$N*i*Pr$_2$][GaCl$_4$] (**7**) (links) und [*i*Pr$_2$NPNP(Cl)$_2$N(SiMe$_3$)$_2$][GaCl$_4$] (**8**) (rechts). Thermische Ellipsoide entsprechen 50 % Wahrscheinlichkeit bei 173 K.

Des Weiteren wurde die Reaktivität dieser komplexen Phosphenium-Spezies gegenüber dmb und 2,2'-Bipyridin (bipy) getestet. Wird **7** mit dmb umgesetzt, konnte das Produkt einer chelotropen [4+1]-Cycloaddition **7[dmb]** isoliert werden, was den Phospheniumcharakter des N_3P_2-Kations verdeutlicht. Die Reaktion mit äquimolaren Mengen bipy führte zu der Bildung des Chlorphosphans *i*Pr$_2$NP(Cl)NP(Cl)$_2$N*i*Pr$_2$ **7[Cl]**, wobei $GaCl_3$ in Form des unlöslichen Komplexes [GaCl$_2$(bipy)$_2$][GaCl$_4$] abgetrennt werden konnte (Schema 19).[61]

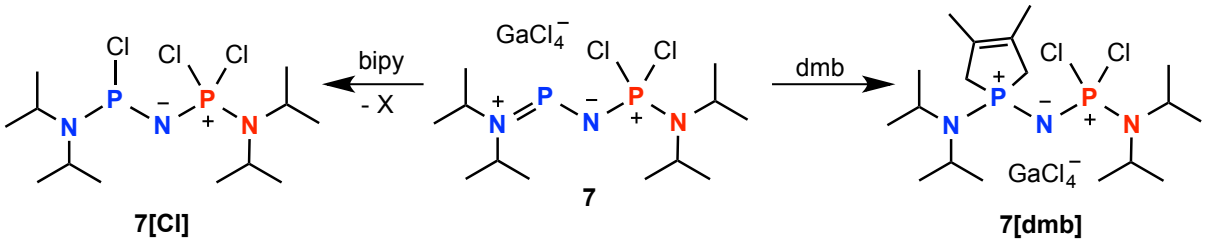

7[Cl] **7** **7[dmb]**

Schema 19. Reaktivität von [*i*Pr$_2$NPNP(Cl)$_2$N*i*Pr$_2$][GaCl$_4$] gegenüber dmb und bipy (X = [GaCl$_2$(bipy)$_2$][GaCl$_4$]).

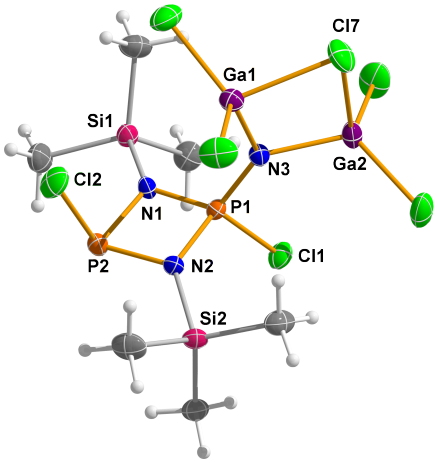

Abbildung 4. ORTEP-Darstellung der Molekülstruktur [(Me$_3$Si)$_2$N$_2$P$_2$Cl$_2$N(Ga$_2$Cl$_5$)] (**11**). Thermische Ellipsoide entsprechen 50 % Wahrscheinlichkeit bei 173 K.

Ausgehend von diesen Resultaten sollte in weiteren Experimenten die Zersetzung von **4** näher untersucht werden. Auf der Basis von ^{31}P-NMR-Experimenten bei Temperaturen zwischen −80 °C und 25 °C konnte gezeigt werden, dass **4** beim Auftauen ebenfalls in einer Staudinger-Reaktion zu [(Me$_3$Si)$_2$NPNP(Cl)$_2$N(SiMe$_3$)$_2$][GaCl$_4$] (**9**) und [(Me$_3$Si)$_2$NPNP(Cl)(N$_3$)N(SiMe$_3$)$_2$][GaCl$_4$] (**10**) reagiert (Schema 20). Die Reaktion ist jedoch nicht selektiv und neben der Dichlorverbindung **9** wurde auch ein gemischtes Chlor/Azid-Derivat **10** gefunden. Die Umsetzung von **4** mit einem Äquivalent **2** führte zur Bildung des *cyclo*-1λ^3,3λ^5-Diphospha-2,4-diazans [{ClP(μ-NSiMe$_3$)}$_2$N(Ga$_2$Cl$_5$)] (**11**) (Abbildung 4), welches als das Produkt einer [1,3]-Silyl-Verschiebung anzusehen ist und direkt aus dem acyclischen Staudinger-Produkt **9** durch zweifache Me$_3$SiCl-Eliminierung hervorgeht. Die Molekülstruktur zeichnet sich durch ein trigonal-pyramidales P^{III}-Zentrum und ein zweites verzerrt tetraedrisch koordiniertes P^{V}-Atom auf, die in einem annähernd planaren P$_2$N$_2$-Ring liegen. Die beiden exocyclischen Chloratome befinden sich dabei in *trans*-Position zueinander und an das Phosphonium-Zentrum ist außerdem ein weiteres exocyclisches Stickstoffatom gebunden, welches mit einer

Ga_2Cl_5-Einheit verknüpft ist. Auf der Basis einer NBO-Analyse kann die Bildung dieser Spezies als Stabilisierung eines $[(Me_3Si)_2N_2P_2Cl_2N]^-$-Fragmentes durch eine $[Ga_2Cl_5]^+$-Einheit verstanden werden (Schema 20, unten).

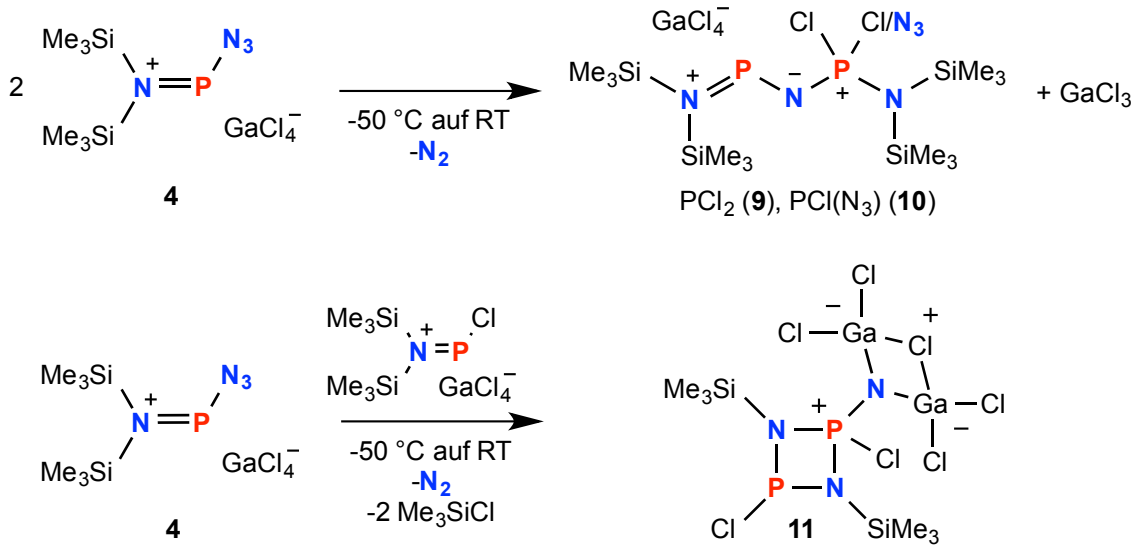

Schema 20. Systematische Untersuchung der Zersetzung von $[(Me_3Si)_2NPN_3][GaCl_4]$.

Tabelle 1: Ausgewählte Strukturparameter und ^{31}P-NMR-Verschiebungen der diskutierten Spezies **1**, **2**, und **4-8.**

Verbindung	1	2	4	5	6	7	8
***d*(P−N_{Amin})**	1.6468(8)	1.595(2)	1.597(3)	1.591(3)	1.6003(9)	1.611(2)	1.612(4)
***d*(P−X[a])**	2.0834(5)	2.003(1)	1.673(2)	2.003(1)	1.665(1)	1.597(2)	1.597(4)
***d*(P−Cl_{Anion})**	2.1074(5)	2.871(4)	3.3923(6)	3.014(1)	3.0448(4)	3.532(1)	3.289(2)
<N1P1X[a]	104.37(4)	107.6(1)	101.03(9)	106.9(1)	100.57(5)	104.97(9)	105.0(2)
***δ*[^{31}P] P^{III} / P^V**	188	285	368	295	311	311 / 27	311 / 30

[a]X = Cl (**1**, **2**, **5**), N_3 (**4**, **6**), $NP(Cl)_2NR_2$ (**7** R = *i*Pr, **8** = $SiMe_3$). [*d*] = Å, [<] = °

3.3 Darstellung Pseudohalogen-substituierter Phosphenium-Ionen

Die vorhergehenden Untersuchungen haben gezeigt, dass es möglich ist, das Chloratom in Chlorphosphenium-Kationen gegen eine Azid-Einheit zu substituieren. Im Rahmen dieses Projektes sollte getestet werden, ob auch andere Pseudohalogen-Gruppen wie Isocyanat-, Isothiocyanat-, Cyanid- oder Fulminat-Gruppen durch die Umsetzung mit dem

entsprechenden Trimethylpseudohalogensilan am Phosphenium-Phosphor eingeführt werden können. Des Weiteren sollte die Reaktivität der Carben-analogen Kationen gegenüber Lewis-Basen und Dienen näher untersucht werden.

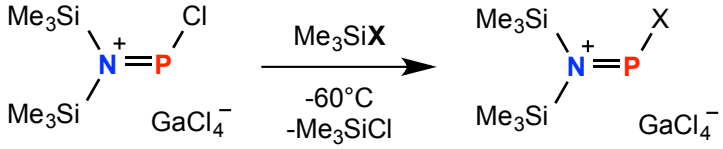

Schema 21. Synthese Pseudohalogen-substituierter Phosphenium-Kationen ausgehend von $[(Me_3Si)_2NPCl][GaCl_4]$ (X = NCO, NCS, $O(SiMe_3)$).

Die Umsetzung von $[(Me_3Si)_2NPCl][GaCl_4]$ mit Me_3SiX (X = N_3, NCO, NCS, CNO) bei −80 °C in CH_2Cl_2 führte in der Tat zur Bildung von Pseudohalogenphosphenium-Salzen (Schema 21). Nach einstündigem Rühren bei dieser Temperatur und anschließender Konzentration der Reaktionslösung bei maximal −50 °C konnten Kristalle der bisher unbekannten Salze des Typs $[(Me_3Si)_2NPX][GaCl_4]$ (X = NCO (**12**), NCS (**13**), $OSiMe_3$ (**14**)) erhalten werden und deren Struktur im Festkörper durch Röntgenkristallstrukturanalyse bestimmt werden (Abbildung 5). Die dargestellten Phosphenium-Spezies sind alle nur in isolierter Form und unterhalb −30 °C stabil, in Lösung setzt beim Erwärmen auf Raumtemperatur Zersetzung zu nicht identifizierten Produkten ein. Durch quantenchemische Rechnungen (NBO, MO) konnte gezeigt werden, dass entlang des NPX-Gerüstes (X = NCO, NCS) eine Delokalisation von π-Elektronen möglich ist. Außerdem tragen Kontakte zwischen Anion und Kation zur Stabilisierung dieser reaktiven Salze im Festkörper bei. Die lokalisierten Molekülorbitale zeigen ebenfalls eine *in-plane*- und *out-of-plane*-Delokalisation von π-Elektronen. Diese Bindungssituation ist analog zu der in Azidophosphenium-Spezies **4**.

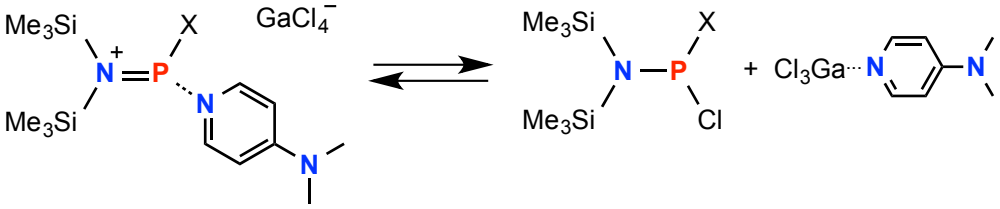

Schema 22. Gleichgewicht in CH_2Cl_2 Lösung von $[(Me_3Si)_2NP(dmap)X][GaCl_4]$ (X = Cl, NCO, NCS).

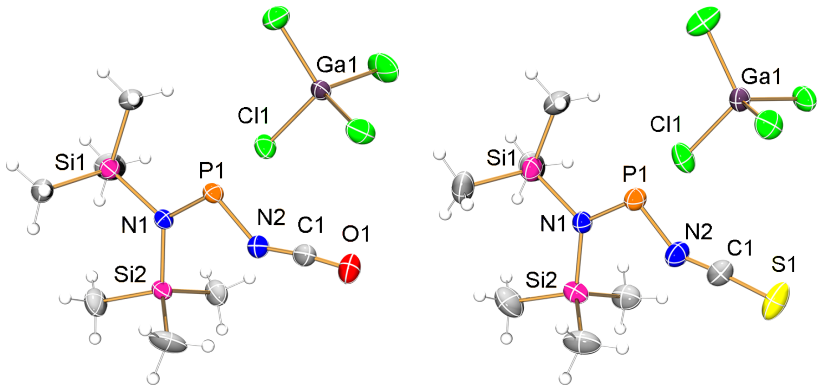

Abbildung 5. ORTEP-Darstellung der Molekülstruktur der Phosphenium-Salze $[(Me_3Si)_2NPNCO][GaCl_4]$ (**12**) (links) und $[(Me_3Si)_2NPNCS][GaCl_4]$ (**13**) (rechts). Thermische Ellipsoide entsprechen 50 % Wahrscheinlichkeit bei 173 K.

Bei der Umsetzung von $[(Me_3Si)_2NPX][GaCl_4]$ mit der Pyridinbase 4-*N*,*N*-Dimethylaminopyridin (dmap) wurden Addukt-Kationen des Typs $[(Me_3Si)_2NP(dmap)X][GaCl_4]$ (X = Cl (**2dmap**), N_3 (**4dmap**), NCO (**12dmap**)) erhalten und diese konnten strukturell charakterisiert werden. (Abbildung 6, links) Im Gegensatz zu ihren Vorstufen sind sie Raumtemperatur-stabil und eine Zersetzung setzt erst oberhalb von 100 °C ein. Auf der Basis von ^{31}P-NMR-Experimenten konnte in Lösung ein Gleichgewicht dieser Lewis-Base-stabilisierten Kationen mit den Chlor-rücksubstituierten neutralen Phosphanen $(Me_3Si)_2NPClX$ und dem dmap-Addukt von $GaCl_3$ beobachtet werden (Schema 22). Die Stabilisierung ist durch eine Delokalisation der positiven Ladung in das aromatische System des dmap zu erklären, sodass es sich nicht mehr um Phosphor-zentrierte Kationen handelt. Aus den Molekülstrukturen geht hervor, dass die Phosphoratome trigonal pyramidal koordiniert sind und das dmap kovalent an das P-Atom gebunden ist.

Die Umsetzung von $[(Me_3Si)_2NPX][GaCl_4]$ mit geeigneten konjugierten Dienen wie 2,3-Dimethyl-1,3-butadien (dmb) oder 1,3-*cyclo*-Hexadien (chd) führte zur Bildung von Salzen mit Phospholenium-Kationen des Typs $[(Me_3Si)_2NP(dmb)X][GaCl_4]$ (X = Cl (**2dmb**), N_3 (**4dmb**), NCO (**12dmb**); Abbildung 6, Mitte) und Phosphanorbornenium-Kationen des Typs $[(Me_3Si)_2NP(chd)X][GaCl_4]$ (X = Cl (**2chd**), N_3 (**4chd**), NCO (**12chd**); Abbildung 6, rechts), welche Produkte einer chelotropen [4+1]-Cycloaddition sind (Schema 23). Es konnte erstmalig gezeigt werden, dass die Doppelbindung innerhalb der 7-Phosphanorbornenium-Einheit im Festkörper immer auf der gleichen Seite wie der Substituent liegt; diese Konfiguration wird als *anti* bezeichnet. Alle Derivate konnten strukturell, NMR- und schwingungsspektrokopisch charakterisiert werden und sind im Festkörper bis 100 °C stabil.

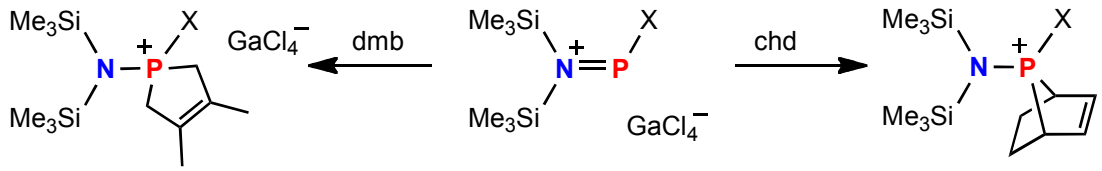

Schema 23. Synthese neuartiger Phospholenium- und Phosphanorbornenium-Salze.

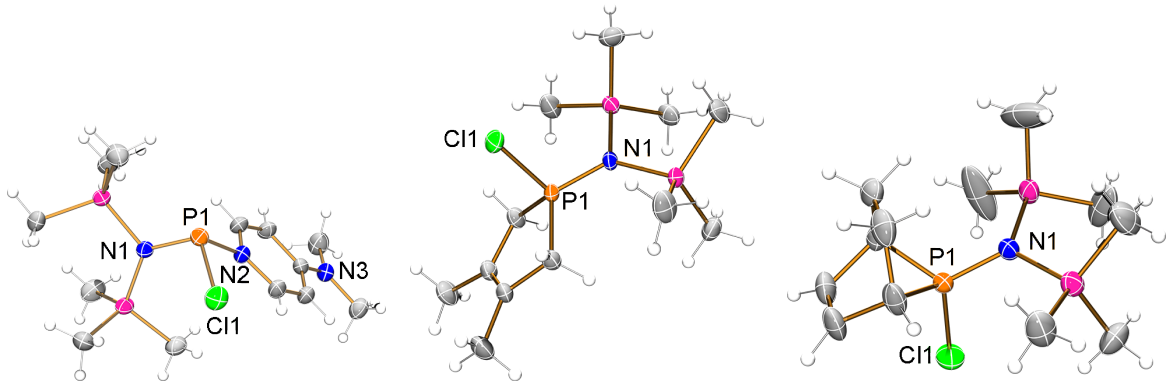

Abbildung 6. ORTEP-Darstellung der Molekülstruktur des Addukt-Kations $[(Me_3Si)_2NP(dmap)Cl][GaCl_4]$ (**2dmap**), des Phospholenium-Kations $[(Me_3Si)_2NP(dmb)Cl][GaCl_4]$ (**2dmb**) und des Phosphanorbornenium-Kations $[(Me_3Si)_2NP(chd)Cl][GaCl_4]$ (**2chd**). Thermische Ellipsoide entsprechen 50 % Wahrscheinlichkeit bei 173 K.

3.4 Synthese eines *cyclo*-Tetraphosphazan – Übertragung von PN

Es konnte bereits gezeigt werden, dass es möglich ist durch die Zugabe von $GaCl_3$ ein Äquivalent Me_3SiCl aus $(Me_3Si)_2NPCl_2$ zu eliminieren. Dabei wird das Iminophosphenium-Salz $[Me_3SiN{\equiv}P][GaCl_4]$ gebildet. Die Eliminierung eines zweiten Moleküls Me_3SiCl sollte formal zur Bildung von molekularem Phosphornitrid (PN) mit einer PN-Dreifachbindung führen, welches jedoch im Gegensatz zum molekularem Stickstoff sehr reaktiv ist und zu undefinierten PN-Polymeren reagiert. In der Gegenwart von geeigneten Abfangreagenzien sollte es gelingen molekulares PN zu stabilisieren.

Zunächst wurde eine Toluol-Lösung von $(Me_3Si)_2NPCl_2$ auf 120 °C erhitzt und die Bildung von unlöslichen polymeren Produkten beobachtet. Diese polymeren Spezies wiesen immer noch Silylgruppen und Chloratome auf, wie eine Elementaranalyse zeigte. Die Zugabe eines Überschusses von dmb zu solch einer Reaktionsmischung und anschließendes Erhitzen auf 120 °C im Hochvakuum resultierte in der Bildung eines cyclischen Phosphazans

[$(Me_3Si)_2N(dmb)PCl$] (**15**), das im ^{31}P-NMR-Spektrum eine Resonanz bei 126 ppm (GIAO:[56] 123 ppm) zeigte (Schema 24).

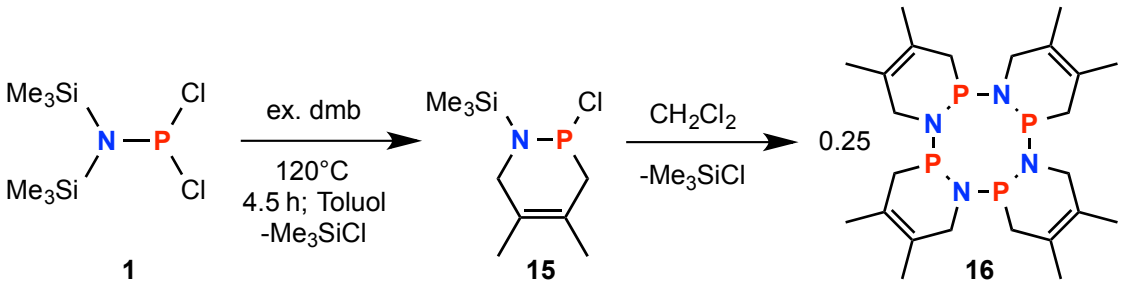

Schema 24. Darstellung des *cyclo*-Tetraphosphazans [PN(dmb)]$_4$, welches formal vier Äquivalente molekulares PN inkorporiert.

Neben diesem Phosphazan entstanden ebenso unlösliche oligo- und polymere Nebenprodukte, welche durch Filtration leicht abgetrennt werden konnten. Nach Entfernen des Lösemittels vom Filtrat im Vakuum und anschließende Aufarbeitung aus CH_2Cl_2 konnten farblose Kristallblöcke isoliert werden, welche röntgenografisch als das *cyclo*-Tetraphosphazan [PN(dmb)]$_4$ (**16**) identifiziert wurden (Abbildung 7, links). **16** kann formal als abgefangenes Phosphornitrid (PN) angesehen werden, wobei vier PN-Moleküle jeweils eine [4+2] Cycloaddition mit dmb eingegangen sind. Die Struktur von **16** ähnelt den *cone*-Calixarenen[62] mit einem unpolaren Käfig. Dieser wird durch die PNC_4-Ringe gebildet, die unterhalb einer Ebene liegen, welche durch die vier Phosphoratome aufgespannt wird. Die freien Elektronenpaare der Phosphoratome besitzen einen großen s-Charakter (NBO) und liegen alle oberhalb des P_4N_4-Ringes, so dass sie für die Reaktion mit Lewis-Säuren, wie z.B. Metallcarbonyl-Fragmenten, zur Verfügung stehen. Die Isolierung eines $Mo(CO)_3$-Komplexes (**16[Mo]**) von **16** gelang bei der Umsetzung mit $Mo(CO)_6$ in einer Toluol-Lösung bei 95 °C oder bei Raumtemperatur in der Reaktion mit [$Mo(C_2H_5CN)_3(CO)_3$] (Abbildung 7, rechts).

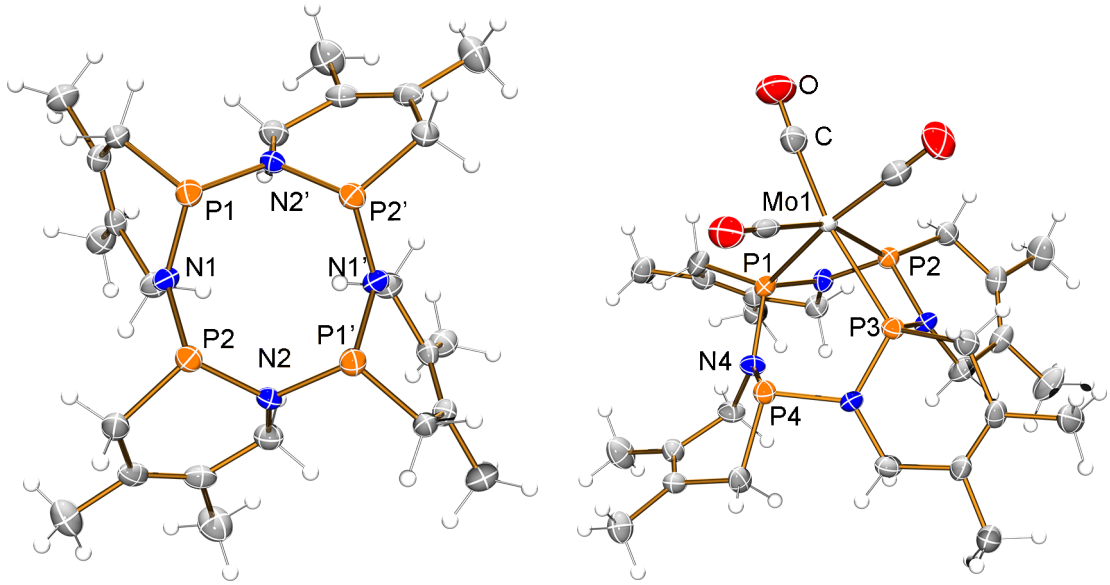

Abbildung 7. ORTEP-Darstellung der Molekülstruktur des *cyclo*-Tetraphoshazan $[PN(dmb)]_4$ (**16**) (links) und des $Mo(CO)_3$ Komplexes **16[Mo]** (rechts). Thermische Ellipsoide entsprechen 50 % Wahrscheinlichkeit bei 173 K.

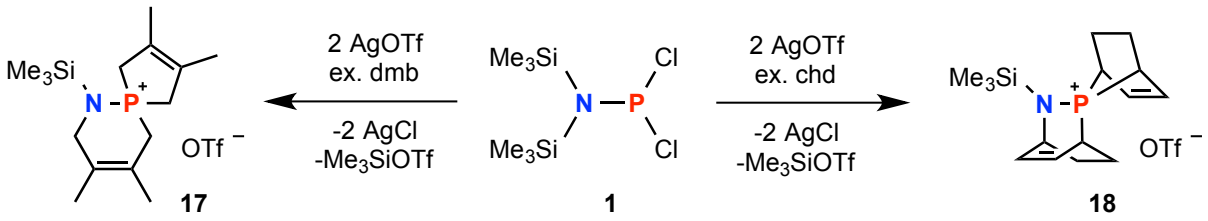

Schema 25. Die Umsetzung von $(Me_3Si)_2NPCl_2$ mit zwei Äquivalenten AgOTf in der Gegenwart von dmb oder chd, führte zur Bildung von Phosphonium-Salzen mit spirocyclischen Kationen.

Im Anschluss sollte untersucht werden, ob es möglich ist, die beiden Chloratome in **1** gegen Trifluormethansulfonat-Gruppen (OTf) auszutauschen und so die thermische Labilität zu erhöhen, da die Eliminierung des Silylesters Me_3SiOTf eine häufig angewandte Methode zur Freisetzung reaktiver Intermediate darstellt. Die Salzeliminierungsreaktion von **1** mit AgOTf in CH_2Cl_2 führte zur Bildung einer unlöslichen Substanz, jedoch konnte die Bildung von Me_3SiOTf beobachtet werden. Die Reaktion wurde daher in der Gegenwart von dmb oder chd wiederholt und nach Abtrennen des gebildeten AgCl konnten zwei Derivate von Phosphonium-Salzen mit einem spirocyclischen Kation $[Me_3SiN(dmb)P(dmb)][OTf]$ (**17**) und $[Me_3SiN(chd)P(chd)][OTf]$ (**18**) isoliert und kristallografisch charakterisiert werden (Schema 25, Abbildung 8). Intermediär wird zunächst durch einfache Me_3SiOTf-Eliminierung ein Iminophosphenium-Kation gebildet, das in einer [4+2]-Cycloaddition zuerst zu einem cyclischen Phosphenium-Kation reagiert, welches dann in einer zweiten chelotropen [4+1]-

Cycloaddition zum spirocyclischen Phosphonium-Kation reagiert. [$Me_3SiN(dmb)P(dmb)$][OTf] ist sehr hydrolyseempfindlich und im Rahmen dieses Projektes ist es gelungen, ein Zersetzungsprodukt zu isolieren. Die cyclische Phosphinsäure [$PO(H)(dmb)_2NH_2$][OTf] konnte als Hydrolyse-Produkt von **17** identifiziert werden. Die dargestellten Phosphonium-Salze konnten durch multinukleare NMR-Spektroskopie, CHN-Analyse und IR-Spektroskopie vollständig charakterisiert werden. Sie sind bis 90 °C thermisch stabil, jedoch extrem feuchtigkeitsempfindlich, können unter einer Schutzgasatmosphäre aber über einen langen Zeitraum gelagert werden.

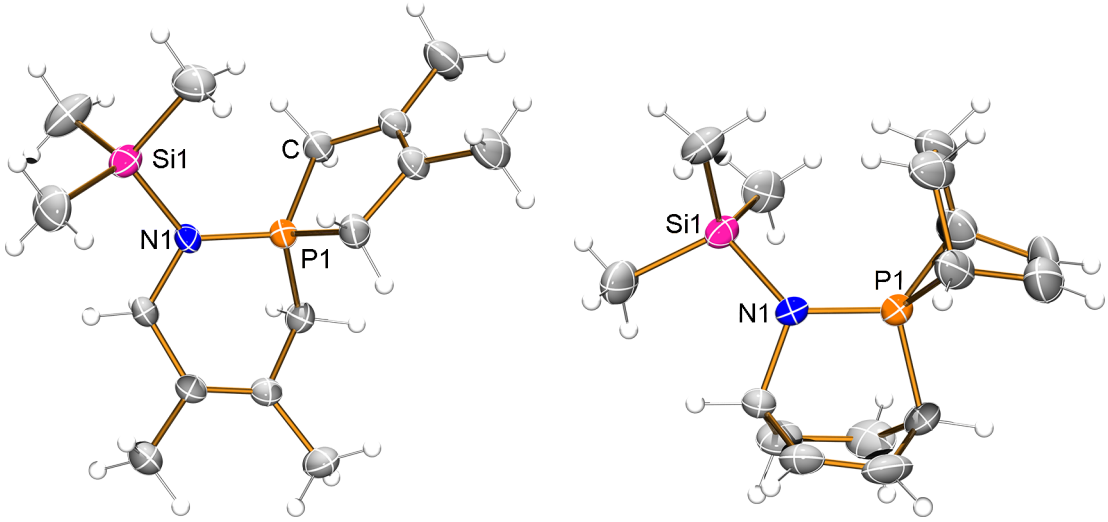

Abbildung 8. Molekülstruktur der spirocyclischen Kationen in den Phosphonium-Salzen [$Me_3SiN(dmb)P(dmb)$][OTf] (**17**) (links) und [$Me_3SiN(chd)P(chd)$][OTf] (**18**) (rechts). Thermische Ellipsoide entsprechen 50 % Wahrscheinlichkeit bei 173 K.

3.5 Untersuchungen zur Reaktivität von Bisaminochlorpniktanen

In vorhergehenden experimentellen Untersuchungen konnte im Arbeitskreis gezeigt werden, dass $(Me_3Si)_2NAsCl_2$ mit $GaCl_3$ unter Bildung von Methylarsanen und cyclischen 1,3-Disila-2,4-diazanen reagiert.[63] $GaCl_3$ vermittelt in dieser Reaktion einen Methyl/Chloraustausch zwischen Silizium und Arsen. Intermediär wird, wie quantenchemische Rechnungen zeigten, ein Aminoarsenium-Kation gebildet, das wiederum in der Lage ist, eine Methylgruppe aus dem Silyl-Rückgrat abzubauen. Es ist jedoch bisher nicht möglich gewesen, dieses Salz mit einem Aminochlorarsenium-Kation zu isolieren. Eine Möglichkeit der thermodynamischen Stabilisierung von reaktiven Pniktenium-Kationen ist die Delokalisation der positiven

Ladung. Dies gelingt durch Einbau des Pniktogen-Atoms in ein delokalisiertes π-System oder durch zwei π-Donatoren, wie z.B. Aminofunktionen, welche an das Pniktenium-Zentrum gebunden sind.[44]

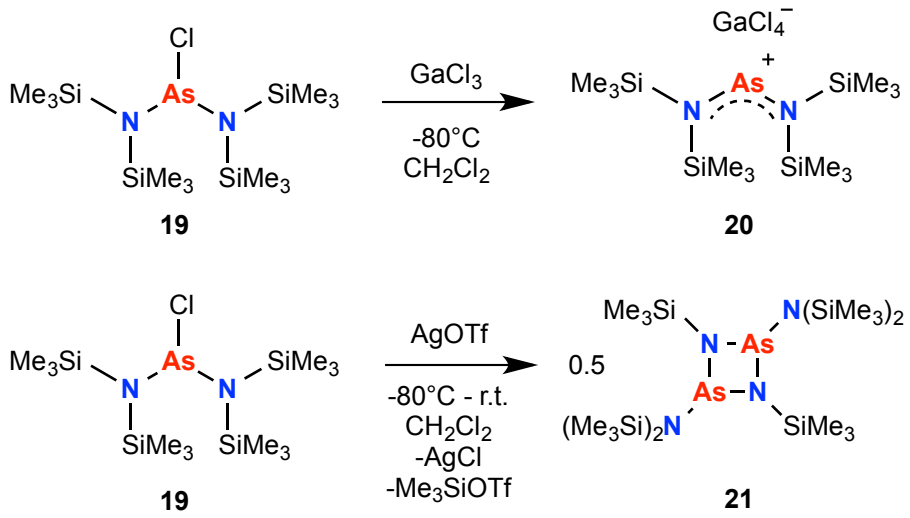

Schema 26. Synthese des Bisaminoarsenium-Salzes **20** und des *cyclo*-1,3-Diarsa-2,4-diazan **21**.

Im Folgenden wurde ausgehend von $[(Me_3Si)_2N]_2AsCl$ (**19**) versucht, acyclische Arsenium-Kationen herzustellen. Das Chlorarsan **19** konnte in moderaten Ausbeuten (< 56%) dargestellt und die Molekülstruktur röntgenografisch bestimmt werden. Anschließend wurde **19** mit einem Äquivalent $GaCl_3$ in CH_2Cl_2 bei −80 °C zur Reaktion gebracht und ein gelber kristalliner Feststoff wurde isoliert, der mit Hilfe von Röntgenkristallstrukturanalyse als das acyclische Arsenium-Salz $[\{(Me_3Si)_2N\}_2As][GaCl_4]$ (**20**) identifiziert werden konnte (Schema 26, oben; Abbildung 9, links). Wird **19** mit zwei Äquivalenten $GaCl_3$ in einer analogen Reaktion umgesetzt, so kann die Bildung des Heptachlorodigallat-Salzes beobachtet werden. In Lösung konnte die Salzbildung mit Hilfe von multinuklearer ^{29}Si-INEPT- und ^{1}H-NMR-Spektroskopie bei tiefen Tieftemperaturen visualisiert werden. Des Weiteren kann die Bildung des Arsenium-Kations sehr gut mit Hilfe der RAMAN-Spektroskopie verfolgt werden. Die asymmetrische Ga−Cl Streckschwingung im Anion weist einen charakteristischen Wert von $\tilde{\nu} = 348$ cm^{-1} auf.

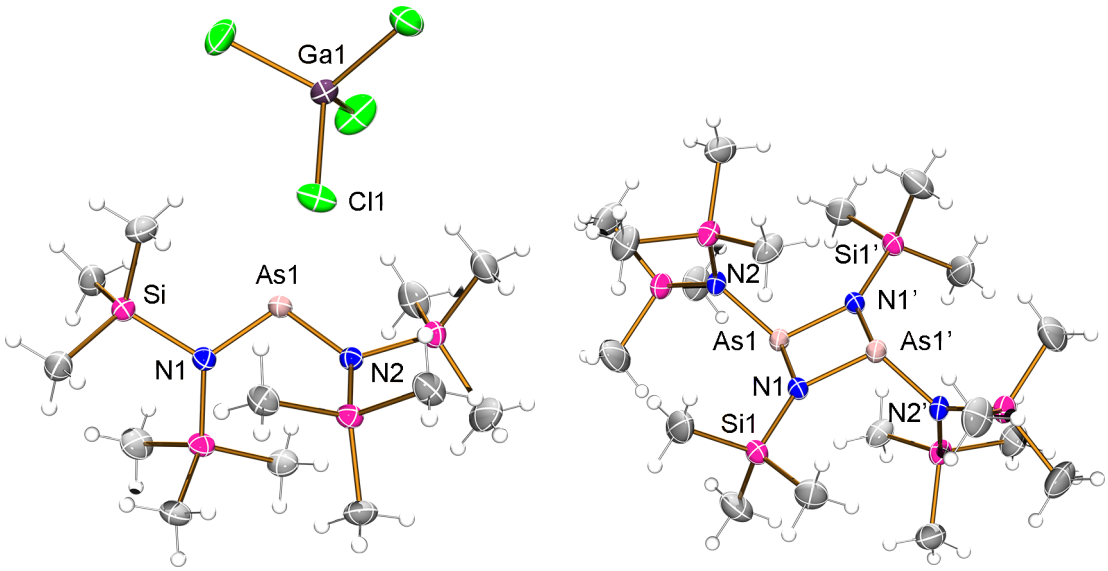

Abbildung 9. ORTEP-Darstellung der Molekülstruktur von $[\{(Me_3Si)_2N\}_2As][GaCl_4]$ (**20**) (links) und $[(Me_3Si)_2NAs(\mu\text{-}NSiMe_3)]_2$ (**21**) (rechts). Thermische Ellipsoide entsprechen 50 % Wahrscheinlichkeit bei 173 K.

Die Generierung eines Triflat-substituierten Arsans gelang nicht, bereits bei tiefen Temperaturen wurde die thermische Eliminierung des Silylesters Me_3SiOTf beobachtet. Das dabei intermediär entstehende Iminoarsan $[(Me_3Si)_2N{=}AsNSiMe_3]$ ist in monomerer Form nicht stabil und dimerisiert zum cyclo-1,3-Diarsa-2,4-diazan $[(Me_3Si)_2NAs(\mu\text{-}NSiMe_3)]_2$ (**21**) (Schema 26, unten; Abbildung 9, rechts), welches kristallografisch charakterisiert wurde. Die hier erarbeitete Synthese stellt eine effektive Möglichkeit der Generierung von **21** in hohen Ausbeuten dar (> 90%).

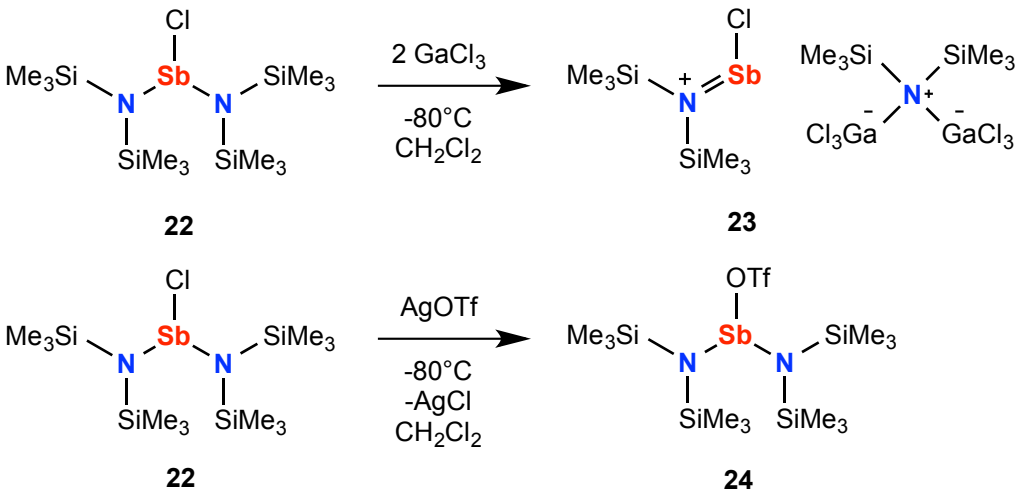

Schema 27. Reaktivität des Bisaminochlorstibans **22** gegenüber $GaCl_3$ und AgOTf.

Im Rahmen dieser Studie sollte des Weiteren die Reaktivität der analogen Antimonverbindung $[(Me_3Si)_2N]_2SbCl$ (**22**) näher untersucht werden. Die Reaktion mit einem Äquivalent $GaCl_3$ bei −80 °C resultierte nicht in der Bildung des zu **20** analogen Stibenium-Kations. Aus einer konzentrierten Reaktionslösung konnten Kristalle für die Röntgenkristallstrukturanalyse erhalten werden und das Produkt dieser Reaktion als das Aminochlorstibenium-Salz $[(Me_3Si)_2NSbCl][(Me_3Si)_2N(GaCl_3)_2]$ (**23**) mit einem komplexen Amid-Anion identifiziert werden (Schema 27, oben; Abbildung 10, links). Dieses Salz ist nur bei tiefen Temperaturen stabil und zersetzt sich beim Auftauen in einer Methyl/Chloraustauschreaktion. Auf die Produkte dieser Austauschreaktion wird in Kapitel 3.5 näher eingegangen. Die Reaktion mit zwei Äquivalenten $GaCl_3$ führte zur stöchiometrischen Bildung von **23**, so dass die Bildung von **23** als eine $GaCl_3$-assistierte Amid-Abstraktion zu verstehen ist.

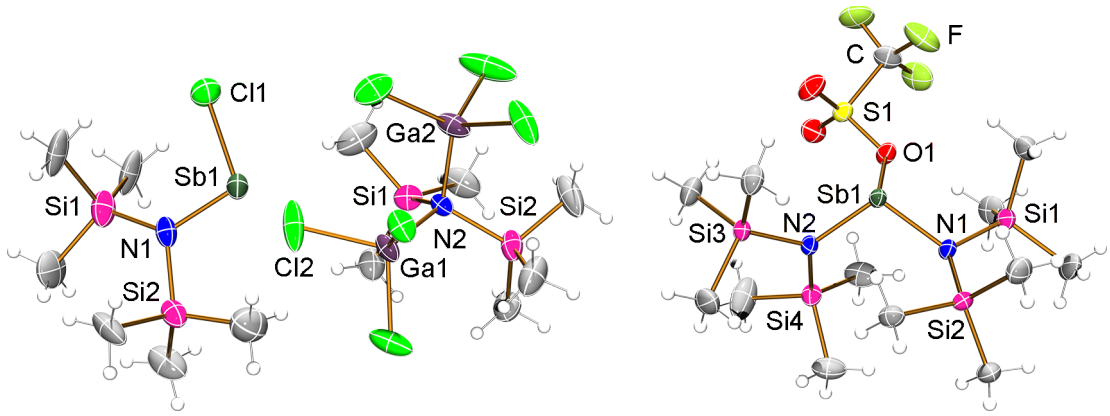

Abbildung 10. ORTEP-Darstellung der Molekülstruktur von $[(Me_3Si)_2NSbCl][(Me_3Si)_2N(GaCl_3)_2]$ (**23**) (links) und $[(Me_3Si)_2N]_2SbOTf$ (**24**) (rechts). Thermische Ellipsoide entsprechen 50 % Wahrscheinlichkeit bei 173 K.

Wurde **22** bei −60°C mit AgOTf umgesetzt, so konnte nach Abtrennen des AgCl und Extraktion des Rückstandes mit *n*-Hexan $[(Me_3Si)_2N]_2SbOTf$ (**24**) als farbloser kristalliner Feststoff in sehr guten Ausbeuten (> 75%) isoliert werden (Schema 27, unten; Abbildung 10, rechts). **24** schmilzt bei 68°C ohne Zersetzung und setzt auch bei 100 °C in einer Toluol-Lösung kein Me_3SiOTf frei. In früheren Arbeiten konnte unsere Arbeitsgruppe zeigen, dass Sb−OTf Bindungen einfach durch die Zugabe von Trimethylsilanen $Me_3Si{-}X$ (X = Br, I, N_3) gespalten werden können,[64] so dass $[(Me_3Si)_2N]_2SbOTf$ eine ideale Vorstufe für weitere Funktionalisierungen am Antimon darstellen könnte.

3.6 Methyl/Chloraustauschreaktionen in silylierten Aminodichlorstibanen

Die $GaCl_3$-assistierte [3+2]-Cycloaddition stellt einen einfachen Zugang zu binären Azapniktolen dar, wobei die benötigten Dipolarophile zuerst *in situ* ausgehend von „versteckten Dipolarophilen“ generiert werden. Diese Syntheseroute liefert für silylierte Aminopniktane des Typs $Mes^*N(SiMe_3)PnCl_2$ (Pn = P, As) in der Gegenwart von Me_3SiN_3 die gewünschten $GaCl_3$-Addukte eines Tetrazapniktols. Im Fall von $TerN(SiMe_3)NAsCl_2$ wurde die Freisetzung des Dipolarophils und eine anschließende Cyclisierung in Gegenwart von Me_3SiN_3 nicht beobachtet. Vielmehr konnten die Produkte eines ungewöhnlichen Methyl/Chloraustausches zwischen Arsen und der Silylgruppe isoliert werden.[63] Im Rahmen dieser Arbeit sollte die Reaktivität der analogen silylierten Aminodichlorstibane des Typs $RN(SiMe_3)SbCl_2$ (R = $SiMe_3$, Mes*, Ter) gegenüber $GaCl_3$ und Me_3SiN_3 näher untersucht werden.

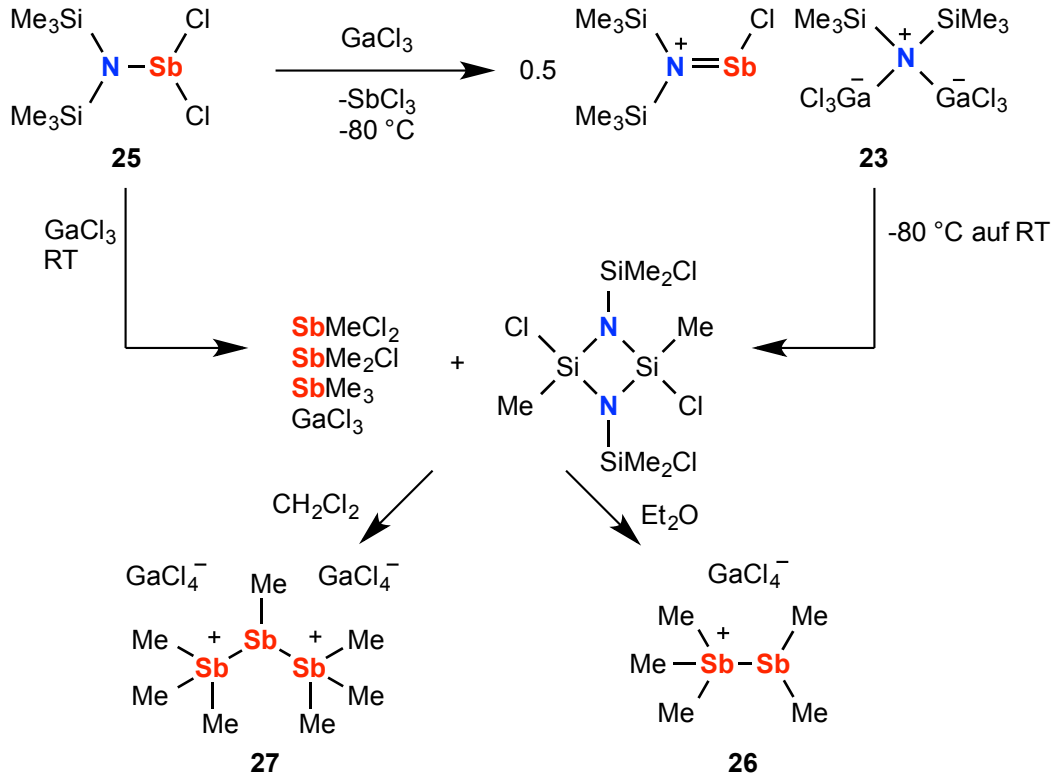

Schema 28. Untersuchungen der Reaktivität von $(Me_3Si)_2NSbCl_2$ gegenüber der Lewis-Säure $GaCl_3$.

Das einfachste silylierte Aminodichlorstiban, $(Me_3Si)_2NSbCl_2$ (**25**), konnte in einer modifizierten Synthese in moderaten Ausbeuten (> 50%) dargestellt und die Molekülstruktur

erstmals röntgenografisch bestimmt werden. Die Reaktion mit einem Äquivalent $GaCl_3$ führte bei −80 °C zur Bildung des Aminochlorstibenium-Salzes $[(Me_3Si)_2NSbCl][(Me_3Si)_2N(GaCl_3)_2]$ (**23**), welches beim Auftauen auf Raumtemperatur unter Bildung eines *cyclo*-Disilazans reagiert. Diese Reaktivität ist mit der des analogen Arsen-Systems vergleichbar,[63] nur dass es im Rahmen dieser Arbeit erstmals gelang, das intermediär gebildete Stibenium-Salz zu kristallisieren. Der in Vorarbeiten im Arbeitskreis Schulz vorgeschlagene Reaktionsmechanismus für den Methyl/Chloraustausch zwischen Arsen und Silizium konnte somit experimentell bewiesen werden. Ebenso werden verschiedene Methylchlorstibane $SbMe_xCl_{3-x}$ (x = 0 – 3) gebildet, welche in der Gegenwart von $GaCl_3$ zu den neuartigen Stibino-Stibonium-Salzen $[Me_3SbSbMe_2][GaCl_4]$ (**26**) und dem Stibino-Distibonium-Salz $[(Me_3Sb)_2SbMe][GaCl_4]_2$ (**27**) reagieren (Schema 28; Abbildung 11). Es ist ebenso möglich, diese Salze als Interpniktogen-Koordinationsverbindung aufzufassen, in denen $SbMe_3$ als Lewis-Base fungiert und an die *in situ* gebildeten Stibenium-Spezies $[SbMe_2]^+$ und $[SbMe]^{2+}$ koordiniert. Die Gegenwart von $SbMe_3$ in dieser Reaktionsmischung konnte durch die Isolierung und strukturelle Charakterisierung eines $GaCl_3$-Addukt von $SbMe_3$ belegt werden.

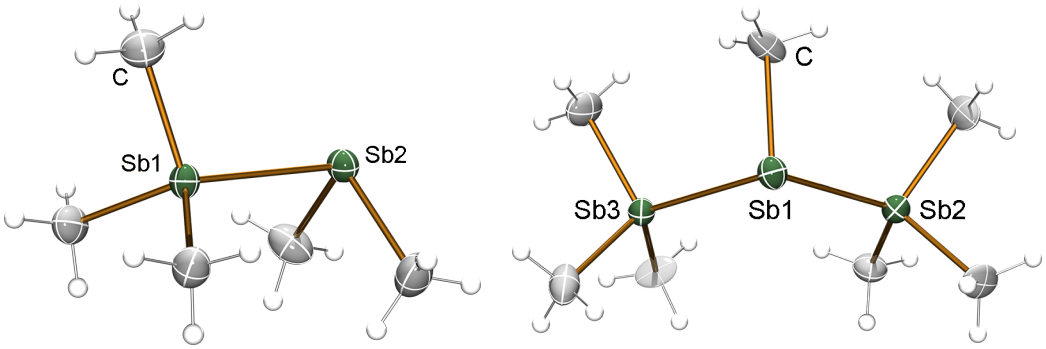

Abbildung 11. ORTEP-Darstellung der Molekülstruktur der Kationen in den Stibino-Stibonium Salzen **26** (links) und **27** (rechts). Thermische Ellipsoide entsprechen 50 % Wahrscheinlichkeit bei 173 K.

Außerdem wurden verschiedene Versuche mit *N*-Trimethylsilyl-*N*-(*m*-terphenyl)aminodichlorstiban $TerN(SiMe_3)SbCl_2$ (**28**) durchgeführt, welches in guten Ausbeuten (> 75 %) ausgehend von $TerN(SiMe_3)H$ erstmals synthetisiert werden konnte.

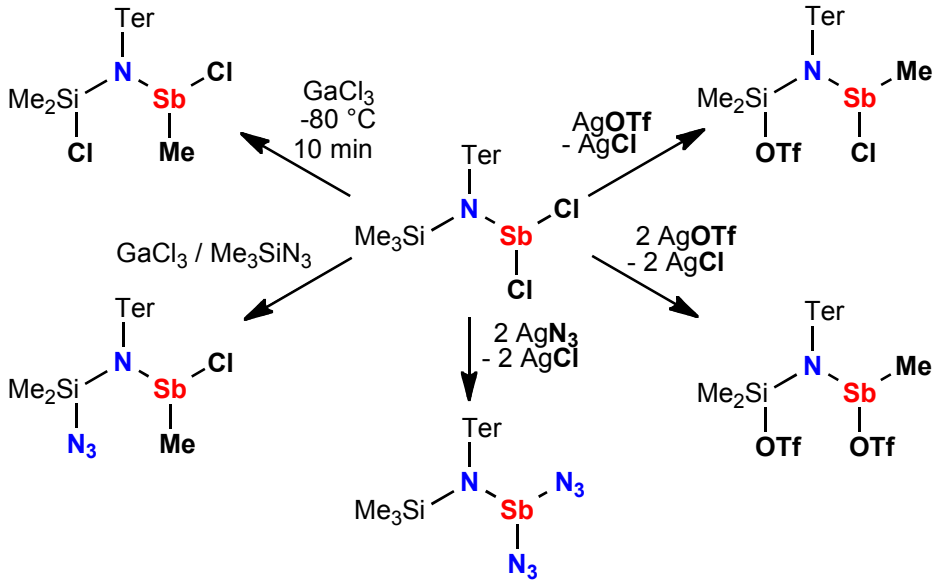

Schema 29. Verschiedene Methyl-Austauschreaktionen ausgehend von TerN(SiMe$_3$)SbCl$_2$ (**28**) in der Reaktion mit GaCl$_3$, GaCl$_3$/Me$_3$SiN$_3$, AgOTf und AgN$_3$.

Die Umsetzung mit einem Äquivalent GaCl$_3$ verlief unter partiellem Methyl/Chloraustausch zum Methyl(chlor)stiban, TerN(SiMe$_2$Cl)NSb(Cl)Me (**29**), in einer analogen Reaktion wurde in der Gegenwart von Me$_3$SiN$_3$ ein Methyl/Azidaustausch beobachtet, der zur Bildung von TerN(SiMe$_2$N$_3$)NSb(Cl)Me (**30**) führt (Schema 29, Abbildung 12).

In Analogie zum System Mes*N(SiMe$_3$)SbCl$_2$ sollte des Weiteren untersucht werden, ob die Substitution beider Chloratome im TerN(SiMe$_3$)SbCl$_2$ gegen eine Triflat-Funktion durch die Umsetzung mit zwei Äquivalenten AgOTf realisiert werden kann. Hierbei konnte TerN(SiMe$_2$OTf)Sb(Me)Cl (**31**) als Produkt eines einfachen Methyl/Triflataustausches bei der Reaktion mit einem Äquivalent AgOTf isoliert werden (Schema 29, Abbildung 12). Diese Verbindung wurde ebenfalls erhalten, wenn TerN(SiMe$_3$)H zunächst bei −80 °C mit *n*BuLi versetzt und anschließend mit Sb(OTf)$_3$ umgesetzt wurde. Ebenso konnte dieser einfache Methyl/Triflataustausch bei der Umsetzung von TerN(SiMe$_3$)Sb(OtBu)$_2$ mit zwei Äquivalenten Me$_3$SiOTf beobachtet werden. Durch Zugabe eines weiteren Äquivalentes an AgOTf wurde das verbliebene Chloratom am Antimon gegen eine OTf-Gruppe substituiert und TerN(SiMe$_2$OTf)Sb(Me)OTf (**32**) erhalten (Schema 29). Im Gegensatz dazu vermittelt AgN$_3$ keinen Methyl/Azidaustausch und bei der Umsetzung mit einem oder zwei Äquivalenten AgN$_3$ wurde das Diazidostiban TerN(SiMe$_3$)Sb(N$_3$)$_2$ als Produkt erhalten. Die Austauschreaktionen verlaufen in moderaten bis sehr guten Ausbeuten. Alle synthetisierten Verbindungen konnten vollständig charakterisiert werden.

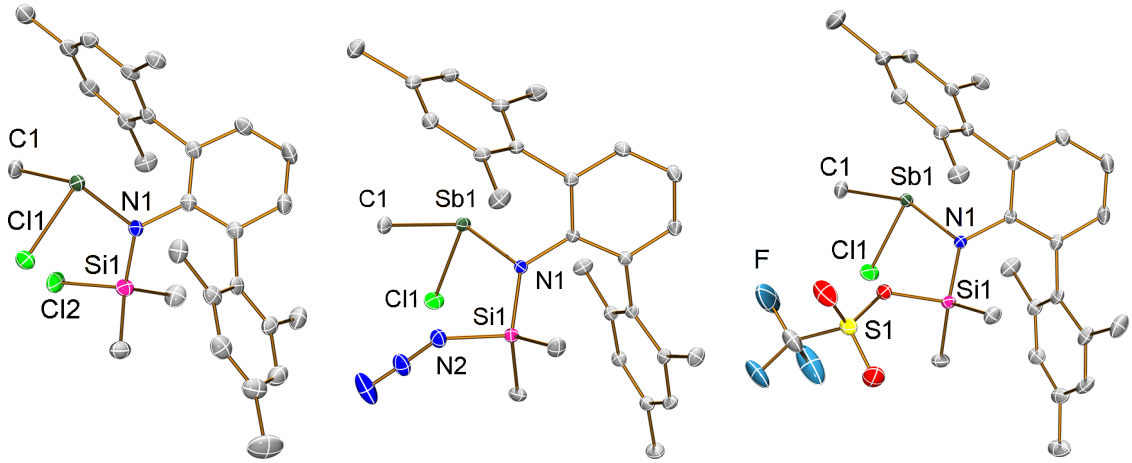

Abbildung 12. ORTEP-Darstellung der Molekülstruktur der Methyl-Austauschprodukte **29** (links), **30** (mitte) und **31** (rechts). Thermische Ellipsoide entsprechen 30 % Wahrscheinlichkeit bei 173 K, Wasserstoffatome sind nicht dargestellt.

Die durchgeführten Reaktionen zeigen deutlich, dass Methylaustauschreaktionen ein genereller Reaktionstyp der schweren Pniktogene Arsen und Antimon darstellen. Es konnte erstmals gezeigt werden, dass ein Aminochlorstibenium-Salz im ersten Reaktionsschritt gebildet wird, welches dann in einer Methyl/Chloraustauschreaktion weiter zu verschiedenen Methylchlorstibanen reagiert, die in Gegenwart von $GaCl_3$ weiter zu Stibino-Stibonium-Kationen reagieren. Darüber hinaus wurde gezeigt, dass $TerN(SiMe_3)SbCl_2$ kein geeignetes „verstecktes Dipolarophil“ für die $GaCl_3$-assistierte Me_3SiCl-Eliminierung darstellt, sondern dieses in definierten Methylaustauschreaktionen reagiert.

4 Literaturverzeichnis

[1] A. Michaelis, G. Schroeter, *Eur. J. Inorg. Chem.* **1894**, *27*, 490–497.

[2] H. J. Chen, R. C. Haltiwanger, T. G. Hill, M. L. Thompson, D. E. Coons, A. D. Norman, *Inorg. Chem.* **1985**, *24*, 4725–4730.

[3] E. Niecke, W. Flick, *Angew. Chem.* **1973**, *85*, 586–587; *Angew. Chem. Int. Ed. Engl.* **1973**, *12*, 585–586.

[4] E. Niecke, W. Flick, S. Pohl, *Angew. Chem.* **1976**, *88*, 305–306; *Angew. Chem. Int. Ed. Engl.* **1976**, *15*, 309–310.

[5] E. Niecke, D. Gudat, *Angew. Chem.* **1991**, *103*, 251–270; *Angew. Chem. Int. Ed. Engl.* **1991**, *30*, 217–237.

[6] F. Zurmühlen, M. Regitz, *Angew. Chem.* **1987**, *99*, 65–67; *Angew. Chem. Int. Ed. Engl.* **1987**, *26*, 83–84.

[7] E. Niecke, M. Nieger, C. Gärtner Winkhaus, B. Kramer, *Eur. J. Inorg. Chem.* **1990**, *123*, 477–479.

[8] J. Boeske, E. Niecke, M. Nieger, E. Ocando, J. P. Majoral, G. Bertrand, *Inorg. Chem.* **1989**, *28*, 499–504.

[9] E. Niecke, R. Rüger, W. W. Schoeller, *Angew. Chem.* **1981**, *93*, 1110–1112; *Angew. Chem. Int. Ed. Engl.* **1981**, *20*, 1034–1036.

[10] O. J. Scherer, W. Gläβel, *Chem. Ber.* **1977**, *110*, 3874–3888.

[11] D. Gudat, E. Niecke, B. Krebs, M. Dartmann, *Organometallics* **1986**, *5*, 2376–2377.

[12] M. Lehmann, A. Schulz, A. Villinger, *Struct. Chem.* **2010**, *22*, 35–43.

[13] E. Niecke, M. Nieger, F. Reichert, *Angew. Chem.* **1988**, *100*, 1781–1782; *Angew. Chem. Int. Ed. Engl.* **1988**, *27*, 1715–1716.

[14] G. Märkl, H. Sejpka, *Tetrahedron Lett.* **1986**, *27*, 171–174.

[15] A. Villinger, P. Mayer, A. Schulz, *Chem. Commun.* **2006**, 1236.

[16] D. Michalik, A. Schulz, A. Villinger, N. Weding, *Angew. Chem.* **2008**, *120*, 6565–6568; *Angew. Chem. Int. Ed.* **2008**, *47*, 6465–6468.

[17] S. Herler, P. Mayer, J. Schmedt auf der Günne, A. Schulz, A. Villinger, J. J. Weigand, *Angew. Chem.* **2005**, *117*, 7968–7971; *Angew. Chem. Int. Ed. Engl.* **2005**, *44*, 7790–7793.

[18] P. Mayer, A. Schulz, A. Villinger, *J. Organomet. Chem.* **2007**, *692*, 2839–2842.

[19] M. Kuprat, A. Schulz, A. Villinger, *Angew. Chem.* **2013**, *125*, 7266–7270; *Angew. Chem. Int. Ed.* **2013**, *52*, 7126–7130.

[20] A. Schulz, A. Villinger, *Angew. Chem.* **2008**, *120*, 614–617; *Angew. Chem. Int. Ed. Engl.* **2008**, *47*, 603–606.

[21] M. Lehmann, A. Schulz, A. Villinger, *Angew. Chem.* **2011**, *123*, 5327–5331; *Angew. Chem. Int. Ed.* **2011**, *50*, 5221–5224.

[22] R. Hoffman, *Angew. Chem. Int. Ed. Engl.* **1982**, *21*, 711−723.

[23] A. H. Cowley, R. A. Kemp, *Chem. Rev.* **1985**, *85*, 367–382.

[24] A. Schmidpeter, *Multiple Bonds and Low Coordination Chemistry. In Phosphorus Chemistry*; M. Regitz, O. Scherer, Eds.; Georg Thieme Verlag: Stuttgart, Germany **1990**, *D2*, 149.

[25] K. Dimroth, P. Hoffmann, *Angew. Chem.* **1964**, *76*, 433; *Angew. Chem. Int. Ed. Engl.* **1964**, *3*, 384.

[26] E. Niecke, R. Kröher, *Angew. Chem.* **1976**, *88*, 758–759; *Angew. Chem. Int. Ed. Engl.* **1976**, *15*, 692−693.

[27] N. Burford, T. S. Cameron, J. A. Clyburne, K. Eichele, K. N. Robertson, S. Sereda, R. E. Wasylishen, W. A. Whitla, *Inorg. Chem.* **1996**, *35*, 5460–5467.

[28] F. Reiß, A. Schulz, A. Villinger, *Eur. J. Inorg. Chem.* **2012**, *2*, 261–271.

[29] D. Gudat, *Coord. Chem. Rev.* **1997**, *163*, 71–106.

[30] D. Gudat, *Acc. Chem. Res.* **2010**, *43*, 1307–1316.

[31] L. Rosenberg, *Coord. Chem. Rev.* **2012**, *256*, 606–626.

[32] C. W. Schultz, R. W. Parry, *Inorg. Chem.* **1976**, *15*, 3046–3050.

[33] R. W. Kopp, A. C. Bond, R. W. Parry, *Inorg. Chem.* **1976**, *15*, 3042–3046.

[34] M. G. Thomas, C. W. Schultz, R. W. Parry, *Inorg. Chem.* **1977**, *16*, 994–1001.

[35] M.-R. Marre, M. Sanchez, R. Wolf, *J. Chem. Soc., Chem. Commun.* **1984**, 566–567.

[36] N. Burford, P. Losier, C. Macdonald, V. Kyrimis, P. K. Bakshi, T. S. Cameron, *Inorg. Chem.* **1994**, *33*, 1434–1439.

[37] R. W. Reed, Z. Xie, C. A. Reed, *Organometallics* **1995**, *14*, 5002–5004.

[38] A. Dumitrescu, H. Gornitzka, W. W. Schoeller, D. Bourissou, G. Bertrand, *Eur. J. Inorg. Chem.* **2002**, *8*, 1953–1956.

[39] A. Schulz, A. Villinger, *Inorg. Chem.* **2009**, *48*, 7359–7367.

[40] M. Lehmann, A. Schulz, A. Villinger, *Angew. Chem.* **2012**, *124*, 8211–8215; *Angew. Chem. Int. Ed.* **2012**, *51*, 8087–8091.

[41] D. Bourissou, O. Guerret, F. P. Gabbaï, G. Bertrand, *Chem. Rev.* **2000**, *100*, 39–92.

[42] C. K. SooHoo, S. G. Baxter, *J. Am. Chem. Soc.* **1983**, *105*, 7443–7444.

[43] A. H. Cowley, R. A. Kemp, J. G. Lasch, N. C. Norman, C. A. Stewart, *J. Am. Chem.*

Soc. **1983**, *105*, 7444–7445.

[44] N. Burford, B. W. Royan, P. S. White, *J. Am. Chem. Soc.* **1989**, *111*, 3746–3747.

[45] N. Burford, T. M. Parks, B. W. Royan, B. Borecka, T. S. Cameron, J. F. Richardson, E. J. Gabe, R. Hynes, *J. Am. Chem. Soc.* **1992**, *114*, 8147–8153.

[46] E. Conrad, N. Burford, R. McDonald, M. J. Ferguson, *J. Am. Chem. Soc.* **2009**, *131*, 17000–17008.

[47] C. Payrastre, Y. Madaule, J.-G. Wolf, *Tetrahedron Lett.* **1992**, *33*, 1273–1276.

[48] N. L. Kilah, S. B. Wild, *Organometallics* **2012**, *31*, 2658–2666.

[49] N. L. Kilah, S. Petrie, R. Stranger, J. W. Wielandt, A. C. Willis, S. B. Wild, *Organometallics* **2007**, *26*, 6106–6113.

[50] E. Conrad, N. Burford, R. McDonald, M. J. Ferguson, *J. Am. Chem. Soc.* **2009**, *131*, 5066–5067.

[51] H. Althaus, H. J. Breunig, E. Lork, *Chem. Commun.* **1999**, 1971–1972.

[52] P. Jutzi, T. Wippermann, C. Krüger, H. J. Kraus, *Angew. Chem.* **1983**, *95*, 244; *Angew. Chem. Int. Ed. Engl.* **1983**, *22*, 250.

[53] M. H. Holthausen, J. J. Weigand, *Z. Anorg. Allg. Chem.* **2012**, *638*, 1103–1108.

[54] P. Pyykkö, M. Atsumi, *Chem. Eur. J.* **2009**, *15*, 12770–12779.

[55] a) M. Mantina, A. C. Chamberlin, R. Valero, C. J. Cramer, D. G. Truhlar, *J. Phys. Chem. A* **2009**, *113*, 5806–5812; b) S. Alvarez, *Dalton Trans.* **2013**, *42*, 8617−8636.

[56] a) F. London, *J. Phys. Radium* **1937**, *8*, 397–409; b) R. McWeeny, *Phys. Rev.* **1962**, *126*, 1028; c) R. Ditchfield, *Mol. Phys.* **1974**, *27*, 789–807, d) K. Wolinski, J. F. Hilton, P. Pulay, *J. Am. Chem. Soc.* **1990**, *112*, 8251–8260; e) J. R. Cheeseman, G. W. Trucks, T. A. Keith, M. J. Frisch, *J. Chem. Phys.* **1996**, *104*, 5497–5509.

[57] M. H. Holthausen, K.-O. Feldmann, S. Schulz, A. Hepp, J. J. Weigand, *Inorg. Chem.* **2012**, *51*, 3374–3387.

[58] H. Staudinger, J. Meyer, *Helv. Chim. Acta* **1919**, *2*, 612–618.

[59] O. Guerret, G. Bertrand, *Acc. Chem. Res.* **1997**, *30*, 486–493.

[60] A. Westenkirchner, A. Villinger, K. Karaghiosoff, R. Wustrack, D. Michalik, A. Schulz, *Inorg. Chem.* **2011**, *50*, 2691–2702.

[61] R. Restivo, G. J. Palenik, *J. Chem. Soc., Dalton Trans.* **1972**, 341–344.

[62] C. Wieser, C. B. Dieleman, D. Matt, *Coord. Chem. Rev.* **1997**, *165*, 93–161.

[63] D. Michalik, A. Schulz, A. Villinger, *Inorg. Chem.* **2008**, *47*, 11798–11806.

[64] M. Lehmann, A. Schulz, A. Villinger, *Eur. J. Inorg. Chem.* **2012**, *5*, 822–832.

5 Ausgewählte Originalpublikationen

Dieses Kapitel beinhaltet die Original-Publikationen zu den im Kapitel 3 vorgestellten Arbeiten. Der eigene Beitrag zu der betreffenden Publikation ist jeweils gesondert hervorgehoben.

Die im Kapitel 5.1. gezeigte Publikation wurde von mir selbstständig verfasst, ein Großteil der Experimente und Rechnungen wurden von mir durchgeführt. Im Rahmen seiner Bachelorarbeit, die von mir betreut wurde, arbeitete B. Sc. Maximilian Hertrich an diesem Projekt mit.

Die im Kapitel 5.2 und 5.3 gezeigten Publikationen wurden von mir selbstständig verfasst, alle Experimente und Rechnungen wurden von mir durchgeführt.

Die im Kapitel 5.4 gezeigte Publikation wurde von mir selbstständig verfasst, alle Experimente und Rechnungen wurden von mir durchgeführt. Im Rahmen ihres Forschungspraktikums, das von mir betreut wurde, arbeitete B. Sc. Julia Rothe an diesem Projekt mit.

Die im Kapitel 5.5 gezeigte Publikation wurde von mir selbstständig verfasst. Sie basiert auf experimentellen Arbeiten, die teilweise schon während der Diplomphase unter der Betreuung von Dr. Mathias Lehmann von mir durchgeführt wurden. Ich verweise darauf, dass ausgewählte Verbindungen sowohl in meiner Diplomarbeit als auch in der Dissertation von Dr. Mathias Lehmann diskutiert wurden. Die Arbeiten wurden während der Promotion von mir fortgeführt, analytische Daten vervollständigt und durch die umfassenden Untersuchungen zur Reaktivität von $(Me_3Si)_2NSbCl_2$ ergänzt.

Die im Anhang (Kapitel 6.1) gezeigte Publikation wurde von mir verfasst. Ein Teil der Rechnungen wurde von Prof. Dr. Axel Schulz durchgeführt. Sie fußt auf Experimenten, die zum größten Teil während der Diplomphase durchgeführt wurden und deren Ergebnisse bereits in meiner Diplomarbeit diskutiert wurden. Zu Beginn der Promotion wurden jedoch noch essentielle analytische Daten gesammelt, welche zur Veröffentlichung der Ergebnisse nötig waren.

5.1 Azidophosphenium Cations: Versatile Reagents in Inorganic Synthesis

Christian Hering, Maximilian Hertrich, Axel Schulz, Alexander Villinger.

Inorganic Chemistry, **2014**, *53*, 3880−3892.

DOI: 10.1021/ic500332s

In dieser Publikation wurde ein Großteil der experimentellen Arbeiten von mir durchgeführt. Der eigene Beitrag liegt bei ca. 80 %.

Inorganic Chemistry

Article

pubs.acs.org/IC

Azidophosphenium Cations: Versatile Reagents in Inorganic Synthesis

Christian Hering,[†] Maximilian Hertrich,[†] Axel Schulz,*[,†,‡] and Alexander Villinger[†]

[†]Institut für Chemie, Abteilung Anorganische Chemie, Universität Rostock, Albert-Einstein-Strasse 3a, 18059 Rostock, Germany

[‡]Leibniz-Institut für Katalyse eV, Universität Rostock, Albert-Einstein-Strasse 29a, 18059 Rostock, Germany

Supporting Information

ABSTRACT: This work describes the synthesis and characterization of a series of iminophosphorane-substituted phosphenium cations of the type $[R_2NPNP(Cl)_2NPNR'_2][GaCl_4]$ [R = *i*Pr; R′ = *i*Pr (**7**[**GaCl$_4$**]), $SiMe_3$ (**8**)], which are directly derived from azidophosphenium salt $[iPrNPN_3][GaCl_4]$ (**2*i*Pr**[**GaCl$_4$**]) and the corresponding chlorophosphane R_2NPCl_2. The reactivity of **7**[**GaCl$_4$**] toward 2,3-dimethylbutadiene (dmb) and 2,2′-bipyridine (bipy) was investigated, resulting in the formation of **7-dmb**[**GaCl$_4$**] and **7-Cl**. In addition, self-condensation of $[(Me_3Si)_2NPN_3][GaCl_4]$ (**2SiMe$_3$**[**GaCl$_4$**]) was studied in detail, and $[(Me_3Si)_2NPNP(XY)N(SiMe_3)_2][GaCl_4]$ [X = Cl; Y = Cl (**13**), N_3 (**14**)] were determined as products on the basis of ^{31}P NMR spectroscopy. The reaction of **2SiMe$_3$**[**GaCl$_4$**] with $[(Me_3Si)_2NPCl][GaCl_4]$ (**1SiMe$_3$**[**GaCl$_4$**]) yielded an unprecedented bicyclic 1,3,2λ^3,4λ^5-diazadiphosphetidine (**15**), which was formed via a $GaCl_3$-assisted Me_3SiCl elimination starting from **13**. Furthermore, cations of the type $[R_2NPNPR'_3][GaCl_4]$ [R = *i*Pr; R′ = *c*Hex (**19**)] were obtained by the effective combination of **2R**[**GaCl$_4$**] (R = *i*Pr, $SiMe_3$) with PR'_3 (R′ = Ph, *c*Hex). Azidochlorophosphanes $R_2NP(N_3)Cl$ [R = *i*Pr, $SiMe_3$ (**20R**)] are shown to be accessible when **2R**[**GaCl$_4$**] was combined with bipy. All new compounds were fully characterized by means of X-ray, vibrational spectroscopy, CHN analysis, and NMR experiments. All compounds were further investigated by means of density functional theory, and the bonding situation was accessed by natural bond orbital analysis.

INTRODUCTION

Dimroth and Hoffmann reported on the synthesis of the first low-valent dicoordinated phosphorus compounds in phosphamethine cyanines in 1964.[1] The term "phosphenium cation" indicates a positively charged divalent phosphorus atom, which formally possesses an empty p orbital and a lone pair (LP) of electrons and thus can be considered as a main-group carbenoid, in which the central carbon atom is replaced by an isovalent P^+. These highly reactive species $[R^1{-}P{-}R^2]^+$ are stabilized best when R^1 and R^2 are π-electron-donating groups, such as amino functions NR_2 (R = Me, *i*Pr). The first examples of acyclic aminophosphenium salts of the type $[(R_2N)_2P][AlCl_4]$ and $[R_2NPCl][AlCl_4]$ [R = Me, Et, *i*Pr (**1R**[**AlCl$_4$**])] were prepared by Parry et al. by the effective combination of chlorophosphane and halogen-abstracting reagent ECl_3 (E = Al, Ga, Fe) in CH_2Cl_2 (Scheme 1).[2] Since then, the reactivity and coordination properties of these species have been studied in detail and reviewed regularly.[3−5] Nevertheless, the molecular structure of chlorophosphenium cations of the type $[R_2NPCl]^+$ remained unknown until recently [R = $SiMe_3$ (**1SiMe$_3$**$^+$),[6] *c*Hex[7]].

In 1984, Wolf et al. reported for the first time that $[R_2NPCl]^+$ [R = Me, *i*Pr (**1*i*Pr**$^+$)] can be further functionalized on the phosphenium center by treatment with pseudohalogensilanes such as Me_3SiN_3, whereupon Me_3SiCl is liberated (Scheme 2).[8]

In the absence of X-ray crystal structures, the intermediate formation of azidophosphenium cation $[R_2NPN_3]^+$ [R = Me, *i*Pr (**2*i*Pr**$^+$)] was established by ^{31}P NMR spectroscopy.[9]

Scheme 1. Synthesis of Bis(aminophosphenium) Salts by the Combination of Chlorophosphane (R = Me, Et, *i*Pr) and ECl_3 (E = Al, Ga, Fe) as a Halogen-Abstracting Reagent

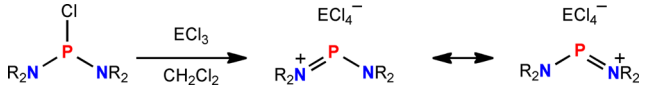

Scheme 2. Synthesis of Azidophosphenium Salts Starting from Chlorophosphenium Salts in the Reaction with Me_3SiN_3 at −50 °C, Whereupon Me_3SiCl Is Released [E = Al (R = Me, *i*Pr), Ga (R = $SiMe_3$)]

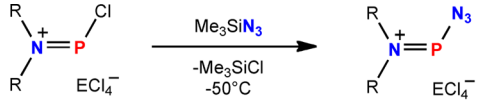

R = Me, *i*Pr (**1*i*Pr**$^+$), $SiMe_3$ (**1SiMe$_3$**$^+$) R = Me, *i*Pr (**2*i*Pr**$^+$), $SiMe_3$ (**2SiMe$_3$**$^+$)

E = Al, Ga

Received: February 11, 2014
Published: March 21, 2014

   dx.doi.org/10.1021/ic500332s | *Inorg. Chem.* 2014, 53, 3880−3892

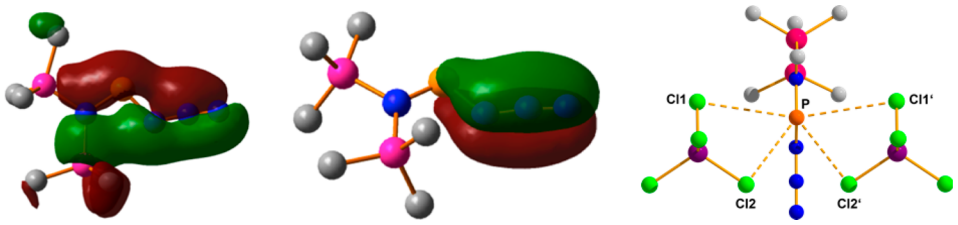

Figure 1. Depiction of selected Kohn–Sham orbitals calculated for the azidophosphenium cation $\mathbf{2SiMe_3}^+$ (left, middle). Ball-and-stick drawing of the anion···cation interactions in the azidophosphenium salt $\mathbf{2SiMe_3[GaCl_4]}$ (right). Four close contacts are observed (distances in angstroms): P1–Cl1 3.1582(6), P1–Cl3 3.7630(7), P1–Cl3′ 3.273(7), P1–Cl4′ 4.0212(9).

Scheme 3. (i) Formation of the Phosphenium–Phosphonium Dication 3^{2+} as a $AlCl_4^-$ Salt According to Early Studies by Wolf et al.[6,7,16] and (ii) Preparation of the First Isolable Iminophosphorane Cation $[4Me][CF_3SO_3]$[14,15]

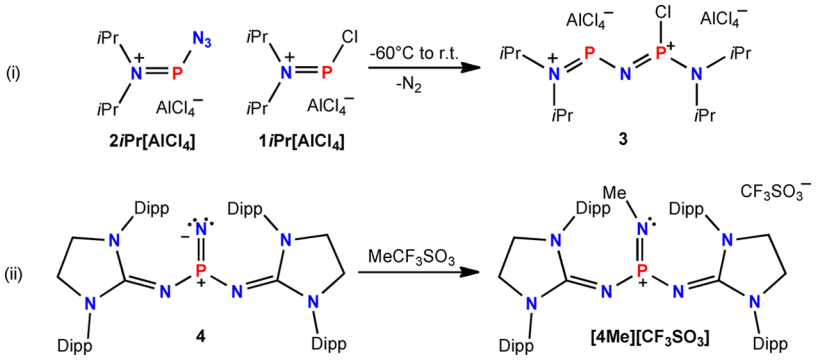

Scheme 4. Formation of Iminophosphorane–Iminophosphanes 5 and Rearrangement in a 1–3-Trimethylsilyl Shift toward Diazadiphosphetidines 6 According to Studies by Boeske et al.[17,18]

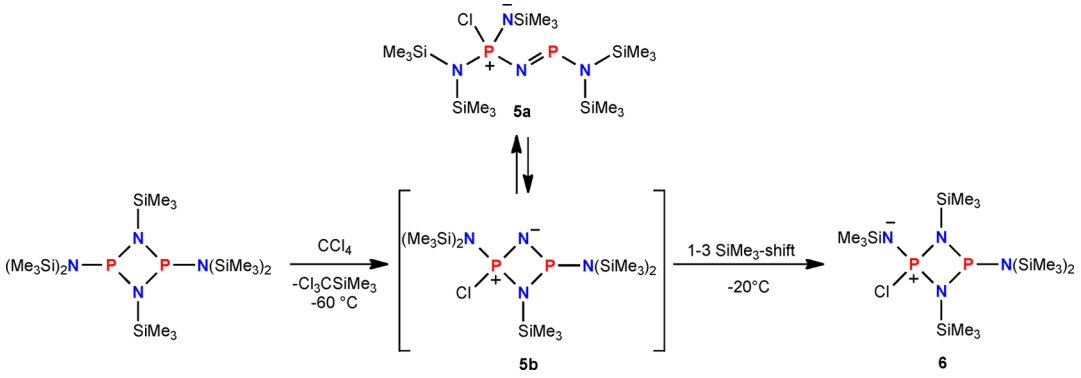

Azidophosphenium ions are considered highly labile and only of transient nature because they can decompose in a Staudinger reaction.[10] In the classical Staudinger reaction, organic azides react with P^{III} compounds in an oxidative coupling between phosphorus and nitrogen, in which phosphorus is oxidized to P^V and dinitrogen is liberated, affording a great variety of iminophosphoranes, which are an important class of substances in organic synthesis and can be further hydrolyzed to give amines.[11]

Nevertheless, our group succeeded in the isolation of an azidophosphenium cation in the salt $[(Me_3Si)_2NPN_3][GaCl_4]$ ($\mathbf{2SiMe_3[GaCl_4]}$) at −50 °C, which, as an isolated crystalline solid, is stable below −30 °C for at least 1 year.[6] This astonishing stability stems from delocalization of the positive charge and formal π-electron density along the NPN_3 skeleton (Figure 1, left) as well as from four close van der Waals contacts to chlorine atoms of the $GaCl_4^-$ anion (Figure 1, right). Furthermore, we succeeded in isolation of the analogous pseudohalogen-substituted salts $[(Me_3Si)_2NPX][GaCl_4]$ (X = NCO, NCS, $OSiMe_3$), which were shown to react with Lewis bases such as 4-(*N*,*N*-dimethylamino)pyridine and as dienophiles with dienes such as 2,3-dimethyl-1,3-butadiene (dmb) or 1,3-*cyclo*-hexadiene.[12]

However, in solution, only traces of $\mathbf{2SiMe_3[GaCl_4]}$ [$\delta(^{31}P)$ = 368.6 ppm, at −65 °C] were detected by means of low-temperature ^{31}P NMR techniques because the salt readily precipitates from cold CH_2Cl_2 solutions. At room temperature, only the resonances of unidentified decomposition products could be detected. A thorough search of the literature revealed that Wolf and co-workers investigated the reactivity of $\mathbf{2}i\mathbf{Pr[AlCl_4]}$, which they assumed to self-condense, affording polymers and phosphenium–phosphonium salts of the type $[i\mathrm{Pr_2NPNP(Cl)N}i\mathrm{Pr_2}][AlCl_4]_2$ (**3**; Scheme 3, reaction i). In accordance with the proposed molecular structure of $\mathbf{3}^{2+}$, an AX spin system was observed in the $^{31}P\{^1H\}$ NMR spectrum with distinct resonances for the phosphenium phosphorus and phosphonium center (cf. $[i\mathrm{Pr_2NPNP(Cl)N}i\mathrm{Pr_2}]^+$ $\delta_{\mathrm{phosphenium}}(^{31}P)$ = 311 ppm, $\delta_{\mathrm{phosphonium}}(^{31}P)$ = 26 ppm,

dx.doi.org/10.1021/ic500332s | Inorg. Chem. 2014, 53, 3880–3892

$J(^{31}P-^{31}P)$ = 111.5 Hz; Scheme 3). However, the formation of a tricoordinated iminophosphonium species is unlikely. Because of the high electrophilicity of the phosphorus center in such iminophosphorane cations, the counterion usually binds covalently to the phosphorus center.[13] Just recently, the first isolable cationic iminophosphorane cation ([**4Me**][CF_3SO_3]) was prepared by methylation of an isolable $\sigma^3\lambda^5$-nitridophosphorane [**4**; also $\sigma^3\lambda^5$-nitridophosphane(V)], which is stabilized by bulky imidazolin-2-iminato substituents, therefore effectively denying interaction with the anion (Scheme 3, reaction ii).[14,15]

Systems that are related to the phosphenium−phosphonium species **3** are iminophosphane−iminophosphoranes of the type $(Me_3Si)_2NP(Cl)(NSiMe_3)NPN(SiMe_3)_2$ (**5a**), which possesses similar ^{31}P NMR shifts for the dicoordinated P^{III} and tetracoordinated P^V atoms, respectively (cf. **5a** $\delta(^{31}P)$ = 341.1 (P^{III}) and −10.6 (P^V) ppm, J(P−P) = 79.9 Hz; Scheme 4).[17] Moreover, they display an N−P−N−P−N backbone similar to that found in $\mathbf{3}^{2+}$. Furthermore, **5a** was shown to be in equilibrium with its cyclic form **5b**, which undergoes a 1,3-trimethylsilyl migration to yield a cyclic 1,3,2λ^3,4λ^5-diazadiphosphetidine (**6**; Scheme 4).[18]

Herein, by utilizing **2*i*Pr**[$GaCl_4$] as a model compound, we describe the decomposition products of azidophosphenium species **2SiMe$_3$**[$GaCl_4$]. The work of Wolf and co-workers has been reevaluated, the missing solid-state structures of **1*i*Pr**$^+$ and **2*i*Pr**$^+$ have been determined, and self-condensation products of **2*i*Pr**[$AlCl_4$] need to be revised on the basis of our findings. Furthermore, **2*i*Pr**[$GaCl_4$] is shown to be a versatile starting material for the formation of complex cations with an N−P−N−P−N backbone. Starting from **2SiMe$_3$**[$GaCl_4$], we succeeded in isolating a unique bicyclic system bearing a P_2N_2 ring, which is connected to a NGa_2Cl four-membered ring representing the first structurally characterized 1,3-diaza-2λ^3,4λ^5-diphosphetidine.

RESULTS AND DISCUSSION

Phosphenium salts of the type [R_2NPCl][$GaCl_4$] [R = *i*Pr, $SiMe_3$ (**1R**[$GaCl_4$])] are most efficiently generated by the combination of dichlorophosphane R_2NPCl_2 and $GaCl_3$ in CH_2Cl_2 at −80 °C. Concentration of the respective reaction mixtures at −50 °C yielded colorless crystalline materials, which in the case of **1*i*Pr**[$GaCl_4$] are stable at ambient temperatures for at least 1 h (vide infra). In contrast to **1*i*Pr**[$GaCl_4$], **1SiMe$_3$**[$GaCl_4$] decomposes in isolated form even at temperatures below −30 °C by thermal elimination of Me_3SiCl. The dynamic solution chemistry of **1*i*Pr**[$GaCl_4$] and **1SiMe$_3$**[$GaCl_4$] was extensively studied by means of variable-temperature ^{31}P NMR spectroscopy, and a dynamic equilibrium between R_2NPCl_2 and $GaCl_3$ and the respective phosphenium salt [R_2NPCl][$GaCl_4$] is characteristic for these species.[7,19] Although **1*i*Pr**[$AlCl_4$] was first reported in 1976 by Parry and co-workers, its solid-state structure has not been reported so far.[2,20] Crystal structures have just been reported for products in which **1*i*Pr**$^+$ was incorporated by means of the oxidative addition of substrates to the phosphenium center (**A**,[21] **B**,[22] and **C**;[23] Figure 2).

Treating iPr_2NPCl_2 with $GaCl_3$ in a CH_2Cl_2 solution at −80 °C and letting the mixture stand overnight at −80 °C afforded crystals of **1*i*Pr**[$GaCl_4$] suitable for X-ray analysis. **1*i*Pr**[$GaCl_4$] crystallizes solvent free in the monoclinic space group $P2_1/c$ with four formula units in the unit cell (Figure 3, left). The short P−N_{amino} distance [1.591(3) Å] is best described as a P−N $p_\pi p_\pi$ double bond [cf. P−N_{amino} of **1SiMe$_3$**[$GaCl_4$] (avg)

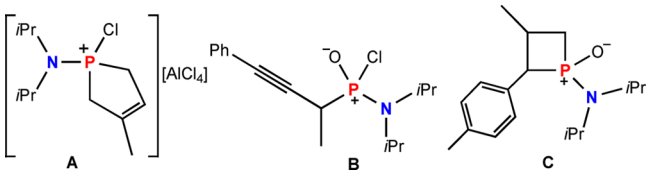

Figure 2. Crystallographically determined structures of molecules formally incorporating **1*i*Pr**$^+$.

1.590 Å; $\sum r_{cov}$(P=N) = 1.60 Å], in accordance with natural bond orbital (NBO) analysis.[19,24] The P−Cl bond is shortened with respect to the sum of the covalent radii [2.003(1) Å; $\sum r_{cov}$(P−Cl) = 2.04 Å; cf. [$(Me_3Si)_2NPCl$][$GaCl_4$] 2.019(4) Å].[19,24] The $GaCl_4^-$ counteranion significantly interacts with the electron-deficient phosphenium center because two P1−Cl_{anion} contacts are detected within the sum of the respective van der Waals radii of phosphorus and chlorine [3.014(1) Å; $\sum r_{vdW}$(P−Cl) = 3.55 Å].[25] Hence, a significant charge transfer of 0.15e from the anion to the cation further enhances its stability by ion pairing. Salt formation is also visualized in the Raman spectrum, which reveals a sharp band at 347 cm^{-1} for the A_1 asymmetric Ga−Cl stretching mode, whereas free $GaCl_3$ is not observed.[26]

For the first time, Wolf and co-workers discussed the existence of an azidophosphenium salt of the type [iPr_2NPN_3][$AlCl_4$] (**3**) in 1984. They reported that **1*i*Pr**[$AlCl_4$] reacts with Me_3SiN_3 to intermediately yield **2*i*Pr**[$AlCl_4$], which self-condenses to yield phosphorus bis(cations) (Scheme 3, reaction i).[8,9] However, the solid-state structure of such phosphenium azides remained unknown until our group uncovered the molecular structure of [$(Me_3Si)_2NPN_3$][$GaCl_4$] (**2SiMe$_3$**[$GaCl_4$]).[19] **2SiMe$_3$**[$GaCl_4$] can be prepared at −50 °C by treating a CH_2Cl_2 solution of **1SiMe$_3$**[$GaCl_4$] with Me_3SiN_3. Nevertheless, **2SiMe$_3$**[$GaCl_4$] is only stable in the solid state below −30 °C and decomposes rapidly in a CH_2Cl_2 solution as vigorous gas evolution is observed upon thawing.[6]

Following the synthetic protocol that yielded **2SiMe$_3$**[$GaCl_4$], **2*i*Pr**[$GaCl_4$] was prepared in good yield (81%) and its structure was determined by X-ray crystallographic measurements. **2*i*Pr**[$GaCl_4$] possesses two major advantages compared to **2SiMe$_3$**[$GaCl_4$]: (i) **2*i*Pr**[$GaCl_4$] cannot be engaged in chlorine/methyl exchange reactions in the presence of $GaCl_3$, which is common for silylated aminopnictanes;[27−30] (ii) **2*i*Pr**[$GaCl_4$] is not sensitive toward the thermal release of Me_3SiCl, which is well documented for silylated aminopnictanes in the presence of $GaCl_3$.[19,31,32] Moreover, **2*i*Pr**[$GaCl_4$] is thermally stable up to 78 °C. Therefore, we envisaged **2*i*Pr**[$GaCl_4$] as a model system for thermal decomposition reactions of azidophosphenium salts. **2*i*Pr**[$GaCl_4$] crystallizes solvent-free in the monoclinic space group $C2/c$ with eight formula units in the unit cell (Figure 3, right). The geometry of the NPN_3 skeleton resembles that of the azidophosphenium ion in **2SiMe$_3$**[$GaCl_4$] with a N_{amino}−P1 double bond [**2*i*Pr**$^+$ 1.6003(9) Å; cf. **2SiMe$_3$**$^+$ 1.597(3) Å][19] and a short P1−N_{azide} distance [1.665(1) Å; cf. $\sum r_{cov}$(P=N) = 1.60, $\sum r_{cov}$(P−N) 1.82 Å].[24] The N−P−N angle [100.57(5)°; cf. **2SiMe$_3$**$^+$ 101.03(9)°][6] is rather acute, and the azide group shows the typical trans-bent configuration (regarding the phosphorus atom, P1−N1−N2−N3 180°) with an N1−N2−N3 angle of 171.4(2)°, with a formally sp^2-hybridized N_α atom [P1−N1−N2 121.19(9)°]. The closest P1−Cl_{anion} contact [3.0448(4) Å] is shorter than the sum of the respective van der

dx.doi.org/10.1021/ic500332s | Inorg. Chem. 2014, 53, 3880−3892

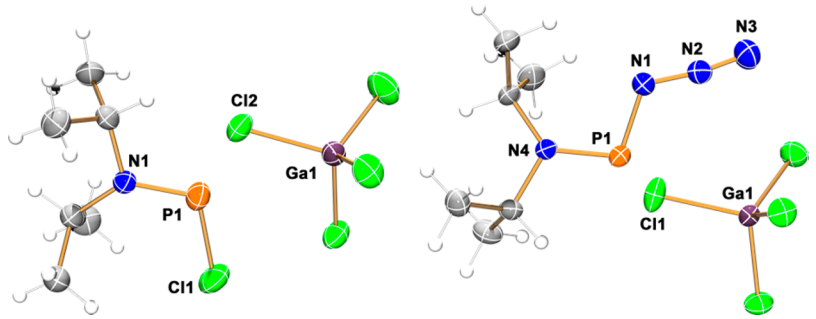

Figure 3. ORTEP drawings of the molecular structures of **1*i*Pr**[$GaCl_4$] (left) and **2*i*Pr**[$GaCl_4$] (right). Ellipsoids are drawn at 50% probability. Selected bond lengths (Å) and angles (deg): **1*i*Pr**[$GaCl_4$], P1−N1 1.591(3), P1−Cl1 2.003(1), P1−Cl2 3.014(1), N1−C1 1.502(4), N1−C4 1.520(4); N1−P1−Cl1 106.9(1); Σ(<N1) 360.0; C1−N1−P1−Cl1 −0.6(3), C1−N1−P1−Cl2 94.9(3); **2*i*Pr**[$GaCl_4$], P1−N4 1.6003(9), P1−N1 1.665(1), N1−N2 1.248(1), N2−N3 1.114(2), N4−C1 1.509(1), N4−C4 1.504(1); N1−P1−N4 100.57(5), N1−N2−N3 171.4(1); Σ(<N4) 359.97; C4−N4−P1−N1 2.8(1), P1−N1−N2−N3 171.6(9).

Scheme 5. Different Pathways for the Preparation of 7[$GaCl_4$] (Reactions i and ii) and Examples of Transformations Starting from 7[$GaCl_4$] (Reactions iii and iv)

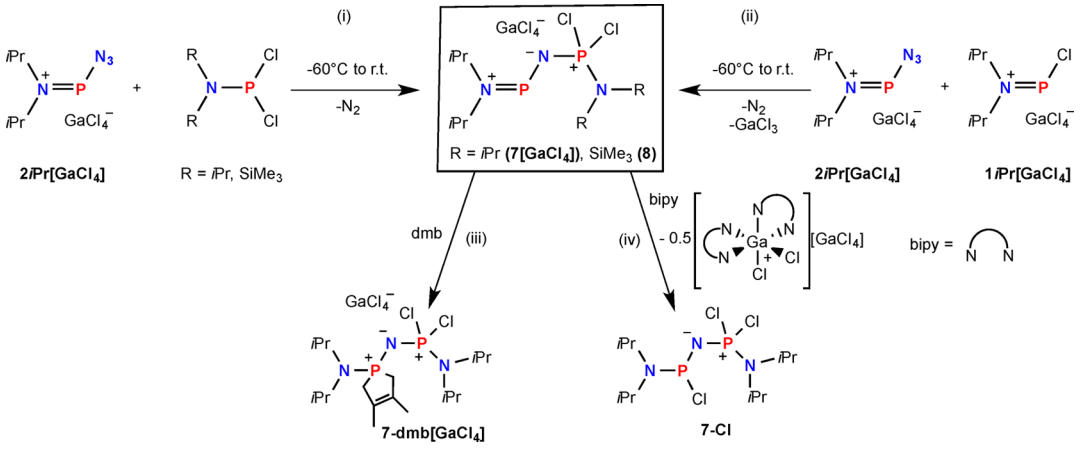

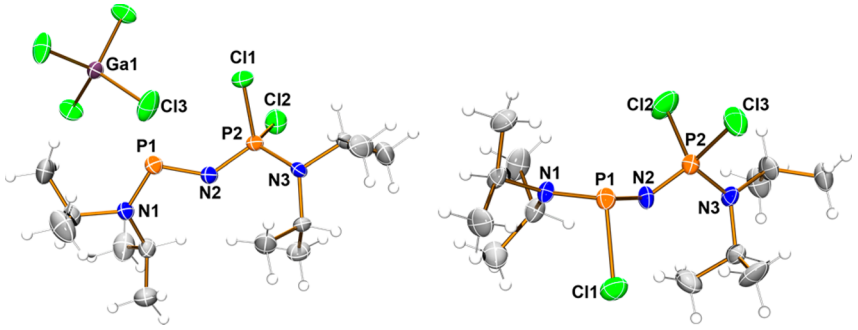

Figure 4. ORTEP drawings of the molecular structures of 7[$GaCl_4$] (left) and **7-Cl** (right). Ellipsoids are drawn at 50% probability at −100 °C. Selected bond lengths (Å) and angles (deg): 7[$GaCl_4$], P1−N1 1.1611(2), P1−N2 1.597(2), P2−N2 1.557(2), P2−N3 1.597(2), P2−Cl1 1.9987(8), P2−Cl2 2.0055(8), P1−Cl5 3.532(1); N1−P1−N2 104.97(9), P2−N2−P1 129.4(1), N2−P2−N3 112.4(1), ∑(<P2) 334.58; ∑(<N1) 359.95; ∑(<N3) 359.88; N2−P1−N1−C4 178.0(2), N1−P1−N2−P2 176.6(2), N3−P2−N2−P1 −165.0(2), N2−P2−N3−C10 178.6(2); **7-Cl**, P1−N1 1.640(4), P1−N2 1.660(4), P2−N2 1.504(2), P2−N3 1.603(4), P1−Cl1 2.207(2), P2−Cl2 2.020(2), P2−Cl3 2.038(2); N1−P1−N2 101.8(2), P2−N2−P1 138.1(3), N2−P2−N3 114.7(2), ∑(<P1) 301.1, ∑(<P2) 333.3, ∑(<N1) 358.6, ∑(<N3) 359.1; N2−P1−N1−C4 28.4(4), N3−P2−N2−P1 149.7(4).

Waals radii [$\sum r_{vdw}$(P−Cl) = 3.55 Å].[25] Additionally, three more contacts between chlorine atoms from the anion and the phosphenium center are found, a geometrical arrangement that is in accordance with other pseudohalogen-substituted phosphenium salts (e.g., Figure 1).[12] This implicates a small charge transfer from the anion to the phosphenium ion, which was calculated by means of NBO analysis and amounts to only 0.08 e; therefore, the cation can be considered almost "naked".[33]

In a first series of experiments, we followed the procedure described by Wolf et al., in which they carried out the reaction of **2*i*Pr**[$GaCl_4$] with 1 equiv of the chlorophosphenium salt **1*i*Pr**[$GaCl_4$], which resulted according to their interpretation in the formation of a bis(cation) ($\mathbf{3}^{2+}$) on the basis of ^{31}P NMR spectroscopy (Scheme 3, reaction i).[8] Treating **2*i*Pr**[$GaCl_4$]

dx.doi.org/10.1021/ic500332s | Inorg. Chem. 2014, 53, 3880−3892

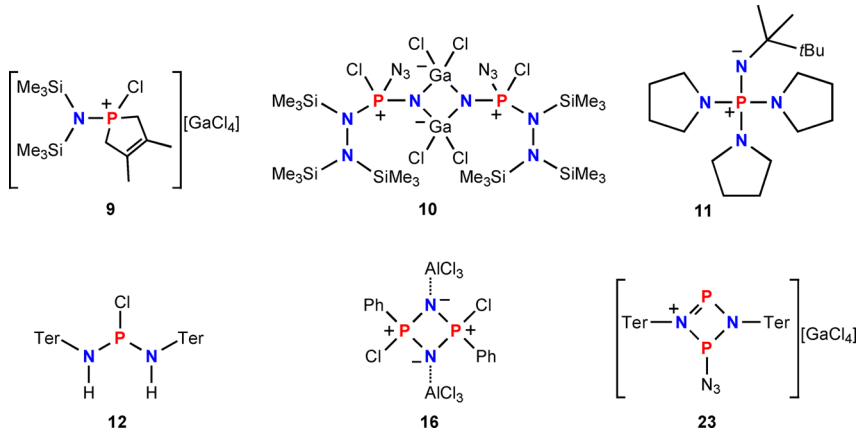

Figure 5. Structures of phospholenium salt **9**, Staudinger product **10**, triaminoiminophosphorane **11**, terphenyl-substituted aminochlorophosphane **12**, cyclodiphospha(V)diazene **16**, and *cyclo*-diphospha(III)diazenium salt **23**.

with equimolar amounts of **1*i*Pr**[**GaCl$_4$**] in CH_2Cl_2 at −50 °C and subsequent warming to room temperature led to vigorous gas evolution, and after workup and recrystallization from CH_2Cl_2, phosphenium species [*i*Pr$_2$NPNP(Cl)$_2$N*i*Pr$_2$][GaCl$_4$] (**7**[**GaCl$_4$**]) could be isolated (Scheme 5, reaction ii; Figure 4, left). The formation of **7**[**GaCl$_4$**] was unequivocally proven by X-ray crystallographic analysis and is best described as a Staudinger reaction between the azide **2*i*Pr**[**GaCl$_4$**] and the parent phosphine *i*Pr$_2$NPCl$_2$, which is present in solutions of **1*i*Pr**[**GaCl$_4$**] according to ^{31}P NMR experiments (vide infra). Hence, in this reaction, 1 equiv of $GaCl_3$ must remain in the mixture.

7[**GaCl$_4$**] is a thermally robust (T_{dec} = 125 °C) colorless crystalline solid that dissolves in polar solvents such as CH_2Cl_2 and C_6H_5F and is insoluble in *n*-hexane and benzene. **7**[**GaCl$_4$**] features an AX spin system in the ^{31}P NMR spectrum with two distinct doublets for the phosphenium phosphorus and the iminophosphorane moiety [**7**[**GaCl$_4$**]; $\delta_{phosphenium}(^{31}P)$ = 311.2, $\delta_{iminophosphorane}(^{31}P)$ = 27.4; $^2J(^{31}P-^{31}P)$ = 111.5 Hz], which lies in the typical range of four-coordinate P^V compounds [cf. $\delta(^{31}P)$ = 33.4 ppm for (*i*Pr)$_2$NP(Cl)(N$_3$)N(Ph)·AlCl$_3$].[34] In the ^{1}H spectrum, four sets of signals are detected for the *i*Pr groups, with one of the septets of the methine protons being split into a septet of doublets, indicating interaction of that proton with the phosphenium phosphorus atom, which results in deshielding and therefore a rather strong downfield-shifted signal.

To render the formation of **7**[**GaCl$_4$**] stoichiometrically, **2*i*Pr**[**GaCl$_4$**] and an equimolar amount of *i*Pr$_2$NPCl$_2$ were combined at −50 °C and allowed to slowly warm to room temperature, which was accompanied by the evolution of dinitrogen (Scheme 5, reaction i). **7**[**GaCl$_4$**] is the sole product and can be crystallized by gradually cooling the saturated reaction mixture to −24 °C overnight (isolated yield 63%). The formation of **7**[**GaCl$_4$**] underlines the Staudinger-type reactivity of azidophosphenium species with phosphanes. In the Staudinger reaction, organic azides typically react with PPh_3 in an oxidative addition to yield iminophosphoranes as an intermediate, which can be further hydrolyzed to give amines and phosphane oxides.[10] In the case of **2*i*Pr**[**GaCl$_4$**] in the first reaction step, either the phosphenium cation **1*i*Pr**$^+$ or *i*Pr$_2$NPCl$_2$ adds with its phosphorus atom to the N_{azide} atom while eliminating dinitrogen and forming the corresponding iminophosphorane-substituted phosphenium cation. The dicationic structure proposed by Wolf and co-workers was not observed;[8] even if such a species was formed transiently, it can be assumed that it forms the iminophosphorane moiety by abstracting a chloride from the $GaCl_4^-$ anion.[13]

Adding (Me$_3$Si)$_2$NPCl$_2$ instead of *i*Pr$_2$NPCl$_2$ to a solution of **2*i*Pr**[**GaCl$_4$**] at −50 °C and warming to room temperature yielded after workup a colorless solid, which was recrystallized from fluorobenzene (C_6H_5F) at 5 °C and found to be the addition product of (Me$_3$Si)$_2$NPCl$_2$ to **2*i*Pr**[**GaCl$_4$**], the iminophosphorane−phosphenium salt [*i*Pr$_2$NPNP(Cl$_2$)N-(SiMe$_3$)$_2$][GaCl$_4$] (**8**). **8** displays the expected AX spin system in the ^{31}P NMR spectrum, with the phosphenium center resonating at 311.3 ppm (cf. **7**[**GaCl$_4$**] 311.2 ppm), whereas the P^V atom is detected at 30.4 ppm, which is downfield-shifted compared to that of **7**[**GaCl$_4$**] (27.4 ppm). The compound was characterized by X-ray analysis, and a representation of the molecular structure of **8** is shown in Figure 6 (right). Owing to their similarity, the molecular structures of **7**[**GaCl4**] and **8** are discussed in one context.

7[**GaCl$_4$**] crystallizes in the monoclinic space group $P2_1/c$ with eight formula units in the cell and thus two independent formula units in the asymmetric unit, whereas **8** crystallizes in the monoclinic space group $P2_1/n$ with four formula units in the unit cell. The discussion of the structure is led for one independent formula unit, respectively. The cations in **7**[**GaCl$_4$**] and **8** possess both a dicoordinated phosphenium phosphorus atom P1 with a P1−N$_{amino}$ double bond [**7**[**GaCl$_4$**] 1.611(2) Å; **8** 1.612(4) Å] and a phosphonium phosphorus atom P2, which is also bound to another amino group with a short P2−N3 distance [**7**[**GaCl$_4$**] 1.597(3) Å, **8** 1.588(5) Å; cf. **9** P−N 1.6089(8) Å,[12] **10** P^V−N$_{amino}$ 1.634(5) Å; Figure 5],[35] which can be considered a P^V−N single bond. The imino−nitrogen phosphorus distances N2−P1 [**7**[**GaCl$_4$**] 1.557(2) Å; **8** 1.597(4) Å] and N2−P2 [**7**[**GaCl$_4$**] 1.597(2) Å; **8** 1.550(4) Å] are rather short (cf. **10** P^V−N$_{imino}$ 1.558(4) Å],[35] with both distances being shorter than the sum of the respective covalent radii for a P−N double bond [$\sum r_{cov}$(P=N) = 1.60 Å],[24] indicating a certain degree of π delocalization along the N_2P_2 moiety, which is further underlined by the two canonical Lewis formulas for **7**[**GaCl$_4$**] shown in Scheme 6. Overall, N_3P_2 is W-shaped, with a rather acute N1−P1−N2 angle [**7**[**GaCl$_4$**] 104.97(9)°; **8** 105.0(2)°], a slightly larger N2−P2−N3 angle [**7**[**GaCl$_4$**] 112.4(1)°; **8** 113.6(2)°], and a typical P1−N2−P2 angle (**7**[**GaCl$_4$**] 129.4(1)°; **8** 133.2(3)°] for the sp^2-hybridized imino nitrogen, with a LP of electrons on the nitrogen site according to NBO analysis. The closest contacts between

dx.doi.org/10.1021/ic500332s | *Inorg. Chem.* 2014, 53, 3880−3892

Scheme 6. Two Canonical Lewis Formulas of the Cation in 7[GaCl$_4$] Displaying π Delocalization along the N−P−N−P−N Backbone in 7$^+$

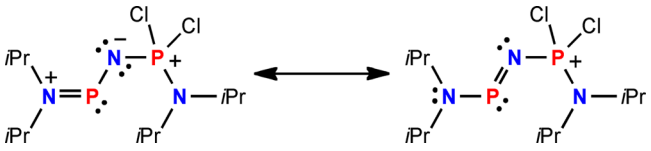

phosphorus and GaCl$_4^-$ [7[**GaCl$_4$**] 3.532(1) Å; **8** 3.289(2) Å] are in the range of the respective van der Waals radii of phosphorus and chlorine [$\sum r_{vdw}$(P−Cl) = 3.55 Å].[25] Therefore, the anion and cation are well separated, which is supported by the calculated charge transfer.[33] Overall, P2 is distorted tetrahedrally coordinated, which is in accordance with a four-coordinate phosphonium phosphorus.

To test the reactivity of 7[**GaCl$_4$**] as a dienophile, we added 2,3-dimethyl-1,3-diene (dmb) because phosphenium cations, which might be regarded as nucleophilic carbenes with respect to the reactivity, are known to react with suitable dienes in chelotropic [4 + 1] cycloaddition reactions. This reaction resulted in the formation of the expected phospholenium species **7-dmb**[**GaCl$_4$**] (Scheme 5, reaction iii), which was crystallographically characterized (Figure 5, left). **7-dmb**-[**GaCl$_4$**] crystallizes in the monoclinic space group $P2_1/n$ with four formula units in the unit cell. Upon the addition of dmb, the P−N$_{amino}$ [1.624(2) Å] and N$_{imino}$−P1 [1.618(2) Å] bonds elongate, whereas the P2−N$_{imino}$ [1.533(2) Å] bond shortens significantly compared to 7[**GaCl$_4$**] (cf. **11** 1.511 Å; Figure 5).[36] The anion and cation are well separated, and no contacts are observed between them. The phosphole moiety is almost planar and slightly bent toward the P^{V}Cl$_2$ fragment.

Furthermore, we wanted to set free the parent chlorophosphane *i*Pr$_2$NPClNP(Cl)$_2$N*i*Pr$_2$ (**7-Cl**). Therefore, GaCl$_3$ needs to be removed from the reaction mixture, which can easily be achieved by adding 2,2′-bipyridine (bipy) to a CH$_2$Cl$_2$ solution of 7[**GaCl$_4$**] because GaCl$_3$ is known to form a chelating complex with bipy in [GaCl$_2$(bipy)$_2$][GaCl$_4$], which is hardly soluble in CH$_2$Cl$_2$ and can be removed by filtration (Scheme 5, reaction iv).[37,38] In the course of this reaction, chlorine is back-substituted to the phosphenium phosphorus and **7-Cl** is obtained by extracting the crude reaction mixture with *n*-hexane and identified by ^{31}P and ^{1}H NMR spectroscopy. As expected, the tricoordinated P^{III} resonates in the ^{31}P NMR spectrum at 156.2 ppm (cf. **12** 129.9 ppm; Figure 5),[17,18,39] whereas P^V is high-field-shifted compared to the starting material 7[**GaCl$_4$**] [δ_{P^V}(^{31}P) = −6.4; cf. 7[**GaCl$_4$**] 27.4 ppm], indicating the loss of positive charge. **7-Cl** crystallizes in the monoclinic space group $P2_1$ with two molecules in the unit cell (Figure 6, right). Upon chlorine back-substitution, the N1−P1 [1.640(4) Å] and N2−P1 [1.660(4) Å] distances elongate significantly toward values typical for N−P single bonds in chlorophosphanes [cf. **12** (avg) 1.644 Å; Figure 5].[39] The N2−P2 [1.504(4) Å] bond is found to be shorter than that in the parent cation 7$^+$, indicating a localized P^V−N double bond, whereas the P2−N3 [1.603(4) Å] distance can still be considered a P^V−N single bond. The P^{III} atom P1 is trigonal-pyramidally coordinated, whereas P2 exhibits the expected distorted tetrahedral environment. The striking structural feature of **7-Cl** is the P−Cl bond [2.207(2) Å], which is significantly elongated with respect to the respective sum of the covalent radii of phosphorus and chlorine [cf. $\sum r_{cov}$(P−Cl) = 2.10 Å]. Therefore, it is plausible to discuss a certain degree of phosphenium character due to strong hyperconjugative effects, which is underlined by a calculated positive charge of 0.43e for the isolated 7$^+$ cation, which is only slightly more positive than the formal cation in [(Me$_3$Si)$_2$NPCl][Cl] with a cationic charge of 0.34e.[19]

Having fully characterized 7[**GaCl$_4$**], we turned back to our initial starting point to uncover the decomposition products of azidophosphenium salt **2SiMe$_3$**[**GaCl$_4$**] (Scheme 7). In a first series of experiments, a CH$_2$Cl$_2$ solution of **2SiMe$_3$**[**GaCl$_4$**] was allowed to slowly warm to room temperature and the reaction was followed by ^{31}P NMR spectroscopy. At −40 °C, only minimal amounts of the parent azidophosphenium cation **2SiMe$_3^+$** were present in solution (green, Figure 7). In addition, two broad doublets could be detected in the downfield region of the spectrum at 357.6 and 354.4 ppm, respectively, with a splitting of 90.8 and 79.9 Hz and a corresponding second set of doublets at 29.3 and 22.1 ppm, respectively, supportive of a species that contains both a phosphenium phosphorus atom and a four-coordinated P^V. Alongside these three species, impurities are detected in the high-field region, which could not be identified. Hence, these data are supportive of the formation

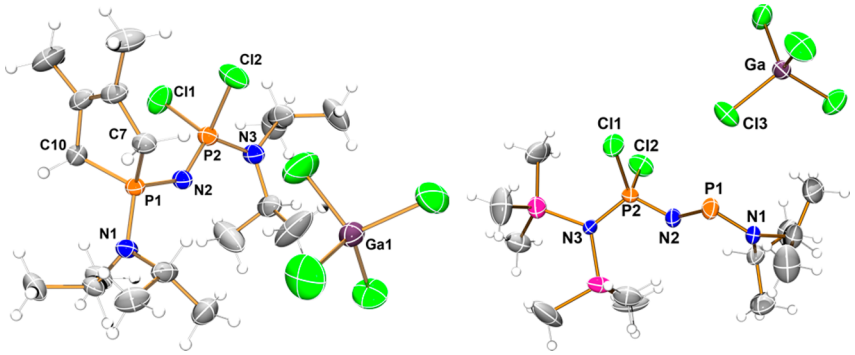

Figure 6. ORTEP drawings of the molecular structures of **7-dmb**[**GaCl$_4$**] (left) and **8** (right). Ellipsoids are drawn at 50% probability at −100 °C, and only the major part is displayed. Selected bond lengths (Å) and angles (deg): **7-dmb**[**GaCl$_4$**], P1−N1 1.624(2), P1−N2 1.618(2), P2−N2 1.533(2), P2−N3 1.607(2), P2−Cl1 2.0207(9), P2−Cl2 2.0073(9), P1−C7 1.799(2), P1−C10 1.796(2); P2−N2−P1 137.7(1), N2−P2−N3 114.1(1); Σ(<P1) 335.26, Σ(<P2) 335.62, Σ(<N1) 358.76, Σ(<N3) 360; N2−P1−N1−C1 79.8(2), P1−C7−C8−C11 −164.9(2); **8**, P1−N1 1.612(4), P1−N2 1.597(4), P2−N2 1.550(4), P2−N3 1.588(5), P2−Cl1 1.996(2), P2−Cl2 2.010(2), P1−Cl3 3.289(2); N1−P1−N2 105.0(2), P2−N2−P1 133.2(3), N2−P2−N3 113.6(2); Σ(<P1) 337.64, Σ(<N1) 359.9, Σ(<N3) 359.4; N2−P1−N1−C4 178.0(2), N1−P1−N2−P2 9.4(4), N3−P2−N2−P1 −130.5(4), Cl2−P2−N3−Si1 120.8(3).

dx.doi.org/10.1021/ic500332s | Inorg. Chem. 2014, 53, 3880−3892

Scheme 7. Self-Condensation via a Staudinger Reaction in Azidophosphenium Species $2SiMe_3[GaCl_4]$

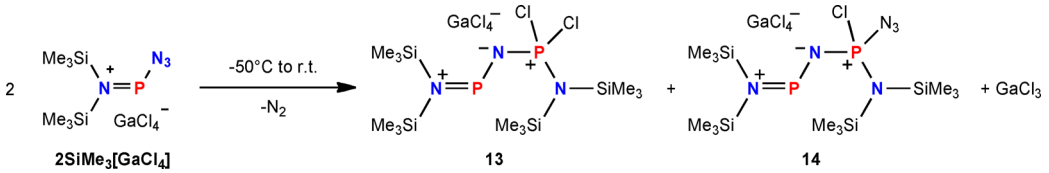

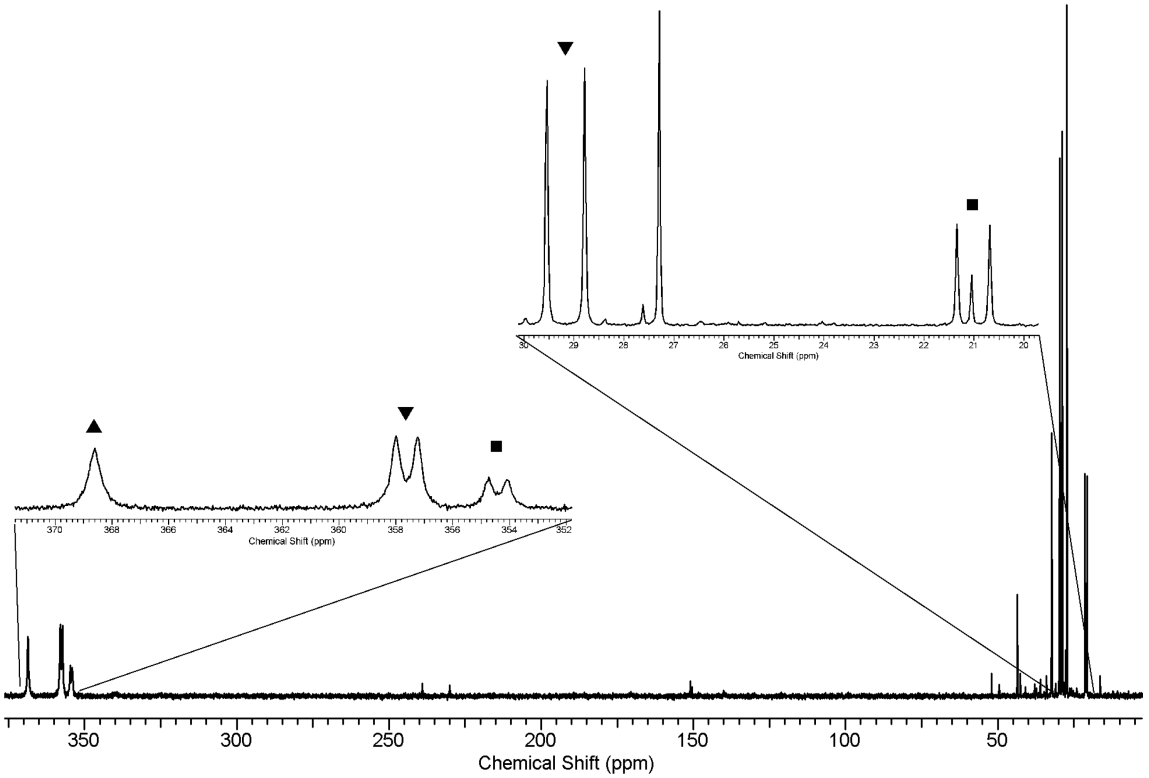

Figure 7. ^{31}P NMR spectrum of a CH_2Cl_2 solution of $2SiMe_3[GaCl_4]$ recorded at −40 °C. The signal at 368.6 ppm (▲) corresponds to the cation $2SiMe_3^+$, and the doublets correspond to 13^+ (▼) and 14^+ (■), respectively, and unidentified impurities.

of $[(Me_3Si)_2NPNP(Cl)_2N(SiMe_3)_2][GaCl_4]$ (**13**) as the major product [$\delta_{phosphenium}(^{31}P)$ = 357.6 ppm, $\delta_{P^V}(^{31}P)$ = 29.3 ppm; Figure 7]. However, the second set of doublets indicates the formation of mixed species $[(Me_3Si)_2NPNP(Cl)(N_3)N(SiMe_3)_2][GaCl_4]$ (**14**; $\delta_{phosphenium}(^{31}P)$ = 354.3 ppm, $\delta_{P^V}(^{31}P)$ = 22.1 ppm; Figure 7 and Scheme 7). In analogy to the formation of $7[GaCl_4]$, $2SiMe_3[GaCl_4]$ was treated with an equimolar amount of $(Me_3Si)_2NPCl_2$, which afforded **13** in a higher purity according to ^{31}P NMR experiments. However, traces of **14** are still present in the reaction mixture, indicating a dynamic solution chemistry of $2SiMe_3[GaCl_4]$, $GaCl_3$, and $(Me_3Si)_2NP(N_3)Cl$ with respect to chlorine/azide scrambling, which is regularly observed in CH_2Cl_2 solutions.[40] Neither crystals of **13** nor **14** could be grown because in all cases oily residues remained and showed no propensity to become solid.

Interestingly, treating $1SiMe_3[GaCl_4]$ with 0.5 equiv of Me_3SiN_3 at −50 °C in CH_2Cl_2 and warming the mixture to room temperature over a period of 2 h yielded after concentration and storage at −24 °C under exclusion of light for 48 h a colorless crystalline solid. The compound was characterized by X-ray crystallography as the unprecedented bicyclic compound $[(Me_3Si)_2N_2P_2Cl_2N(Ga_2Cl_5)]$ (**15**; Scheme 8 and Figure 8, left). The formation of **15** is best understood as $GaCl_3$-assisted elimination of two molecules of Me_3SiCl from

Scheme 8. Comprehensive Solution Chemistry of $(Me_3Si)_2NPCl_2$ in the Presence of $GaCl_3$ and Me_3SiN_3

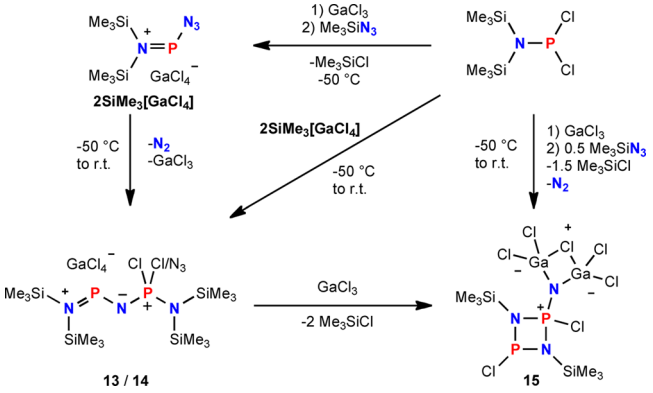

13 and rearrangement of the naked $[(Me_3Si)_2N_3P_2Cl_2]^-$ fragment to a cyclic intermediate, which is subsequently stabilized by adduct formation with a $Ga_2Cl_5^+$ fragment. Intermediates of this transformation could not be observed. To test this hypothesis, we added $GaCl_3$ to a solution containing **13** and followed the reaction with ^{31}P NMR spectroscopy, which clearly indicated the formation of **15**. The stabilization of anionic intermediates by a $Ga_2Cl_5^+$ fragment has

dx.doi.org/10.1021/ic500332s | Inorg. Chem. 2014, 53, 3880−3892

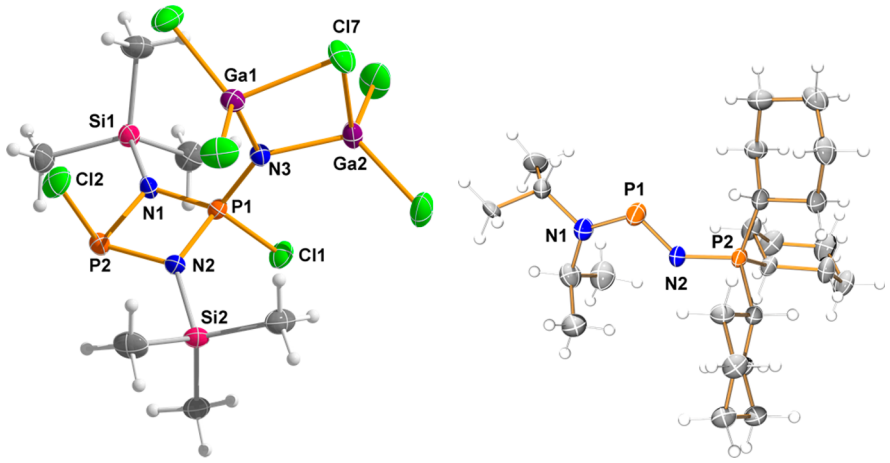

Figure 8. ORTEP drawings of **15** (left) and **19**$^+$ (right). The anion is omitted for clarity. Ellipsoids are drawn at 50% probability. Selected bond lengths (Å) and angles (deg): **15**, P1−N1 1.634(2), C1−P1 1.773(3), N1−C4 1.504(3), N1−Si1 1.769(2), C1−C2 1.518(3), C2−C3 1.331(3), P1−C7 1.801(3), P1−C10 1.797(3), C7−C8 1.498(4), C8−C9 1.322(4); Σ(<N1) 359.26, Σ(<P1) 324.63; Si1−N1−P1−C7 59.5(2), C4−N1−P1−C10 115.27(19), C2−C1−P1−N1 51.2, C4−N1−P1−C1 −7.0(2); **5**, P2−N2 1.643(2), P2−C23 1.812(3), P2−C26 1.824(3), P2−C29 1.833(3), N2−C20 1.539(3), N2−Si2 1.790(2), C20−C21 1.499(4), C21−C22 1.328(4), C26−C27 1.538(5), C27−C28 1.298(5); Σ(<N2) 356.74, Σ(<P2) 340.59. Selected bond lengths and angles of **19**$^+$ are listed in Table 1

Scheme 9. Different Reactivities Observed in the Reaction of 2R[GaCl$_4$] with Phosphanes PPh$_3$ and P*c*Hex$_3$

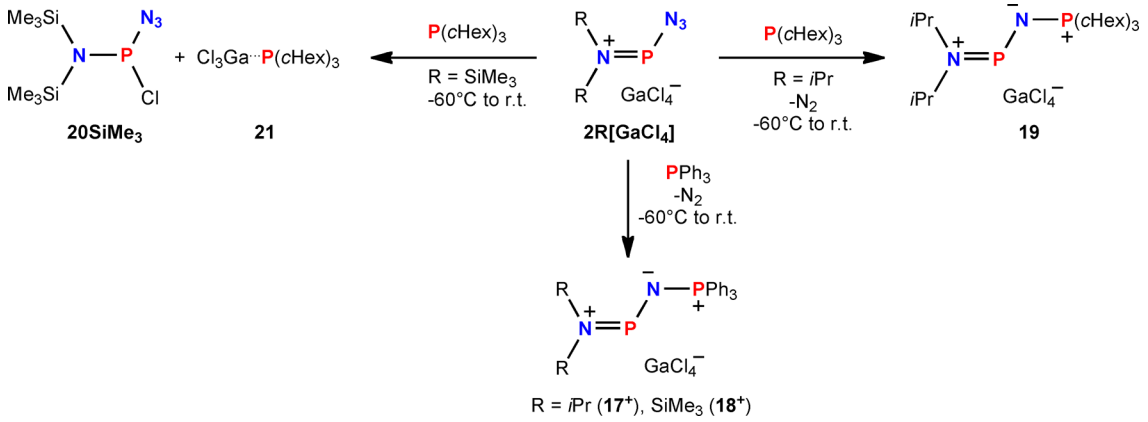

been previously described in the reaction of HypN(SiMe$_3$)PCl$_2$ (Hyp = Si(SiMe$_3$)$_3$) with GaCl$_3$.[41] In the ^{31}P NMR spectrum of isolated **15**, two resonances were detected for the NP(Cl)N group at 142.6 ppm, in good agreement with other strained NP^{III} heterocyclic compounds [cf. **6** $\delta(^{31}P)$ = 102.5 ppm; Scheme 4],[18] and for the tetracoordinated P^V at 23.9 ppm, with both signals being split into doublets with a $^2J(^{31}P-^{31}P)$ coupling of 64.5 Hz, which is in good agreement with the few examples of 1,3,2λ^3,4λ^5-diazaphosphetidines, which were shown to form by a 1,3-SiMe$_3$ shift from iminophosphane−iminophosphoranes (Scheme 4).[17,18] **15** crystallizes in the orthorhombic space group *Pbca* with eight molecules in the cell (Figure 8, left). The characteristic structural feature of **15** is the (Me$_3$Si)$_2$N$_2$P$_2$Cl$_2$ four-membered ring with two long P2−N$_{amino}$ bonds [1.733(2) and 1.736(2) Å] and two significantly shorter P1−N$_{amino}$ distances [1.640(2) and 1.636(2) Å], in accordance with related systems that also incorporate a four-coordinated phosphorus atom [cf. **16** P−N 1.665(2) Å; Figure 5].[42] The N1−P2−N2 angle [83.5(1)°] is rather acute, whereas the N1−P1−N2 angle is close to 90°. The exocyclic SiMe$_3$ groups are attached to the amino nitrogen by single bonds [1.789(2) and 1.786(2) Å; $\sum r_{cov}$(Si−N) = 1.87 Å][24] and lie below a plane that is formed by the central P$_2$N$_2$ ring. The exocyclic NGa$_2$Cl ring is attached to the central P$_2$N$_2$ moiety via the nitrogen atom N3 with a comparably short P1−N3 [1.565(2) Å] distance, which can be regarded as a P^V−N single bond, with a partial charge on N3 of −1.87e according to NBO analysis and an overall negative charge of the [(Me$_3$Si)$_2$N$_3$P$_2$Cl$_2$] fragment of −0.95e. The charge is compensated for via the unusual Ga$_2$Cl$_5$ fragment, which is covalently bound to N3 with Ga−N single bonds [1.903(2) and 1.906(2) Å; $\sum r_{cov}$(Ga−N) = 1.92 Å, cf. **10** Ga−N$_{imino}$ 1.946 Å; Figure 5].[35] Within the Ga$_2$Cl$_5$ moiety, two long Ga−Cl bonds are detected between Ga and the bridging chlorine atom Cl7 [2.3273(8) and 2.3450(7) Å, $\sum r_{cov}$(Ga−Cl) = 2.23 Å],[24] whereas the exocyclic Ga−Cl distances can be considered as typical polar covalent single bonds (avg 2.121 Å). In agreement with this observation is the calculated partial charge of −0.40e for Cl7, which is less negative than the other chlorine atoms at −0.47e.

Having prepared 7[**GaCl$_4$**], we wanted to investigate the possibility of utilizing azidophosphenium cations as building blocks for the generation of cations with multiple phosphorus atoms. Reacting **2*i*Pr**[**GaCl$_4$**] or **2SiMe$_3$**[**GaCl$_4$**] with phosphanes of the type PR$_3$ (R = *c*Hex, Ph) should yield iminophosphorane-substituted phosphenium cations of the type [R$_2$NPNPR′$_3$][GaCl$_4$] (Scheme 9). In the earlier studies

dx.doi.org/10.1021/ic500332s | *Inorg. Chem.* 2014, 53, 3880−3892

Table 1. Selected Structural Data (Distances in Å and Angles in deg) and ^{31}P NMR Data (Chemical Shifts in ppm) of Aminophosphenium Species 1*i*Pr$^+$, 2*i*Pr$^+$, 2SiMe$_3^+$, 7[GaCl$_4$], 8, 15, 7-dmb[GaCl$_4$], and 7-Cl

	P−N1	P−X[a]	N2−P2	P2−N3	N$_{amino}$−P−X[a]	P1−N$_{imino}$−P2	Σ(<P2)	^{31}P P1	^{31}P P2
1*i*Pr$^+$	1.591(3)	2.003(1)			106.8(1)			294.7	
2*i*Pr$^+$	1.6003(9)	1.665(2)			100.57(5)			310.9	
2SiMe$_3^+$								367.5	
7[GaCl$_4$]	1.611(2)	1.597(2)	1.557(2)	1.597(2)	104.97(9)	129.4(1)	334.58	311.2	27.4
7-dmb[GaCl4]	1.624(2)	1.618(2)	1.533(2)	1.607(2)	112.4(1)	137.7(1)	335.26	48.1	−4.4
7-Cl	1.640(4)	1.660(4)					333.26	156.2	−6.4
8	1.612(4)	1.597(4)	1.550(4)	1.588(5)	105.0(2)	133.2(3)	335.62	311.3	30.4
15	1.62[b]	1.573(3)	1.628(3)		107.6(4)	128.3(2)	327.48	303.8	49.1

[a]X = Cl (1), N$_{azide}$ (2*i*Pr$^+$, 2SiMe$_3^+$), N$_{imino}$ (8−15). [b]N*i*Pr moiety disordered; therefore, averaged P−N distance.

by Wolf and co-workers, such cations were prepared in the reaction of 2*i*Pr[AlCl$_4$] with PBu$_3$ and PPh$_3$, whereas at low temperatures, PBu$_3$ formed a Lewis acid base adduct with a phosphenium cation, as indicated by the characteristic ^{31}P NMR shifts for these adducts and a large P−P coupling constant [cf. [4···PBu$_3$][AlCl$_4$] $\delta_{phosphenium}(^{31}P)$ = 102.3 ppm, $\delta_{PBu_3}(^{31}P)$ = 20 ppm, $J(^{31}P-^{31}P)$ = 327 Hz].[43] We therefore treated 2*i*Pr[GaCl$_4$] and 2SiMe$_3$[GaCl$_4$] with PR$_3$ (R = Ph, *c*Hex) at −50 °C, and the mixtures were rapidly warmed to room temperature, resulting in vigorous gas evolution. The ^{31}P NMR spectra showed a species with an AX spin system supportive of a iminophosphorane-substituted phosphenium salt of the type [*i*Pr$_2$NNPPPh$_3$][GaCl$_4$] [17[GaCl$_4$]; $\delta_{phosphenium}(^{31}P)$ = 310.9 ppm, $\delta_{PBu_3}(^{31}P)$ = 28.8 ppm, $J(^{31}P-^{31}P)$ = 68 Hz] because Wolf et al. reported identical values for [*i*Pr$_2$NNPPPh$_3$][AlCl$_4$] (17[AlCl$_4$]), indicating that there is no electronic effect upon a change in the anion from GaCl$_4^-$ to AlCl$_4^-$. 2SiMe$_3$[GaCl$_4$] as a starting material yielded [(Me$_3$Si)$_2$NPNPPh$_3$][GaCl$_4$] (18[GaCl$_4$]) with a more deshielded phosphenium phosphorus atom because the resonance for this atom at 361.5 ppm is 50 ppm downfield-shifted compared to 17[GaCl$_4$], which clearly shows that the (Me$_3$Si)$_2$N substituent is more electron-withdrawing than *i*Pr$_2$N (vide infra). However, the molecular structure of 17[GaCl$_4$] and 18[GaCl$_4$] could not be determined. The introduction of P(*c*Hex)$_3$ as a base in the reaction with 2*i*Pr[GaCl$_4$] in CH$_2$Cl$_2$ resulted after concentration of the reaction mixture in the deposition of colorless crystals, which were identified by a single-crystal structure determination as [*i*Pr$_2$NNP(*c*Hex)$_3$][GaCl$_4$] (19). 19 crystallizes in the monoclinic space group $P2_1/c$ with two formula units and one molecule of CH$_2$Cl$_2$ in the asymmetric unit. In one cation, the *i*Pr$_2$NP group is disordered and split into two parts. In the other independent cation, one N*i*Pr moiety is found to be disordered. Because the molecular geometry is similar in both formula units, just one of the two cations is discussed. The metrical parameters are in the expected range and compare well with the values in 7$^+$ and 8$^+$ (Table 1). The bond distances N1−P1 (avg 1.62 Å), P1−N2 [1.573(3) Å], and N2−P2 [1.628(3) Å] are supportive of a phosphonium formulation similar to that discussed for 9$^+$.

In contrast, the addition of P(*c*Hex)$_3$ to a CH$_2$Cl$_2$ of 2SiMe$_3$[GaCl$_4$] was not accompanied by gas evolution, and in the ^{31}P NMR spectrum of the reaction mixture, two species were detected. On the one hand, the azidochlorophosphane (Me$_3$Si)$_2$NP(N$_3$)Cl (20SiMe$_3$) and, on the other hand, the GaCl$_3$ adduct of P(*c*Hex)$_3$ (*c*Hex)$_3$P···GaCl$_3$ (21),[44] which crystallize from concentrated reaction mixtures (Scheme 9), were observed. The main reason for the different reactivities observed supposedly lies in the steric congestion that stems from the N(SiMe$_3$)$_2$ moiety in 2SiMe$_3^+$, which effectively denies the formation of an iminophosphorane-substituted phosphenium salt.

The formation of 20SiMe$_3$ prompted us to investigate the possibility of using 2*i*Pr[GaCl$_4$] and 2SiMe$_3$[GaCl$_4$] as precursors for azido(chloro)phosphanes because these species cannot be prepared using standard routes such as the addition of 1 equiv of AgN$_3$, Me$_3$SiN$_3$, or NaN$_3$ because in all cases a mixture of mono- and disubstituted azidophosphanes was obtained. In contrast, in the presence of an excess of Me$_3$SiN$_3$, complete conversion to *i*Pr$_2$NP(N$_3$)$_2$ (22*i*Pr) and (Me$_3$Si)$_2$NP(N$_3$)$_2$ (22SiMe$_3$) was accomplished. It is worth noting that the synthesis of 22R can also be achieved by addition of 2 equiv of AgN$_3$ or NaN$_3$ in CH$_2$Cl$_2$ and workup from *n*-hexane (Scheme 10).

Scheme 10. Attempted Synthesis of Azidochlorophosphanes Resulting in the Formation of Diazides 22R (R = *i*Pr, SiMe$_3$) and Synthetic Access to 20R via bipy-Induced Chlorine Back-substitution to Azidophosphenium Species 2R[GaCl$_4$]

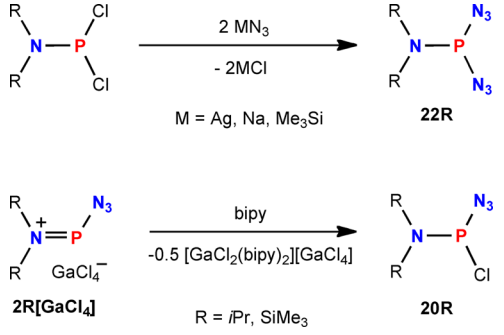

To circumvent these drawbacks, to a CH$_2$Cl$_2$ solution of 2R[GaCl$_4$] (R = iPr, SiMe$_3$) was added a stoichiometric amount of bipy to remove GaCl$_3$ and obtain the chloride-back-substituted chlorophosphane. Removal of the solvents in vacuo and extraction of the residues with *n*-hexane afforded in the case of 2*i*Pr[GaCl$_4$] a mixture of chlorophosphanes *i*Pr$_2$NP(N$_3$)Cl (20*i*Pr) [20*i*Pr $\delta(^{31}P)$ 155.1 ppm] and *i*Pr$_2$NPCl$_2$ (in an analogous procedure, 20SiMe$_3$ is obtained; 20SiMe$_3$ $\delta(^{31}P)$ 173.4 ppm). This mixture solidifies at ca. −25 °C, crystals suitable for X-ray analysis were selected at −50 °C, and the molecular structure was successfully determined (Figure 9). The crystal structure revealed, in good accordance with the ^{31}P NMR data, a mixture of both 20*i*Pr and *i*Pr$_2$NPCl$_2$ in an occupational disorder of 0.79/0.21 (Figure 9). 20*i*Pr crystallizes

dx.doi.org/10.1021/ic500332s | Inorg. Chem. 2014, 53, 3880−3892

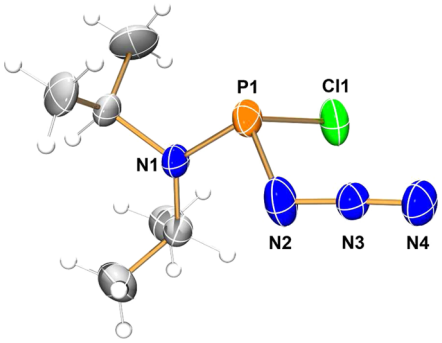

Figure 9. ORTEP drawing of the molecular structure of **20*i*Pr**. Ellipsoids are drawn at 50% probability, and just the main part of the mixed phosphane is shown because **20*i*Pr** crystallizes as a mixture of the general formula $iPr_2NPCl(N_3)_{0.79}(Cl)_{0.21}$. Selected bond lengths (Å) and angles (deg): P1−N1 1.658(1), N2−P1 1.76(3), N2−N3 1.24(1), N3−N4 1.125(4), P1−Cl1 2.1075(9); Σ(<N1) 359.26, Σ(<P1) 324.63; N2−N3−N4 177.3; N2−P1−N1−C4 −44.9.

in the monoclinic space group $P2_1/m$ with two molecules in the unit cell. **20*i*Pr** lies on a crystallographically imposed mirror plane, which results in disorder of the whole molecule. The P−N_{amino} bond [1.658(1) Å] is in the expected range for a P−N single bond in chlorophosphanes [cf. $(Me_3Si)_2NPCl_2$ 1.6468(8) Å],[19] with the azido group bound to the phosphorus via a P−N_{azide} [1.76(3) Å] single bond [cf. **10**[35] P−N_{azide} 1.698(5) Å, **23**[32] P−N_{azide}1.706(3) Å; Figure 5]. Conclusively, chlorine back-substitution with the aid of bipy is a viable route toward chlorophosphanes starting from phosphenium precursors, but in the presence of an azide substituent, scrambling of the substituents might result in mixed phosphanes.[40]

CONCLUSION

Azidophosphenium cations **2R**[$GaCl_4$] (R = *i*Pr, $SiMe_3$) were shown to be susceptible to the loss of dinitrogen in the presence of phosphanes. Starting from **2*i*Pr**[$GaCl_4$] or **2SiMe$_3$**[$GaCl_4$], different iminophosphorane-substituted polyphosphorus salts **7**[$GaCl_4$], **8**, **13**, and **14** could be obtained from Staudinger reactions with different chlorophosphanes, and the comprehensive chemistry of **7**[$GaCl_4$] was studied in detail. This study clearly demonstrates a misinterpretation of data published by Wolf and co-workers. In an effort to develop a route toward chlorophosphanes, phosphenium cations were shown to be transformed to chlorophosphanes by the addition of bipyridine as the chelating ligand, which effectively removes $GaCl_3$ from $GaCl_4^-$ salts. The new topology of the NPNPN cations formulated in this work might result in the formation and design of new polyphosphorus ligands for transition-metal fragments.

EXPERIMENTAL SECTION

Synthesis of [*i*Pr$_2$NPCl][$GaCl_4$] (1*i*Pr[$GaCl_4$]). A CH_2Cl_2 (2 mL) solution of $GaCl_3$ (0.189 g, 1.07 mmol) was added dropwise to a stirred solution of iPr_2NPCl_2 (0.213 g, 1.05 mmol) in CH_2Cl_2 (3 mL) at −75 °C. The clear colorless mixture was allowed to stir for 15 min and concentrated to incipient crystallization at −50 °C. Standing overnight at −80 °C yielded, after removal of the supernatant solution, 0.203 g (0.53 mmol, 51%) of **1*i*Pr**[$GaCl_4$] as colorless crystals.

Mp: 51 °C. Anal. Calcd (found): C, 19.06 (19.10); H, 3.73 (3.70); N, 3.70 (3.72). ^{1}H NMR (25 °C, CD_2Cl_2, 500.13 MHz): δ 1.49−1.59 (m, 12H, $CH(CH_3)_2$), 4.41−4.63 (m, 2H, $CH(CH_3)_2$). $^{13}C\{^1H\}$ NMR (25 °C, CD_2Cl_2, 125.76 MHz): δ 23.48 (d, $J(^{31}P-^{13}C)$ = 8.25 Hz, $CH(CH_3)_2$), 56.24−57.74 (m, $CH(CH_3)_2$), 58.19 (d, $J(^{31}P-^{13}C)$ = 8.25 Hz, $CH(CH_3)_2$). $^{31}P\{^1H\}$ NMR (25 °C, CD_2Cl_2, 202.46 MHz): δ 294.7 (br s, NPCl). Raman (100 mW, 25 °C, 3 scans, cm^{-1}): 3305(1), 3237(1), 3181(1), 2976(1), 2944(1), 1459(2), 1399(2), 1360(2), 1320(2), 1263(2), 1201(2), 1163(2), 1131(2), 1121(2), 1032(5), 927(2), 884(2), 634(3), 567(5), 506(3), 479(3), 397(3), 374(4), 360(3), 345(10), 265(3), 201(4).

Synthesis of [*i*Pr$_2$NPN$_3$][$GaCl_4$] (2*i*Pr[$GaCl_4$]). A CH_2Cl_2 (5 mL) solution of $GaCl_3$ (0.283 g, 1.61 mmol) was added dropwise to a stirred solution of iPr_2NPCl_2 (0.325 g, 1.61 mmol) in CH_2Cl_2 (2 mL) at −75 °C. The clear colorless mixture was allowed to stir for 30 min at this temperature and treated with a CH_2Cl_2 solution (5 mL) of Me_3SiN_3 (0.186 g, 1.61 mmol) afterward. The yellowish solution was concentrated to incipient crystallization, whereas the temperature was maintained below −30 °C. Standing overnight in a freezer (−80 °C) afforded, after removal of the supernatant liquid, 0.460 g (1.20 mmol, 75%) of **2*i*Pr**[$GaCl_4$] as colorless crystals.

Mp: 78 °C (dec). Anal. Calcd (found): C, 18.73 (19.32); H, 4.21 (3.90); N, 14.56 (14.30). ^{1}H NMR (−20 °C, CD_2Cl_2, 500.13 MHz): δ 1.44−1.57 (m, 12H, $CH(CH_3)_2$), 4.31−4.44 (m, 2H, $CH(CH_3)_2$). $^{13}C\{^1H\}$ NMR (0 °C, CD_2Cl_2, 125.76 MHz): δ 20.20 (s, $CH(CH_3)_2$), 21.70−22.24 (m, $CH(CH_3)_2$), 50.29−50.44 (m, $CH(CH_3)_2$), 51.01 (s, $CH(CH_3)_2$). $^{31}P\{^1H\}$ NMR (−20 °C, CD_2Cl_2, 202.46 MHz): δ 310.93 (s, NPN_3). IR (ATR, 25 °C, 32 scans, cm^{-1}): 3174 (w), 3101 (w), 2981 (w), 2939 (w), 2899 (w), 2879 (w), 2505 (w), 2159 (s), 1574 (w), 1468 (m), 1460 (w), 1411 (m), 1391 (w), 1373 (m), 1558 (s), 1207 (s), 1181 (m), 1165 (s), 1154 (s), 1139 (s), 1111 (s), 1020 (s), 965 (s), 909 (m), 885 (m), 848 (s), 754 (m), 638 (m), 569 (s), 552 (s), 542 (s). Raman (100 mW, 25 °C, 3 scans, cm^{-1}): 2988(1), 2969(1), 2947(1), 2896(1), 2873(1), 2733(1), 2174(10), 2166(4), 1464(3), 1441(3), 1413(3), 1372(3), 1307(3), 1207(3), 1167(3), 1023(6), 967(3), 886(3), 759(3), 639(3), 554(3), 543(3), 469(3), 398(3), 362(3), 347(7), 275(4), 241(3), 203(4).

Synthesis of [*i*Pr$_2$NPNP(Cl)$_2$N*i*Pr$_2$][$GaCl_4$] (7[$GaCl_4$]). *Procedure 1.* A CH_2Cl_2 (5 mL) solution of $GaCl_3$ (0.283 g, 1.6 mmol) was added dropwise to a stirred solution of iPr_2NPCl_2 (0.325 g, 1.6 mmol) in CH_2Cl_2 (2 mL) at −80 °C. The colorless mixture was allowed to stir for 30 min at this temperature. Afterward, a CH_2Cl_2 solution (2.5 mL) of Me_3SiN_3 (0.093 g, 0.8 mmol) was added at −60 °C, and the mixture was allowed to slowly warm to ambient temperature and stirred for 2 h. The mixture attained a yellow color, and gas evolution could be observed. After removal of the solvent in vacuo, a yellow oil is obtained as the crude product, from which colorless crystals grew. The crude mixture was taken up in fresh CH_2Cl_2 (0.5 mL) and placed in a freezer (−24 °C) for 12 h. After removal of the supernatant liquid, 0.394 g (0.71 mmol, 44%) of **7**[$GaCl_4$] was isolated as colorless crystals.

Procedure 2. A CH_2Cl_2 (3 mL) solution of $GaCl_3$ (0.186 g, 1.06 mmol) was added dropwise to a stirred solution of iPr_2NPCl_2 (0.213 g, 1.05 mmol) in CH_2Cl_2 (3 mL) at −80 °C. The colorless mixture was allowed to stir for 30 min at this temperature. Afterward, a CH_2Cl_2 solution (2.5 mL) of Me_3SiN_3 (0.123 mg, 1.05 mmol) was added at −60 °C, and the mixture was stirred for another 30 min, followed by the addition of another 1 equiv of iPr_2NPCl_2 (0.213 g, 1.05 mmol). Subsequently, the mixture was rapidly warmed to room temperature, which was accompanied by vigorous gas evolution. After stirring for 1 h and removal of the solvent in vacuo, a yellow oil was obtained as the crude product, which was washed with *n*-hexane (1 mL). The crude mixture is redissolved in CH_2Cl_2 (0.5 mL) and placed in a freezer (−24 °C) for 12 h. After removal of the supernatant liquid, 0.370 g (0.66 mmol, 63%) of **7**[$GaCl_4$] was isolated as colorless crystals.

Mp: 122−123 °C. Anal. Calcd (found): C, 25.79 (25.69); H, 5.05 (5.13); N, 7.52 (7.59). ^{1}H NMR (25 °C, CD_2Cl_2, 300.13 MHz): δ 1.41 (d, $J(^1H-^1H)$ = 6.80 Hz, 12H, $CH(CH_3)_2$), 1.44 (d, $J(^1H-^1H)$ = 6.99 Hz, 6H, $CH(CH_3)_2$), 1.61 (d, $J(^1H-^1H)$ = 6.80 Hz, 6H, $CH(CH_3)_2$), 3.91 (sept, $J(^1H-^1H)$ = 6.80 Hz, $CH(CH_3)_2$), 4.03 (sept, $J(^1H-^1H)$ = 6.80 Hz, $CH(CH_3)_2$), 4.08−4.25 (sept, $CH(CH_3)_2$), 4.88−4.98 (sept, $CH(CH_3)_2$). $^{13}C\{^1H\}$ NMR (25 °C, CD_2Cl_2, 75.48 MHz): δ 22.16 (d, $J(^{31}P-^{13}C)$ = 2.20 Hz, $CH(CH_3)_2$), 22.31 (d, $J(^{31}P-^{13}C)$ = 2.75 Hz, $CH(CH_3)_2$), 27.09 (d, $J(^{31}P-^{13}C)$ = 11.55 Hz, $CH(CH_3)_2$), 51.67 (d, $J(^{31}P-^{13}C)$ = 5.50 Hz, $CH(CH_3)_2$), 52.63 (d, $J(^{31}P-^{13}C)$ = 27.51 Hz, $CH(CH_3)_2$), 54.23 (d, $J(^{31}P-^{13}C)$ = 11.00 Hz,

dx.doi.org/10.1021/ic500332s | Inorg. Chem. 2014, 53, 3880−3892

$CH(CH_3)_2$). $^{31}P\{^1H\}$ NMR (25 °C, C_6D_6, 121.51 MHz): δ 27.40 (d, $J(^{31}P-^{31}P)$ = 111.5 Hz, $NPCl_2N$), 311.16 (d, $J(^{31}P-^{31}P)$ = 111.5 Hz, NPN). IR (ATR, 25 °C, 16 scans, cm^{-1}): 3167 (w), 2976 (w), 2935 (w), 2874 (w), 2164 (w), 1454 (w), 1413 (m), 1400 (w), 1390 (w), 1375 (m), 1282 (m), 1251 (m), 1237 (s), 1203 (m), 1170 (m), 1146 (s), 1122 (m), 1109 (s), 1027 (s), 989 (s), 968 (s), 887 (w), 859 (m), 797 (m), 738 (w), 659 (m), 754 (m), 636 (w), 607 (w), 564 (s), 551 (s). Raman (12 mW, 25 °C, 3 scans, cm^{-1}): 3238(1), 2984(1), 2940(1), 2456(1), 1456(1), 1444(1), 1415(1), 1318(1), 1205(1), 1168(1), 1144(1), 1123(1), 1031(1), 969(1), 945(1), 893(2), 861(1), 799(1), 756(1), 706(1), 660(1), 637(1), 570(1), 554(1), 504(2), 485(1), 469(1), 406(1), 378(1), 346(10), 326(1), 300(1), 289(1), 252(1), 220(1), 202(1).

Synthesis of $[i\mathrm{Pr_2NPNP(Cl)_2N(SiMe_3)_2}][\mathrm{GaCl_4}]$ (8). To a cooled sample of $\mathbf{2}i\mathbf{Pr}[\mathbf{GaCl_4}]$ (0.326 g, 0.85 mmol) at −50 °C was added a CH_2Cl_2 (3 mL) solution of $(Me_3Si)_2NPCl_2$ (0.223 g, 0.85 mmol) at that temperature, and the mixture was slowly warmed to room temperature over a period of 2 h. At ca. −30 °C, vigorous gas evolution was observed. Removal of the solvents in vacuo resulted in an oily colorless residue, which was washed with *n*-hexane (1 mL). The residual oil was redissolved in minimal amounts of C_6H_5F, and standing at 5 °C for 12 h afforded colorless crystals of **8** (0.280 g, 0.45 mmol, 53%).

Anal. Calcd (found): C, 23.29 (23.59); H, 5.21 (4.92); N, 6.79 (7.32). ^1H NMR (25 °C, CD_2Cl_2, 300.13 MHz): δ 1.38 (d, $^3J(^1H-^1H)$ = 6.8 Hz, 6H, $C(CH_3)_2$), 1.61 (d, $^3J(^1H-^1H)$ = 6.8 Hz, 6H, $C(CH_3)_2$), 4.1 (sept, $^3J(^1H-^1H)$ = 6.8 Hz = 1H, $CH(CH_3)_2$), 5.03 (sept, d, $^3J(^1H-^1H)$ = 6.8 Hz, $J(^{31}H-^1H)$ = 2.8 Hz, $CH(CH_3)_2$). $^{31}P\{^1H\}$ NMR (25 °C, CD_2Cl_2/CH_2Cl_2, 121.51 MHz): δ 311.3 (d, $^2J(^{31}P-^{31}P)$ = 111.5 Hz, $NPNiPr_2$), 30.4 (d, $NP(Cl)_2N$). Raman (100 mW, 25 °C, 4 scans, cm^{-1}): 2986(3), 2970(2), 2944(2), 2906(4), 2732(1), 1459(3), 1361(2), 1331(2), 1168(2), 1142(2), 1136(2), 1033(3), 1011(2), 972(2), 969(2), 892(3), 862(2), 773(2), 659(6), 641(5), 576(2), 554(2), 500(3), 471(2), 451(3), 419(2), 402(2), 370(3), 345(10), 290(2), 213(2).

Synthesis of $[i\mathrm{Pr_2NP(dmb)NP(Cl)_2N}i\mathrm{Pr_2}][\mathrm{GaCl_4}]$ (7-dmb-$[\mathrm{GaCl_4}]$). A CH_2Cl_2 (5 mL) solution of dmb (0.071 g, 0.86 mmol) was added dropwise to a CH_2Cl_2 solution of $\mathbf{7}[\mathbf{GaCl_4}]$ (0.200 g, 0.36 mmol) at −20 °C. The colorless mixture was allowed to slowly warm to room temperature over a period of 2 h. Afterward, the solvent was removed in vacuo, and the white solids were washed with *n*-hexane, taken up in CH_2Cl_2 (0.5 mL), and placed in a freezer (−40 °C) for 12 h. After removal of the supernatant liquid, 0.100 g (0.16 mmol, 44%) of $\mathbf{7\text{-}dmb}[\mathbf{GaCl_4}]$ was isolated as colorless crystals.

Mp: 156 °C. Anal. Calcd (found): C, 33.73 (33.53); H, 5.98 (5.36); N, 6.56 (6.46). ^1H NMR (25 °C, CD_2Cl_2, 300.14 MHz): δ 1.34 (d, $J(^1H-^1H)$ = 6.80 Hz, 24H, $CH(CH_3)_3$), 1.84 (s, 6H, CCH_3), 2.87–3.18 (m, 4H, $PCCH_2$), 3.64 (sept, $J(^1H-^1H)$ = 6.80 Hz, $CH(CH_3)_3$), 3.69 (sept, $J(^1H-^1H)$ = 6.80 Hz, $CH(CH_3)_3$), 3.79 (sept, $J(^1H-^1H)$ = 6.80 Hz, $CH(CH_3)_3$), 3.89 (sept, $J(^1H-^1H)$ = 6.80 Hz, $CH(CH_3)_3$). $^{13}C\{^1H\}$ NMR (25 °C, CD_2Cl_2, 75.48 MHz): δ 16.88 (d, $J(^{31}P-^{13}C)$ = 15.41 Hz, CCH_3), 21.89 (d, $J(^{31}P-^{13}C)$ = 2.20 Hz, $CH(CH_3)_2$), 23.32 (d, $J(^{31}P-^{13}C)$ = 3.30 Hz, $CH(CH_3)_2$), 38.64 (d, $J(^{31}P-^{13}C)$ = 3.30 Hz, $PCCH_2$), 39.79 (d, $J(^{31}P-^{13}C)$ = 3.30 Hz, $PCCH_2$), 49.87 (d, $J(^{31}P-^{13}C)$ = 2.20 Hz, $CH(CH_3)_2$), 50.73 (d, $J(^{31}P-^{13}C)$ = 6.05 Hz, $CH(CH_3)_2$), 128.22 (d, $J(^{31}P-^{13}C)$ = 12.11 Hz, $C_2C{=}CC_2$). $^{31}P\{^1H\}$ NMR (25 °C, CD_2Cl_2, 121.51 MHz): δ −4.35 (d, $J(^{31}P-^{31}P)$ = 5.87 Hz, $NPCl_2N$), 48.08 (d, $J(^{31}P-^{31}P)$ = 5.87 Hz, NPC_2N). IR (ATR, 25 °C, 32 scans, cm^{-1}): 2981 (w), 2937 (w), 2913 (w), 2877 (w), 2856 (w), 2168 (w), 1468 (w), 1441 (w), 1412 (m), 1391 (m), 1375 (m), 1288 (s), 1215 (m), 1206 (m), 1192 (w), 1175 (m), 1153 (m), 1136 (m), 1112 (m), 1082 (w), 1018 (s), 990 (s), 949 (w), 926 (w), 894 (w), 866 (w), 852 (m), 841 (m),796 (m), 742 (w), 709 (m), 658 (m), 646 (w), 547 (s), 527 (m). Raman (100 mW, 25 °C, 4 scans, cm^{-1}): 2990(1), 2971(1), 2945(1), 2930(1), 2907(1), 2737(1), 2722(1), 1667(1), 1468(1), 1445(1), 1416(1), 1405(1), 1385(1), 1326(1), 1311(1), 1292(1), 1210(1), 1180(1), 1154(1), 1137(1), 1127(1), 1117(1), 1033(1), 1000(1), 946(1), 928(1), 895(3), 854(1), 842(1), 797(1), 720(1), 711(1), 660(1), 647(1), 551(1), 527(1), 493(1), 456(3), 429(1), 408(3), 377(1), 347(10), 296(1), 254(1), 201(2).

Synthesis of $[i\mathrm{Pr_2NP(Cl)NP(Cl)_2N}i\mathrm{Pr_2}][\mathrm{GaCl_4}]$ (7-Cl). A CH_2Cl_2 (5 mL) solution of 2,2′-bipyridine (0.157 g, 1.01 mmol) was dropwise added to a CH_2Cl_2 solution of $\mathbf{7}[\mathbf{GaCl_4}]$ (0.559 g, 1.00 mmol) at 0 °C. The obtained suspension was allowed to stir at room temperature over a period of 2 h, the solvent was removed in vacuo afterward, and the residues were extracted with *n*-hexane and filtered. Removal of *n*-hexane in vacuo yielded 0.283 g (0.74 mmol, 74%) of **7-Cl** as a colorless crystalline solid.

Mp: 60 °C (dec). Anal. Calcd (found): C, 37.66 (38.091); H, 7.37 (7.31); N, 10.98 (11.30). ^1H NMR (25 °C, CD_2Cl_2, 300.14 MHz): δ 1.09–1.43 (m, 24H, $CH(CH_3)_3$), 3.76 (sept, $J(^1H-^1H)$ = 6.80 Hz, $2CH(CH_3)_3$), 3.86 (sept, $J(^1H-^1H)$ = 6.80 Hz, $2CH(CH_3)_3$). $^{31}P\{^1H\}$ NMR (25 °C, CD_2Cl_2, 121.51 MHz): δ 156.2 (d, $J(^{31}P-^{31}P)$ = 140.85 Hz, NPClN), −6.4 (d, $J(^{31}P-^{31}P)$ = 140.85 Hz, $NPCl_2N$). IR (ATR, 25 °C, 32 scans, cm^{-1}): 2971 (m), 2932 (w), 2871 (w), 2835 (w), 2760 (w), 2722 (w), 1463 (w), 1407 (m), 1395 (w), 1367 (m), 1315 (s), 1273 (m), 1199 (m), 1173 (s), 1150 (s), 1116 (s), 1021 (m), 991 (s), 972 (s), 880 (m), 857 (m), 725 (m), 653 (m), 634 (m), 551 (s), 528 (s). Raman (632 nm, 100 mW, 25 °C, 5 scans, cm^{-1}): 2973(5), 2957(5), 2946(7), 2934(7), 2896(4), 2874(4), 2725(2), 2715(2), 1463(4), 1455(4), 1408(2), 1391(2), 1380(3), 1372(3), 1323(3), 1315(3), 1200(2), 1174(2), 1142(2), 1120(2), 1031(2), 1023(2), 992(2), 974(3), 944(2), 936(2), 924(1), 892(4), 880(3), 858(1), 655(2), 634(5), 552(2), 504(4), 494(2), 453(7), 407(5), 398(3), 386(3), 366(2), 337(2), 318(1), 287(10), 235(2).

Decomposition of $[(\mathrm{Me_3Si})_2\mathrm{NPN_3}][\mathrm{GaCl_4}]$. A CH_2Cl_2 solution of freshly prepared $\mathbf{2SiMe_3}[\mathbf{GaCl_4}]$ in CH_2Cl_2 (5 mL) at −75 °C was allowed to slowly warm to room temperature over a period of 4 h, resulting in a yellowish reaction mixture, while gas evolution was observed. The solvents were removed in vacuo, and the oily residues were washed with *n*-hexane (1 mL). The residual yellowish oil was redissolved in CH_2Cl_2 (2 mL) and concentrated to a volume of 0.3 mL. Crystallization attempts from CH_2Cl_2 and C_6H_5F and vapor diffusion of *n*-hexane into a saturated CH_2Cl_2 solution failed in all cases, and the products were identified by ^{31}P NMR spectroscopy.

$^{31}P\{^1H\}$ NMR (−40 °C, CD_2Cl_2, 121.49 MHz): for $\mathbf{2Si\text{-}Me_3}[\mathbf{GaCl_4}]$, 368.6 (s); $\mathbf{13}^+$), 357.6 (d, $J(^{31}P-^{31}P)$ = 90.8 Hz), 29.3 (d, $J(^{31}P-^{31}P)$ = 90.8 Hz); for $\mathbf{14}^+$, 354.4 (d, $J(^{31}P-^{31}P)$ = 79.9 Hz), 22.1 (d, $J(^{31}P-^{31}P)$ = 79.9 Hz).

Synthesis of $[(\mathrm{Me_3Si})_2\mathrm{N_2P_2Cl_2N(Ga_2Cl_5)}]$ (15). A CH_2Cl_2 solution (4 mL) of $GaCl_3$ (0.177 g, 1.00 mmol) was dropwise added to a stirred solution of $(Me_3Si)_2NPCl_2$ (0.263 g, 1.00 mmol) in CH_2Cl_2 (2 mL) at −75 °C. The resulting colorless solution was maintained at that temperature for 30 min and treated with a CH_2Cl_2 (2 mL) solution of Me_3SiN_3 (0.060 g, 0.52 mmol) afterward. The colorless clear mixture was slowly warmed to room temperature, with bubbling setting in at −20 °C. Stirring at room temperature for 1 h resulted in a yellowish solution, from which the solvents were removed in vacuo and the oily residues were washed with *n*-hexane (1 mL). The residual yellowish oil was redissolved in CH_2Cl_2 and concentrated to incipient crystallization. After standing at −24 °C for 72 h, colorless crystalline plates of **15** were obtained but could not be effectively separated from the supernatant oil.

Anal. Calcd (found): C, 11.30 (12.63); H, 2.84 (3.13); N, 6.59 (5.61). ^1H NMR (25 °C, CD_2Cl_2, 300.13 MHz): δ 0.50 (s, 18H, $Si(CH_3)_3$). $^{13}C\{^1H\}$ NMR (25 °C, CD_2Cl_2, 75.48 MHz): δ 0.37 (dd, $J(^{31}P-^{13}C)$ = 2.7 Hz, $J(^{31}P-^{13}C)$ = 3.7 Hz, $Si(CH_3)_3$). INEPT ^{29}Si NMR (25 °C, CD_2Cl_2, 59.62 MHz): δ 16.09 (s, $Si(CH_3)_3$). $^{31}P\{^1H\}$ NMR (25 °C, CD_2Cl_2, 121.49 MHz): δ 23.86 (d, $J(^{31}P-^{31}P)$ = 64.5 Hz), 142.64 (d, $J(^{31}P-^{31}P)$ = 64.5 Hz).

Synthesis of $[\mathrm{R_2NPNPPh_3}][\mathrm{GaCl_4}]$ [R = $i\mathrm{Pr_2}$ (17), $\mathrm{SiMe_3}$ (18)]. A CH_2Cl_2 solution of $GaCl_3$ (0.174 g, 0.99 mmol) was dropwise added to a stirred solution of R_2NPCl_2 (R = *i*Pr, $SiMe_3$) (0.202 or 0.263 g, 1 mmol) in CH_2Cl_2 (2 mL) −75 °C. The resulting colorless solution was maintained at that temperature for 30 min and treated with a CH_2Cl_2 (2 mL) solution of Me_3SiN_3 (113 mg, 0.98 mmol) afterward, resulting in the formation of a colorless crystalline solid that precipitates from the reaction mixture. Subsequently, a CH_2Cl_2 (5 mL) solution of PPh_3 (263 mg, 1.0 mmol) was dropwise added at −50 °C and the mixture rapidly warmed to ambient temperature, which

dx.doi.org/10.1021/ic500332s | Inorg. Chem. 2014, 53, 3880–3892

was accompanied by vigorous gas evolution. Stirring for 1 h resulted in a yellowish solution, from which the solvent was removed in vacuo, and the oily residues were washed with *n*-hexane (1 mL). Crystallization attempts from CH_2Cl_2 and C_6H_5F and vapor diffusion of *n*-hexane into a saturated CH_2Cl_2 solution failed in all cases, and the products were identified by ^{31}P NMR spectroscopy.

[*i*Pr$_2$NPNPPh$_3$][GaCl$_4$] (**17**). ^1H NMR (25 °C, CD_2Cl_2/CH_2Cl_2, 300.13 MHz): δ 1.47 (d, $J(^1H-^1H)$ = 6.80 Hz, 6H, CH(CH_3)$_2$), 1.52 (d, $J(^1H-^1H)$ = 6.80 Hz, 6H, CH(CH_3)$_2$), 4.08 (sept, $J(^1H-^1H)$ = 6.80 Hz, C*H*(CH$_3$)$_2$), 4.77−4.88 (m, C*H*(CH$_3$)$_2$), 7.57−7.70 (m, 12H, *m*-C*H*, *o*-C*H*), 7.76−7.82 (m, 3H, *p*-C*H*). $^{31}P\{^1H\}$ NMR (25 °C, CD_2Cl_2/CH_2Cl_2, 121.51 MHz): δ 28.82 (d, $J(^{31}P-^{31}P)$ = 67.5 Hz, N*P*Ph$_3$), 310.85 (d, $J(^{31}P-^{31}P)$ = 67.5 Hz, N*P*N).

[(Me$_3$Si)$_2$NPNPPh$_3$][GaCl$_4$] (**18**). ^1H NMR (25 °C, CD_2Cl_2, 300.13 MHz): δ 0.47 (d, $J(^{31}P-^1H)$ = 1.51 Hz, 18H, Si(CH_3)$_3$), 7.52−7.70 (m, 12H, *o*-C*H*, *m*-C*H*), 7.75−7.84 (m, 3H, *p*-C*H*). $^{31}P\{^1H\}$ NMR (25 °C, CD_2Cl_2, 121.51 MHz): δ 30.09 (d, $J(^{31}P-^{31}P)$ = 59 Hz, N*P*Ph$_3$), 361.50 (d, $J(^{31}P-^{31}P)$ = 59 Hz, N*P*N).

Synthesis of [*i*Pr$_2$NPNP*c*Hex$_3$][GaCl$_4$] (19). A CH_2Cl_2 solution of $GaCl_3$ (0.174 g, 0.99 mmol) was dropwise added to a stirred solution of *i*Pr$_2$NPCl$_2$ (0.263 g, 1.0 mmol) in CH_2Cl_2 (2 mL) at −75 °C. The resulting colorless solution was maintained at that temperature for 30 min and was treated with a CH_2Cl_2 (2 mL) solution of Me_3SiN_3 (113 mg, 0.98 mmol) afterward, resulting in the formation of a colorless crystalline solid that precipitates from the reaction mixture. Subsequently, a CH_2Cl_2 (4 mL) solution of P*c*Hex$_3$ (278 mg, 0.99 mmol) was added dropwise at −60 °C and the mixture rapidly warmed to ambient temperature, which was accompanied by vigorous gas evolution. Stirring for 1 h resulted in a yellowish solution from which the solvents were removed in vacuo, and the oily residues were washed with *n*-hexane (1 mL). The residual yellowish oil was redissolved in CH_2Cl_2 and concentrated to incipient crystallization. After standing for 48 h at −24 °C, colorless crystals of **19** were obtained (0.275 g, 0.41 mmol, 41%).

Mp: 159−164 °C (dec). Anal. Calcd (found): C, 43.80 (43.58); H, 7.06 (6.98); N, 4.09 (3.78). ^1H NMR (25 °C, CD_2Cl_2, 300.13 MHz): δ 1.23−1.52 (m, 14H, P(C$_6$H$_{11}$)$_3$), 1.37 (d, $J(^1H-^1H)$ = 6.80 Hz, 6H, CH(CH_3)$_2$), 1.48 (d, $J(^1H-^1H)$ = 6.80 Hz, 6H, CH(CH_3)$_2$), 1.76−1.83 (m, 3H, P(C$_6$H$_{11}$)$_3$), 1.87−1.98 (m, 12H, P(C$_6$H$_{11}$)$_3$), 2.11−2.27 (m, 4H, P(C$_6$H$_{11}$)$_3$), 4.00 (sept, $J(^1H-^1H)$ = 6.80 Hz, C*H*(CH$_3$)$_2$), 4.60−4.74 (m, C*H*(CH$_3$)$_2$). $^{13}C\{^1H\}$ NMR (25 °C, CD_2Cl_2, 75.46 MHz): δ 19.90 (s, P(C$_6$H$_{11}$)$_3$), 22.24 (d, $J(^{31}P-^{13}C)$ = 2.20 Hz, P(C$_6$H$_{11}$)$_3$), 25.49 (s, P(C$_6$H$_{11}$)$_3$), 26.11 (d, $J(^{31}P-^{13}C)$ = 1.10 Hz, CH(*C*H$_3$)$_2$), 26.25 (s, P(C$_6$H$_{11}$)$_3$), 26.61 (s, P(C$_6$H$_{11}$)$_3$), 26.78 (s, P(C$_6$H$_{11}$)$_3$), 26.83−27.06 (m, P(C$_6$H$_{11}$)$_3$), 28.48 (s, P(C$_6$H$_{11}$)$_3$), 28.61 (d, $J(^{31}P-^{13}C)$ = 3.85 Hz, P(C$_6$H$_{11}$)$_3$), 34.75 (d, $J(^{31}P-^{13}C)$ = 55 Hz, P(C$_6$H$_{11}$)$_3$), 49.62 (s, *C*H(CH$_3$)$_2$), 49.85−50.17 (m, *C*H(CH$_3$)$_2$), 50.54 (s, *C*H(CH$_3$)$_2$). $^{31}P\{^1H\}$ NMR (25 °C, CD_2Cl_2/CH_2Cl_2, 121.51 MHz): δ 49.1 (d, $J(^{31}P-^{31}P)$ = 23.5 Hz, N*P*(C$_6$H$_{11}$)$_3$), 303.81 (s, N*P*N). IR (ATR, 25 °C, 32 scans, cm^{-1}): 3183 (w), 2973 (w), 2933 (s), 2856 (s), 2725 (w), 2674 (w), 2092 (w), 1591 (w), 1447 (s), 1408 (w), 1397 (w), 1386 (w), 1371 (m), 1296 (m), 1260 (s), 1228 (m), 1202 (s), 1174 (s), 1157 (m), 1116 (s), 1041 (m), 1004 (s), 981 (s), 919 (m), 889 (s), 850 (s), 824 (m), 773 (m), 760 (m), 739 (m), 693 (w), 636 (w), 578 (w), 540 (s), 530 (s). Raman (12 mW, 25 °C, 3 scans, cm^{-1}): 3237(1), 2977(1), 2941(1), 2904(1), 2877(1), 2858(1), 2398(1), 1445(1), 1389(1), 1381(1), 1354(1), 1331(1), 1294(1), 1284(1), 1217(1), 1206(1), 1174(1), 1119(1), 1087(1), 1051(1), 1023(2), 1005(1), 982(1), 942(1), 887(1), 848(1), 818(2), 792(1), 774(1), 761(1), 740(1), 694(1), 687(1), 637(2), 556(2), 541(1), 518(1), 506(1), 469(1), 444(1), 421(1), 375(2), 343(10), 321(1), 309(1), 298(1), 220(3).

Synthesis of R$_2$NP(Cl)N$_3$ (20*i*Pr, 20SiMe$_3$). To a solution of **2*i*Pr**[**GaCl$_4$**] (0.385 g, 1.0 mmol) in CH_2Cl_2 (4 mL) was added dropwise a solution of bipy (0.157 g, 1.0 mmol) at −75 °C, and the resulting colorless suspension was allowed to warm to ambient temperatures, which resulted in a color change to orange. After stirring at room temperature for 1 h, the solvent was removed in vacuo, and the residual solids were extracted with *n*-hexane (5 mL). The colorless filtrate was concentrated to incipient crystallization and stored at −40 °C for 4 days, resulting in the deposition of colorless crystals of **20*i*Pr**. At room temperature, crystals of **20*i*Pr** rapidly melt, whereas only NMR data could be collected for this compound. **20SiMe$_3$** can be obtained in an analogous procedure.

^1H NMR (25 °C, CD_2Cl_2, 500.13 MHz): δ 1.19 (d, $J(^1H-^1H)$ = 6.94 Hz, 6H, CH(CH_3)$_2$), 1.28 (d, $J(^1H-^1H)$ = 6.62 Hz, 6H, CH(CH_3)$_2$), 3.76 (sept, $J(^1H-^1H)$ = 6.94 Hz, C*H*(CH$_3$)$_2$), 3.92 (sept, $J(^1H-^1H)$ = 6.62 Hz, 6H, C*H*(CH$_3$)$_2$). $^{13}C\{^1H\}$ NMR: δ 23.56 (d, $J(^{31}P-^{13}C)$ = 11.00 Hz, CH(*C*H$_3$)$_2$), 24.25 (d, $J(^{31}P-^{13}C)$ = 3.67 Hz, CH(*C*H$_3$)$_2$), 48.12 (d, $J(^{31}P-^{13}C)$ = 11.91 Hz, *C*H(CH$_3$)$_2$), 48.94 (d, $J(^{31}P-^{13}C)$ = 13.75 Hz, *C*H(CH$_3$)$_2$). $^{31}P\{^1H\}$ NMR (25 °C, CD_2Cl_2, 202.46 MHz): δ 155.12 (s, N*P*ClN$_3$), 173.4 (s, N*P*ClN$_3$) (**20SiMe$_3$**).

■ ASSOCIATED CONTENT

Ⓢ Supporting Information

X-ray crystallographic data in CIF format, general information, structure elucidation, synthesis, and computational details. This material is available free of charge via the Internet at http://pubs.acs.org.

■ AUTHOR INFORMATION

Corresponding Author

*E-mail: axel.schulz@uni-rostock.de.

Notes

The authors declare no competing financial interest.

■ ACKNOWLEDGMENTS

Dr. Dirk Michalik is gratefully acknowledged for his help with variable-temperature ^{31}P NMR experiments. Financial support by the Fonds der chemischen Industrie (fellowship to C.H.) and the DFG (Grant SCHU 1170/8-1) is gratefully acknowledged.

■ REFERENCES

(1) Dimroth, K.; Hoffmann, P. *Angew. Chem., Int. Ed. Engl.* **1964**, *3*, 384−384.
(2) Kopp, R. W.; Bond, A. C.; Parry, R. W. *Inorg. Chem.* **1976**, *15*, 3042−3046.
(3) Cowley, A. H.; Kemp, R. A. *Chem. Rev.* **1985**, *85*, 367−382.
(4) Gudat, D. *Coord. Chem. Rev.* **1997**, *163*, 71−106.
(5) Gudat, D. *Acc. Chem. Res.* **2010**, *43*, 1307−1316.
(6) Hering, C.; Schulz, A.; Villinger, A. *Angew. Chem., Int. Ed.* **2012**, *51*, 6241−6245.
(7) Holthausen, M. H.; Weigand, J. J. *Z. Anorg. Allg. Chem.* **2012**, *638*, 1103−1108.
(8) Marre, M.-R.; Sanchez, M.; Wolf, R. *J. Chem. Soc., Chem. Commun.* **1984**, 566−567.
(9) Mazieres, M. R.; Sanchez, M.; Bellan, J.; Wolf, R. *Phosphorous Sulfur Relat Elem.* **1986**, *26*, 97−99.
(10) Staudinger, H.; Meyer, J. *Helv. Chim. Acta* **1919**, *2*, 612−618.
(11) Gololobov, Y. G.; Zhmurova, I. N.; Kasukhin, L. F. *Tetrahedron* **1981**, *37*, 437−472.
(12) Hering, C.; Schulz, A.; Villinger, A. *Inorg. Chem.* **2013**, *52*, 5214−5225.
(13) Guerret, O.; Bertrand, G. *Acc. Chem. Res.* **1997**, *30*, 486−493.
(14) Dielmann, F.; Back, O.; Henry-Ellinger, M.; Jerabek, P.; Frenking, G.; Bertrand, G. *Science* **2012**, *337*, 1526−1528.
(15) Dielmann, F.; Moore, C. E.; Rheingold, A. L.; Bertrand, G. *J. Am. Chem. Soc.* **2013**, *135*, 14071−14073.
(16) Schmidpeter, A. Multiple Bonds and Low Coordination Chemistry. In *Phosphorus Chemistry*; Regitz, M., Scherer, O., Eds.; Georg Thieme Verlag: Stuttgart, Germany, 1990; Vol. D2, p 149.
(17) Boeske, J.; Ocando-Mavarez, E.; Niecke, E.; Majoral, J. P.; Bertrand, G. *J. Am. Chem. Soc.* **1987**, *109*, 2822−2823.
(18) Boeske, J.; Niecke, E.; Nieger, M.; Ocando, E.; Majoral, J. P.; Bertrand, G. *Inorg. Chem.* **1989**, *28*, 499−504.

(19) Hering, C.; Schulz, A.; Villinger, A. *Angew. Chem., Int. Ed.* **2012**, *51*, 6241−6245.
(20) Schultz, C. W.; Parry, R. W. *Inorg. Chem.* **1976**, *15*, 3046−3050.
(21) Cowley, A. H.; Kemp, R. A.; Lasch, J. G.; Norman, N. C.; Stewart, C. A.; Whittlesey, B. R.; Wright, T. C. *Inorg. Chem.* **1986**, *25*, 740−749.
(22) Kasaka, T.; Matsumura, A.; Kyoda, M.; Fujimoto, T.; Ohta, K.; Yamamoto, I.; Kakehi, A. *J. Chem. Soc., Perkin Trans. 1* **1994**, 2867.
(23) Huang, T.-B.; Wang, K.; Liu, L.-F.; He, F.-H. *Main Group Chem.* **1999**, *3*, 5−14.
(24) Pyykkã, P.; Atsumi, M. *Chem.—Eur. J.* **2009**, *15*, 12770−12779.
(25) (a) Mantina, M.; Chamberlin, A. C.; Valero, R.; Cramer, C. J.; Truhlar, D. G. *J. Phys. Chem. A* **2009**, *113*, 5806−5812. (b) Alvarez, S. *Dalton Trans.* **2013**, *42*, 8617−8636.
(26) Holthausen, M. H.; Feldmann, K.-O.; Schulz, S.; Hepp, A.; Weigand, J. J. *Inorg. Chem.* **2012**, *51*, 3374−3387.
(27) Michalik, D.; Schulz, A.; Villinger, A. *Inorg. Chem.* **2008**, *47*, 11798−11806.
(28) Hering, C.; Lehmann, M.; Schulz, A.; Villinger, A. *Inorg. Chem.* **2012**, *51*, 8212−8224.
(29) Westenkirchner, A.; Villinger, A.; Karaghiosoff, K.; Wustrack, R.; Michalik, D.; Schulz, A. *Inorg. Chem.* **2011**, *50*, 2691−2702.
(30) Schulz, A.; Mayer, P.; Villinger, A. *Inorg. Chem.* **2007**, *46*, 8316−8322.
(31) Herler, S.; Mayer, P.; Schmedt auf der Günne, J.; Schulz, A.; Villinger, A.; Weigand, J. J. *Angew. Chem., Int. Ed.* **2005**, *44*, 7790−7793.
(32) Michalik, D.; Schulz, A.; Villinger, A.; Weding, N. *Angew. Chem., Int. Ed.* **2008**, *47*, 6465−6468.
(33) Computational details can be found in the Supporting Information (SI) on p 37.
(34) Marre-Mazieres, M. R.; Sanchez, M.; Wolf, R.; Bellan, J. *Nouv. J. Chim.* **1985**, *9*, 605−615.
(35) Schulz, A.; Villinger, A. *Eur. J. Inorg. Chem.* **2008**, *27*, 4199−4203.
(36) Schwesinger, R.; Willaredt, J.; Schlemper, H.; Keller, M.; Schmitt, D.; Fritz, H. *Eur. J. Inorg. Chem.* **1994**, *127*, 2435−2454.
(37) Restivo, R.; Palenik, G. J. *J. Chem. Soc. D* **1969**, 867.
(38) Restivo, R.; Palenik, G. J. *J. Chem. Soc., Dalton Trans.* **1972**, 341−344.
(39) Reiß, F.; Schulz, A.; Villinger, A. *Eur. J. Inorg. Chem.* **2012**, *2*, 261−271.
(40) Rosenstengel, K.; Schulz, A.; Villinger, A. *Inorg. Chem.* **2013**, *52*, 6110−6126.
(41) Villinger, A.; Westenkirchner, A.; Wustrack, R.; Schulz, A. *Inorg. Chem.* **2008**, *47*, 9140−9142.
(42) Hubrich, C.; Michalik, D.; Schulz, A.; Villinger, A. *Z. Anorg. Allg. Chem.* **2008**, *634*, 1403−1408.
(43) Mazieres, M. R.; Roques, C.; Sanchez, M.; Majoral, J. P.; Wolf, R. *Tetrahedron* **1987**, *43*, 2109−2118.
(44) The structure of **21** was determined by X-ray crystallography, and the molecular structure is shown in the SI, Figure S2.

5.2 On the Synthesis and Reactivity of Highly Labile Pseudohalogen Phosphenium Ions

Christian Hering, Axel Schulz, Alexander Villinger.

Inorganic Chemistry, **2013**, *52*, 5214−5225.

DOI: 10.1021/ic4001285

In dieser Publikation wurden sämtliche experimentelle Arbeiten von mir durchgeführt. Der eigene Beitrag liegt bei ca. 90 %.

Inorganic Chemistry

Article

pubs.acs.org/IC

On the Synthesis and Reactivity of Highly Labile Pseudohalogen Phosphenium Ions

Christian Hering,[†] Axel Schulz,*[,†,‡] and Alexander Villinger[†]

[†]Institut für Chemie, Abteilung Anorganische Chemie, Universität Rostock, Albert-Einstein-Strasse 3a, 18059 Rostock, Germany

[‡]Leibniz-Institut für Katalyse e.V. an der Universität Rostock, Albert-Einstein-Strasse 29a, 18059 Rostock, Germany

Supporting Information

ABSTRACT: The synthesis and characterization of salts bearing highly labile pseudohalogen-substituted aminophosphenium cations of the type $[(Me_3Si)_2NPX][GaCl_4]$ (X = NCO, NCS, $O(SiMe_3)$) and their respective reactivity toward Lewis bases (4-dimethylaminopyridine, dmap) and dienes (2,3-dimethyl-1,3-butadiene, dmb; 1,3-*cyclo*-hexadiene, chd) are described. As π-acidic species, aminophosphenium cations react with dmap at low temperatures to yield adduct salts of the type $[(Me_3Si)_2NP(dmap)X][GaCl_4]$ (X = Cl, N_3, NCO) which were fully characterized. In the reaction with dienes at −50 °C, salts bearing phospholenium cations were obtained that could be structurally characterized. The crystal structures of novel 7-phosphanorbornenium cations of the type $[(Me_3Si)_2NP(C_6H_8)X][GaCl_4]$ (X = Cl, N_3, NCO) are reported. All compounds were further investigated by means of density functional theory, and the bonding situation was accessed by Natural Bond Orbital (NBO) analysis.

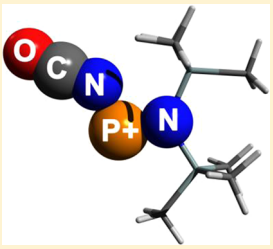

INTRODUCTION

Phosphenium cations are phosphorus analogues of the carbenes, as they possess a dicoordinated, formally positively charged phosphorus atom, isolobally replacing the carbon. Consequently phosphenium cations of the type X-P-Y are stabilized best when X and Y are π-electron donors stabilizing the electron deficient phosphorus atom.[1] Schmidpeter suggested to categorize phosphenium cations into two groups which differ in the charge distribution in the π-electron system. On the one hand the positive charge of the cation is localized exclusively on the substituents, with a nucleophilic phosphorus (type A), and on the other hand the phosphorus is positively charged in the π-bond system and may be regarded as an ambiphilic center exhibiting both electrophilic and nucleophilic character (type B) (Scheme 1).[2] Dimroth and co-workers reported on the first phosphenium species in phosphamethine cyanines as early as 1964 (Figure 1, species **1**).[3] In 1975 the first acylic phosphenium cations, $[(Me_2N)_2P]^+$ and $[(Me_2N)PCl]^+$, were prepared by Parry et al. utilizing halide ion abstraction from the precursor aminohalophosphines (Figure 1, species **2**).[4] Dimroth's phosphamethine cyanines represent type A cations, whereas aminophosphenium ions exemplify type B cations (Scheme 1). Also in the 1970s, $AlCl_3$ and $GaCl_3$ adducts of aminoiminophosphines have been synthesized as acyclic zwitterions which further cyclize to the four-membered ylidic rings by elimination of $Me_3Si{-}Cl$ (Figure 1, species **3**).[5]

The first cationic phosphorus azide, a 1-azido-*cyclo*-1,3-diphospha-2,4-diazenium ion, $[Ter_2N_2P_2(N_3)]^+$ (**4**) (Ter = 2,6-mesityl-phenyl, with $[N_3(GaCl_3)_2]^-$ as counterion), was reported by Schulz et al. (Figure 1, species **4**).[6,7] Furthermore, diaminophosphenium species are known and have been observed in the aminolysis of phosphadiazonium salts by the group of Burford (Figure 1, species **5**).[8] Only recently, the terphenyl-substituted bisaminophosphenium phosphadiazonium ion (**5**, R = Ter) has been utilized as a powerful probe for cation−anion interactions in solution and in the solid state with a series of different anions.[9]

With their ambiphilic nature, type B phosphenium cations display a similar reactivity as electrophilic carbenoids. Therefore, the reaction of type B phosphenium cations with Lewis bases such as 4-dimethylaminopyridine (dmap) should lead to the formation of adduct cations, as carbenes are well-known to form true ylides in the reaction with pyridines.[10] Extending this concept, type B ions may also engage in chelotropic [4 + 1]-cycloaddition reactions with suitable dienes such as 2,3-dimethyl-1,3-butadiene (dmb) or 1,3-*cyclo*-hexadiene (chd).[11]

Phosphenium ions show a fascinating variety of structural motifs, and their unique solution and coordination chemistry has been reviewed frequently.[1,12] Following our interest in unusual bonding motifs in compounds bearing a binary NPn-core (Pn = P,[13] As,[14] Sb,[15] Bi[16]), we are concerned with the synthesis of low coordination phosphorus compounds. Despite the great structural variety of phosphenium species, structural data on acyclic phosphenium ions is scarcely found and only a few amino substituted examples are known: $[(iPr_2N)_2P]X$ (X = $[AlCl_4]^-$, $[GaCl_4]^-$, $[BPh_4]^-$).[17] The solid state structures of acyclic amino(chloro)phosphenium ions of the type $[R_2N{=}P{-}Cl]^+$ (R = $SiMe_3$,[18] Cy[19]) were not known until recently. Astonishingly, substitution of the chlorine atom in the cation of $[(Me_3Si)_2N{=}P{-}Cl][GaCl_4]$ (**6**) was achieved by treatment with $Me_3Si{-}N_3$ at −50 °C in methylene dichloride, and the first salt $[(Me_3Si)_2N{=}P{-}N_3][GaCl_4]$ (**7**) with an azide group

Received: January 17, 2013
Published: April 24, 2013

   dx.doi.org/10.1021/ic4001285 | *Inorg. Chem.* 2013, 52, 5214−5225

Scheme 1. Different Lewis Representations of (Top) Type A Phosphenium Cations, Displaying the Delocalization of the Positive Charge over the Substituent System in Addition to a Nucleophilic Phosphorus Center,[3] and of (Bottom) Type B Phosphenium Cations Displaying Their Ambiphilic Nature[4,18]

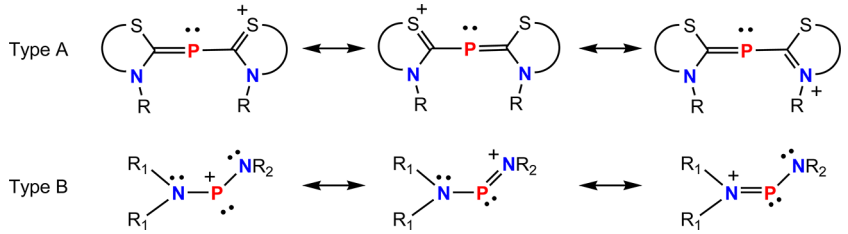

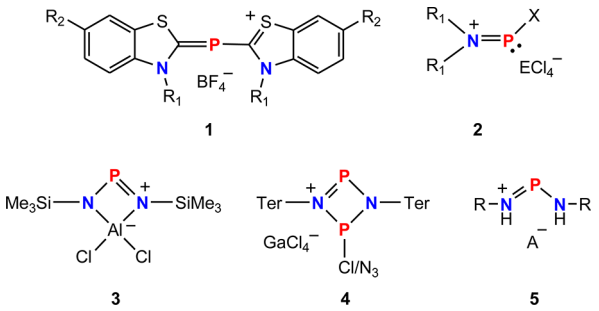

Figure 1. Different types of phosphenium salts: **1** phosphamethine cyanines,[3] **2** aminophosphenium tetrachloridometallates (R_1 = Me, *i*Pr, Cy and X = NR_2, Cl;[4,19] R_1 = $SiMe_3$ and X = Cl, N_3;[18] E = Al, Ga, Fe, **3** 4-membered zwitterionic rings with a phosphenium center,[5] **4** μ-chloro/azido-*cyclo*-1,3,-diphospha-2,4-diazenium tetrachloridogallate,[6] **5** aminoiminophosphenium salts (R = Mes*,[8] Ter;[9] A = Cl, OTf, $B(C_6F_5)_4$).

attached to a two-coordinate phosphorus was successfully isolated and structurally characterized (Scheme 2).[18]

7 is highly reactive and unstable in solution, but can be handled as a solid at temperatures below −30 °C. To the best of our knowledge pseudohalogen-substituted phosphenium salts have not been isolated or structurally characterized so far and can be expected to be highly reactive and unstable in solution.[20] Following the preparation of **7** we were intrigued by the idea to further extend this synthetic scope, by reacting **6** with other silylated pseudohalogens Me_3Si-X (X = NCO, NCS, NCSe, CN, CNO) to obtain the labile pseudohalogen phosphenium salts of the type $[(Me_3Si)_2N{=}P{-}X][GaCl_4]$. In this work we report on the synthesis, structure, and properties of such highly labile pseudohalogen substituted phosphenium salts. The ambiphilic nature of such cations was studied in reactions with (i) bases leading to the isolation of thermally stable σ-donor stabilized adduct cations of the type $[(Me_3Si)_2NP(base)X][GaCl_4]$ (X = Cl, N_3, NCO; base = dmap), and (ii) dienes resulting in the formation of pseudohalogen substituted phospolenium salts of the type $[(Me_3Si)_2NP(diene)X][GaCl_4]$ (X = Cl, N_3, NCO; diene = dmb, chd) in formal [4 + 1] chelotropic cycloaddition reactions. Moreover, the bonding situation in all these systems was investigated by density functional calculations.

RESULTS AND DISCUSSION

The starting material $[(Me_3Si)_2NPCl][GaCl_4]$ (**6**) can be prepared in situ, when $(Me_3Si)_2NPCl_2$ is reacted with $GaCl_3$ in CH_2Cl_2 at temperatures below −50 °C. Isolation of the amino(azido)phosphenium cation was achieved when $Me_3Si{-}N_3$ was added to **6** at −50 °C.[18] Since this synthetic route represents a high-yielding procedure, which allows for the isolation of **7** as crystalline solid, we were encouraged to react **1** with other trimethylpseudohalogenosilanes Me_3Si-X (X = NCO, NCS, NCSe, CNO, CN). Me_3Si-X (X = NCO, NCS) were added to a CH_2Cl_2 solution of **1** at −60 °C and subsequent concentration of the reaction mixture and storage at −40 °C for 24 h afforded the desired salts $[(Me_3Si)_2N{=}P\text{-}NCO][GaCl_4]$ (**8**) and $[(Me_3Si)_2N{=}P\text{-}NCS][GaCl_4]$ (**9**) as colorless crystalline solids (Scheme 3, middle). **8** and **9** are the first examples of structurally characterized acyclic phosphenium cations with an isocyanato or isothiocyanato group attached to a dicoordinated phosphorus atom. It should be noted that in 1987 Mazieres et al. reported on the spectroscopic detection of an $[i Pr_2N{=}P\text{-}NCS]^+$ cation by ^{31}P NMR spectroscopy ($\delta(^{31}P)$ = 276 ppm); however, isolation of this compound was not achieved.[21] It is noteworthy that both salts can be prepared in good yields (**8**: 80%; **9**: 92%), but decomposition occurs even in the freezer of a high quality glovebox (<1 ppm O_2/H_2O) indicating their transient character. Isolated **9** was stable only 24 h in the freezer and decomposed to a brownish oil. In the IR spectrum, taken from cooled samples of **8** and **9**, the asymmetric stretching modes of the NCO and NCS functional groups are found at 2248 cm^{-1} and 1921 cm^{-1}, respectively, indicating that both groups are covalently attached to the phosphorus via the N atom (ν_{OCN}(KOCN) = 2130 cm^{-1}; ν_{SCN}(KSCN) = 2020 cm^{-1}).[22] In solution only traces of the cation in **8** could be detected ($\delta(^{31}P\{^1H\})$ = 338 ppm; cf. $\delta(^{31}P\{^1H\})$ = 363 ppm in $[(Me_3Si)_2N{=}P{-}N_3]^+$ at −70 °C). In the literature ^{31}P NMR data for differently substituted aminophosphenium salts can be found, which were mostly recorded at ambient temperatures.[4,12,21] This is in contrast to the bissilylamino-substituted systems, where only traces of the phosphenium cations can be detected in solution, which arises from two major facts: (i) The solubility of salts **8** and **9** in CH_2Cl_2 is rather low as both salts precipitate out even at −50 °C from highly diluted reaction mixtures. (ii) Trimethylsilyl

Scheme 2. Synthesis of Azidophosphenium Salt 7 Starting from $(Me_3Si)_2NPCl_2$

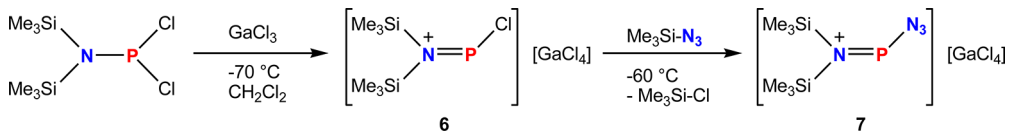

dx.doi.org/10.1021/ic4001285 | Inorg. Chem. 2013, 52, 5214−5225

Scheme 3. Synthesis of Pseudohalogen-Substituted Phosphenium Salts (7, 8, 9), Adduct Stabilized Cationic Species (14, 15, 16), and Cyclic Phospholenium Salts (17−19 dmb/chd) in Chelotropic [4 + 1] Cycloaddition Reactions with dmb or chd, Respectively

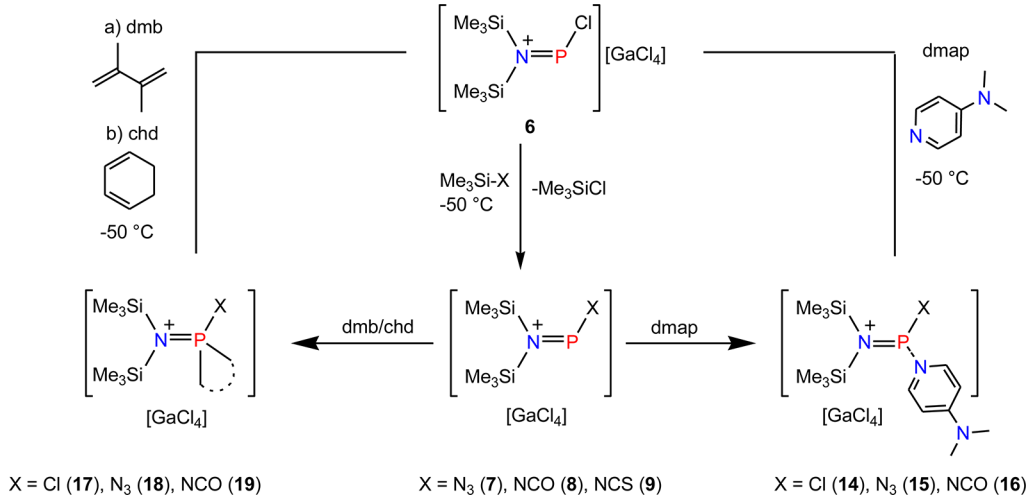

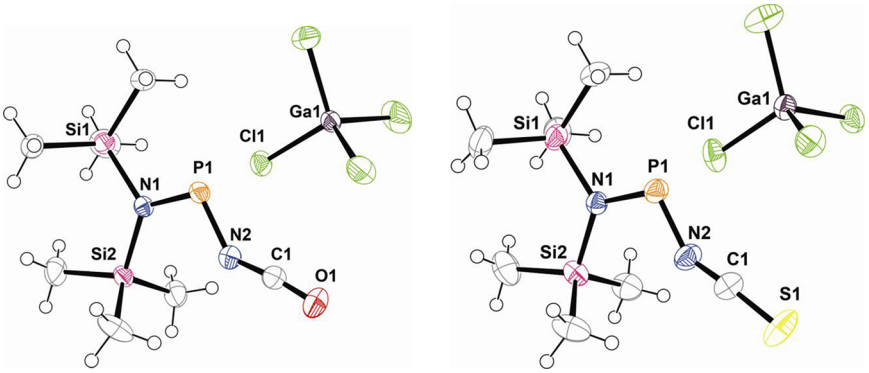

Figure 2. ORTEP drawing of **8** (left) and **9** (right). Ellipsoids are drawn at 50% probability. Selected bond lengths (Å) and angles (deg), (**8**): P1−N1 1.592(1), P1−N2 1.656(2), N1−Si 1.843(1), N1−Si2 1.846(1), N2−C1 1.211(2), O1−C1 1.155(2), P1−Cl1 3.1582(6); N1−P1−N2 103.65(7), O1−C1−N2 173.3(2); N2−P1−N1-Si1 −178.17. (**9**) P1−N1 1.593(1), P1−N2 1.651(2), N1−Si 1.835(2), N1−Si2 1.839(1), N2−C1 1.205(2), S1−C1 1.5421(2), P1−Cl1 3.0926(6); N1−P1−N2 103.79(8), S1−C1−N2 176.08; N2−P1−N1-Si2 −0.33.

groups are unstable in solution in the presence of $GaCl_3$ or other strong Lewis acidic centers such as phosphenium cations. Triggered by the action of the Lewis acid methyl exchange reactions might occur as previously reported by our group.[23] Furthermore, a dynamic equilibrium chemistry between $R_2NPClX/GaCl_3$ and $[R_2NPX][GaCl_4]$ is observed. This was also observed before by our group and the group of Weigand in solution ^{31}P NMR spectra of mixtures containing chlorophosphines and galliumtrichloride in different ratios.[18,19] However, **8** and **9** could be isolated at low temperatures nearly quantitatively since both salts are stabilized significantly in the solid state.

X-ray quality crystals of **8** were obtained directly from the reaction mixture at −40 °C, and crystals of **9** suitable for structural analysis were grown in a similar manner. **8** and **9** crystallize in the orthorhombic space groups $P2_12_12_1$ and *Pbca*, respectively, with four formula units per cell (Figure 2). The amino nitrogen atom sits in a planar environment in both cations indicating a formal sp^2 hybridization. Similarly to amino(azido)phosphenium species **7**, the NCO or NCS moieties nearly lie in the NPSi1Si2 plane, as only a minimal deviation from planarity is observed (**8**: Si1−N2−P1−N1 = −178.1°; **9**: −0.33°). The N_{amino}−P distance is in the typical range of a P−N double bond (**8** 1.592(1), **9** 1.593(1) Å) compared with the sum of the covalent radii (Σr_{cov}(P═N) = 1.60 Å).[24] The isocyanato moiety in **8** and the isothiocyanato group in **9** are slightly bent (∠NCO = 175°; ∠NCS = 174°). This trans-bent configuration was also observed in azido-species **7** and is a common feature for covalently bound triatomic pseudohalide groups. Furthermore, a rather short P−$N_{pseudohalogen}$ (**8** 1.656(2), **9** 1.651(2) Å) bond length is indicative of a partial double bond character (cf. Σr_{cov} (P═N) = 1.60 Å, (P−N) = 1.82 Å). As expected the C1−O1 and C1−S1 (**8** 1.155(2), **9** 1.5421(2) Å) distances are between a double and triple bond (cf. Σr_{cov} (C═O) = 1.24 Å, Σr_{cov} (C≡O) = 1.13 Å; (C═S) = 1.61, (C≡S) = 1.55), whereas the N1−C2 (**3** 1.211(2), **4** 1.205(2) Å) distances are indicative of a shortened double bond (cf. Σr_{cov} (C═N) = 1.27 Å, (C≡N) = 1.14). These values compare nicely with known phosphorus compounds that incorporate isocyanate (cf. P−N_{NCO} 1.673(3), N_{NCO}−C 1.168(4), C−O 1.146(4) Å in **10**, Figure 4)[25] or isothiocyanate (cf. P−N_{NCS} 1.707(7), N_{NCS}−C 1.165(9), S−C 1.551(9) Å; N_{NCS}−C−S 176.8(8)° in $P^{(III)}$ isothiocyanate **11**, Figure 4)[26] groups. Strong cation···anion interactions are observed for **8** and **9** in the crystal. For example, four contacts to neighboring chlorine atoms of the anion are detected in **8**

dx.doi.org/10.1021/ic4001285 | *Inorg. Chem.* 2013, 52, 5214−5225

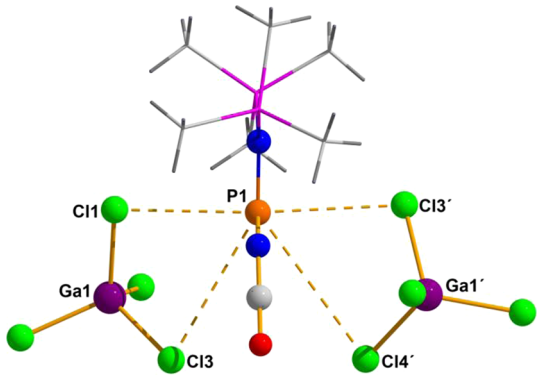

Figure 3. Ball and Stick drawing of the anion−cation interactions in amino(isocyanato)phosphenium salt **8**. Four close contacts are observed (distances in Å): P1−Cl1 3.1582(6), P1−Cl3 3.7630(7), P1−Cl3′ 3.273(7), P1−Cl4′ 4.0212(9).

whose lone pairs (LPs) offer effective donor sites. The three closest P−Cl distances (**8**: P1−Cl1 3.1582(6) Å, P1−Cl3′ 3.273(7) Å, P1−Cl3 3.7630(7) Å) are all in the range of the sum of the van der Waals radii (cf. Σr_{vdw}(P−Cl) = 3.70 Å). Therefore, electrostatic interactions, that stabilize the reactive phosphenium center, can be assumed (Figure 3). A similar situation is found in species **9**.

To access the bonding in these unique cations, we carried out Natural Bond Orbital (NBO) analyses and molecular orbital (MO) calculations for the salts **8** and **9** at the pbe1pbe/aug-cc-pVDZ level of density functional theory.[27] NBO analysis displays a localized p_π-p_π P−N_{amino} double bond, which is highly polarized, with 80% of the electron density being located on the nitrogen atom and a positive net charge on the phosphorus atom of +1.47*e* in **8** and 1.38*e* in **9**. This finding highlights the fact that pseudohalogen phosphenium ions are phosphorus-centered cations. An empty p-type orbital is found at the phosphorus atom, which is accessible for electron pair donors. The LPs located on the chlorine atoms of the anion can effectively interact with the positively charged phosphorus center and therefore a significant charge transfer (**8**: 0.11 and **9**: 0.12 *e*) from the anion to the cation is calculated. Thus the overall charge of the cation is significantly decreased ($q(X_{cat})$ = 0.89 and 0.88 *e* for the cations in **8** and **9**). The bonding situation in **8** and **9** is best described by at least four canonical Lewis formulas (Scheme 4) with formula I being the energetically favored Lewis representation according to NBO analysis. Lewis representation **I** of the cation in **8** shows two σ P−N single bonds and as described before an additional π P−N_{amino} bond. Two LPs are found on the N_{NCO} and N_{NCS} atoms, respectively, which are highly delocalized into the π^* orbital of the P−N_{amino} bond and into the π^* orbital of the C1−O1 bond,

Scheme 4. Resonance Scheme of Lewis Formulae for the Cation in 8 According to NBO Analysis

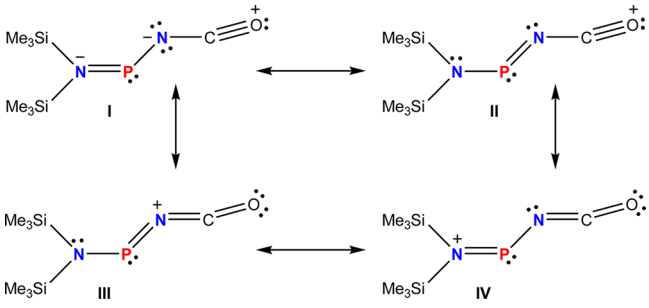

with hyperconjugative energies ($\Delta E^{(2)}$) of 41.9 and 115.9 kcal/mol, respectively. The postulated π-acidity of phosphenium cations is underlined by MO analysis, in which a lowest unoccupied MO (LUMO) with a large coefficient for a p-type orbital on the phosphenium center is found (Figure 5, top). Additionally, π bonding in the cation allows for delocalization of the positive charge, as shown by selected MOs of **8** and **9** (Figure 5).

Isolation and Characterization of a Siloxy Substituted Phosphenium Cation in $[(Me_3Si)_2N{=}P\text{-}OSiMe_3][GaCl_4]$. In a next series of experiments we were interested in the synthesis of the remaining pseudohalogen-substituted species $[(Me_3Si)_2N{=}P{-}X][GaCl_4]$ (X = NCSe, CN, CNO). Treating **1** with Me_3Si-CNO led to an immediate color change and the deposition of colorless crystals, after concentrating the reaction mixture at −50 °C. Surprisingly, crystal structure analysis revealed the formation of an amino(trimethylsiloxy)-phosphenium salt $[(Me_3Si)_2N{=}P\text{-}OSiMe_3][GaCl_4]$ (**12**) indicating decomposition of Me_3Si-CNO and the formal elimination of "CNCl" (Scheme 5). The crystalline material obtained in this reaction was found to be exclusively **12**, nevertheless byproducts of the reaction could not be identified. To date reactions employing Me_3Si-CNO as a $OSiMe_3$ transfer reagent remain elusive, and this reaction might open a new way to effectively transfer siloxy units. **12** is the first structurally characterized acyclic phosphenium cation with a siloxy moiety directly attached to the dicoordinated phosphorus atom. Crystals suitable for X-ray analysis were selected at −50 °C. It should be noted that only one aminooxyphosphenium $[Mes^*N(H)P\text{-}OMes^*][GaCl_4]$ (Mes^* = 2,4,6-tri-*tert*-butylphenyl) ion has been reported to date in the alcoholysis of an iminophosphenium salt.[28] Furthermore the structures of alkoxyphosphenium transition metal complexes are known; Muetterties and co-workers reported on an bisalkoxy phosphenium ligand in a cationic molybdenum complex $\{Mo[P(OCH_3)_3]_5[P(OCH_3)_2]\}[PF_6]$ in 1978, and an aryloxy

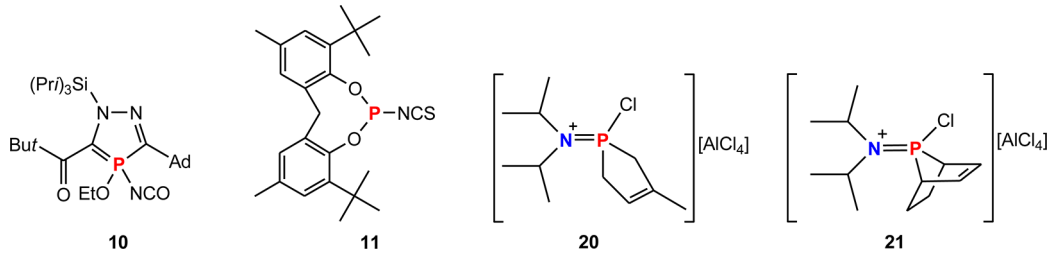

Figure 4. Structures of structurally characterized P-isothiocyanates and -isocyanates **10** and **11**.[25,26] Structures of phospholenium salts **20** and **21** prepared by Cowley et al.[11b].

dx.doi.org/10.1021/ic4001285 | *Inorg. Chem.* 2013, 52, 5214−5225

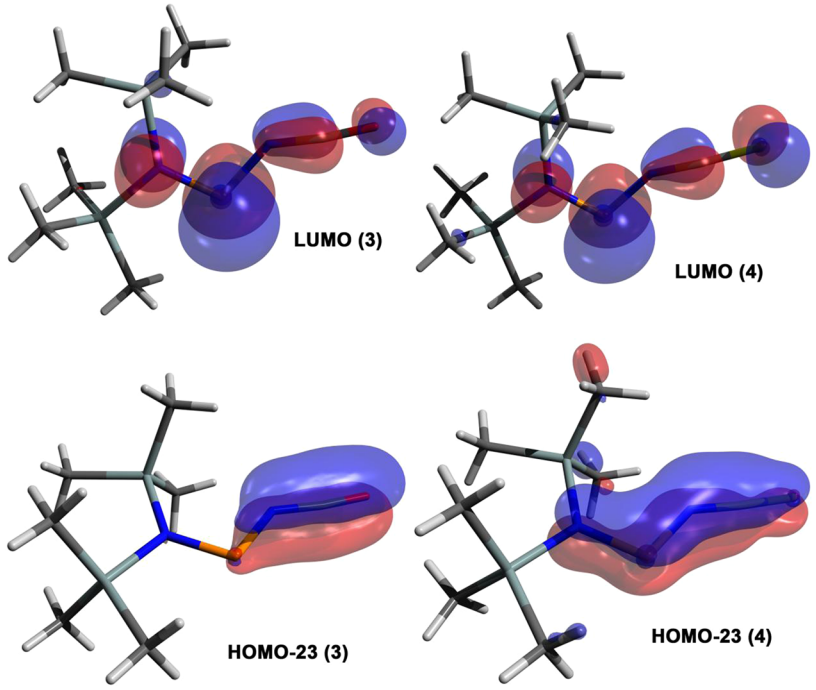

Figure 5. Top: LUMOs calculated for $[(Me_3Si)_2N{=}P\text{-}NCO]^+$ (left) and $[(Me_3Si)_2N{=}P\text{-}NCS]^+$ (right) at the pbe1pbe/aug-cc-pVDZ level of theory . Bottom: MOs displaying out-of-plane π delocalization in the cation in **8** (left) and over the whole N−P−N−C−S chain in **9** (right).

Scheme 5. Attempted Synthesis of Isoselenocyanato- and Cyano-Substituted Phosphenium Ions Starting from 1[a]

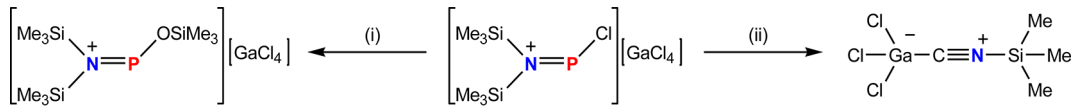

12 6 13

[a]Left, formation of **12**; right, formation **13**. (i) Me_3Si-CNO at −50°C; −CNCl, -Me_3Si−Cl; (ii) Me_3Si-NCSe or Me_3Si-CN (decomposition products could not be identified).

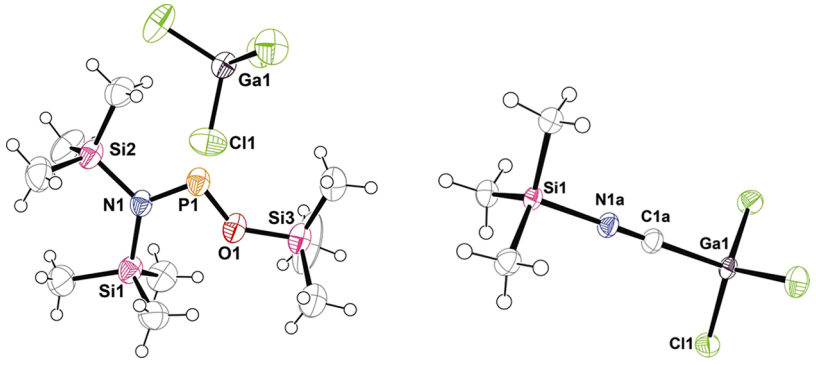

Figure 6. ORTEP drawing of **12** (left) and **13** (right). Ellipsoids are drawn at 50% probability. Selected bond lengths (Å) and angles (deg): (**5**): P1−N1 1.600(3), P1−O1 1.557(3), N1−Si 1.825(3), N1−Si2 1.845(3), O1−Si3 1.715(3), P1−Cl1 3.133(2); N1−P1−O1 105.2(2); N1−P1−O1-Si3 175.2(2). (**6**) N1a-C1a 1.141(4), Si1−N1a 1.858(3), C1a-Ga1 2.029(4), Si1−C 1.836(2), Ga1−Cl 2.1452(5); Σ(∠Si) 343.7, Σ(∠Ga) 336.2; Si1−N1a−C1a−Ga1 180.

phosphenium stabilized in the coordination sphere of cobalt in $[Co(CO)_3(Mes^*O\text{-}PCp^*)]$ was reported by Lang et al. in 1996.[29] Aminosulfidophosphenium ions are also known; however, the sulfide groups were introduced prior to the formation of the cation, and the solid state structures were not reported. **12** crystallizes in the monoclinic space group $P2_1/n$ with four formula units per cell (Figure 6). The structural parameters found for **12** compare nicely with those of the other phosphenium species (**8**, **9**), as the P−N_{amino} distance (**12** 1.600(3) Å) (cf. Σr_{cov} (P═N) = 1.60 Å) is a typical double bond and the NPO angle of 105.2(2)° is in the same range observed for the NPN angle in the cations of **8** and **9** ($\angle N_{amino}$−P−N_{NCX} (deg): **8** 103.65(7), **9** 103.79(8); X = O, S). The P−O distance (**12** 1.557(3) Å) gives rise to a double bond (cf. Σr_{cov} (P═O) = 1.59 Å) with two LPs being located on oxygen as supported by NBO analysis. As observed in **7**−**9**, these LPs are highly delocalized into the π^* of the P−N_{amino} bond ($\Delta E^{(2)}$ = 33.9 kcal mol^{-1}) and furthermore into the σ^*

dx.doi.org/10.1021/ic4001285 | Inorg. Chem. 2013, 52, 5214−5225

orbitals of the Si−C bonds in the trimethylsilyl group. Again close contacts to the anion are observed (P1···Cl1 = 3.133(2); Σr_{vdw}(P−Cl) = 3.70 Å). This kind of ion pairing seems to be a prominent feature in the structure of phosphenium cations with weakly coordinating anions. However, these weak cation−anion interactions cannot be neglected since they substantially contribute to the stability of phosphenium salts in the solid state. Nevertheless, all phosphenium salts discussed in this article are highly labile in solution, and **12** could not be detected in solution in the ^{31}P NMR spectrum, as precipitation occurs below −30 °C and above this temperature decomposition to unidentified products begins.

When trying to prepare the isoselenocyanato substituted phosphenium cation, the color of the reaction mixture changed to deep brown, but at no time was the formation of red selenium observed in the reaction vessel. Concentration of the reaction mixture after several days at −80 °C afforded small yellowish crystals, which decomposed when brought into an atmosphere of nitrogen at −50 °C for crystal selection. In this case red selenium formed, and the residual crystals were found to be a $GaCl_3$ adduct of *N*-trimethylisonitrilesilane (**13**) (Scheme 5). The same product was obtained and characterized by means of X-ray analysis in the attempted synthesis of the amino(cyano)phosphenium cation when **6** was treated with Me_3Si-CN. However, this adduct compound decomposes within 5 min at ambient temperatures in an argon atmosphere. Crystals suitable for structural analysis were collected at low temperatures, and the molecular structure could be determined. **13** crystallizes in the trigonal spacegroup *R*3 with three molecules in the unit cell (Figure 6). The linear Si1−N1−C1−Ga1 moiety lies on a 3-fold axis, and the bond lengths detected in **13** are indicative for the formulation of a dative bond between carbon and gallium (C1−Ga = 2.029(4) ; Σr_{cov} (C−Ga) = 1.99 Å). The nitrogen carbon distance is a typical triple bond (N1−C1 = 1.141(4) Å, cf. Σr_{cov} (C≡N) = 1.14 Å), and the sum of angles around silicon and gallium are in agreement with tetrahedrally coordinated centers (Σ(∠Si) 343.7°, Σ(∠Ga) 336.2°). It is noteworthy that the positions of the carbon and nitrogen atoms in **13** are found to be partially occupied by nitrogen and carbon respectively. Consequently **13** is best described as a mixture of Me_3Si-NC···$GaCl_3$ and Me_3Si-CN···$GaCl_3$. Astonishingly, the group of Mazieres reported a ^{31}P NMR chemical shift of 78 ppm for $[i Pr_2N{=}P\text{-}CN]^+$.[20] However, we were neither able to detect a similar signal at low temperature in ^{31}P NMR experiments nor could we find any further indications for the formation of $[(Me_3Si)_2N{=}P\text{-}CN]^+$.

Investigation of the Lewis Acidic Properties of Phosphenium Species 7−9. In earlier studies it was shown that phosphenium cations can be stabilized by the addition of Lewis bases that act as electron pair donors to the electron deficient π-acidic phosphenium center.[30] This reactivity is best understood in analogy to the carbenes which form ylides in the reaction with Lewis bases (Scheme 6).

Bases usually employed for such reactions are phosphines, carbenes, or pyridine bases such as 4-dimethylaminopyridine (dmap) or 2,2′-bipyridine.[31] The catenation of phosphenium ions in the presence of phosphines is also well described and especially the group of Burford established a huge library of catena-phosphinophospenium salts in the past decade.[32] We therefore decided to add the strong pyridine base and σ-donor dmap to a solution of **6**, **7**, or **8** in CH_2Cl_2. It is well described in the literature that dmap can be utilized to remove $GaCl_3$ from mixtures as a dmap-adduct which does not dissolve in

Scheme 6. Comparison of the Reactivity of Carbenes of the Type X−C−Y with the Isolobal $[X{-}P{-}Y]^+$ Ion in the Reaction with Lewis Bases[a]

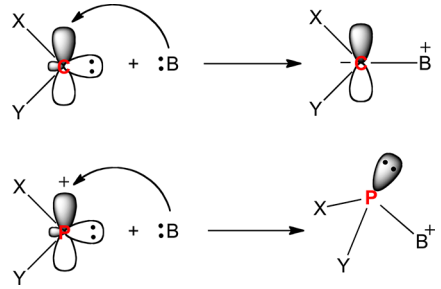

[a]Carbenes (top) form ylides whereas phosphenium cations (bottom) form adduct cations. In both cases the LP located on the Lewis base interacts with an empty p-orbital of the Lewis acidic center (C or P).

nonpolar solvents such as *n*-hexane.[23] Conclusively, two reaction channels are possible in this reaction: (i) The formation of adduct cations in salts of the type $[(Me_3Si)_2NP(dmap)X][GaCl_4]$ or the removal of $GaCl_3$ as $Cl_3Ga{\cdot}dmap$ adduct along with the formation of the corresponding chlorophosphines $(Me_3Si)_2NPClX$ (X = Cl, N_3, NCO) (Scheme 7 and Figure 7). Indeed both reaction pathways

Scheme 7. Synthesis of $[(Me_3Si)_2NP(dmap)X][GaCl_4]$ (X = Cl (14), N_3 (15), NCO (16)) When dmap is Added to a Solution of 6 in CH_2Cl_2 at −50 °C

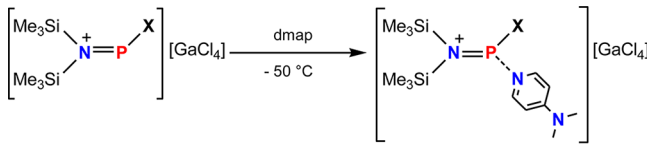

X = Cl (**14**), N_3 (**15**), NCO (**16**)

were observed. Upon addition of dmap at −50 °C to **6**, **7**, and **8** and subsequent concentration of the reaction mixture, colorless crystals of $[(Me_3Si)_2NP(dmap)X][GaCl_4]$ (X = Cl (**14**), N_3 (**15**), NCO (**16**)) were isolated and structurally characterized (Figure 7, only structures of **14** and **15** are shown).

All cationic adduct salts (**14**, **15**, and **16**) are stable at room temperature, moisture and air sensitive. They can be stored over a long period of time in an inert atmosphere. Decomposition of these salts begins at around 100 °C nicely illustrating the ability of bases such as dmap to inhibit the reactivity of cationic Lewis acidic compounds by adduct formation.[33] As mentioned before, a second reaction channel is possible which is observed when **14**−**16** are redissolved in CD_2Cl_2 as demonstrated in ^{31}P NMR experiments. Accordingly in the ^{31}P NMR spectrum of **14** two resonances are detected (see Figure 8). A resonance at 163 ppm corresponds to the dmap adduct cations $[(Me_3Si)_2NP(dmap)Cl]^+$ whose chemical shift is in the typical range of neutral phosphines with two electronegative substituents on the phosphorus atom. Furthermore, a signal at 188 ppm, that corresponds to the starting material $(Me_3Si)_2NPCl_2$, is observed. Therefore, it can be concluded that there is an equilibrium in solution between $GaCl_3$-dmap and $[(Me_3Si)_2NP(dmap)X]^+$ (Figure 8).

Such an equilibrium is observed for all species **14**−**16**. It is noteworthy that in the crystal a substitutional disorder of the type $[(Me_3Si)_2NP(dmap)Cl_yX_{1-y}]^+$ (y = 0.14) is observed for **16**. This mixed compound gives the expected solution ^{31}P

dx.doi.org/10.1021/ic4001285 | Inorg. Chem. 2013, 52, 5214−5225

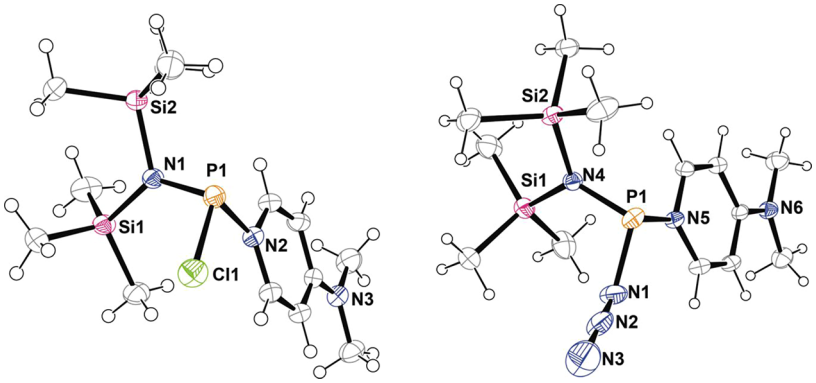

Figure 7. ORTEP drawings of the cations in **14** (left) and **15** (right). Ellipsoids are drawn at 50% probability, anions are omitted for clarity. Selected bond lengths (Å) and angles (deg): (**14**): P1−N1 1.641(1), P1−N2 1.829(1), P1−Cl1 2.0799(6), N1−Si 1.801(1), N1−Si2 1.817(1); N1−P1−O1 105.2(2); Σ(∠N1) 359.86, Σ(∠P1) 305.51; Si2−N1−P1-Cl1 129.46(6). (**15**) P1−N4 1.649(3), P1−N1 1.757(3), P1−N5 1.810(3), N1−N2 1.157(4), N2−N3 1.162(5), N1−Si 1.797(3), N1−Si2 1.808(3); N1−N2−N3 173.6(5), Σ(∠N4) 359.18, Σ(∠P1) 298.08; Si2−N4−P1−N1 138.5(2).

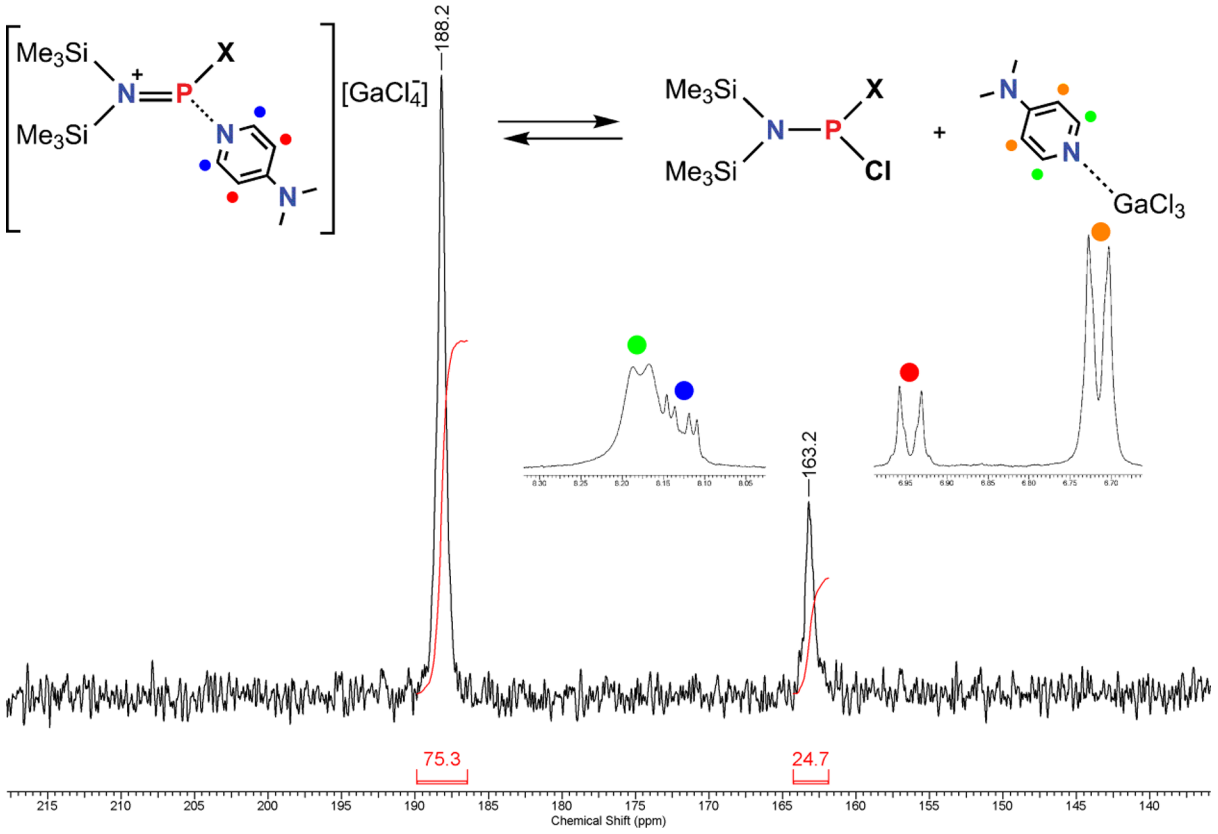

Figure 8. ^{31}P NMR (bottom) and ^{1}H NMR (top, proton positions indicated by colored dots) spectrum of a CD_2Cl_2 of **14** at room temperature, displaying the solution equilibrium between $[(Me_3Si)_2NP(dmap)X][GaCl_4]$ (X = Cl (**14**), N_3 (**15**), NCO (**16**)) and the corresponding chlorophosphine $(Me_3Si)_2NP(X)Cl$ in solution. The resonance in the ^{31}P NMR spectrum at 188 ppm corresponds to $(Me_3Si)_2NPCl_2$ and at 163 ppm the cation in **14** is detected.

NMR spectrum with four species present, $(Me_3Si)_2NPCl_2$, $[(Me_3Si)_2NP(dmap)Cl]^+$, $[(Me_3Si)_2NP(dmap)X]^+$, and $(Me_3Si)_2NPClX$. This kind of partial chlorine occupancy of a pseudohalogen position is a well-known phenomenon and regularly observed in binary azides when prepared in chlorinated solvents or from chlorine precursors.[14b,23c] Species **14**−**16** crystallize in the monoclinic space groups $P2_1/c$ (**14**, **16**) and $P2_1/n$ (**15**), respectively. In the molecular structures of the cations in **14**−**16** the P−N_{amino} distance is rather long (**14** 1.644(1), **15** 1.649(3), **16** 1.645(2) Å) compared with the phosphenium precursor ions and falls in the range of the starting material $(Me_3Si)_2NPCl_2$ (P−N_{amino} = 1.6468(8) Å). The dmap binds with its pyridine N atom, and the P−N_{dmap} distance (**14** 1.829(1), **15** 1.810(3), **16** 1.848(2) Å) is in the range of a typical P−N single bond (cf. Σr_{cov} (P−N) = 1.82 Å). The phosphine character of the adduct cation is also supported by the sum of angles around the central P atom (Σ∠(P): **14** 305.51, **15** 298.08, **16** 298.21°) and therefore in the typical range of a tricoordinated, trigonal pyramidal coordinated phosphorus in the oxidation state +III (cf. $(Me_3Si)_2NPCl_2$

dx.doi.org/10.1021/ic4001285 | Inorg. Chem. 2013, 52, 5214−5225

$\Sigma\angle$(P): 305.99°).[18] NBO analyses were carried out to gain insight into the bonding in these adduct cations, which show, that the positive charge is delocalized mainly over the π-system of the dmap moiety. The LP on the N_{amino} atom, located in a p-type orbital, is delocalized into the σ^* orbitals of the Si−C backbone and also negative hyperconjugation with the σ^* orbitals of the P−X bond contributes to the rather short P−N_{amino} distance and elongation of the P−X bond (**14** 2.0799(6), **15** 1.757(3), **16** 1.740(4) Å) underlining the phosphine character of these adduct cations (cf. Σr_{cov} (P−N) = 1.82, Σr_{cov} (P−Cl) = 2.04; $[Ter_2N_2P_2N_3]^+$ d(P−N_{azide}) = 1.706 (3) Å).[6] The natural charge on phosphorus is still positive with nearly 1.2−1.4 *e* (**14** 1.25, **15** 1.43, and **16** 1.45 *e*); however, no empty p orbital on phosphorus is found, and thus the adduct cations do not have any phosphenium characteristics, as dmap transfers electron density to the phosphenium fragment (e.g., $q_{charge\text{-}transfer}$ = 0.38 *e* in **14**).

Investigation of the Carbenoid Reactivity of 6−8. It is known that dienes such as dmb or chd can easily add to carbenes in chelotropic [4 + 1] cycloaddition reactions.[34] Therefore the formation of differently substituted phospholenium salts can be assumed when phosphenium ions are utilized instead of carbenes. Phosphenium species **6**−**8** are related to carbenes of the type X−C−Y and accordingly possess orbitals suitable for the [4 + 1] chelotropic cycloaddition with dienes (Figure 9 and 10).[10,11b] Computational studies were carried out

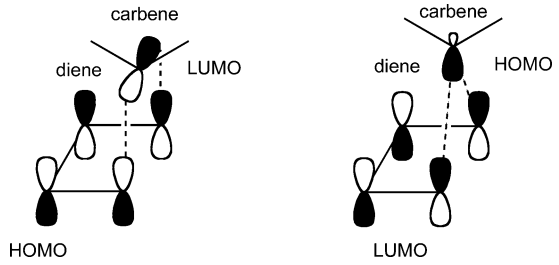

Figure 9. HOMO−LUMO interactions in a [4 + 1] chelotropic cycloaddition process.

to assess the bonding situation in the phosphenium cations which support the idea that these cycloadditions are symmetry allowed (Figure 10). Accordingly, addition of dmb to a freshly prepared solution of **6** in CH_2Cl_2 at −60 °C resulted in a clean conversion to one new phosphorus species as shown by ^{31}P NMR studies (Scheme 8).

Similar chelotropic [4 + 1] cycloaddition reactions have been utilized as early as 1983 when Soo and co-workers prepared the first phospholenium cations.[11a] They treated $[(Me_2N)_2P]^+$ with dmb in an attempt to optimize the McCormack reaction which is used to synthesize phosphorus-containing heterocycles.[35] The ^{31}P NMR chemical shifts of 95.9 ppm for $[(Me_3Si)_2NP(dmb)Cl][GaCl_4]$ (**17dmb**) compare well with similar literature values (cf. $\delta(^{31}P\{^1H\})$: **20** = 100.3, Figure 4).[11b] To grow X-ray quality crystals of **17dmb** a concentrated solution was stored in the freezer at −80 °C for 24 h. Structural analysis indeed revealed the formation of **17dmb**. To add to the diverse library of such salts and to investigate the possibility to synthesize room temperature stable derivatives of **7** and **8** we decided to additionally react **6** with 1,3-*cyclo*-hexadiene and treated **7** and **8** with both dmb and chd. According to ^{31}P NMR experiments the reaction of **6** with chd occurs immediately and $[(Me_3Si)_2NP(chd)Cl][GaCl_4]$ is formed. With respect to the position of the phosphorus LP, there are two possible conformers (*syn*/*anti*) in such 7-phosphanorbornenium cations (Figure 11).

The *anti* species of **17chd** is observed at 117 ppm, and the *syn* conformer is detected at 94 ppm in a 3:2 ratio. GIAO calculations of the magnetic field tensors were carried out to assign ^{31}P NMR shift of the *syn*- and *anti*-conformer of **17chd**.[36] In the ^{1}H NMR spectrum four different kinds of protons are detected for each conformer. As expected, two aromatic protons (multiplet at 6.67 ppm), two methine protons (multiplet at 3.8 ppm), and two sets of multiplets are observed for the CH_2-groups as both protons are magnetically inequivalent. All attempts to crystallize **17chd** directly from the reaction mixture in CH_2Cl_2 always resulted in the formation of microcrystalline material. Layering a CH_2Cl_2 solution of **17chd** with *n*-pentane and storage at −25 °C for 24 h yielded minimal amounts of crystals suitable for structural analysis. The *anti*-conformer of **17chd** is exclusively found in the solid state, which is in good agreement with the calculated structure of a similar, but neutral system, in *anti*-*i*Pr_2N-7-phosphanorbornene just recently reported by Cummins et al.[37] In addition the reactivity of metal phosphinidene complexes is well studied, and various examples of metal stabilized *anti*-7-phosphanorbornadienes have been structurally characterized.[38] Compound **17chd** is the first example of a structurally characterized 7-

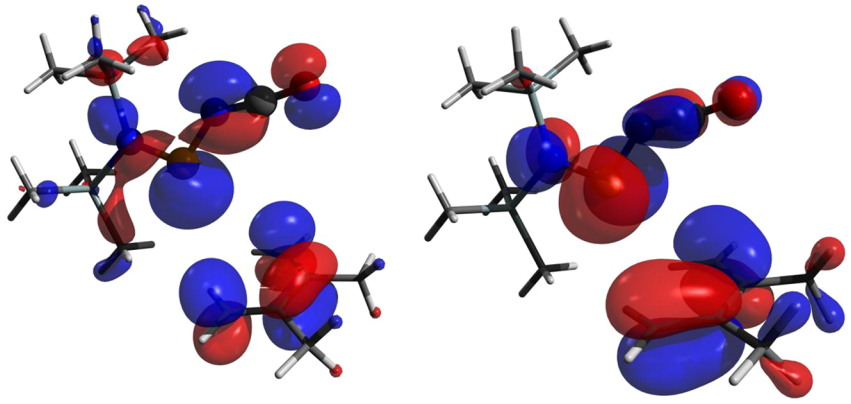

Figure 10. HOMO and LUMO combinations calculated for the cation in $[(Me_3Si)_2NPNCO]^+$ (**8**) and dmb (pbe1pbe/aug-cc-pVDZ) displaying the correct symmetry for chelotropic [4 + 1] cycloaddition. Left: Interaction of the HOMO-4 of **8** and the LUMO of dmb. Right: Interaction of the LUMO of **8** and the HOMO of dmb.

dx.doi.org/10.1021/ic4001285 | *Inorg. Chem.* 2013, 52, 5214−5225

Scheme 8. Synthesis of Phospholenium Salts 17dmb−19dmb and 17chd−19chd[a]

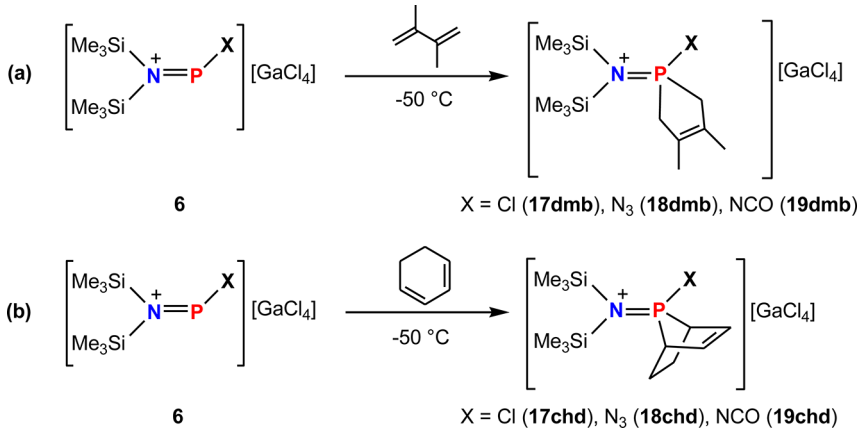

[a](**a**) By addition of 2,3-dimethyl-1,3-butadiene to a solution of **1** in CH_2Cl_2 at −50 °C; (**b**) by addition of 1,3-*cyclo*-hexadiene to a solution of **1** in CH_2Cl_2 at −50 °C.

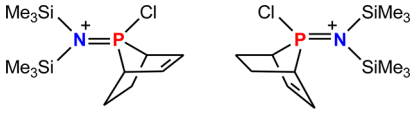

Figure 11. *Syn*- and *anti*-conformers of 7-phosphanorbornenium salt **17chd**.

phosphanorbornenium cation obtained in the [4 + 1]-cycloaddition between chd and a phosphenium cation, underlining the assumption made by Cowley and co-workers that the sterically less encumbered configuration, that places the double bond on the same side as the chlorine atom, is indeed favored.[11b] Additionally, the ^{31}P NMR data reported for a mixture containing both *syn*- and *anti*-[*i*Pr_2NP(chd)Cl][$AlCl_4$] (**21**) (cf. $\delta(^{31}P\{^1H\})$: syn-**21** = 98.7, anti-**21** = 117.2; Figure 4), correspond well with the values detected for **17chd**.[11b] Adopting the same synthetic procedure that yielded **17dmb** to **7** and **8** phosphapentene moieties containing phospholenium salts of these phosphenium salts have been prepared. [$(Me_3Si)_2$NP(dmb)N_3][$GaCl_4$] (**18dmb**) and [$(Me_3Si)_2$NP(dmb)NCO][$GaCl_4$] (**19dmb**) could be prepared in moderate yields of nearly 50% and are, in contrast to their transient precursors, thermally stable up to 100 °C. In **18dmb** a partial chlorine occupancy (0.03) of the azide position was observed by means of X-ray crystallographic methods. Depending on tiny changes in the reaction conditions a slightly different, small contamination with chlorine was observed (see Supporting Information). Furthermore, the addition of chd to pseudohalogen-containing phosphenium salts **7** and **8** resulted, according to X-ray crystallographic methods, exclusively in the formation of *anti*-[$(Me_3Si)_2$NP(chd)N_3][$GaCl_4$] (**18chd**) and *anti*-[$(Me_3Si)_2$NP(chd)NCO][$GaCl_4$] (**19chd**). In the ^{31}P NMR spectrum also only one species is detected (Table 1). The molecular structures of dmb containing phospholenium salts **17dmb−19dmb** and chd-added species **17chd−19chd** are quite similar and will be discussed only briefly (Figure 12). The dmb derivative **17dmb** crystallizes in the monoclinic space group $P2_1/n$, whereas **18dmb**, **19dmb**, and **19chd** crystallize in the space group $P2_1/c$, respectively, all with four formula units in the unit cell. **17chd** and **18chd** crystallize in $P\bar{1}$ with two formula units in the cell. The NPCl(C_6H_8) moiety in **17chd** is disordered, and only the main part is shown. **18chd** crystallizes as a toluene solvate with one solvent molecule in the asymmetric unit. In **18dmb** a partial occupation of the azide position with chlorine is detected, a feature also detected in **16**. Interestingly upon reaction only modest changes within the [$(Me_3Si)_2$NPX]$^+$ moiety are observed. The most striking feature is that the group X (X = Cl, N_3, NCO) attached to the phosphorus atom is nearly perpendicular to the Si1−N_{amino}−Si2 plane, which is in contrast to the phosphenium

Table 1. Selected Bond Lengths (Å) and Angles (deg) of Phospholenium Salts 17dmb−19dmb/17chd−19chd along with $\delta(^{31}P)$ NMR Shifts (ppm)[a]

	d(P1−N_{amino})	d(P1−X)[b]	d(P1−C)[c]	d(N_{amino}−Si)[c]	Σ∠P1	$\delta(^{31}P)$
17dmb	1.6089(9)	2.0065(4)	1.801	1.824	333.98	95.9
18dmb	1.608(1)	1.683(2)	1.795	1.820	333.95	78.6
19dmb	1.612(2)	1.661(2)	1.792	1.819	333.5	66.2
17chd	1.592(2) /1.657(3)	1.994(2)[e]	1.822	1.824	322.83	116.6
11chd	1.609(2)	1.682(2)	1.826	1.815	322.01	91.4
12chd	1.612(2)	1.661(2)	1.792	1.819	320.87	83.7
8	1.592(1)	1.656(2)		1.844	103.65(7)	337
14	1.644(1)	2.0799(6)	1.829(1)[d]	1.809	305.51	163
$(Me_3Si)_2NPCl_2$	1.6468(8)	2.0834(5)[e]	2.1074(5)[f]	1.795	305.99	189

[a]In addition, the corresponding values for **8**, **14** and $(Me_3Si)_2NPCl_2$ are given for comparison. [b]X: **17** Cl, **18** N_3, **19** NCO. [c]Bond lengths are similar, therefore average value is presented. [d]d(P−N_{dmap}) is presented. [e]d(P−Cl1) in $(Me_3Si)_2NPCl_2$. [f]d(P−Cl2) in $(Me_3Si)_2NPCl_2$.

dx.doi.org/10.1021/ic4001285 | *Inorg. Chem.* 2013, 52, 5214−5225

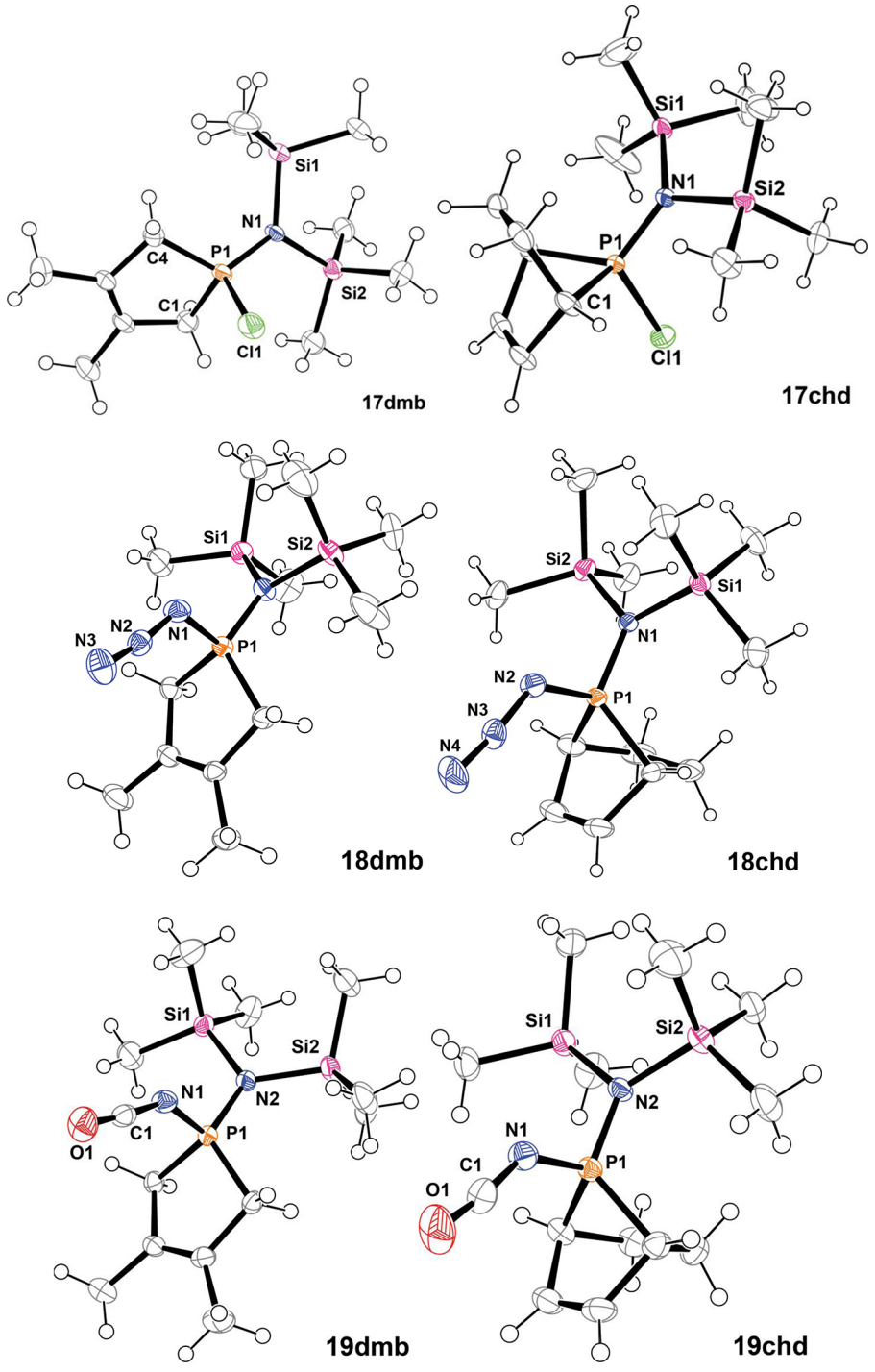

Figure 12. ORTEP drawings of the cations in **17dmb**−**19dmb** (left) and **17chd**−**19chd** (right). In **18dmb** a partial occupation of the azide position with chlorine is detected; the chlorine is omitted for clarity. Ellipsoids are drawn at 50% probability; anions are omitted for clarity. Selected bond lengths and angles are listed in Table 1.

cations and is similar to the situation in the dmap adducts **14**−**16**. As a result of this geometrical arrangement an interaction between the LP located in a p-type orbital at the N_{amino} and a σ^*-orbital of the P−X bond is possible and therefore the P−N_{amino} bond is significantly shortened (1.60 Å, Table 1). Additionally, the P−X distance is longer than in the precursor cations. The phosphapentene moiety in **17dmb**−**19dmb** adopts an envelope conformation, and the C−C double bond points toward the group X (**17dmb**: N1−P1−C7−C8 = 146.19(7)°). A similar situation is found for the phosphapentene groups in **17chd**−**19chd**, in which the olefinic double bond is in a proximal arrangement with the group X and therefore the five-membered PC_4-ring also adopts an envelope conformation. The carbon distances within the phosphole unit are in the expected range for such compounds with a C−C double bond in the ring. The P−C distances represent short single bonds (Table 1, cf. Σr_{cov}(P−C) = 1.86, Σr_{cov}(P═C) = 1.69 Å). As a consequence of negative hyperconjugation between the LP on N_{amino} and the antibonding σ^* Si−C orbitals the N_{amino}−Si distances are shortened which is clearly

dx.doi.org/10.1021/ic4001285 | Inorg. Chem. 2013, 52, 5214−5225

shown by NBO analysis. In contrast to the phosphenium cations **1**−**5**, in which contacts between anion and cation are detected, the phospholenium species can be considered as almost "naked" cations underlined by the overall natural charge of the cation of +0.99 *e* and by the fact that no short contacts to the counteranions are observed.

CONCLUSIONS

In this study we present for the first time the crystal structures of pseudohalogen-substituted phosphenium salts of the type $[R_2NPX][GaCl_4]$ (R = $SiMe_3$; X = NCO (**8**), NCS (**9**)) which are highly reactive and labile in solution. These salts are only stable below −40 °C; however, even at these low temperatures decomposition occurs within two weeks. Attempts to prepare $[R_2NPX][GaCl_4]$ (R = $SiMe_3$, X = CNO) resulted in the formation of $[(Me_3Si)_2NPO(SiMe_3)][GaCl_4]$ (**12**), the first salt with an oxygen atom directly attached to the phosphenium center. The reaction pathway gives rise to a trimethylsiloxy transfer from trimethylnitrileoxidosilane to the phosphorus, a reaction with no precedence in the literature so far. In subsequent reactions the ambiphilic nature of phosphenium cations was demonstrated as they react readily at low temperatures with σ-donors such as dmap to yield adduct cations in **14**−**16**. In solution these dmap adducts, which cannot be referred to as phosphorus centered cations, show a fascinating equilibrium chemistry that was studied by means of solution ^{31}P NMR spectroscopy. Moreover, phosphenium salts **6**−**8** were shown to react with dienes such as dmb and chd to afford 7-phosphanorbornenium salts **17dmb**−**19dmb**/**17chd**−**19chd** which are room temperature stable derivatives of the parent, transient phosphenium salts. We succeeded in the structural characterization of the first 7-phosphanorbornenium salts $[(Me_3Si)_2NPX(C_6H_8)][GaCl_4]$, which revealed the formation of the *anti*-conformer as the dominant species, when chd is added to the phosphenium salt. These findings are further supported by ^{31}P NMR data and DFT calculations. In future studies the potential of the phospholenium salts as starting materials for the synthesis of phosphaazenes will be investigated, and preliminary results show that interesting polymeric materials might be accessible.

ASSOCIATED CONTENT

Supporting Information

This material contains experimental and computational details, crystallographic information, and further experimental and theoretical data of all considered species. This material is available free of charge via the Internet at http://pubs.acs.org.

AUTHOR INFORMATION

Corresponding Author

*E-mail: axel.schulz@uni-rostock.de.

Notes

The authors declare no competing financial interest.

ACKNOWLEDGMENTS

Martin Ruhmann and Fabian Reiß (University of Rostock) are acknowledged for the measurement of Raman spectra. Financial support by the Fonds der chemischen Industrie (fellowship to C.H.) and the DFG are gratefully acknowledged.

REFERENCES

(1) (a) Fluck, E. *Top. Phosphorus Chem.* **1980**, *10*, 193. (b) Elian, M.; Chen, M. M. L.; Mingos, D. M. P.; Hoffmann, R. *Inorg. Chem.* **1976**, *I S*, 1148. (c) Hoffmann, R. *Angew. Chem., Int. Ed. Engl.* **1982**, *21*, 711.
(2) Schmidpeter, A. Multiple Bonds and Low Coordination Chemistry. In *Phosphorus Chemistry*; Regitz, M., Scherer, O., Eds.; Georg Thieme Verlag: Stuttgart, Germany, 1990; Vol. *D2*, p 149.
(3) Dimroth, K.; Hoffmann, P. *Angew. Chem.* **1964**, *76*, 433; *Angew. Chem., Int. Ed. Engl.* **1964**, *3*, 384.
(4) (a) Kopp, R. W.; Bond, A. C.; Parry, R. W. *Inorg. Chem.* **1976**, *15*, 3042. (b) Schultz, C. W.; Parry, R. W. *Inorg. Chem.* **1976**, *15*, 3046.
(5) Niecke, E.; Kroher, R. *Angew. Chem.* **1976**, *88*, 758; *Angew. Chem., Int. Ed. Engl.* **1976**, *15*, 692.
(6) Michalik, D.; Schulz, A.; Villinger, A.; Weding, A. *Angew. Chem.* **2008**, *120*, 6565−6568; *Angew. Chem., Int. Ed.* **2008**, *47*, 6465.
(7) Villinger, A.; Mayer, P.; Schulz, A. *Chem. Commun.* **2006**, 1236.
(8) Burford, N.; Cameron, T. S.; Clyburne, J. A. C.; Eichele, K.; Robertson, K. N.; Sereda, S.; Wasylishen, R. E.; Whitla, W. A. *Inorg. Chem.* **1996**, *35*, 5460.
(9) Reiss, F.; Villinger, A.; Schulz, A. *Eur. J. Inorg. Chem.* **2012**, *2*, 261.
(10) Bourissou, D.; Guerret, O.; Gabbai, F. P.; Bertrand, G. *Chem. Rev.* **2000**, *100*, 39.
(11) (a) SooHoo, C. K.; Baxter, S. G. *J. Am. Chem. Soc.* **1983**, *105*, 7443. (b) Cowley, A. H.; Kemp, R. A.; Lasch, J. G.; Norman, N. C.; Stewart, C. A.; Whittlesey, B. R. *Inorg. Chem.* **1986**, *25*, 740.
(12) (a) Cowley, A. H.; Kemp, R. A. *Chem. Rev.* **1985**, *85*, 367. (b) Sanchez, M.; Mazieres, M.-R.; Lamande, L.; Wolf, R. Phosphenium Cations. In *Multiple Bond and Low Coordination in Phosphorus Chemistry*; Regitz, M., Scherer, O., Eds.; Georg Thieme: Stuttgart, Germany, 1990; Chapter 0.1, p 129. (c) Gudat, D. *Coord. Chem. Rev.* **1997**, *163*, 71.
(13) (a) Mayer, P.; Schulz, A.; Villinger, A. *Chem. Commun.* **2006**, 1236. (b) Mayer, P.; Schulz, A.; Villinger, A. *J. Organomet. Chem.* **2007**, *692*, 2839. (c) Beweries, T.; Kuzora, R.; Rosenthal, U.; Schulz, A.; Villinger, A. *Angew. Chem., Int. Ed.* **2011**, *50*, 8974. (d) Kuprat, M.; Lehmann, M.; Schulz, A.; Villinger, A. *Inorg. Chem.* **2011**, *50*, 5784.
(14) (a) Schulz, A.; Villinger, A. *Angew. Chem., Int. Ed.* **2008**, *47*, 603. (b) Michalik, D.; Schulz, A.; Villinger, A. *Inorg. Chem.* **2008**, *47*, 11798. (c) Schulz, A.; Villinger, A. *Inorg. Chem.* **2009**, *48*, 7359.
(15) (a) Lehmann, M.; Schulz, A.; Villinger, A. *Eur. J. Inorg. Chem.* **2010**, *35*, 5501. (b) Lehmann, M.; Schulz, A.; Villinger, A. *Angew. Chem., Int. Ed.* **2011**, *50*, 5221. (c) Lehmann, M.; Schulz, A.; Villinger, A. *Eur. J. Inorg. Chem.* **2012**, *5*, 822.
(16) (a) Baumann, W.; Schulz, A.; Villinger, A. *Angew. Chem., Int. Ed.* **2008**, *47*, 9530. (b) Michalik, D.; Schulz, A.; Villinger, A. *Angew. Chem., Int. Ed.* **2010**, *49*, 7575. (c) Lehmann, M.; Schulz, A.; Villinger, A. *Angew. Chem., Int. Ed.* **2012**, *51*, 8087.
(17) Burford, N.; Losier, P.; Macdonald, C.; Kyrimis, V.; Bakshi, P. K.; Cameron. *Inorg. Chem.* **1994**, *33*, 1434.
(18) Hering, C.; Schulz, A.; Villinger, A. *Angew. Chem.* **2012**, *124*, 6345; *Angew. Chem., Int. Ed.* **2012**, *51*, 6241.
(19) Holthausen, M. H.; Weigand, J. J. *Z. Anorg. Allg. Chem.* **2012**, *638*, 1103.
(20) Mazieres, M. R.; Sanchez, M.; Bellan, J.; Wolf, R. *Phosphorus, Sulfur Relat. Elem.* **1986**, *26*, 97.
(21) Mazieres, M. P.; Roques, C.; Sanchez, M.; Majoral, J. P.; Wolf, R. *Tetrahedron* **1987**, *43*, 2109.
(22) (a) Miller, F. A.; Wilkins, C. H. *Anal. Chem.* **1952**, *24*, 1253. (b) Sowerby, D. B. *J. Inorg. Nucl. Chem.* **1961**, *22*, 205. (c) Oba, K.; Watari, F.; Aida, K. *Spectrochim. Acta* **1967**, *23A*, 1515.
(23) (a) Schulz, A.; Mayer, P.; Villinger, A. *Inorg. Chem.* **2007**, *46*, 8316. (b) Westenkirchner, A.; Villinger, A.; Karaghiosoff, K.; Wustrack, R.; Michalik, D.; Schulz, A. *Inorg. Chem.* **2011**, *50*, 2691−2702. (c) Hering, C.; Lehmann, M.; Schulz, A.; Villinger, A. *Inorg. Chem.* **2012**, *51*, 8212.
(24) Pyykkö, P.; Atsumi, M. *Chem.—Eur. J.* **2009**, *15*, 12770.
(25) (a) Kerth, J.; Werz, U.; Maas, G. *Tetrahedron* **2000**, *56*, 35. (b) Hubner, T.; Gieren, A. *Z. Kristallogr.* **1986**, *174*, 95. (c) Ishmaeva, E. A.; Vereshchagina, Y. A.; Yarkova, E. G.; Burnaeva, L. M.; Litvinov,

I. A.; Krivolapov, D. B.; Gubaidullin, A. T.; Mironov, V. F.; Fattakhova, G. R. *Zh. Obshch. Khim.* **2002**, *72*, 1276.
(26) Kumaraswamy, S.; Kumar, K. S.; Kumar, N. S.; Swamy, K. C. *Dalton Trans.* **2005**, *10*, 1847.
(27) Weinhold, F.; Landis, C. *Valency and Bonding. A Natural Bond Orbital Donor-Acceptor Perspective*; Cambridge University Press: New York, 2005, and references therein.
(28) (a) Huang, T.; Liu, L.; Zhang, J.; Xu, X.; Huang, W.; Chen, R.; Wang, K.; Yu, X.; Liu, X. *Phosphorus, Sulfur and Silicon* **1998**, *140*, 183−193. (b) Burford, N.; Cameron, T. S.; Clyburne, J. A. C.; Eichele, K.; Robertson, K. N.; Sereda, S.; Wasylishen, R. E.; Whitla, W. A. *Inorg. Chem.* **1996**, *35*, 5460.
(29) (a) Muetterties, E. L.; Kirner, J. F.; Evans, W. J.; Watson, P. L.; Abdel-Meguid, S.; Tavanaiepou, I.; Day, V. W. *Proc. Natl. Acad. Sci. U.S.A.* **1978**, *75*, 1056. (b) Lang, H.; Eberle, U.; Leise, M.; Zsolnai, l. *J. Organomet. Chem.* **1996**, *519*, 137.
(30) (a) Cowley, A. H.; Lattman, M.; Wilburn, J. C. *Inorg. Chem.* **1981**, *20*, 2916. (b) Baxter, S. G.; Collins, R. L.; Cowley, A. H.; Sena, S. F. *Inorg. Chem.* **1983**, *22*, 3475. (c) Payrastre, C.; Madaule, Y.; Wolf, J. G. *Heteroat. Chem.* **1992**, *3*, 157. (d) Burford, N.; Cameron, T. S.; Ragogna, P. J. *J. Am. Chem. Soc.* **2001**, *123*, 7947. (e) Burford, N.; Ragogna, P. J. *J. Chem. Soc., Dalton Trans.* **2002**, 4307.
(31) (a) Davidson, J.; Weigand, J. J.; Burford, N.; Cameron, T. S.; Decken, A.; Zwanziger, W. *Chem. Commun.* **2007**, 4671. (b) Weigand, J. J.; Feldman, K.-O.; Henne, F. D. *J. Am. Chem. Soc.* **2010**, *132*, 16321.
(32) Burford, N.; Dyker, C. A.; Decken, A. *Angew. Chem., Int. Ed.* **2005**, *44*, 2364.
(33) (a) Weiss, P.; Pomrehn, B.; Hampel, F.; Bauer, W. *Angew. Chem., Int. Ed.* **1995**, *34*, 1319. (b) Boomishankar, R.; Ledger, J.; Guilbaud, J.; Campbell, N. L.; Bacsa, J.; Bonar-Law, R.; Khimyak, Y. Z.; Steiner, A. *Chem. Commun.* **2007**, 5152.
(34) Fleming, I. *Frontier Orbitals and Organic Chemical Reactions*; John Wiley & Sons: London, U.K., 1976, and references therein.
(35) W. B. McCormack, W. B.; Lewis, S. N.; Emmons, W. D. *Org. Synth.* **1973**, *5*, 787.
(36) The structures of *syn*- and *anti*-$[(Me_3Si)_2NP(C_6H_8)Cl][GaCl_4]$ were optimized on the pbe1pbe/aug-cc-pVDZ level of density functional theory. Optimized structures were analyzed for being a minimum on the energy hyper surface and in the last step the magnetic field tensors were calculated with the GIAO-package implemented in GAUSSIAN09 using the NMR-command. For example: $\delta(^{31}P)_{anti,\ calc}$ = 79.15 ppm; $\delta(^{31}P)_{syn,\ calc}$ = 33.58 ppm.
(37) Velian, A.; Cummins, C. C. *J. Am. Chem. Soc.* **2012**, *134*, 13978.
(38) Lammertsma, K. *Top. Curr. Chem.* **2003**, *229*, 95.

dx.doi.org/10.1021/ic4001285 | *Inorg. Chem.* 2013, 52, 5214−5225

5.3 Diatomic PN – trapped in a *cyclo*-tetraphosphazane

Christian Hering, Axel Schulz, Alexander Villinger.

Chemical Science, **2014**, *5*, 1064−1073.

DOI: 10.1039/C3SC52322E

In dieser Publikation wurden sämtliche experimentelle Arbeiten von mir durchgeführt. Der eigene Beitrag liegt bei ca. 90 %.

Chemical Science

EDGE ARTICLE

Diatomic PN – trapped in a *cyclo*-tetraphosphazene†

Cite this: *Chem. Sci.*, 2014, **5**, 1064

Christian Hering,[a] Axel Schulz*[ab] and Alexander Villinger[a]

$(Me_3Si)_2NPCl_2$, which is formally capable of eliminating two equivalents of Me_3SiCl, is shown to be a suitable starting material to prepare highly reactive PN species by successive elimination of Me_3SiCl. Me_3SiCl elimination can be triggered either thermally and/or by addition of a Lewis acid such as $GaCl_3$, thus leading to the formation of a highly labile aminochlorophosphenium cation in $[(Me_3Si)_2NPCl][GaCl_4]$ and iminophosphenium salt $[Me_3Si{-}N{\equiv}P][GaCl_4]$ upon warming to ambient temperatures. This work describes the synthesis and characterization of a *cyclo*-tetraphosphazane in $[PN(dmb)]_4$ (**5**) (dmb = 2,3-dimethyl-1,3-butadiene) obtained by thermal elimination of Me_3SiCl from $(Me_3Si)_2NPCl_2$ at 120 °C in toluene solution. The reactive intermediate $Me_3SiN{=}PCl$ was trapped with dmb to form the cyclic phosphazane $Me_3SiN(dmb)PCl$, which eventually oligomerizes to give **5**. In the presence of dmb or chd (chd = 1,3-cyclohexadiene) $(Me_3Si)_2NP(OTf)_2$ reacts by eliminating Me_3SiOTf to yield the spirocyclic phospholenium salts $[Me_3SiN(dmb)P(dmb)][OTf]$ (**7**) and $[Me_3SiN(chd)P(chd)][OTf]$ (**8**), of which the solid state structures were successfully determined. **7** decomposes when exposed to moisture to give an unprecedented cyclic ammonium phosphinoxide $[P(O)H(dmb)_2NH_2][OTf]$ (**9**). Tetraphosphazane **5** is shown to be a versatile ligand in transition metal chemistry. It coordinates in an η^3-fashion in $\{[PN(dmb)]_4Mo(CO)_3\}$ (**5·Mo**) and is able to coordinate a second metal fragment, exemplified by the formation of the ditungsten complex$\{[PN(dmb)]_4W_2(CO)_7\}$ (**5·W$_2$**) with a semi-bridging carbonyl ligand. All compounds were structurally characterized and the bonding situation was investigated by density functional theory and natural bond orbital analysis (NBO).

Received 19th August 2013
Accepted 4th November 2013

DOI: 10.1039/c3sc52322e

www.rsc.org/chemicalscience

Introduction

An interesting field in group 15 element chemistry is the search for molecular precursors that can release *in situ* the highly reactive heavier homologs of dinitrogen N_2. Just recently Cummins *et al.* described a multistep method in which P_2 can be thermally transferred from (Mes*NPP)Nb(N[Np]Ar)$_3$ (Mes* = 2,4,6-tri-*tert*-butylphenyl, Np = neopentyl, Ar = 3,5-$Me_2C_6H_3$) to 1,3-dienes.[1] This synthetic approach mimics the reaction between a transition metal platform and an organic azide, in which N_2 and a metal imido complex are liberated. This protocol was successfully adapted to various systems that can accept P_2.[2,3] In a similar synthetic procedure (Mes*NPAs)Nb(N[Np]Ar)$_3$ was used to access unsaturated (As≡P)–W(CO)$_5$, which retains its triple bond reactivity towards 1,3-dienes and was also transferred to terminal metal phosphide complexes to generate *cyclo*-AsP_2 molybdenum species.[4] An atom-economical and operationally simple procedure starting from P_4 was also described.[5] Under UV light irradiation (256 nm) P_4 was split into P_2 in hexane solution and could be sufficiently trapped by conjugated 1,3-dienes such as 2,3-dimethyl-1,3-butadiene (dmb) to give in moderate yields the corresponding diphosphine (Scheme 1), which has been shown to be a versatile reagent.[6,7]

In contrast, molecular PN is only known as an exotic gas-phase species of astronomical interest as it is most commonly detected in interstellar clouds.[8] The first spectroscopic evidence for the existence of phosphorus nitride was found by Curry *et al.* in 1933, when they exposed P_4 and N_2 to an electrical discharge

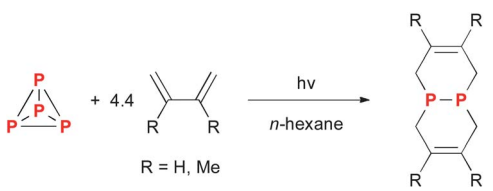

Scheme 1 Photochemical *in situ* generation of P_2 starting from P_4 and its trapping by dienes.[5]

[a]*Institut für Chemie, Abteilung Anorganische Chemie, Universität Rostock, Albert-Einstein-Strasse 3a, 18059 Rostock, Germany. E-mail: axel.schulz@uni-rostock.de*

[b]*Leibniz-Institut für Katalyse e.V. an der Universität Rostock, Albert-Einstein-Strasse 29a, 18059 Rostock, Germany*

† Electronic supplementary information (ESI) available: Full synthetic, spectroscopic, and X-ray crystallography details. CCDC 956156, 956157, 956159–956165. For ESI and crystallographic data in CIF or other electronic format see DOI: 10.1039/c3sc52322e

in the gas phase.[9] Under lab conditions PN is commonly generated by pyrolysis of either P_3N_5 at 1050 K or at 1300 K from *cyclo*-hexachlorotriphosphazene $(NPCl_2)_3$ and silver metal in a dehalogenation reaction.[10] By microwave spectroscopy the length of the PN triple bond was found to be 1.49 Å, which is in reasonable agreement with the calculated value of 1.462 Å.[10] However, molecular systems, that can be thought of as PN delivery platforms, are rare. Bertrand and co-workers reported on the reaction of NHC=N–PCl_2 (NHC = $(HCN(Dipp))_2C$, Dipp = 2,6-(diisopropyl)phenyl) with a cyclic alkyl amino carbene (CAAC, Scheme 2) and subsequent reduction with excess magnesium to yield the stable formal carbene diadduct of phosphorus mononitride NHC=N–P=CAAC (**A**) (Scheme 2, reaction (i)).[11] Compound **A** can be described as either a phosphazabutadiene ($\mathbf{A_1}$) or as the carbene diadduct of a phosphinidine-nitrene fragment ($\mathbf{A_2}$) (Scheme 2). Cummins and Velian presented another interesting molecule that possesses a hidden PN moiety in **An**N–P**An** (**B**) (**An** = $C_{14}H_{10}$, anthracene), which was shown to be susceptible to the loss of two molecules of anthracene upon thermolysis, accompanied by the formation of an insoluble yellow solid (Scheme 2, reaction (ii)).[12] Moreover, Klapötke *et al.* structurally characterized P_3N_{21}, the smallest discrete binary PN molecule so far.[13] However, to the best of our knowledge there are no reports in the literature that PN can be released directly from molecular precursors in solution.

$(Me_3Si)_2NPCl_2$ (**1**), which is formally capable of eliminating two equivalents of Me_3SiCl, should be a suitable starting material to release PN in solution, as it incorporates a PN fragment and is known to decompose within hours by Me_3SiCl elimination to give unidentified oligomeric materials.[15,16] Just recently we succeeded in the preparation of an aminochlorophosphenium cation in $[(Me_3Si)_2NPCl][GaCl_4]$ (**2**) starting from **1**. Me_3SiCl was released from **2** in CH_2Cl_2 solution upon warming to ambient temperatures, to form an iminophosphenium salt $[Me_3Si–N\equiv P][GaCl_4]$ (**3[GaCl$_4$]**) (Scheme 3), which was visualized by variable temperature ^{31}P NMR experiments.[14]

Thermal elimination of Me_3SiCl from **1** results in the formation of $Me_3Si–N=P–Cl$ (**4**) in the first step, as was previously shown by photoelectron spectroscopy (Scheme 4, reaction (i)).[17] There is just one report of **4** being released in solution when a phosphoranimine was reductively dechlorinated by a tertiary phosphine (Scheme 4, reaction (ii)).[18] Phosphoranimines are usually ideal precursors for the synthesis of polyphosphazenes, which in contrast to oligo- and polyphosphazanes incorporate oxidized P(v) centers.[19] Polyphosphazenes are the largest class of inorganic macromolecules and owing to their broad range of properties are of significant industrial importance.[20]

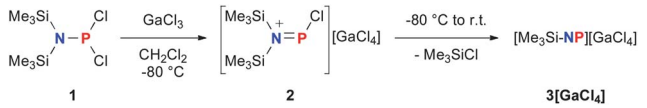

Scheme 3 Formation of iminophosphenium salt **3[GaCl$_4$]**, upon thermal release of Me_3SiCl starting from chloroaminophosphenium salt **2**.[14]

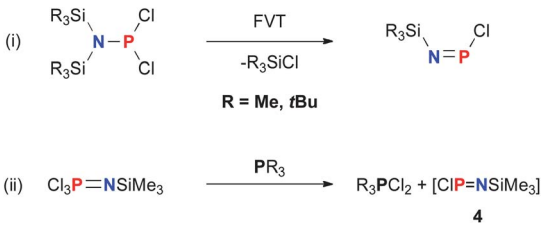

Scheme 4 (i) Formation of the iminophosphane (**4**, R = Me) in the flash vacuum thermolysis (FVT) of silylated dichlorophosphanes.[17] (ii) Tertiary phosphine induced dechlorination of phosphoranimines to generate **4** in solution.[18]

However, the iminophosphane **4** is likely to be highly reactive, prone to polymerize to oligophosphazanes and could be detected only intermediately by ^{31}P NMR spectroscopy. In contrast to **4**, Niecke and Flick prepared a stable iminophosphane $(Me_3Si)_2N–P=N(SiMe_3)$ (**5**) by eliminating Me_3SiF from $(Me_3Si)_2NP(F)N(SiMe_3)_2$ at room temperature.[21]

A class of compounds, that can be regarded as oligomers of iminophosphanes, are *cyclo*-phosphazanes $[RP^{(III)}–NR']_n$

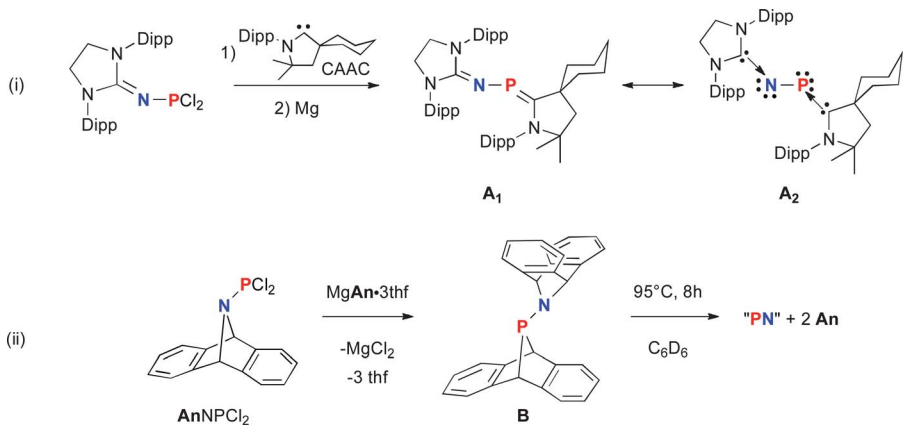

Scheme 2 (i) Formation of PN-container molecule **A** along with the two Lewis representations ($\mathbf{A_1}$ and $\mathbf{A_2}$). (ii) Reduction of **An**$NPCl_2$ with Mg**An**·3thf yielding phosphanorbornenium species **B**, which releases two equivalents of anthracene upon warming.[14]

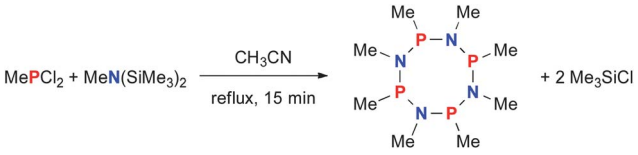

Scheme 5 Generation of $[P(Me)N(Me)]_4$ in the thermolysis of $MePCl_2$ and $MeN(SiMe_3)_2$.

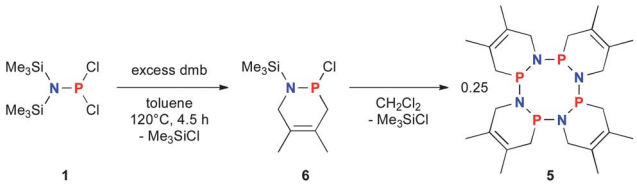

Scheme 6 Synthesis of tetraphosphazane **5** in a thermolysis reaction starting from **1**.

(R, R′ = Me, Et; n = 2, 3, 4). Pioneering work in this field was carried out by the working group of Zeiss, who reported on the first cyclic tetraphosphazane $[P(Me)N(Me)]_4$ in 1977, which was obtained in the condensation reaction of $PMeCl_2$ in the presence of $(Me_3Si)_2NMe$ by elimination of Me_3SiCl (Scheme 5).[22]

This synthetic protocol was further explored and several rings of the type $[P(R^1)N(R^2)]_4$ (R^1 = Me,[22] Et,[22] Ph,[23] Mes;[24] R^2 = Me, *t*Bu) were prepared and their potential as ligands in transition metal chemistry was explored successfully.[23,25,26] However, to the best of our knowledge there are no reports, in which *cyclo*-tetraphosphazanes can be directly prepared from molecules, that already incorporate a PN moiety. Herein we present attempts to release molecular PN directly from **1** by thermal treatment in the presence of a trapping reagent (dmb) resulting in the formation of an unprecedented *cyclo*-tetraphosphazane. Additionally, **1** was converted into $(Me_3Si)_2N$-$P(OTf)_2$, a thermally labile intermediate, which could only be trapped *in situ*. This work follows our interest in the chemistry of highly reactive molecules that incorporate binary PnN moieties (Pn = P,[27,28] As,[29,30] Sb,[31,32] Bi[33,34]) with a low coordination number on the pnictogen atom.

Results and discussion

Thermal chlorosilane elimination from $(Me_3Si)_2NPCl_2$

1 can be regarded as a molecule with a disguised PN moiety, since elimination of two equivalents of Me_3SiCl should result in the formation of "naked", molecular PN. We therefore wanted to thermally release Me_3SiCl by refluxing **1** in toluene *in vacuo* at 120 °C in a sealed flask, which resulted in the formation of an undefined polymer that still contained trimethylsilyl groups according to elemental analysis.[17] In accordance with a procedure described by Cummins and Tofan in 2010, in which they successfully quenched the triple bond reactivity of P_2 by the addition of suitable dienes (Scheme 1),[5] we added dmb to prevent the intermediate formed in the thermolysis of **1** from polymerizing.

Consequently, **1** dissolved in toluene and an excess of dmb were refluxed at 120 °C for 5 h, which resulted according to ^{31}P NMR spectroscopy in the formation of one phosphorus containing species that resonates at 126 ppm. This indicated a phosphazane with at least one carbon substituent (*cf.* δ (^{31}P): 10-chloro-9,10-dihydro-9-aza-10-phosphaphenanthrene[35] (**10**) 84.2, Fig. 5; $(Me_3Si)_2N$–$N(SiMe_3)$–$P(C_6F_5)Cl$[36] 105 ppm). In addition, polymeric side products that can be removed by filtration were formed. After removal of toluene and addition of CH_2Cl_2, the hitherto unknown *cyclo*-tetraphosphazane $[PN(dmb)]_4$ (**5**) could be isolated from the filtrate (Scheme 6, Fig. 1). Interestingly, in the ^{31}P NMR spectrum of isolated **5** only one resonance at 69.7 ppm was detected (*cf.* $[P(Ph)N(Me)]_4$ (ref. 23) 107.0 ppm), which indicated that in the thermolysis reaction the monomeric *cyclo*-phosphazane $[(Me_3Si)N(dmb)PCl]$ (**6**) was formed in the first reaction step, as the highly reactive iminophosphane $Me_3SiN{=}PCl$ (**4**) reacted in a [4 + 2] cycloaddition reaction to yield **6** (Scheme 6).[18] However, attempts to isolate **6** failed, as in all cases **5** was isolated as the oligomerization product. The polymeric side products presumably consist of higher aggregates, as exemplified by the structural characterization of a cyclic pentamer $[PN(dmb)]_5$ (**5b**) from a saturated C_6H_5F solution of **6** (Fig. 2), which could also be detected in a concentrated CH_2Cl_2 solution at 71.6 ppm in the ^{31}P NMR spectrum. The preference for the formation of **5** was further supported by calculations at the B3LYP/6-31G(d,p) level of density functional theory that render the tetramerization of **6** to be exothermic by −13.86 kcal mol^{-1} (exergonic by −17.64 kcal mol^{-1}). **5** can be prepared in isolated yields of *ca.* 25% and was fully characterized by means of NMR spectroscopy, elemental analysis, IR and Raman spectroscopy. In the Raman spectrum of **5** a stretching mode, that corresponds to the C=C double bond within the PNC_4 moieties, is detected at 1695 cm^{-1}, which is in good agreement with the C=C stretching mode observed in $[(Me_3Si)_2NP(dmb)Cl]$-$[GaCl_4]$ (**14**) (*cf.* ν (C=C) = 1672 cm^{-1}). In the CI (isobutane)

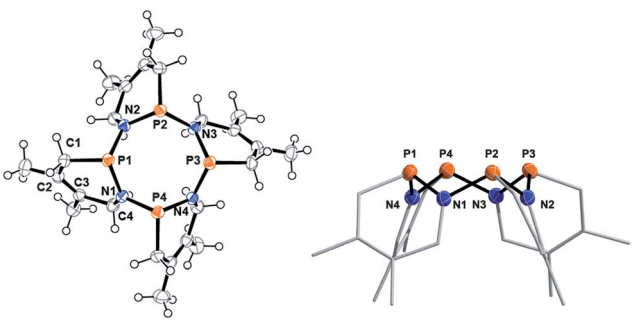

Fig. 1 Left: ORTEP drawing of the molecular structure of **5** (triclinic polymorph **5_1**) (top view). Ellipsoids are drawn at 50% probability at −100 °C. Right: molecular structure of **5** (side view, C atoms as stick representation, H atoms omitted for clarity) displaying the puckered eight-membered P_4N_4 ring. Selected bond lengths (Å) and angles (°): P1–N1 1.715(2), P1–N4 1.730(2), P2–N2 1.711(2), P2–N1 1.726(2), P3–N3 1.712(2), P3–N2 1.723(2), P4–N4 1.710(2), P4–N3 1.723(2), P1–C1 1.835(2), N1–C4 1.470(2), C2–C3 1.334(3); Σ(∠P1) 308.8, Σ(∠P2) 311.7, Σ(∠P3) 309.7, Σ(∠P4) 309.4, Σ(∠N1) 357.1; P1–C1–N1–C4 40.2(2).

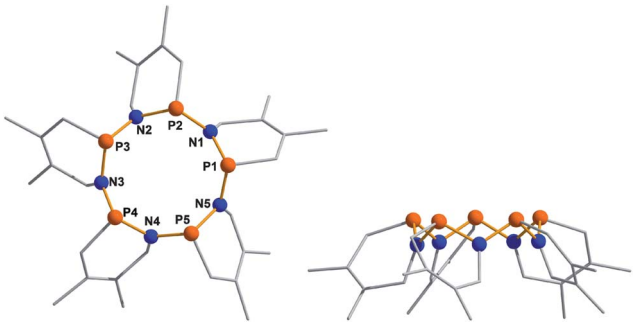

Fig. 2 Left: Ball and stick representation of the molecular structure of **5b** (top view). Right: molecular structure of **5b** side view, displaying the puckered ten-membered P_5N_5 ring. For a list of bond lengths (Å) and angles (°), see ESI.†

mass spectrum of **5** the molecular ion is detected at 509 *m*/*z*. In good agreement with the postulated reaction pathway for the formation of **5** the monomeric ion $[PN(dmb)H]^+$ is observed along with its dimer $\{[PN(dmb)]_2H\}^+$.

Depending on the temperature **5** crystallizes in two polymorphs from CH_2Cl_2. At −80 °C **5** crystallizes in the triclinic space group $P\bar{1}$ with two molecules in the unit cell and two solvent molecules per molecule of **5**. Whereas between −24 °C and −40 °C **5** crystallizes in the monoclinic space group $C2/c$ and adopts perfect C_2-symmetry as it lies on a twofold axis with one solvent molecule per molecule of **5** and four molecules per cell. Only the structural parameters of the triclinic modification are discussed, since similar metrical parameters were determined in both polymorphs. The averaged P–N distance of 1.719 Å (range: 1.710(2)–1.730(2) Å) in the monomeric unit of **5** can be considered as a shortened single bond (*cf.* Σr_{cov}(P=N) = 1.60; (P–N) = 1.82 Å)[42] and compares well with values found for $[P(Me)N(Me)]_4$ (*cf.* P–N = 1.723 Å).[22,37] Interestingly, shorter PN distances always alternate with slightly longer (*cf.* P1–N1 1.715(2), P1–N4 1.730(2), P2–N2 1.711(2), P2–N1 1.726(2), P3–N3 1.712(2), P3–N2 1.723(2), P4–N4 1.710(2), P4–N3 1.723(2) Å). As depicted in Fig. 1, the most prominent structural feature is the central puckered eight-membered P_4N_4 ring with each PN unit being part of a twisted PNC_4 six-membered ring. The phosphorus atoms in **5** are trigonal pyramidally coordinated ($\Sigma(\angle P1) = 308.78°$), which is in good agreement with $[P(Me)N(Me)]_4$ (*cf.* $\Sigma(\angle P) = 309.5°$).[22] The nitrogen atoms in **5** display only a small deviation from planarity ($\Sigma(\angle N1) = 357.05°$) which might be due to steric hindrance. According to NBO analysis a p-type lone pair (LP) is located on the four N_{amino} atoms and a LP with 50% s-character is located on each phosphorus atom. The LPs at the nitrogen atoms are delocalized into each of the neighboring σ*-orbitals of the PN bonds, imposing a certain degree of π-bonding in the PN skeleton. All six-membered PNC_4 heterocycles point in one direction, resulting in the formation of a hydrophobic cage below the plane that is formed by all four phosphorus atoms (Fig. 1, right), a structural feature that is also observed in cone-calixarenes.[38] Phosph(III)azane donor cavity molecules are rare and to the best of our knowledge cone-like derivatives are without precedent.[39–41] However, there are examples of cyclic triphosphanes that also place the phosphorus atoms in one direction, for example $(PRC_2H_4)_3$[42] (**11**) obtained in a CpFe(II) templated reaction or the chair-like 1,3,5-triphospha-2,4,6-trisilahexane[43] (**12**) which was first synthesized in 1971 (Fig. 5). Hence all four lone pairs (LP) in **5**, one located on each phosphorus site, point in one direction above the ring (see Fig. S10† in the ESI) and can be utilized to bind Lewis acids such as metal carbonyl fragments (*vide infra*). The dmb moiety is covalently attached to phosphorus and nitrogen (P1–C1 1.835(2); N1–C4 1.470(2) Å), as both distances are in the range of single bonds (*cf.* Σr_{cov}(P–C) = 1.86; (N–C) = 1.46 Å).[42] A carbon double bond (C2–C3 1.334(3) Å) is detected within the six-membered ring system (*cf.* Σr_{cov}(C=C) = 1.34 Å).[37] The PNC_4 moieties are twisted, with the P1–C1–N1 plane being rotated against the N1–C4–P1 plane by 40.2°. **5b** crystallizes in the monoclinic space group $P2_1$ with two molecules in the unit cell. The quality of the data obtained is rather poor and therefore only the connectivity is shown and does not allow for a detailed discussion of bond lengths and angles. As in **5** the PNC_4 moieties in **5b** point in one direction, forming a cavity below the plane that is formed by all five phosphorus atoms. Consequently all five LPs on the phosphorus atoms point in one direction, offering five donor sites for transition metal fragments.

Preparation of highly labile $(Me_3Si)_2NP(OTf)_2$

In a next series of experiments we wanted to explore the ability of the triflate-substituted aminophosphane $(Me_3Si)_2NP(OTf)_2$ (OTf = $CF_3SO_3^-$, trifluoromethylsulfonate) to serve as a PN-precursor, as Me_3Si–OTf is a common leaving group in main group chemistry.[44,45] In the absence of a trapping reagent the addition of two equivalents of AgOTf to a solution of **1** in CH_2Cl_2 at −80 °C yielded according to ^{31}P NMR spectroscopy no phosphorus-containing product. However, the evolution of Me_3Si–OTf was observed. We therefore added dmb to trap the reactive intermediate that is formed *in situ* upon thermal elimination of Me_3Si–OTf. Indeed, in the presence of two equivalents of dmb a clean conversion to one phosphorus-containing species was observed in the ^{31}P NMR spectrum, which gave rise to a resonance at 59.8 ppm, a region typical for phosphonium salts (Scheme 7).

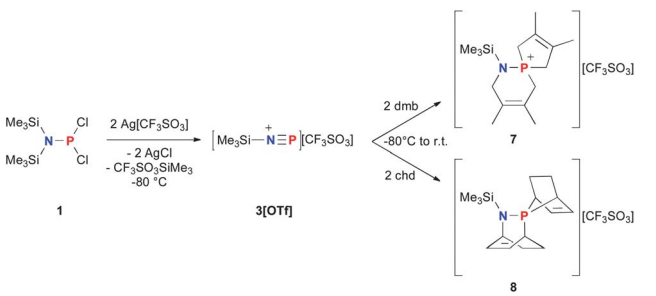

Scheme 7 Synthesis of spirocyclic phospholenium salt **7**, when **1** is treated with AgOTf in the presence of dmb. **8** is obtained in a similar synthetic protocol when chd is utilized instead of dmb.

In addition, two different dmb moieties and one Me_3Si-group were identified in the ^1H NMR spectrum, which was indicative of the spirocyclic phospholenium salt $[Me_3SiN(dmb)P(dmb)][CF_3SO_3]$ (**7**) (Fig. 3, left). In the ^{13}C NMR spectrum six magnetically inequivalent carbon atoms are detected for the six-membered P(dmb)N moiety and furthermore a C_2 symmetric $PC_4H_4(Me)_2$ five-membered ring (a formal phosphapentene) with three distinguishable resonances. Examples of cationic spirocyclic phosphorus compounds are scarcely found in the literature.[46–48] Niecke *et al.* described a related heterocyclic system in 1992, when they treated $[Mes^*–N{\equiv}P]^+$ with diphenylacetylene. In the presence of dmb a spirocyclic phospholenium salt (**13**, Fig. 5) was obtained.[49] It was also possible to prepare the cyclohexa-1,3-diene (chd) derivative $[Me_3SiN(chd)P(chd)][CF_3SO_3]$ (**8**) (Fig. 3, right), which resonates at 82.1 ppm in the ^{31}P NMR spectrum. We assume that in the first reaction step an iminophosphenium cation of the type $[Me_3Si–N{\equiv}P][CF_3SO_3]$ (**3[OTf]**) was formed, which shows triple bond reactivity towards dienes and firstly reacted with dmb/chd in a [4 + 2] cycloaddition forming a cyclic phosphenium cation. This heterocyclic phosphenium cation further reacted in a second chelotropic [4 + 1] cycloaddition to yield **7** and **8**, respectively. This reaction is the first example of PN triple bond reactivity utilized in the formation of PN heterocycles, whereas AsP and P_2 triple bond reactivity has been described before (Scheme 1).[1,4,5] Serendipitously, we found that **7** can be hydrolyzed to form a cyclic ammonium phosphine oxide salt $[(O)PH(dmb)_2NH_2][CF_3SO_3]$ (**9**) (Scheme 8), which could be structurally characterized (Fig. 4). It incorporates phosphorus and nitrogen atoms, respectively, indicating that it is indeed possible to transfer PN starting from **1**. To the best of our knowledge, **9** is the first 10-membered cyclic phosphine oxide that also possesses an ammonium center. However, **9** is only stable at temperatures below −30 °C and decomposes rapidly at ambient temperature, consequently no further data could be collected.

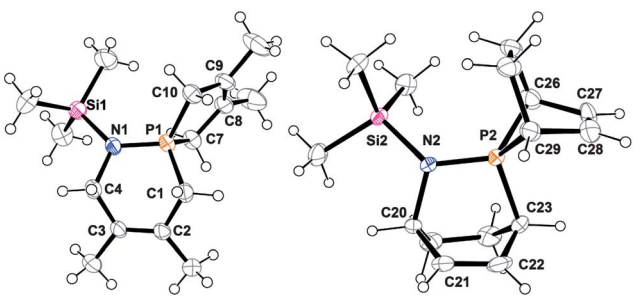

Fig. 3 ORTEP drawing of one of the three independent cations in the asymmetric unit of **7** (left) and one of the two independent cations in the asymmetric unit of **8** (right), $CF_3SO_3^-$ anions are omitted for clarity. Ellipsoids are drawn at 50% probability at −100 °C. Selected bond lengths (Å) and angles (°), (**7**): P1–N1 1.634(2), C1–P1 1.773(3), N1–C4 1.504(3), N1–Si1 1.769(2), C1–C2 1.518(3), C2–C3 1.331(3), P1–C7 1.801(3), P1–C10 1.797(3), C7–C8 1.498(4), C8–C9 1.322(4); Σ(∠N1) 359.3, Σ(∠P1) 324.6; Si1–N1–P1–C7 59.5(2), C4–N1–P1–C10 115.3(2), C2–C1–P1–N1 51.2, C4–N1–P1–C1 −7.0(2); (**8**): P2–N2 1.643(2), P2–C23 1.812(3), P2–C26 1.824(3), P2–C29 1.833(3), N2–C20 1.539(3), N2–Si2 1.790(2), C20–C21 1.499(4), C21–C22 1.328(4), C26–C27 1.538(5), C27–C28 1.298(5); Σ(∠N2) 356.7, Σ(∠P2) 340.6.

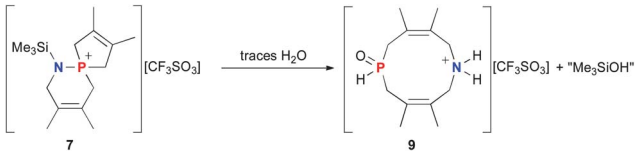

Scheme 8 Hydrolysis of phospholenium species **7** to afford cyclic ammonium phosphine oxide **9**.

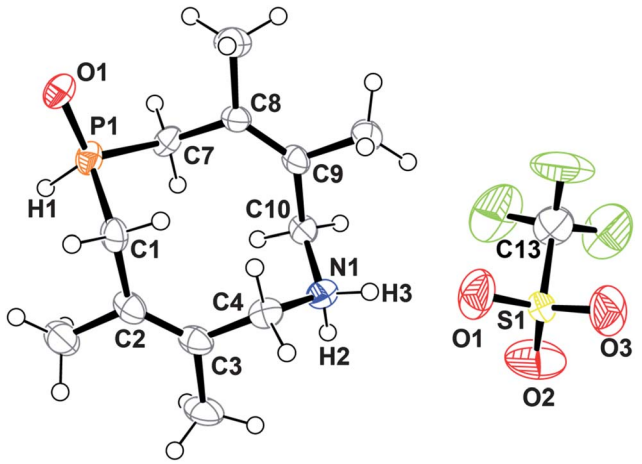

Fig. 4 ORTEP drawing of **9**. Ellipsoids are drawn at 50% probability at −100 °C. Selected bond lengths (Å) and angles (°): P1–O1 1.500(3), P1–C1 1.795(5), P1–C7 1795(4), N1–C4 1.509(6), N1–C10 1.497(6); Σ(∠P1) 334.1, Σ(∠N1) 332.3; C7–P1–C1–C2 −64.4(4).

7 crystallizes in the triclinic space group $P\bar{1}$ with three independent formula units in the asymmetric unit. **8** crystallizes in the monoclinic space group $P2_1/n$ with eight formula units in the unit cell. Two ion pairs are found per asymmetric unit of which the cation in one of these pairs is partially disordered. Since similar structural parameters are observed for the different independent formula units, the discussion is led for only one of the formula units of **7** and **8**, respectively.

The P–N distance in **7** and **8** (**7**: 1.634(2); **8**: 1.643(2) Å) is in the range of the starting material **1** (*cf.* $(Me_3Si)_2NPCl_2$: P–N 1.6468(8) Å)[14] and might be considered as an elongated double bond (*cf.* $\Sigma r_{cov}(P{=}N) = 1.60$; $(P–N) = 1.82$ Å).[37] As **7** and **8** are derived from the corresponding phosphenium species the bonding is similar to the recently reported phospholenium salt $[(Me_3Si)_2NP(dmb)Cl][GaCl_4]$ (**14**, Fig. 5) and the 7-phosphanorbornenium salt $[(Me_3Si)_2NP(chd)Cl][GaCl_4]$ (**15**, Fig. 5), in which the P–N distances are shorter (*cf.* **14**: 1.6089(9), **15**: 1.592(2) Å). A reason for the elongation seems to be the steric congestion that is applied to the P–N bond by the cycloaddition of the dmb or chd moiety, respectively.[50] Spirocyclic phosphorus cations have already been prepared, however, structural data of such species are not found in the literature; the structures of **7** and **8** close this gap.[46,47,53,54] The carbon atoms of the dmb and chd moieties in **7** and **8** are covalently attached to both nitrogen and phosphorus by a single bond (**7**: N–C 1.504(3), P–C 1.773(3); **8**: N–C 1.539(3), P–C 1.812(3) Å; *cf.* $\Sigma r_{cov}(P–C) = 1.86$; $\Sigma r_{cov}(N–C) = 1.46$ Å),[37]

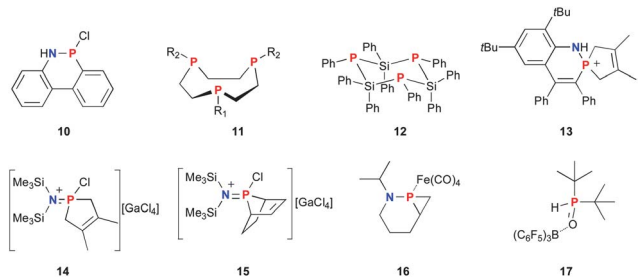

Fig. 5 Structures of chlorophosphine **10**, triphosphine **11**, 1,3,5-triphospha-2,4,6-trisilahexane **12**,[43] spirocyclic phospholenium cation **13**,[49] phospholenium salts **14** and **15**,[50] $(PNC_8)Fe(CO)_4$ **16**[51] and $(C_6F_5)_3B\cdots PH(O)tBu_2$ **17**.[52]

with the longer distances detected in chd derivative **8** due to steric hindrance. These values compare nicely with those detected in related phosphazanes coordinated to $Fe(CO)_4$ (*cf.* $(PNC_8)Fe(CO)_4$ (**16**): P–C 1.805(2), P–N 1.470(2) Å, Fig. 5).[51] The second diene fragment is also covalently attached to the phosphorus atom (**7**: 1.801(3)/1.797(3); **8**: P2–C26 1.824(3)/1.833(3) Å), which furthermore exhibits a tetrahedral coordination environment (Σ(∠P), **7**: 324.6, **8**: 340.6°). These bond lengths are similar to those observed in **14** (*cf.* averaged P–C 1.801 Å) and **15** (*cf.* averaged P–C 1.822 Å).[50] The nitrogen atom is trigonal planar coordinated in both salts (Σ(∠N), **7**: 359.3, **8**: 356.7°). In **7** the $PNC_4H_4(Me)_2$ moiety shows an envelope conformation, whereas the phosphole moiety is almost planar. The 7-phosphanorbornenium group in **8** is found to place the double bond in a *trans* position with respect to the PN bond, in contrast to the P(chd)N moiety, which is found to have no preferential orientation, indicated by a disorder in the molecular structure. Cation and anion are well separated, thus no significant interionic interactions can be assumed.

Decomposition product **9** crystallizes as the CH_2Cl_2 solvate in the orthorhombic space group $Pna2_1$ with four ion pairs in the cell (Fig. 4). The cation in **9** is disordered and was split into two parts. The P–O distance (P1–O1 1.500(3) Å) is in the expected range for phosphine oxides (*cf.* **17**: P–O 1.534(1) Å, Fig. 5),[52] with a P–O double bond (*cf.* $\Sigma r_{cov}(P{=}O) = 1.50$ Å).[37] The phosphorus and nitrogen atoms are tetrahedrally coordinated. The dmb moieties are both connected to phosphorus and nitrogen by single bonds and the ten-membered ring system in the cation adopts a chair-like conformation in which a central PNC_4 plane is found. The plane of each dmb is angled by 60° with respect to the inner plane. The anion and cation in **9** are well separated.

Utilization of $[PN(dmb)]_4$ as a ligand

Having prepared **5**, we were intrigued by the idea of binding **5** to a suitable transition metal. Reports by Gallicano and co-workers encouraged us to test **5** as a ligand for different group 6 metal complexes.[25] After refluxing a mixture of $Mo(CO)_6$ and **5** for 2 h at 95 °C in toluene the solvent was removed *in vacuo*, residual $Mo(CO)_6$ was removed by sublimation and the remaining brownish solid was re-dissolved in toluene to yield minimal amounts of crystalline material that was identified as a tricarbonylmolybdenum(0) complex of $[PN(dmb)]_4$ (**5·Mo**) by means of X-ray crystallography (Fig. 6, left). **5·Mo** can be prepared independently starting from the labile $[Mo(CO)_3(EtCN)_3]$ precursor complex in which the C_2H_5CN ligands can be replaced easily by stronger donors (Scheme 9, reaction (i)).[55] **5·Mo** was fully characterized by means of elemental analysis, ^{31}P NMR, IR and Raman spectroscopy. In the IR spectrum **5·Mo** shows ν (CO) frequencies of 1930 and 1828 cm^{-1} (*cf.* {[P(Me)N(Me)]$_4$Mo(CO)$_3$} 1928, 1828 cm^{-1}) indicating that **5** is less σ-donating than the tridentate ligand [9]-ane P_3Ph_3 (**11** R_{1-3} = Ph; Fig. 5) (*cf.* ν (CO) = 1902, 1795 cm^{-1}),[56] hence π-back-bonding to the carbonyl ligands is decreased which is supported by the X-ray crystallographic data. In the ^{31}P NMR spectrum of **5·Mo** a single resonance at 79.8 ppm is observed leading to the conclusion that the $Mo(CO)_3$ fragment migrates freely on top of the P_4N_4 platform in solution, so that all phosphorus atoms are equivalent on the NMR time scale. Upon cooling to −80 °C the singlet splits in a rather complex set of broad multiplets between 83 and 69 ppm with a 1 : 2 : 1 ratio, suggesting that the coordination mode of the $Mo(CO)_3$ fragment becomes more rigid (see Fig. S3/S4 in the ESI†) and hence an AB_2C spin system.

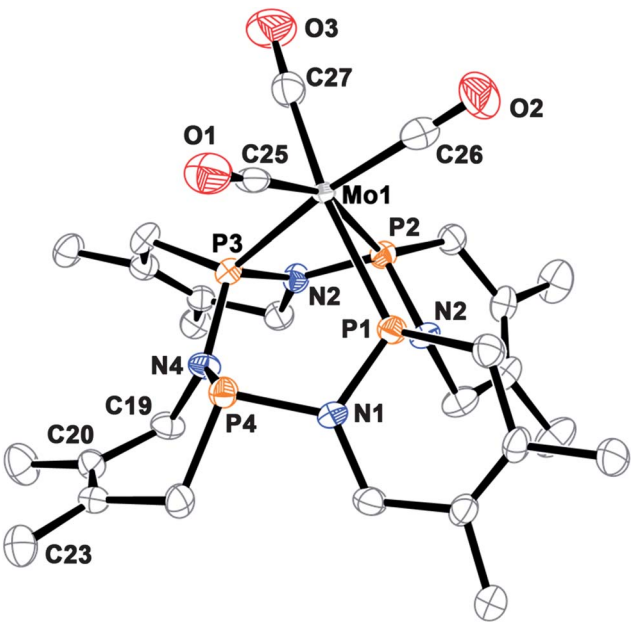

Fig. 6 ORTEP drawing of **5·Mo** (monoclinic polymorph **5·Mo_1**). Ellipsoids are drawn at 50% probability at −100 °C. Selected bond lengths (Å) and angles (°) of **5·Mo**: P1–N1 1.674(3), P1–N2 1.719(4), P2–N2 1.681(3), P2–N3 1.709(3), P3–N3 1.703(3), P3–N4 1.681(3), P4–N4 1.727(3), P4–N1 1.749(4), C25–O1 1.165(5), C26–O2 1.174(6), C27–O3 1.163(5), Mo1–C25 1.960(5), Mo1–C26 1.942(5), Mo1–C27 1.949(5), P1–Mo1 2.469(1), P2–Mo1 2.456(1), P3–Mo1 2.497(1); Σ(∠P1) 315.5, Σ(∠P2) 318.5, Σ(∠P3) 311.9, Σ(∠P4) 303.0, Σ(∠N1) 358.9, Σ(∠N4) 360.0; P4–C19–C20–C23 57.7(5); P3–W1 2.457(1), P4–W2 2.534(1); Σ(∠P1) 321.5, Σ(∠P2) 316.3, Σ(<P3) 307.9, Σ(∠P4) 315.4, Σ(∠N) 360.0, W2–C31–O7 163.3(6). Selected bond lengths and angles of **5·W$_2$**, along with a detailed structure discussion can be found in the ESI (Fig. S6†).

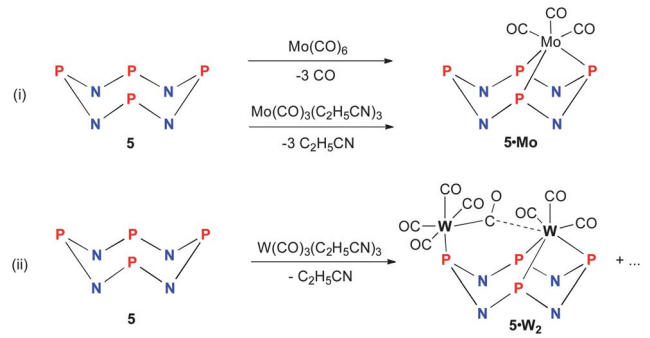

Scheme 9 Top: Synthesis of the *fac*-$Mo(CO)_3$ complex of **5** utilizing ligand replacement in $Mo(CO)_3(C_2H_5CN)_3$. Bottom: illustration of the reaction sequence that yielded **5·W₂** (dmb moieties are omitted for clarity).

Furthermore, we wanted to prepare a tungsten complex starting from the precursor complex $[W(CO)_3(EtCN)_3]$[55] and after stirring a mixture of **5** and $[W(CO)_3(EtCN)_3]$ in CH_2Cl_2 for 21 days different types of crystals had formed (Scheme 9, reaction (ii)). It was possible to isolate a few crystals by manual separation and to determine the molecular structure of the substance. In that case among other unidentified crystalline material, a dinuclear tungsten complex **5·W₂** had formed as a minor product that incorporates two differently coordinated tungsten atoms (see Fig. S6 in the ESI†). However, it was impossible to prepare enough material of **5·W₂** to fully characterize the substance.

5·Mo crystallizes in two modifications depending on the solvent utilized. From a saturated toluene solution **5·Mo** crystallizes in the triclinic space group $P\bar{1}$ with two molecules in the cell and 1.4 molecules of toluene per **5·Mo**. By vapour diffusion of *n*-hexane into a saturated CH_2Cl_2 solution of **5·Mo** crystals were obtained, which were found to crystallize in the monoclinic space group $P2_1/c$ with four molecules in the unit cell. The following detailed structure discussion focuses on the monoclinic polymorph. The X-ray structure shows a distorted octahedral environment around the molybdenum atom consisting of a facially capped P_4N_4 framework and three carbonyl ligands, whereas the crown conformation of the P_4N_4 ligand is retained. The deviation from an ideal octahedral coordination sphere evolves mainly around the P_4N_4 ring, which shows two rather acute P–Mo–P bite angles averaging 64.94°, one angle of 85.14(4)° and the *trans* C–Mo–P angles average 163.34°. The average C–Mo–C bond angles, however, amount to 92.34°, illustrating that the carbonyl ligands nearly sit in idealized octahedral positions around the metal center. The average P–Mo and Mo–C distances are 2.471 Å and 1.950 Å, respectively. Compared with the values observed in $\{[P(Me)N(Me)]_4Mo(CO)_3\}$ (*cf.* Mo–P 2.506, Mo–C 1.984 Å), it appears that **5** is more tightly bound to the molybdenum atom than in the $[P(Me)N(Me)]_4$ complex.[25] The PN distances within the coordinated PNC_4 fragments in **5** compared to **5·Mo** contract significantly upon coordination, with the largest contraction being 0.39 Å (*cf.* **5**: P1–N1 1.715(2), **5·Mo**: 1.674(3) Å). Presumably, the p-type LP located on the N_{amino} atom in the P1N1C4 moiety interacts with the σ*-orbital of the Mo1–P1 bond inducing some degree of π-bonding between P1 and N1. The same situation can be discussed for the other PNC_4 fragments that are coordinated. The three coordinated PNC_4 moieties point downwards and are nearly planar. Interestingly, the uncoordinated PNC_4 fragment adopts an envelope conformation (P4–C19–C20–C23 57.7(5)°).

Conclusions

$(Me_3Si)_2NPCl_2$ can be considered as a molecule with a disguised PN moiety which can be used in formal pericyclic reactions such as [4 + 2] and [4 + 1] cycloadditions. For example, in the presence of dmb the highly reactive intermediate $Me_3SiN{=}PCl$ was trapped in a [4 + 2] cycloaddition to give phosphazane **6**, which undergoes oligomerization by eliminating Me_3SiCl to yield the calixarene-like $[PN(dmb)]_4$. The latter species was shown to be a versatile ligand in transition metal chemistry. Further investigations of its ligand properties might result in interesting applications in catalysis. Additionally, $(Me_3Si)_2NP(OTf)_2$ was also shown to be a suitable PN precursor as in the presence of dmb or chd the spirocyclic phospholenium cations **7** and **8** were formed. For the first time the triple bond reactivity of the $[Me_3Si{-}N{\equiv}P]^+$ cation was exploited to yield stable derivatives, which could be structurally characterized. In future studies the polymerization behavior of $(Me_3Si)_2NPCl_2$ will be explored in more detail.

Experimental section

General information

All manipulations were carried under oxygen- and moisture-free conditions using standard Schlenk and Drybox techniques.

Dichloromethane was purified according to a literature procedure,[1] dried over P_4O_{10}, stored over CaH_2 and was freshly distilled prior to use, as was C_6H_5F. Toluene and benzene were dried over Na/benzophenone and freshly distilled prior to use. *n*-Hexane was dried over Na/benzophenone/tetraglyme and freshly distilled prior to use. *N*,*N*-Bis(trimethylsilyl)aminodichlorophosphane,[14] silver trifluoromethylsulfonate AgOTf[57] and $Mo/W(CO)_3(C_2H_5CN)_3$[55] have been reported previously and were prepared according to modified literature procedures. 2,3-Dimethyl-1,3-butadiene (98%, Aldrich) and 1,3-cyclohexadiene (*stabilized for synthesis*, Merck) were stirred over $NaBH_4$ for 24 h and stored over molecular sieves. $Mo(CO)_6$ (pract., Fluka) was freshly sublimed prior to use.

NMR. $^{31}P\{^1H\}$, ^{29}Si INEPT-, $^{19}F\{^1H\}$-, $^{13}C\{^1H\}$- and ^1H-NMR spectra were recorded on BRUKER spectrometers AVANCE 300 and AVANCE 500, respectively. The ^1H and ^{13}C NMR chemical shifts were referenced to the solvent signals ($CDHCl_2$: δ (^1H) = 5.31; δ (^{13}C) = 54.0). The ^{19}F, ^{29}Si and ^{31}P NMR chemical shifts are referred to $CFCl_3$, TMS and H_3PO_4 (85%), respectively. CD_2Cl_2 was dried over P_4O_{10} and was degassed prior to use.

CHN analysis. Analysator Flash EA 1112 from Thermo Quest.

IR. Nicolet 380 FT-IR with a Smart Orbit ATR module.

Raman. LabRAM HR 800 Horiba Jobin YVON equipped with a high stability BX40 microscope.

(Focus 1 μm) or an Olympus Mplan 50xNA 0.70 lens. For excitation an infrared laser (785 nm, 100 mW, air-cooled diode) or a red laser (633 nm, 17 mW, HeNe-Laser) was utilized.

Melting points are uncorrected (EZ-Melt, Stanford Research Systems). Heating-rate 20 °C min^{-1} (clearing points are reported).

MS. Finnigan MAT 95-XP from Thermo Electron was used.

X-ray structure determination

X-ray quality crystals of **5**, **5b**, **7**, **8**, **9**, **5·Mo**, **5·W$_2$** and $Mo(CO)_3(C_2H_5CN)_3$ were selected in Fomblin YR-1800 perfluoroether (Alfa Aesar) at ambient temperature. The data were collected on a Bruker Kappa Apex-II CCD diffractometer using graphite monochromated Mo-Kα radiation (λ = 0.71073). The structures were solved by direct methods (SHELXS-97)[58] and refined by full-matrix least squares procedures (SHELXL-97).[59] Semi-empirical absorption corrections were applied (SADABS).[60] All non-hydrogen atoms were refined anisotropically; hydrogen atoms were included in the refinement at calculated positions using a riding model.

Synthesis of [PN(dmb)]$_4$ (5)

$(Me_3Si)_2NPCl_2$ (0.821 g, 3.3 mmol) and 2,3-dimethyl-1,3-butadiene (0.662 g, 8.06 mmol) were combined in 10 ml toluene and the mixture degassed properly by three freeze–pump–thaw cycles. Afterwards the flask was placed in an oil bath and refluxed *in vacuo* at 115 °C over a period of 4.5 h. The resulting white suspension was slowly cooled to room temperature and polymers removed by filtration. Afterwards the solvent was removed from the filtrate *in vacuo* and the residual oily liquid re-dissolved in CH_2Cl_2, yielding after concentration to 0.2 ml and placement in the freezer for 12 h (−40 °C) [PN(dmb)]$_4$ (0.112 g, 0.18 mmol, 22%). Taking on the residual oily liquid in C_6H_5F resulted in the deposition of colorless blocks of **5** together with small plates of $[P_5N_5(dmb)_5]$ (**5b**).

Mp. 70 °C (dec). Anal. calc. % (found) [PN(dmb)]$_4\cdot CH_2Cl_2$: C 50.60 (50.74); H 7.13 (7.27); N 9.44 (10.10). ^{1}H NMR (25 °C, CD_2Cl_2, 250.13 MHz): 1.54 (s, 12H, CH_3), 1.73 (s, 12H, CH_3), 1.74 (m, $J(^{13}C–^1H)$ = 119.16 Hz, 8H, PCH_2), 3.59 (m, 8H, NCH_2); $^{13}C\{^1H\}$ NMR (25 °C, CD_2Cl_2, 62.90 MHz): 18.2 (s, CH_3), 20.9 (s, *C*H$_3$), 32.1 (m, P*C*H$_2$), 51.1 (m, N*C*H$_2$), 122.0 (s, C_{vinyl}), 125.3 (s, C_{vinyl}); ^{31}P NMR (25 °C, CD_2Cl_2, 101.27 MHz): (**5**) 69.7 (s), (**5b**) 71.6 (s). IR (ATR, 25 °C, 32 scans, cm^{-1}): 2978 (w), 2906 (m), 2855 (m), 2821 (m), 1436 (m), 1393 (w), 1382 (m), 1361 (w), 1275 (m), 1250 (m), 1218 (m), 1166 (m), 1135 (m), 1091 (m), 1044 (m), 956 (m), 920 (m), 862 (s), 839 (s), 805 (m), 778 (s), 751 (s), 724 (s), 695 (m), 645 (s), 563 (m). Raman: 2907 (7), 2865 (5), 2832 (1), 2797 (1), 1695 (5), 1442 (4), 1397 (6), 1277 (4), 1260 (4), 1166 (1), 1138 (1), 1104 (1), 962 (1), 780 (1), 758 (3), 696 (3), 642 (10), 566 (4), 495 (5), 423 (3), 368 (4), 321 (3), 288 (4), 264 (3), 248 (3). MS (CI, isobutane, *m*/*z*, >10%): $\{[PN(C_6H_{10})]_4 + H\}^+$ 509 (15.8), $\{[PN(C_6H_{10})]_2 + H\}^+$ 255, $\{[PN(C_6H_{10})] + H\}^+$ 128 (52.2); (ESI-TOF, *m*/*z*): $\{[PN(C_6H_{10})]_4 + H\}^+$ 509.22, $\{[PN(C_6H_{10})]_5 + H\}^+$ 636.28.

Synthesis of [Me$_3$SiN(dmb)P(dmb)][CF$_3$SO$_3$] (7)

$(Me_3Si)_2NPCl_2$ (0.269 g, 1.05 mmol) in CH_2Cl_2 (3 ml) was combined with dmb (0.170 g, 2.1 mmol) and added to a slurry of AgOTf (0.523 g, 2.1 mmol) in CH_2Cl_2 (3 ml) at −80 °C. The greyish suspension was allowed to slowly warm to room temperature and was further stirred for one hour. Afterwards the solvent was removed *in vacuo* and the residual off-white solids extracted with CH_2Cl_2 (5 ml). Removal of the solvents and washing of the crude material with minimal amounts of *n*-hexane yielded $[Me_3SiN(dmb)P(dmb)][CF_3SO_3]$ (7) as a white powder (0.325 g, 0.75 mmol, 72%).

When a CH_2Cl_2 solution of **9** was placed in the freezer at −24 °C for 72 h the formation of small colorless needles was observed. These needles were crystallographically analysed to be the hydrolysis product of **9** $[H(O)P(dmb)_2N_2]$ $[CF_3SO_3]$ (**9**). Crystals of **9** decompose rapidly at room temperature.

Mp. 58 °C. ^{1}H NMR (25 °C, CD_2Cl_2, 500.13 MHz): 0.31 (s, $J(^{29}Si–^1H)$ = 6.59 Hz, $J(^{13}C–^1H)$ = 120.02 Hz, 9H, Si(CH_3)$_3$), 1.79 (m, 3 CH_3), 1.91 (s, CH_3), 2.76-2.97 (m, 4H, PCH_2), 3.00 (d, $J(^{31}P–^1H)$ = 12.8 Hz, 2H, PCH_2), 3.58 (d, $J(^{31}P–^1H)$ = 18.00 Hz, 2H, NCH_2); $^{13}C\{^1H\}$ NMR (25 °C, CD_2Cl_2, 125.76 MHz): 0.16 (s, Si(*C*H$_3$)$_3$), 16.5 (d, $J(^{31}P–^{13}C)$ = 14.50 Hz, 2 *C*H$_3$), 18.7 (d, $J(^{31}P–^{13}C)$ = 1.99 Hz, *C*H$_3$), 21.0 (d, $J(^{31}P–^{13}C)$ = 6.47 Hz, *C*H$_3$), 27.2 (d, $J(^{31}P–^{13}C)$ = 56.01 Hz, P*C*H$_2$), 36.6 (d, $J(^{31}P–^{13}C)$ = 60.47 Hz, 2 P*C*H$_2$), 50.0 (d, $J(^{31}P–^{13}C)$ = 3.56 Hz, N*C*H$_2$), 122.0 (d, $J(^{31}P–^{13}C)$ = 10.84 Hz, C_{vinyl}), 128.6 (d, $J(^{31}P–^{13}C)$ = 10.93 Hz, 2 C_{vinyl}), 134.15 (d, $J(^{31}P–^{13}C)$ = 14.73 Hz, C_{vinyl}); $^{19}F\{^1H\}$ NMR (25 °C, CD_2Cl_2, 282.40 MHz): −78.8; ^{29}Si NMR (25 °C, CD_2Cl_2, 59.63 MHz): 7.7 (m); ^{31}P NMR (25 °C, CD_2Cl_2, 202.46 MHz): 59.9 (s). IR (ATR, 25 °C, 32 scans, cm^{-1}): 2954 (w), 2920 (w), 2864 (w), 1444 (w), 1418 (w), 1395 (w), 1255 (s), 1221 (s), 1188 (m), 1149 (s), 1113 (m), 1054 (m), 1028 (s), 978 (m), 904 (m), 841 (s), 802 (m), 755 (m), 711 (m), 695 (m), 666 (m), 634 (s), 572 (m).

Synthesis of [Me$_3$SiN(chd)P(chd)][CF$_3$SO$_3$] (8)

$(Me_3Si)_2NPCl_2$ (0.269 g, 1.05 mmol) in CH_2Cl_2 (3 ml) was combined with chd (0.166 g, 2.1 mmol) and added to a slurry of AgOTf (0.527 g, 2.1 mmol) in CH_2Cl_2 (3 ml) at −80 °C. The greyish suspension was allowed to slowly warm to room temperature and further stirred for one hour. Afterwards the solvent was removed *in vacuo* and the residual off-white solids extracted with CH_2Cl_2 (5 ml). Removal of the solvents and washing of the crude material with minimal amounts of *n*-hexane yielded $[Me_3SiN(chd)P(chd)][CF_3SO_3]$ (**8**) as a greyish powder (0.171 g, 0.40 mmol, 38%).

Mp. 87 °C (dec). ^{1}H NMR (25 °C, CD_2Cl_2, 300.13 MHz): 0.45 (s, $J(^{29}Si–^1H)$ = 6.42 Hz, $J(^{13}C–^1H)$ = 120.30 Hz, 9H, Si(CH_3)$_3$), 1.45–2.53 (m, 8 CH_2), 3.08 (m, 1H, PC*H*), 3.49 (m, 1H, PC*H*), 3.58 (m, 1H, PC*H*), 4.60–4.46 (m, 1H, NC*H*), 6.81–6.46 (m, 4H, vinyl-C*H*); $^{13}C\{^1H\}$ NMR (25 °C, CD_2Cl_2, 75.47 MHz): 2.8 (s, Si(*C*H$_3$)$_3$), 19.1 (d, $J(^{31}P–^{13}C)$ = 5.07 Hz, 1 *C*H$_2$), 22.0 (d, $J(^{31}P–^{13}C)$ = 15.52 Hz, *C*H$_2$), 23.9 (d, $J(^{31}P–^{13}C)$ = 42.28 Hz, P*C*3), 24.0 (d, $J(^{31}P–^{13}C)$ = 59.97 Hz, P*C*H), 24.4 (d, $J(^{31}P–^{13}C)$ = 14.86 Hz, P*C*H$_2$), 28.2 (d, $J(^{31}P–^{13}C)$ = 9.1 Hz, P*C*H$_2$), 37.9 (d, $J(^{31}P–^{13}C)$ = 54.0 Hz, P*C*H), 40.0 (d, $J(^{31}P–^{13}C)$ = 48.2 Hz, P*C*H), 56.4 (d, $J(^{31}P–^{13}C)$ = 6.01 Hz, N*C*H), 130.6 (d, $J(^{31}P–^{13}C)$ = 10.85 Hz, C_{vinyl}), 133.0

(d, $J(^{31}P–^{13}C) = 12.13$ Hz, C_{vinyl}), 134.3 (d, $J(^{31}P–^{13}C) = 12.97$ Hz, C_{vinyl}), 139.2 (d, $J(^{31}P–^{13}C) = 13.65$ Hz, C_{vinyl}); $^{19}F\{^1H\}$ NMR (25 °C, CD_2Cl_2, 282.40 MHz): −78.6; ^{29}Si NMR (25 °C, CD_2Cl_2, 59.63 MHz): 19.2 (m); ^{31}P NMR (25 °C, CD_2Cl_2, 75.46 MHz): 82.1 (s). IR (ATR, 25 °C, 16 scans, cm^{-1}): 3068 (w), 3016 (w), 2954 (w), 2918 (w), 2881 (w), 1622 (w), 1467 (w), 1451 (w), 1423 (w), 1391 (w), 1360 (w), 1330 (w), 1259 (s), 1222 (m), 1143 (s), 1111 (m), 1084 (m), 1073 (m), 1028 (m), 990 (m), 968 (m), 951 (m), 914 (m), 842 (s), 813 (m), 773 (m), 752 (m), 714 (m), 694 (m), 680 (m), 664 (m), 633 (s), 610 (m), 594 (m), 570 (m).

Synthesis of $[PN(dmb)]_4 \cdot Mo(CO)_3$ (5·Mo)

Procedure 1: **5** (0.150 g, 0.30 mmol) and $Mo(CO)_6$ (0.132 g, 0.5 mmol) were combined in 20 ml toluene and the yellow mixture refluxed for 2 h at 95 °C. Afterwards the solvent was evaporated and residual $Mo(CO)_6$ removed by sublimation (10^{-3} mbar) at 50 °C over a period of 6 h. The residual brownish solids were extracted with toluene (5 ml) and from the filtrate colorless needles of $[PN(dmb)]_4$ $Mo(CO)_3$ (0.045 g, 0.05 mmol, 18%) were grown.

Procedure 2: **5** (0.080 g, 0.16 mmol) and $Mo(CO)_3(C_2H_5CN)_3$ (0.055 g, 0.16 mmol) were combined in 6 ml CH_2Cl_2 at −50 °C. The clear brownish solution was allowed to warm slowly to ambient temperature over a period of 5 h. Afterwards the solvent was removed *in vacuo* and the residues dried *in vacuo* at 60 °C for 2 h. The brownish residual solids were re-dissolved in 1 ml CH_2Cl_2 and crystals of $[PN(dmb)]_4 \cdot Mo(CO)_3$ (0.065 g, 0.09 mmol, 54%) were grown by vapour diffusion of *n*-hexane into this CH_2Cl_2 solution.

Mp. 207 °C (dec). Anal. calc.% (found) $[PN(C_6H_{10})]_4 \cdot MoCO_3 \cdot 0.65(CH_2Cl_2)$: C 44.65 (44.63); H 5.60 (5.58); N 7.53 (7.69). ^1H NMR (25 °C, CD_2Cl_2, 250.13 MHz): 1.60 (s, 12H, CH_3), 1.80 (s, 12H, CH_3), 2.2–3.8 (16H, CH_2); $^{13}C\{^1H\}$ NMR (25 °C, CD_2Cl_2, 62.90 MHz): 18.2 (s, CH_3), 21.4 (s, *C*H_3), 33.3 (m, P*C*H_2), 50.4 (m, N*C*H_2), 122.6 (s, C_{vinyl}), 126.0 (s, C_{vinyl}); ^{31}P NMR (25 °C, CD_2Cl_2, 101.27 MHz): 79.8 (s). IR (ATR, 25 °C, 32 scans, cm^{-1}): 2981 (w), 2912 (m), 2856 (m), 1930 (s), 1828 (s), 1435 (m), 1384 (m), 1267 (m), 1251 (m), 1215 (m), 1160 (m), 1097 (m), 1049 (m), 957 (m), 869 (m), 843 (m), 808 (m), 780 (s), 728 (s), 695 (m), 653 (s), 603 (m), 574 (s). Raman: 2907 (3), 2876 (2), 1928 (7), 1854 (8), 1847 (8), 1837 (9), 1679 (8), 1453 (8), 1398 (8), 1380 (8), 1397 (6), 1245 (7), 784 (5), 745 (5), 721 (5), 705 (5), 696 (3), 676 (5), 668 (5), 656 (6), 606 (4), 571 (4), 505 (5), 482 (5), 452 (8), 445 (10), 382 (2), 288 (1), 264 (1), 239 (3), 230 (4), 211 (2). MS (ESI-TOF, *m*/*z*): $\{[PN(C_6H_{10})_4Mo(CO)_2 + H\}^+$ 657.12.

Acknowledgements

We thank Prof. W. W. Seidel (University of Rostock) for his assistance with the metal complexes. We are indebted to Dr Dirk Michalik for carrying out the variable temperature ^{31}P NMR experiments. Denise Heyl, Julia Rothe and Max Thomas (University of Rostock) are gratefully acknowledged for their synthetic contributions. Financial support from the Fonds der Chemischen Industrie (fellowship to C.H.) and the DFG (SCHU 1170/8-1) is gratefully acknowledged.

Notes and references

1 N. A. Piro, J. S. Figueroa, J. T. McKellar and C. C. Cummins, *Science*, 2006, **313**, 1276–1279.
2 N. A. Piro and C. C. Cummins, *Inorg. Chem.*, 2007, **46**, 7387–7393.
3 N. A. Piro and C. C. Cummins, *J. Am. Chem. Soc.*, 2008, **130**, 9524–9535.
4 H. A. Spinney, N. A. Piro and C. C. Cummins, *J. Am. Chem. Soc.*, 2009, **131**, 16233–16243.
5 D. Tofan and C. C. Cummins, *Angew. Chem., Int. Ed.*, 2010, **49**, 7516–7518.
6 D. Tofan and C. C. Cummins, *Chem. Sci.*, 2012, **3**, 2474.
7 D. Tofan, M. Temprado, S. Majumdar, C. D. Hoff and C. C. Cummins, *Inorg. Chem.*, 2013, **52**(15), 8851–8864.
8 L. M. Ziurys, *Astrophys. J.*, 1987, **321**, L81–L85.
9 J. Curry, L. Herzberg and G. Herzberg, *J. Chem. Phys.*, 1933, **1**, 749.
10 R. Ahlrichs, M. Bär, H. S. Plitt and H. Schnöckel, *Chem. Phys. Lett.*, 1989, **161**, 179–184.
11 R. Kinjo, B. Donnadieu and G. Bertrand, *Angew. Chem., Int. Ed.*, 2010, **49**, 5930–5933.
12 A. Velian and C. C. Cummins, *J. Am. Chem. Soc.*, 2012, **134**, 13978–13981.
13 M. Göbel, K. Karaghiosoff and T. M. Klapötke, *Angew. Chem., Int. Ed.*, 2006, **45**, 6037–6040.
14 C. Hering, A. Schulz and A. Villinger, *Angew. Chem., Int. Ed.*, 2012, **51**, 6241–6245.
15 O. J. Scherer and N. Kuhn, *J. Organomet. Chem.*, 1974, **82**, C3–C6.
16 R. H. Neilson, R. C.-Y. Lee and A. H. Cowley, *Inorg. Chem.*, 1977, **16**, 1455–1459.
17 K. Miqueu, J.-M. Sotiropoulos, G. Pfister-Guillouzo and V. D. Romanenko, *New J. Chem.*, 2001, **25**, 930–938.
18 K. Huynh, E. Rivard, W. LeBlanc, V. Blackstone, A. J. Lough and I. Manners, *Inorg. Chem.*, 2006, **45**, 7922–7928.
19 R. H. Neilson and P. Wisian-Neilson, *Chem. Rev.*, 1988, **88**, 541–562.
20 M. Gleria and R. De Jaeger, *Top. Curr. Chem.*, 2005, **250**, 165–251.
21 E. Niecke and W. Flick, *Angew. Chem., Int. Ed. Engl.*, 1973, **12**, 585–586.
22 W. Zeiß, W. Schwarz and H. Hess, *Angew. Chem., Int. Ed. Engl.*, 1977, **16**, 407–408.
23 K. D. Gallicano and N. L. Paddock, *Can. J. Chem.*, 1985, **63**, 314–318.
24 C. Lehousse, M. Haddad and J. Barrans, *Tetrahedron Lett.*, 1982, **23**, 4171–4174.
25 K. D. Gallicano, N. L. Paddock, S. J. Rettig and J. Trotter, *Can. J. Chem.*, 1982, **60**, 2415–2419.
26 K. D. Gallicano, N. L. Paddock, S. J. Rettig and J. Trotter, *Can. J. Chem.*, 1984, **62**, 1869–1873.
27 A. Villinger, P. Mayer and A. Schulz, *Chem. Commun.*, 2006, 1236.
28 S. Herler, P. Mayer, J. Schmedt auf der Günne, A. Schulz, A. Villinger and J. J. Weigand, *Angew. Chem., Int. Ed.*, 2005, **44**, 7790–7793.

29 A. Schulz and A. Villinger, *Angew. Chem., Int. Ed.*, 2008, **47**, 603–606.
30 A. Schulz and A. Villinger, *Inorg. Chem.*, 2009, **48**, 7359–7367.
31 M. Lehmann, A. Schulz and A. Villinger, *Angew. Chem., Int. Ed.*, 2011, **50**, 5221–5224.
32 C. Hering, M. Lehmann, A. Schulz and A. Villinger, *Inorg. Chem.*, 2012, **51**, 8212–8224.
33 W. Baumann, A. Schulz and A. Villinger, *Angew. Chem., Int. Ed.*, 2008, **47**, 9530–9532.
34 M. M. Lehmann, A. A. Schulz and A. A. Villinger, *Angew. Chem., Int. Ed.*, 2012, **51**, 8087–8091.
35 M. Rakotomalala, M. Ciesielski, T. Zevaco and M. Doering, *Phosphorus, Sulfur Silicon Relat. Elem.*, 2011, **186**, 989–996.
36 A. Westenkirchner, A. Villinger, K. Karaghiosoff, R. Wustrack, D. Michalik and A. Schulz, *Inorg. Chem.*, 2011, **50**, 2691–2702.
37 P. Pyykkö and M. Atsumi, *Chem.–Eur. J.*, 2009, **15**, 12770–12779.
38 C. Wieser, C. B. Dieleman and D. Matt, *Coord. Chem. Rev.*, 1997, **165**, 93–161.
39 J. M. Barendt, E. G. Bent, R. C. Haltiwanger and A. D. Norman, *J. Am. Chem. Soc.*, 1989, **111**, 6883–6884.
40 A. D. Norman, E. G. Bent, R. C. Haltiwanger and T. R. Prout, *Phosphorus, Sulfur Silicon Relat. Elem.*, 1989, **41**, 63–67.
41 J. M. Barendt, E. G. Bent, S. M. Young, R. C. Haltiwanger and A. D. Norman, *Inorg. Chem.*, 1991, **30**, 325–331.
42 P. G. Edwards, R. Haigh, D. Li and P. D. Newman, *J. Am. Chem. Soc.*, 2006, **128**, 3818–3830.
43 H. Schumann and H. Benda, *Eur. J. Inorg. Chem.*, 1971, **104**, 333–342.
44 M. Lehmann, A. Schulz and A. Villinger, *Eur. J. Inorg. Chem.*, 2012, 822–832.
45 E. Conrad, N. Burford, R. McDonald and M. J. Ferguson, *J. Am. Chem. Soc.*, 2009, **131**, 17000–17008.
46 C. K. SooHoo and S. G. Baxter, *J. Am. Chem. Soc.*, 1983, **105**, 7443–7444.
47 A. H. Cowley, R. A. Kemp, J. G. Lasch, N. C. Norman, C. A. Stewart, B. R. Whittlesey and T. C. Wright, *Inorg. Chem.*, 1986, **25**, 740–749.
48 R. J. Boyd, N. Burford and C. L. Macdonald, *Organometallics*, 1998, **17**, 4014–4029.
49 G. David, E. Niecke and M. Nieger, *Tetrahedron Lett.*, 1992, **33**, 2335–2338.
50 C. Hering, A. Schulz and A. Villinger, *Inorg. Chem.*, 2013, **52**, 5214–5225.
51 M. L. G. Borst, N. van der Riet, R. H. Lemmens, F. J. J. de Kanter, M. Schakel, A. W. Ehlers, A. M. Mills, M. Lutz, A. L. Spek and K. Lammertsma, *Chem.–Eur. J.*, 2005, **11**, 3631–3642.
52 R. C. Neu, E. Y. Ouyang, S. J. Geier, X. Zhao, A. Ramos and D. W. Stephan, *Dalton Trans.*, 2010, **39**, 4285.
53 A. H. Cowley, R. A. Kemp, J. G. Lasch, N. C. Norman and C. A. Stewart, *J. Am. Chem. Soc.*, 1983, **105**, 7444–7445.
54 C. A. Caputo, J. T. Price, M. C. Jennings, R. McDonald and N. D. Jones, *Dalton Trans.*, 2008, 3461.
55 G. J. Kubas, L. S. V. D. Sluys, R. A. Doyle, and R. J. Angelici, *Inorganic Syntheses: Reagents for Transition Metal Complex and Organometallic Syntheses*, 1990, vol. 28, pp. 29–33.
56 D. J. Lowry and M. L. Helm, *Inorg. Chem.*, 2010, **49**, 4732–4734.
57 G. M. Whitesides and F. D. Gutowski, *J. Org. Chem.*, 1976, **41**, 2882–2885.
58 G. M. Sheldrick, *SHELXS-97, Program for solution of crystal structures*, University of Göttingen, Germany, 1997.
59 G. M. Sheldrick, *SHELXL-97, Program for refinement of crystal structures*, University of Göttingen, Germany, 1997.
60 G. M. Sheldrick, *SADABS, Version 2*, University of Göttingen, Germany, 2004.

5.4 Structure and Bonding of Novel Acyclic Bisaminoarsenium Cations

Christian Hering, Julia Rothe, Axel Schulz, Alexander Villinger.

Inorganic Chemistry, **2013**, *52*, 7781−7790.

DOI: 10.1021/ic4010104

In dieser Publikation wurden sämtliche experimentelle Arbeiten von mir durchgeführt. Der eigene Beitrag liegt bei ca. 85 %.

Inorganic Chemistry

Article

pubs.acs.org/IC

Structure and Bonding of Novel Acyclic Bisaminoarsenium Cations

Christian Hering,[†] Julia Rothe,[†] Axel Schulz,*[,†,‡] and Alexander Villinger[†]

[†]Abteilung Anorganische Chemie, Institut für Chemie, Universität Rostock, Albert-Einstein-Strasse 3a, 18059 Rostock, Germany

[‡]Leibniz-Institut für Katalyse e.V. an der Universität Rostock, Albert-Einstein-Strasse 29a, 18059 Rostock, Germany

Supporting Information

ABSTRACT: The synthesis and characterization of a salt bearing a labile bisaminoarsenium cation of the type $\{[(Me_3Si)_2N]_2As\}^+$ (**9a**) are described, which was obtained in the reaction of the chloroarsane $[(Me_3Si)_2N]_2AsCl$ (**8**) with $GaCl_3$. Reacting **8** with AgOTf did not yield an arsenium salt, but the *cyclo*-diarsadiazane $[(Me_3Si)_2NAs\text{-}\mu\text{-}NSiMe_3]_2$ (**11**) was obtained in excellent yields. Moreover, the reactivity of the analogous antimony species $[(Me_3Si)_2N]_2SbCl$ (**12**) was studied. In the reaction with $GaCl_3$, the aminochlorostibenium salt $[(Me_3Si)_2NSbCl]^+[(Me_3Si)_2N(GaCl_3)_2]^-$ (**5**) was isolated. In the reaction with AgOTf, substitution of the chlorine in **12** resulted in the formation of $[(Me_3Si)_2N]_2SbOTf$ (**13**), a compound with significant stibenium character. All new compounds have been fully characterized by means of X-ray, vibrational spectroscopy, CHN analysis, and NMR experiments. All compounds were further investigated by means of density functional theory and the bonding situation was accessed by natural bond orbital (NBO) analysis.

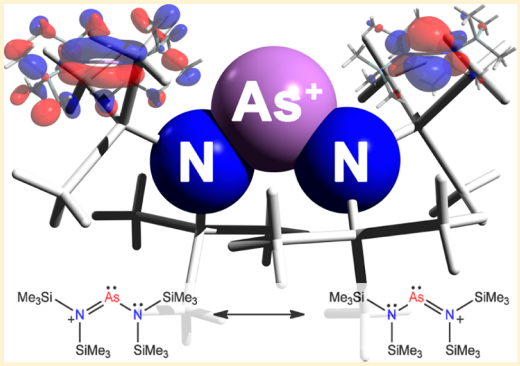

INTRODUCTION

An interesting part of heavier group 15 elements, in terms of both structure and reactivity, that continuously receives attention is the field of cationic species with a low coordination number.[1] Pnictenium cations are electron-deficient and coordinatively unsaturated group 15 species that resemble the reactivity of nucleophilic carbenes of the type X−C−Y, in which the central carbon is isolobally replaced by a positively charged pnictogen atom, $[X\text{−}Pn\text{−}Y]^+$ (Pn = P, As, Sb, Bi; X, Y = π-donating groups).[2] They display Lewis acidic as well as Lewis basic properties, as they possess on the one hand a vacant p-orbital and on the other hand a lone pair of electrons (LP).[3] The introduction of bulky substituents, charge delocalization, and charge transfer by means of Lewis bases such as DMAP [4-(*N*,*N*-dimethylamino)pyridine] or ER_3 (E = P, As, Sb; R = Me, Et, Ph) are among typical approaches to stabilize such reactive cationic pnictogen species.[4] Within this field, the compounds most thoroughly studied are the phosphenium ions $[PR_2]^+$ (R = good π-donor group, such as amino groups).[5]

However, a thorough search of the literature revealed that structural data on acyclic pnictenium cations of arsenic, antimony, and bismuth is still limited to only a few examples. In the early 1990s, Wolf and co-workers[6] reported on the isolation of the first acyclic dialkylaminoarsenium cation $[R_2NAs\text{-}Cl]^+[OTf]^-$ (**1**) (OTf = $[CF_3SO_3]^-$) in the reaction of R_2NAsCl_2 (R = Me, Et, *i*Pr) with AgOTf at room temperature. In subsequent substitution reactions with $Me_3Si\text{-}NMe_2$, the bis(dialkylamino)arsenium species $[R_2N\text{−}As\text{−}NMe_2]^+[OTf]^-$ (**2**) (R = Me, Et) were prepared, but nevertheless crystal structures of these arsenium salts were not reported (Scheme 1). In our opinion $[R_2NAs\text{-}Cl]^+[OTf]^-$ is not a true salt bearing an arsenium cation but an arsane with a highly polarized As−O bond, which is better represented as $R_2NAs(Cl)\text{-}OTf$.

Scheme 1. Preparation of the First Acyclic Aminochloroarsenium Salts by Wolf and Co-workers[6] in 1992

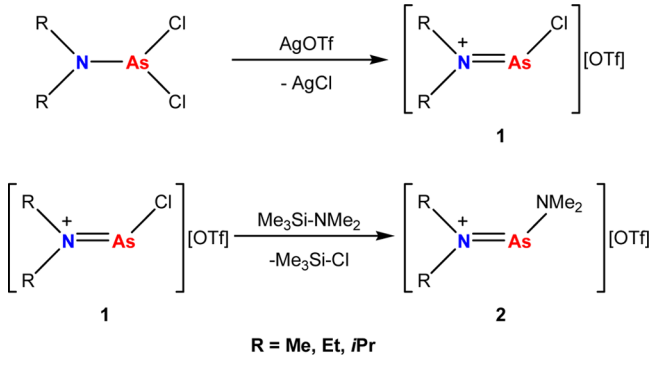

Pnictenium ions are most efficiently generated by combination of a chloropnictine R_2PnCl and a halide abstracting agent (e.g., $Me_3Si\text{-}OTf$, $AlCl_3$, $GaCl_3$, AgOTf).[5] The generated cations $[R_2Pn]^+$ (R = alkyl, phenyl, NR_2) are ideal building blocks in inorganic synthesis and can be stabilized by the addition of Lewis bases such as ER_3 (E = P, As, Sb; R = alkyl, phenyl), and in this case different pnictino-pnictonium

Received: April 23, 2013
Published: June 17, 2013

   dx.doi.org/10.1021/ic4010104 | *Inorg. Chem.* 2013, 52, 7781−7790

frameworks are formed, which can to some degree also be viewed as interpnictogen coordination compounds (Scheme 2).[7]

Scheme 2. Generation of Pnictenium Cations $[R_2Pn]^+$ by Addition of a Halide Abstracting Reagent (LA) to a Chloropnictane and Formation of Pnictino-Pnictonium Frameworks by Addition of the Lewis Base PnR_3

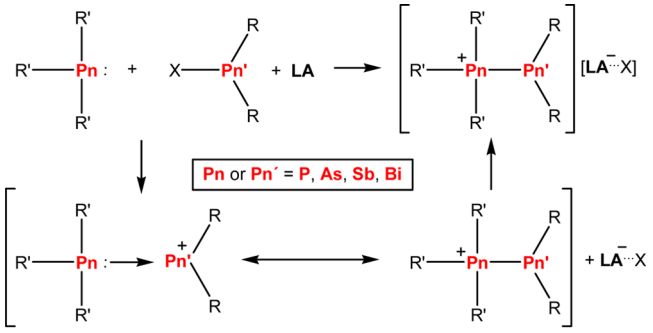

However, the only structurally characterized "naked" acylic arsenium cations (also known as arsacenium ion in analogy to metallocene nomenclature) are the cations in $[Cp^*_2As]^+[BF_4]^-$ (**3**) and in $[Cp^*As{-}Cl]^+[ClAl(OR^F)_3]^-$ (**4**) (Figure 1).[8,9] Of the heavier pnictogens, only the analogous stibenium cation is known. Just recently, we reported on the isolation and structural characterization of an aminostibenium cation in $[(Me_3Si)_2NSbCl]^+[(Me_3Si)_2N(GaCl_3)_2]^-$ (**5**) and a homoleptic bismuth−nitrogen cation in $[((Me_3Si)_2NN(SiMe_3))_2Bi]^+[GaCl_4]^-$ (**6**) that were isolated at low temperatures.[10,11]

In this study, we investigated the ability of the bis-(*N*,*N*-trimethylsilyl)amido group to stabilize the bisaminoarsenium cation in **9**. Furthermore, we investigated different synthetic approaches to generate **9** and compared the reactivity of chloroarsane **8** with its analogous antimony system **12**, which exhibits a completely different reactivity. All compounds that were prepared in the course of this study have been structurally characterized. To gain further insight into the bonding situation, natural bond orbital (NBO) calculations were carried out.

RESULTS AND DISCUSSION

In earlier studies, we have shown that when $GaCl_3$ is added to a CH_2Cl_2 solution of $(Me_3Si)_2NAsCl_2$ at low temperatures, an immediate color change to yellow occurs. But upon warming the mixture to ambient temperatures, the color vanishes, and after standard workup only $[(ClMe_2Si)_2N{-}SiMe_2]_2$ (**7**) was isolated. This indicates that $GaCl_3$ facilitates a chlorine/methyl exchange reaction, which in the end results in the formation of Me_2AsCl and dimeric $(ClMe_2Si)_2N{=}SiMe_2$ in **7** (Scheme 3).[12]

Scheme 3. $GaCl_3$-Assisted Chlorine/Methyl Exchange in $(Me_3Si)_2NAsCl_2$ Yielding *cyclo*-Disiladiazane 7 via Release of Me_2AsCl[12]

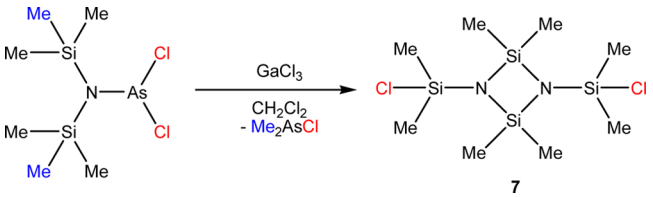

Keeping these results in mind, we targeted $[(Me_3Si)_2N]_2AsCl$ (**8**) to be a better starting material to gain access to the corresponding bisaminoarsenium cation, as the second amide ligand adds both steric bulk and electronic stabilization to the arsenic center.[13]

In a similar synthetic protocol, which also yielded the highly labile phosphenium cations of the type $[(Me_3Si)_2NPX]^+[GaCl_4]^-$ (X = Cl, N_3),[14] $GaCl_3$ was added to a CH_2Cl_2 solution of **8** at −80 °C, whereupon the mixture attained a deep yellow color (Scheme 4, reaction i).

Concentration of the reaction mixture and subsequent crystallization in the freezer at −80 °C yielded a hitherto unknown salt of the type $[(Me_3Si)_2N]_2As]^+[GaCl_4]^-$ (**9a**) as a yellow crystalline solid in decent yields (ca. 50%) (Figure 2). Compound **9a** can be stored in the freezer of the glovebox over a long period of time and is stable even at room temperature in isolated form over a short period of time. In addition to **3** and **4** (Figure 1), **9a** is one of the few examples of structurally

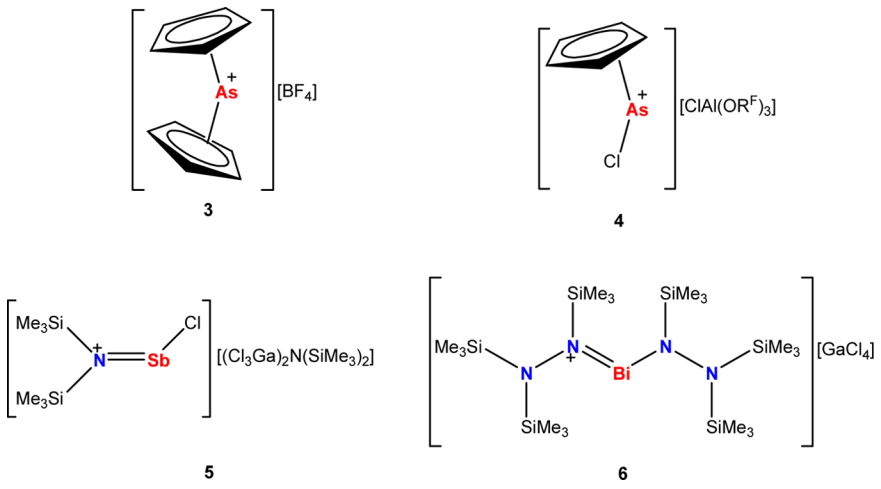

Figure 1. Structurally characterized acyclic arsenium cations **3** and **4** as well as examples of an aminochlorostibenium salt **5** and a bishydrazinobismuthenium salt **6**.

dx.doi.org/10.1021/ic4010104 | Inorg. Chem. 2013, 52, 7781−7790

Scheme 4. Synthesis of Aminoarsenium Salts 9a and 9b[a] and *cyclo*-Diarsadiazan 11[b]

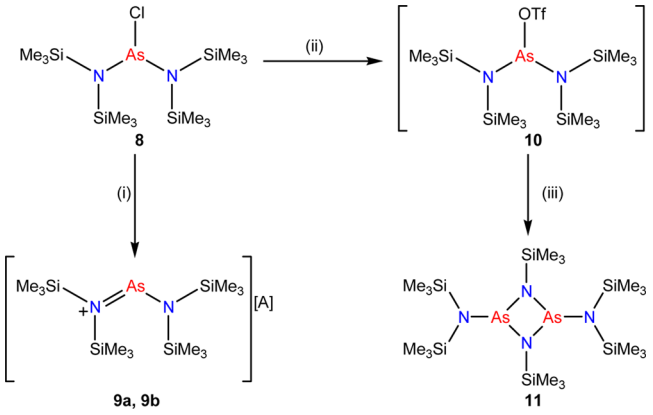

[a] In **9a**, A = $[GaCl_4]^-$; in **9b**, A = $[Ga_2Cl_7]^-$).

[b] Reaction conditions: (i) (a) 1 equiv of $GaCl_3$, −80 °C, CH_2Cl_2; (b) 2 equiv of $GaCl_3$, −80 °C, CH_2Cl_2. (ii) AgOTf, CH_2Cl_2, −60 °C, −AgCl. (iii) $-Me_3Si$-OTf.

characterized acyclic arsenium cations. In Raman experiments carried out at room temperature of isolated crystalline material, the As−Cl stretching mode in **8** is detected at 326 cm^{-1}. This mode vanishes upon chloride abstraction, and instead in **9a** a prominent mode at 349 cm^{-1}, characteristic for the A_1 vibration mode of the tetrahedral $[GaCl_4]^-$, is observed.[15] ^1H NMR and ^{29}Si NMR spectroscopy at low temperatures are also well-suited to distinguish between **8** and **9**, as a significant downfield shift, especially in the ^{29}Si NMR spectrum, is observed (**8**, δ = 6.6 ppm, vs **9a**, δ = 16.7 ppm) upon salt formation. However, in solution **9a** is only stable up to ca. −10 °C. At ambient temperatures, the yellow color of the reaction mixture vanishes and a colorless solution remains. As described above, a chlorine/methyl exchange reaction occurs in solution, leading to the decomposition of **9**.

In analogy to the synthetic approach described by Wolf and co-workers[6] for the preparation of $R_2NAs(Cl)$-OTf (**1**), we wanted to prepare the analogous $[(Me_3Si)_2N]_2As$-OTf (**10**) by adding AgOTf to a stirred solution of **8** in CH_2Cl_2 at −60 °C (Scheme 4, reaction ii). After the mixture was stirred for 1 h at that temperature, the precipitates were filtered off at −80 °C, and from the concentrated reaction mixture, colorless crystals were grown, which were analyzed by low-temperature X-ray crystallographic methods. Interestingly, **10** was not formed but instead a *cyclo*-1,3-diarsa-2,4-diazane of the type $\{[(Me_3Si)_2N]$-$As[\mu$-$NSiMe_3]\}_2$ (**11**) was isolated (Figure 3). The isolation of **11** is indicative of the intermediate formation of **10**; however, it decomposes even at −60 °C by eliminating the silyl ester Me_3Si-OTf, a reaction pathway that has been already observed in similar reactions (Scheme 4, reaction iii).[16] Obviously, elimination of the silyl ester is thermodynamically favored over the formation of a bisaminoarsenium salt **9**. Two major facts play a role here: (1) The formation of a Si−O bond can be regarded as the thermodynamic driving force of the elimination. (2) In addition, the arsenic center is sterically too overcrowded to allow secondary or covalent interactions with the triflate anion for stabilization. In a similar reaction, **11** was synthesized by Niecke and Bitter[17] in the thermolysis of $[(Me_3Si)_2N]_2AsF$ at 150 °C, whereupon Me_3Si-F was eliminated and **11** was obtained. This new synthetic approach allows for a room-temperature preparation of **11** in excellent yields (ca. 95%). In the ^1H NMR spectrum, three distinct singlet resonances for three inequivalent trimethylsilyl groups are detected, in good agreement with literature values.[17] It is also noteworthy that **11** melts without decomposition at 200 °C. In summary, we present here a high-yielding synthetic route toward a bisaminoarsenium salt **9**, and also a room-temperature approach for the synthesis of **11** is presented, which yielded crystals of **11** that allowed the determination of its solid-state structure.

In a next series of experiments, we were interested in the analogous reactions of $[(Me_3Si)_2N]_2SbCl$ (**12**) with $GaCl_3$ and AgOTf. Compound **12** was prepared according to a modified literature procedure.[13a] $SbCl_3$ was suspended in Et_2O and a *n*-hexane solution of $LiN(SiMe_3)_2$ was added at −50 °C, resulting in a light gray suspension. LiCl was separated by extraction with

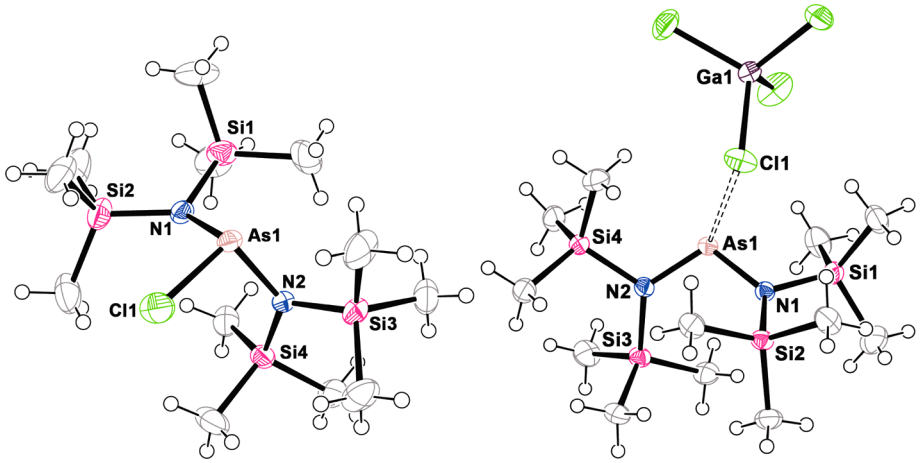

Figure 2. ORTEP drawings of **8** (left) and **9a** (right). Ellipsoids are drawn at 50% probability. Selected bond lengths (angstroms) and angles (degrees) for **8**: As1−Cl1 2.2469(9), As1−N1 1.844(2), As1−N2 1.857(2), N1−Si1 1.764(2), N1−Si2 1.772(2), N2−Si3 1.773(2), N2−Si4 1.765(2); N1−As−N2 105.8(1), $\sum(\angle As1)$ 306.8, $\sum(\angle N1)$ 352.7, $\sum(\angle N2)$ 357.96; Cl1−As1−N1−Si1 20.5(1), N2−As1−N1−Si1 123.9(1), N1−As1−N2−Si3 155.3(1). Selected bond lengths (angstroms) and angles (degrees) for **9a**: As1−N1 1.780(2), As1−N2 1.776(2), N1−Si1 1.807(2), N1−Si2 1.809(2), N2−Si3 1.811(2), N2−Si4 1.823(2), As1−Cl1 3.47, As1−Cl2 3.82; N1−As1−N2 108.88(7), $\sum(\angle N1)$ 357.85, $\sum(\angle N2)$ 358.31; N2−As1−N1−Si1 146.80(8), N1−As1−N2−Si3 150.38(8).

dx.doi.org/10.1021/ic4010104 | *Inorg. Chem.* 2013, 52, 7781−7790

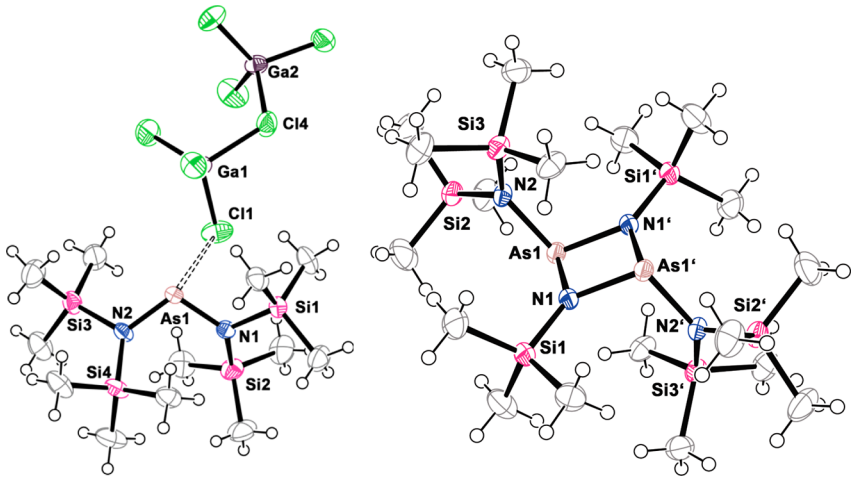

Figure 3. ORTEP drawings of **9b** (left) and **11** (right). Ellipsoids are drawn at 50% probability. Selected bond lengths (angstroms) and angles (degrees) for **9b**: As1−N1 1.782(3), As1−N2 1.772(3), N1−Si1 1.812(3), N1−Si2 1.798(3), N2−Si3 1.824(3), N2−Si4 1.807(3), As1−Cl1 3.813(1), As1−Cl2i 3.497(1); N1−As1−N2 109.5(1), ∑(∠N1) 357.41, ∑(∠N2) 358.08; N1−As1−N2−Si3 −148.1(2). Selected bond lengths (angstroms) and angles (degrees) for **11**: As1−N1 1.866(2), As1−N2 1.881(1), Sb1−N2 2.012(2), N1−Si1 1.725(2), N2−Si2 1.753(2), N2−Si3 1.763(2); ∑(∠As1) 296.16, ∑(∠N1) 359.98, ∑(∠N2) 359.98; As1′−As1−N2−Si2 2.1(2).

Scheme 5. Synthesis of Aminochlorostibenium Salt 5 and Triflate-Substituted Stibane 13[a]

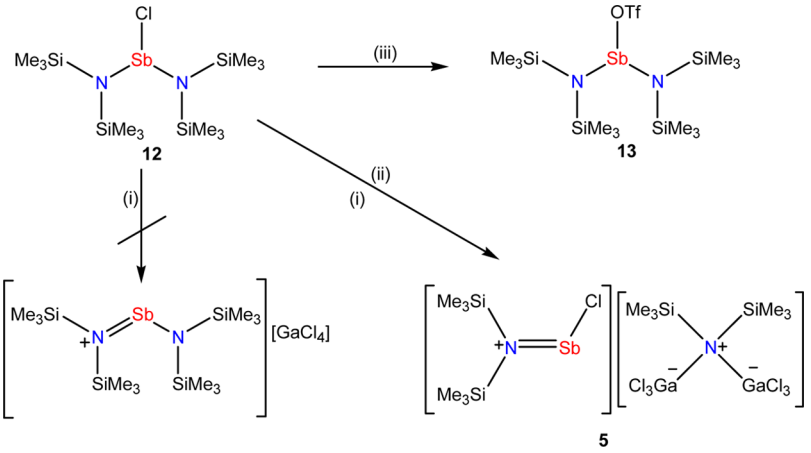

[a]Reaction conditions: (i) 1 equiv of $GaCl_3$, −80 °C, CH_2Cl_2. (ii) 2 equiv of $GaCl_3$, −80 °C, CH_2Cl_2. (iii) AgOTf, CH_2Cl_2, −60 °C, −AgCl.

n-pentane over a Celite-padded frit to remove colloidal dispersed Sb that was formed in the reaction. The crude product was purified by distillation at 130 °C in vacuo to yield **12** as a viscous colorless oil (mp −5 °C) that can be stored over a long period of time in the freezer. In a first experiment, **12** was treated with 1 equiv of $GaCl_3$ in CH_2Cl_2 at −80 °C, leading to an immediate color change to orange. After the solution was stirred for 5 min, a colorless solid precipitated and the supernatant became pale yellow (Scheme 5, reaction i). At ca. −30 °C the solids redissolved and the mixture turned orange again. After concentration of the mixture and placement in the freezer at −40 °C for 24 h, colorless crystalline blocks were deposited that could be analyzed by X-ray crystallography. Astonishingly, the crystals were identified as $[(Me_3Si)_2NSbCl]^+[(Me_3Si)_2N(GaCl_3)_2]^-$ (**5**), an aminochlorostibenium salt that was reported by our group just recently (Figure 4).[10]

Taking a closer look at this result, we realized that we found a new approach to synthesize **5**, which is also formed in the first reaction step, when $(Me_3Si)_2NSbCl_2$ is treated with $GaCl_3$. Nevertheless, **5** finally decomposes in CH_2Cl_2 solution in a

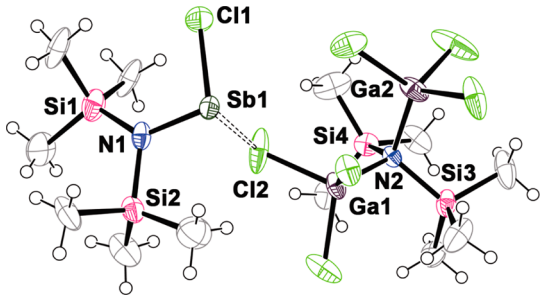

Figure 4. ORTEP drawing of **5**. Ellipsoids are drawn at 50% probability. Selected bond lengths (angstroms) and angles (degrees): Sb1−N1 1.949(3), As1−N2 1.656(2), N1−Si1 1.863(4), N1−Si2 1.725(4), N2−Si3 1.862(3), N2−Si4 1.863(3), Sb1−Cl1 2.330(6), Sb1−Cl2 2.850(1); N1−Sb1−Cl1 97.2(2).

methyl/chlorine exchange reaction to form stibinostibonium cations of the type $[R_3Sb\text{-}SbR_2]^+$ and $[(R_3Sb)_2SbR]^{2+}$ (R = Me), which were identified by means of X-ray crystallography.[10] This underlines again the increasing Lewis acidity as the pnictogen atom becomes heavier in aminochloropnictenium

dx.doi.org/10.1021/ic4010104 | *Inorg. Chem.* 2013, 52, 7781−7790

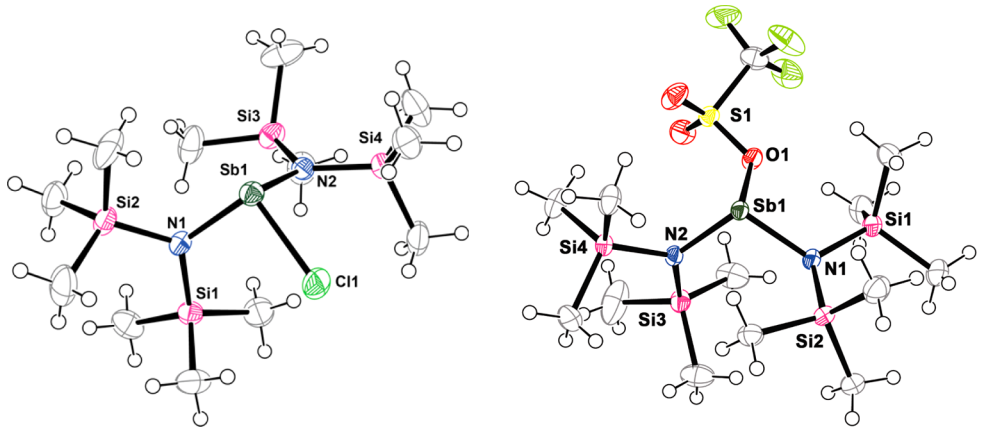

Figure 5. ORTEP drawings of **12** (left) and **13** (right). Ellipsoids are drawn at 50% probability. Selected bond lengths (angstroms) and angles (degrees) for **12**: Sb1−Cl1 2.405(1), Sb1−N1 2.032(4), Sb1−N2 2.050(4), N1−Si1 1.765(4), N1−Si2 1.760(4), N2−Si3 1.748(4), N2−Si4 1.766(4); ∑(∠Sb1) 298.3, ∑(∠N1) 358.0, ∑(∠N2) 358.1; Cl1−Sb1−N1−Si1 −33.1(2), N1−Sb1−N2−Si3 50.9(3). Selected bond lengths (angstroms) and angles (degrees) for **13**: Sb1−O11 2.158(1), Sb1−N1 2.035(2), Sb1−N2 2.012(2), N1−Si1 1.770(2), N1−Si2 1.774(2), N2−Si3 1.770(2), N2−Si4 1.770(2); S1−C13 1.830(2); ∑(∠Sb1) 289.75, ∑(∠N1) 347.89, ∑(∠N2) 360.00; N2−Sb1−N1−Si1 131.90(9), O1−Sb1−N1−Si2 179.05(1).

salts. To gain further insight in the reaction of **12** with $GaCl_3$, we added 2 equiv of $GaCl_3$, resulting again in a deep orange reaction mixture. From this mixture **5** could be isolated in decent yields (ca. 70%) (Scheme 5, reaction ii). This finding is best understood as the elimination reaction of an amide ligand from **12** in the presence of the Lewis acid $GaCl_3$, which further stabilizes the $[(Me_3Si)_2N]^-$ fragment by adduct formation, resulting in the formation of a complex anion. Similar reactions are known, as $Pn(NR_2)_3$ (Pn = Sb, Bi) are well-known to be cleaved in superacidic media such as HOTf, leading to $Pn(OTf)_3$ and the free amine HNR_2.[18] Extrusion of an amide group by the action of $GaCl_3$ as Lewis acid is without precedent. It is worth noting that reacting the cyclic chlorostibane $ClSb(i\text{PrN})_2C_6H_{10}$ with $GaCl_3$ or $AlCl_3$ resulted, even at low temperatures, only in the precipitation of metallic antimony, as described by Richeson and co-workers,[19] mirroring the reactivity found in **12**. To test this synthetic approach, we also reacted **8** with 2 equiv of $GaCl_3$, resulting, according to X-ray crystallography, in formation of the heptachloridogallate salt of $\{[(Me_3Si)_2N]_2As\}^+$ (**9b**), while no extrusion of $[(Me_3Si)_2N]^-$ was observed. As **9b** is highly labile in the solid state as well as in solution even at low temperatures, no further analytical data for **9b** could be obtained. Conclusively, the reactivity of **8** and **12** toward $GaCl_3$ differ significantly, a behavior also found in the reaction of **12** with AgOTf. Addition of **12** to a stirred suspension of AgOTf at −60 °C and subsequent separation of AgCl by extracting the reaction mixture with *n*-hexane at ambient temperature yields $[(Me_3Si)_2N]_2Sb\text{-}OTf$ (**13**) (Scheme 5 reaction iii; Figure 4). Compound **13** is a colorless crystalline solid with a melting point of 68 °C (without decomposition) that can be prepared in good yields (ca. 80%) and that is thermally stable in toluene solution up to 100 °C. It was impossible to eliminate $Me_3Si\text{-}OTf$ from **13** at this temperature, displaying again the different reactivity in the antimony systems. In earlier studies we have shown that Sb-OTf bonds can be easily cleaved by the addition of Me_3SiX (X = Br, I, N_3), so that **13** might be an ideal precursor for functionalized antimony compounds.[16]

Structural Characterization. All compounds reported in this work were structurally characterized. Compound **8** crystallizes in the orthorhombic space group *Pbca* with eight molecules in the cell (Figure 2). The arsenic atom in **8** adopts trigonal-pyramidal coordination geometry [∑(∠As1) = 306.8°; N1−As−N2 105.8(1)°], as expected for arsenic in oxidation state III [cf. $(Me_3Si)_2NAsCl_2$, ∑(∠As) = 301.8°; $Ter(MeCl_2Si)NAsMe_2$, ∑(∠As) = 302.22°][12] without any significantly short intermolecular contacts. The $As\text{−}N_{amino}$ distances [**7**, 1.844(2)/1.857(2) Å] are shortened As−N single bonds [cf. $\sum r_{cov}$(As−N) = 1.92, $\sum r_{cov}$(As=N) = 1.74 Å].[20] The same is detected for the Si−C bonds, which are significantly shorter than the sum of the covalent radii [cf. $\sum r_{cov}$(Si−C) = 1.91 Å].[20] A considerable elongation is detected for the As−Cl bond [**8**, 2.2469(9) Å], which is longer than the respective sum of the covalent radii [cf. $\sum r_{cov}$(As−Cl) = 2.20 Å].[20] Interestingly, a small but obvious deviation from planarity is observed for the N_{amino} atoms (∑(∠N1) 352.7°, ∑(∠N2) 357.96°) indicating that there is high steric strain due to the four $SiMe_3$ groups, which is further underlined by the torsion angle between the As1−N1−Si1 and the As1−N2−Si3 planes of 155°, an arrangement similar to $[(Me_3Si)_2NN(SiMe_3)]_2BiCl$ (cf. torsion angle between NNBi planes ca. 150°).[11]

Addition of $GaCl_3$ to **8** resulted in the formation of **9a** and **9b**, which crystallize in the monoclinic space group $P2_1/n$ with four formula units in the cell. The transition to an ion pair with a bisaminoarsenium cation is best visualized by the significantly shorter As−N distances in **9a** and **9b** [**9a**, 1.780(2)/1.776(2); **9b**, 1.772(3)/1.782(3) Å] compared with **8** [cf. $\sum r_{cov}$(As=N) = 1.74 Å][20] and are in good agreement with the values detected in related *N*-heterocyclic arsenium species (cf. $[C_6H_{10}(i\text{PrN})_2As][GaCl_4]$[19] 1.759 Å and $[(CH_2)_3(NMe)_2As][GaCl_4]$[21] 1.68 Å, averaged values). The N−As−N angle [**9a**, 108.88(7)°; **9b**, 109.5(1)°] opens upon chloride abstraction and is in the expected range for a bisaminoarsenium cation. Furthermore, the Si−N bonds in **9** (**9a** avg 1.81 Å, **9b** avg 1.81 Å) widen significantly upon chloride abstraction, and consequently the deviation from planarity around the N_{amino} centers is less expressed (**9a**, ∑(∠N) 357.85°/358.31°; **9b**, 357.41°/358.08°) compared with **8**, as the steric strain lessens around the nitrogen center. The cations in **9a** and **9b** can be considered almost "naked", as the shortest As···$ClGaCl_3$ distances are detected at 3.5 Å, which is in the range of the

dx.doi.org/10.1021/ic4010104 | *Inorg. Chem.* 2013, 52, 7781−7790

Scheme 6. Lewis Representations of the Cation in Compounds 9 and 13 According to NBO Analysis

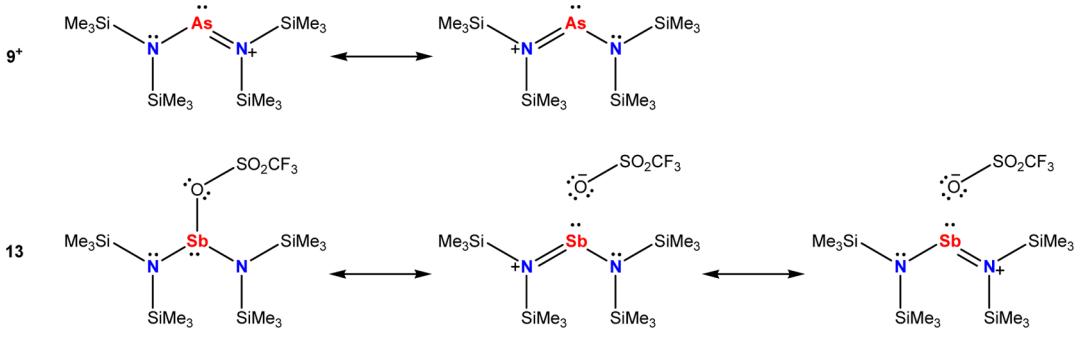

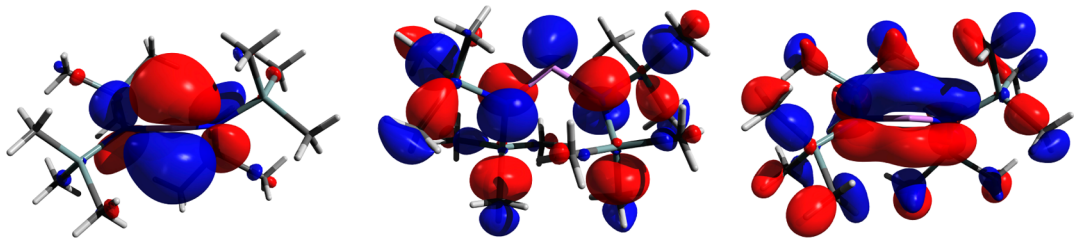

Figure 6. Surface plots (isovalue 0.03) showing the LUMO (left), HOMO (middle), and HOMO − 11 (right) of $[((Me_3Si)_2N)_2As]^+$.

respective sum of the van der Waals radii [$\sum r_{vdW}$(As−Cl) = 3.60 Å].[22]

Compound **11** crystallizes in the monoclinic space group $P2_1/c$ with two molecules in the cell, which lie on a crystallographically imposed center of inversion resulting in an anti configuration for the exocyclic substituents on the arsenic. Compound **11** adopts a square As_2N_2 core with crystallographically indistinguishable As−N distances [**11**, 1.866(2) Å] that are in the typical range for derivatives of *cyclo*-1,3-diarsa-2,4-diazanes (cf. [TerN-μ−As-Cl]$_2$ 1.862 Å).[23,24] In the analogous bismuth system {[$(Me_3Si)_2N$]Bi[μ-N($SiMe_3$)]}$_2$, the ring Bi−N distances differ and also a small deviation from planarity is observed.[25] The exocyclic As−N [**11**, 1.881(2) Å] bonds are slightly shorter than the sum of the covalent radii for an As−N single bond [cf. $\sum r_{cov}$(As−N) = 1.92 Å] and furthermore the exocyclic N−Si bonds [**11**, 1.725(2) Å] are significantly shortened [cf. $\sum r_{cov}$(Si−N) = 1.87 Å and $\sum r_{cov}$(Si=N) = 1.67 Å].[20] As expected the arsenic is trigonal pyramidally coordinated (**11**: $\sum$(∠As) = 296.2°), whereas the sum of angles around nitrogen is close to 360° indicating a planar environment and, hence, a formal sp^2 hybridization. Interestingly, the exocyclic plane Si2−N2−Si3 is nearly perpendicular to the inner As_2N_2 square, which is a result of the hindered rotation around the exocyclic As−N bond, as the $SiMe_3$ groups are sterically too demanding.

The structure of **5** was determined before by our group; however, we were now able to grow high-quality crystals that gave a much better structure model of **5**. Compound **5** crystallizes in the triclinic space group *P*-1 with two formula units per cell. Two disordered CH_2Cl_2 solvent molecules are found in the asymmetric unit. The whole cation in **5** is disordered and was split in two parts, which are occupied in a 1:1 ratio. This new structure determination of **5** allowed for a more reliable determination of the N1−Sb1 distances [**5**, 1.948(3) (part 1)/1.981(3) (part 2) Å] in the cation.[10]

Compounds **12** and **13** crystallize in the monoclinic space group $P2_1/n$ with four molecules in the cell. The antimony adopts trigonal-pyramidal coordination geometry [**12**, $\sum$(∠Sb1) = 298.3°; **13**, $\sum$(∠Sb1) = 289.75°], as expected for a tricoordinated antimony atom [cf. $(Me_3Si)_2NSbCl_2$[10] $\sum$(∠Sb) = 292.99°] without any significantly short intermolecular contacts. The Sb−N_{amino} distances [**12**, 2.032(4)/2.050(4) Å; **13**, 2.035(2)/2.012(2) Å] are shortened Sb−N single bonds [cf. $\sum r_{cov}$(Sb−N) = 2.11 Å, $\sum r_{cov}$(Sb=N) = 1.93 Å],[20] with the shorter distances detected in **13**. This illustrates the transition to a stibenium salt, as the Sb−O bond in **13** [2.158(1) Å] is also significantly elongated [cf. $Sb(R_F)_2OTf$ 2.082(8) Å; $\sum r_{cov}$(Sb−O) = 2.03 Å].[20,26] The Sb−N distances in **13** are in the range of previously reported *N*-heterocyclic stibenium cations (cf. [C_2H_2(*t*BuN)$_2$Sb][$SbCl_4$] 2.024 Å, [Me_2Si(*t*BuN)$_2$Sb][$AlCl_4$] 1.995 Å, averaged values).[27,28] The Sb−Cl distance in **12** is also rather long [**12**, 2.405(3) Å, cf. $\sum r_{cov}$(Sb−Cl) = 2.39 Å, Me_2Si(*t*BuN)$_2$SbCl, 2.646(2) Å].[20] Interestingly, a small but obvious deviation from planarity is observed for one of the N_{amino} atoms in **13** [for **12**, $\sum$(∠N1) 358.1°, $\sum$(∠N2) 358.0°; for **13**, $\sum$(∠N1) 347.9°, $\sum$(∠N2) 360.0°]. The torsion angle between the Si1−N1−Sb1 and Si3−N2−Si4 planes in **13** is rather large, 131.90(9)°, and is larger than in starting material **12**, 33.1(2)°.

To assess the bonding in arsenic compounds **8**−**11** and antimony compounds **12** and **13**, natural bond orbital (NBO)[29] analyses were carried out at the B3LYP level of density functional theory. The NBO analysis of **8** shows three σ bonds and one lone pair (LP) localized at the As atom in a mainly s-type orbital, while in the cation of **9** only two σ bonds, one LP at the As atom, and a p_π−p_π double bond between the As atom and one N_{amino} atom are found. Furthermore, a p-type LP is found on the other N_{amino} atom, which is delocalized into the π^*(N=As) with a hyperconjugative energy of $\Delta E^{(2)}$ = 32.0 kcal·mol^{-1}. Consequently, in the valence band (VB) picture, the π bonding in **9** is best described by at least two resonance formulas as shown in Scheme 6 and can thus be classified as a four-electron, three-center bond. This is further illustrated by the highest occupied molecular orbital (HOMO) − 11 Kohn−Sham molecular orbital, which mainly describes the delocalized π bond (Figure 6). The lowest unoccupied molecular orbital

dx.doi.org/10.1021/ic4010104 | Inorg. Chem. 2013, 52, 7781−7790

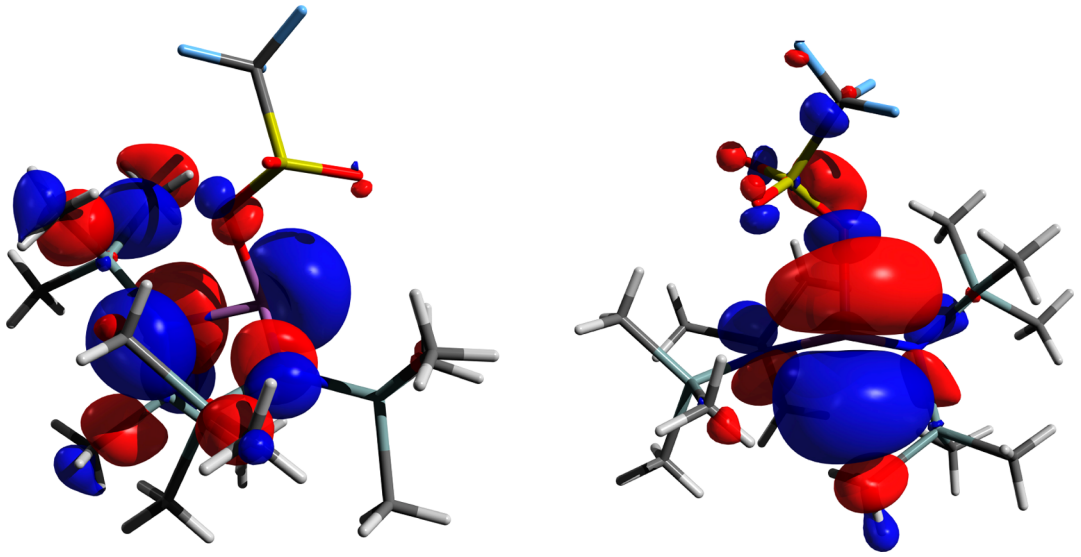

Figure 7. Surface plots (isovalue 0.03) showing the LUMO (left) and HOMO (right) of **13**.

(LUMO) of the cation in **9** represents a π^* orbital with a rather large coefficient at the As atom, while the HOMO describes mainly the LPs located at both N_{amino} atoms and the As center (Figure 6).

All As−N/As-Cl bonds are highly polarized, as for example only 17% of the As=N double bond is located at the As atom. In **8** one of the p-type LPs located on the N_{amino} atom is almost parallel to the As−Cl bond. Hence intramolecular donor−acceptor between the p-LP and the antibonding σ^* orbital are found (hyperconjugative energy $\Delta E^{(2)}$ = 12.7 kcal·mol^{-1}), resulting in the rather long As−Cl bond and a small amount of N−As π bonding. Furthermore, the p-LPs on both N_{amino} atoms donate into the σ^* orbitals of the Si−C backbone, and consequently the N−Si bonds are shortened.

In **11** the p-type LPs on the exocyclic N_{amino} donate into the σ^* orbitals of the As−N bonds in the ring system, with hyperconjugative energies that sum up to $\Delta E^{(2)}$ = 23.0 kcal·mol^{-1} on each side of the ring. The resulting stabilization of that perpendicular arrangement consequently leads, together with steric reasons, to magnetic inequivalence of the three different $SiMe_3$ groups in the ^{1}H NMR spectrum of **11**. In contrast to **11**, in $\{[(Me_3Si)_2N]Bi[\mu\text{-}N(SiMe_3)]\}_2$ only two signals in a 2:1 ratio are detected and a splitting into three resonances is observed at 213 K in variable -temperature ^{1}H NMR experiments. Hence, at room temperature, rotation around the exocyclic Bi−N bond is possible in the *cyclo*-dibismadiazane.[25] Therefore, the steric strain in **11** is a considerable source of its magnificent stability. In addition, the ring N atoms also carry a p-type LP that is also delocalized into the As_2N_2 unit, inducing significant π bonding in the ring and rather short As−N bonds.

The bonding situation in chlorostibane **12** is similar to that discussed before for **8**. Interestingly, **13** has some kind of stibenium character, as the positive charge on the Sb increases upon chloride abstraction [q(Sb) for **12**, +1.62e; for **13**, +1.81e), and the overall charge transfer from the triflate group amounts to only 0.29e, leading formally to a $[(Me_3Si)_2N)_2Sb]^{0.71+}$ unit. Thus **12** is best described by at least three resonances in the VB picture (Scheme 6), which describes best the high polarization of the bonds within the N−Sb(O)−N skeleton and the ionic character of the Sb−O bond (90% located on O1). The Sb1−O1 bond is significantly weakened by negative hyperconjugation of the p-LP located on N2 into the Sb1−O1 σ^* antibonding orbital ($\Delta E^{(2)}$ = 13.9 kcal·mol^{-1}). In the MO picture, a π^* orbital with a rather large coefficient for an empty p-orbital located at the Sb atom is calculated as LUMO. The HOMO has some degree of antibonding character for the Sb−O bond and describes further an s-type LP on the antimony (Figure 7). In both compounds **12** and **13**, the LPs located on antimony have almost the same large amount of s-character (**12**, 80.23%; **13**, 80.84%).

■ CONCLUSION

In conclusion, we present here the first structurally characterized bisaminoarsenium salt in **9** and its full characterization. Upon reaction of **8** with AgOTf, *cyclo*-diarsadiazane **11** was obtained, which was formed by elimination of Me_3Si-OTf from **10**. Interestingly, the analogous chlorostibane **12** was found to display a completely different reactivity: in the reaction with $GaCl_3$, aminochlorostibenium salt **5** was isolated, and with AgOTf, the triflate-substituted stibane **13** was obtained, which in contrast to **10** is stable in solution up to 100 °C.

■ EXPERIMENTAL SECTION

General Information. All manipulations were carried out under oxygen- and moisture-free conditions via standard Schlenk and drybox techniques.

Dichloromethane was purified according to a literature procedure,[1] dried over P_4O_{10}, stored over CaH_2, and freshly distilled prior to use. *N*-Pentane and *n*-hexane were dried over sodium benzophenone/tetraglyme and freshly distilled prior to use. Lithium *N*,*N*-bis-(trimethylsilyl)amide[30] and silver trifluoromethylsulfonate (AgOTf)[31] have been reported previously and were prepared according to a modified literature procedure. $AsCl_3$ (99.99%, Merck) was freshly distilled prior to use. $GaCl_3$ (99.999%, Sigma−Aldrich) and $SbCl_3$ (99.99%, Merck) were freshly sublimed prior to use.

Characterization Techniques. For NMR characterization, ^{29}Si insensitive nuclei enhanced by polarization transfer (INEPT), ^{19}F{^{1}H}, ^{13}C{^{1}H}, and ^{1}H NMR spectra were recorded on a Bruker spectrometer Avance 300. The ^{1}H and ^{13}C NMR chemical shifts were referenced to the solvent signals [$CDHCl_2$, δ (^{1}H) = 5.31; δ (^{13}C) = 54.0]. The ^{19}F and ^{29}Si NMR chemical shifts are referred to

dx.doi.org/10.1021/ic4010104 | Inorg. Chem. 2013, 52, 7781−7790

$CFCl_3$ and tetramethylsilane (TMS), respectively. CD_2Cl_2 was dried over P_4O_{10} and was degassed prior to use.

Elemental analysis (C, H, N) was performed on an Analysator Flash EA 1112 instrument from Thermo Quest.

Infrared spectra were taken on a Nicolet 380 Fourier transform infrared (FT-IR) spectrometer with a Smart Orbit attenuated total reflectance (ATR) module.

Raman spectroscopy was performed on a LabRAM HR 800 Horiba Jobin YVON instrument equipped with a high-stability BX40 microscope (focus 1 μm) or an Olympus Mplan 50× NA 0.70 lens. For excitation, an infrared laser (785 nm, 100 mW, air-cooled diode) or a red laser (633 nm, 17 mW, HeNe laser) was utilized.

Melting points are uncorrected (EZ-Melt, Stanford Research Systems). A heating rate of 20 °C/min was employed (clearing points are reported).

A Finnigan MAT 95-XP spectrometer from Thermo Electron was used for mass spectrometric measurements.

For X-ray structure determination, X-ray-quality crystals of **8**, **11**, and **13** were selected in Fomblin YR-1800 perfluoroether (Alfa Aesar) at ambient temperature. X-ray-quality crystals of **9a**, **9b**, **5**, and **12** were selected in Fomblin Y LVAC 06/6 perfluoroether (Sigma–Aldrich) at 220 K. The samples were cooled to 173(2) K during measurement. Data were collected on a Bruker Kappa Apex-II CCD diffractometer that used graphite monochromated Mo Kα radiation (λ = 0.710 73). The structures were solved by direct methods (SHELXS-97)[32] and refined by full-matrix least-squares procedures (SHELXL-97).[33] Semiempirical absorption corrections were applied (SADABS).[34] All non-hydrogen atoms were refined anisotropically, and hydrogen atoms were included in the refinement at calculated positions by use of a riding model.

Syntheses. *[(Me$_3$Si)$_2$N]$_2$AsCl (**8**).* To a stirred solution of $AsCl_3$ (9.2 mmol, 1.668 g) in *n*-hexane (15 mL) was added dropwise at −60 °C a solution of Li[N(SiMe$_3$)$_2$] (19.4 mmol, 3.246 g) in *n*-hexane (15 mL). The resulting white suspension was slowly warmed to room temperature over a period of 2 h. Afterward the solids were removed over a frit and the solvents were removed from the filtrate in vacuo. The crude orange oil was distilled in vacuo (10^{-3} mbar) at 70 °C to remove $(Me_3Si)_2NAsCl_2$. Upon complete removal, the product crystallized as an orange solid and was further purified by recrystallization from a saturated *n*-hexane solution. After storage of the saturated solution at −24 °C for 24 h, bis-[*N*,*N*-bis(trimethylsilyl)-amino]chloroarsane (2.219 g, 5.14 mmol, 56%) (**8**) was obtained as a colorless crystalline solid, mp 48 °C. Anal. calcd % (found): C 33.43 (33.53); H 8.42 (8.38); N 6.50 (6.51). ^{1}H NMR (25 °C, CD_2Cl_2, 300.13 MHz) 0.33 [s, $J(^{29}Si-^1H)$ = 6.61 Hz, $J(^{13}C-^1H)$ = 119.16 Hz, 36H, Si(CH_3)$_3$]. ^{13}C{^{1}H} NMR (25 °C, CD_2Cl_2, 75.48 MHz) 5.57 [s, Si(CH_3)$_3$]. ^{29}Si INEPT NMR (25 °C, CD_2Cl_2, 49.70 MHz) 6.6 [m, $J(^1H-^{29}Si)$ = 6.6 Hz]. IR (ATR, 25 °C, 32 scans, cm^{-1}) 2947 (w), 2897 (w), 1404 (w), 1265 (m), 1246 (s), 896 (m), 820 (s), 785 (s), 763 (s), 725 (m), 699 (m), 687 (m), 668 (s) 641 (m), 621 (m). Raman 2958 (4), 2900 (10), 2832 (1), 2797 (1), 1411 (1), 1250 (1), 887 (1), 854 (1), 848 (1), 839 (1), 755 (1), 726 (1), 678 (2), 643 (7), 621 (1), 441 (2), 408 (1), 377 (1), 355 (1), 326 (9), 299 (3), 260 (1), 216 (2). MS (CI, isobutene, *m*/*z*, >10%) {[(Me$_3$Si)$_2$N]$_2$As}$^+$ 395 (100), [(Me$_3$Si)$_2$NAsCl]$^+$ 269 (46).

*[[(Me$_3$Si)$_2$N]$_2$As][GaCl$_4$] (**9a**).* To a stirred solution of **8** (0.5 mmol, 0.217 g) in CH_2Cl_2 (3 mL) was added dropwise at −80 °C a solution of $GaCl_3$ (0.51 mmol, 0.091 g) in CH_2Cl_2 (2 mL). The resulting deep yellow solution was stirred for 1 h at this temperature. Afterward the mixture was concentrated to 0.5 mL and placed in the freezer (−80 °C) for 12 h. During this time span, yellow crystalline needles of bis[*N*,*N*-bis(trimethylsilyl)amino]arsenium tetrachloridogallate (**9a**) precipitated, and after removal of the supernatant 0.165 g (0.23 mmol; 48%) of **9a** was isolated. **9a** can be stored in the freezer for at least six months and is stable even at room temperature for a short period of time. Anal. calcd % (found): C 23.74 (23.79); H 5.98 (5.89); N 4.61 (4.70). ^{1}H NMR (−40 °C, CD_2Cl_2, 250.13 MHz) 0.51 [s, $J(^{13}C-^1H)$ = 121.4 Hz, 36H, Si(CH_3)$_3$]. ^{13}C{^{1}H} NMR (−40 °C, CD_2Cl_2, 62.90 MHz) 4.18 [s, Si(CH_3)$_3$]. ^{29}Si INEPT NMR (−40 °C, CD_2Cl_2, 49.70 MHz) 16.9 (s). IR (ATR, 25 °C, 32 scans, cm^{-1}) 2954 (m), 2899 (m), 1409 (m), 1318 (w), 1260 (s), 1173 (w), 1042 (w), 1012 (m), 995 (m), 926 (m), 873 (s), 839 (s) 830 (s), 802 (s), 790 (s), 758 (s), 741 (m), 715 (m), 678 (m), 649 (m), 632 (m), 617 (m), 566 (m). Raman 2994 (1), 2963 (2), 2906 (4), 1411 (2), 1260 (2), 1067 (1), 1018 (1), 911 (3), 856 (1), 809 (1), 784 (1), 763 (1), 744 (1), 693 (2), 674 (2), 644 (3), 636 (3), 572 (2), 528 (1), 427 (3), 390 (3), 362 (2), 349 (10), 293 (1), 271 (1), 251 (1), 228 (1).

*[[(Me$_3$Si)$_2$N]$_2$As][Ga$_2$Cl$_7$] (**9b**).* To a stirred solution of **8** (0.5 mmol, 0.217 g) in CH_2Cl_2 (3 mL) was added dropwise at −80 °C a solution of $GaCl_3$ (1.01 mmol, 0.179 g) in CH_2Cl_2 (2 mL). The resulting deep yellow solution was stirred for 1 h at this temperature. Afterward the mixture was concentrated to 0.5 mL and placed in the freezer (−80 °C) for 96 h. During this time span, yellow crystalline plates of bis[*N*,*N*-bis(trimethylsilyl)amino]arsenium heptachloridodigallate (**9b**) precipitated, and after removal of the supernatant, a yellow crystalline solid was isolated that decomposed when brought into the drybox.

*[(Me$_3$Si)$_2$NAs-μ-NSiMe$_3$]$_2$ (**11**).* To a stirred suspension of AgOTf (1.02 mmol, 0.262 g) in CH_2Cl_2 (3 mL) was added at −60 °C a solution of **8** (1 mmol, 0.432 g) in CH_2Cl_2 (2 mL). The resulting grayish suspension was slowly warmed to room temperature over a period of 2 h, and subsequently the solvents were removed in vacuo. The residual solids were extracted with *n*-hexane (7 mL). Again the solvents were evaporated and an off-white solid (powder) remained, which could be recrystallized from CH_2Cl_2, by gradually cooling a saturated solution to −80 °C over a period of 12 h. After removal of the supernatant liquid, 0.310 g (0.47 mmol; 95%) of 1,3-[*N*,*N*-bis(trimethylsilyl)amino]diarsa-2,4-(*N*-trimethylsilyl)diazan (**11**) was obtained as a colorless crystalline solid. ^{1}H NMR (25 °C, CD_2Cl_2, 300.13 MHz) 0.49 [s, $J(^{29}Si-^1H)$ = 6.61 Hz, 9H, Si(CH_3)$_3$], 0.23 [s, $J(^{29}Si-^1H)$ = 6.61 Hz, 9H, Si(CH_3)$_3$], −0.07 [s, $J(^{29}Si-^1H)$ = 6.61 Hz, 9H, Si(CH_3)$_3$]. ^{13}C{^{1}H} NMR (25 °C, CD_2Cl_2, 75.48 MHz) 5.72 [s, 3C, Si(CH_3)$_3$], 5.20 [s, 3C, Si(CH_3)$_3$], 2.03 [s, 3C, Si(CH_3)$_3$]. ^{29}Si INEPT NMR (25 °C, CD_2Cl_2, 49.70 MHz) 5.5 [m, 1 *Si*(CH_3)$_3$], 1.4 [m, 1 *Si*(CH_3)$_3$], 0.5 [m, 1 *Si*(CH_3)$_3$]. IR (ATR, 25 °C, 32 scans, cm^{-1}) 2951 (m), 2897 (w), 1405 (w), 1336 (w), 1298 (w) 1261 (m), 1246 (s), 1171 (w), 1033 (w), 893 (s), 855 (s), 817 (s), 769 (s), 757 (s), 746 (s), 694 (m), 677 (m), 641 (s), 626 (s). MS (CI, isobutene, *m*/*z*, >10%): [M]$^+$ 654 (100), [M − N(SiMe$_3$)$_2$]$^+$ 484 (99), [H$_2$N(SiMe$_3$)$_2$]$^+$ 162 (37).

*[(Me$_3$Si)$_2$N]$_2$SbCl (**12**).* To a stirred solution of $SbCl_3$ (10.3 mmol, 2.349 g) in Et_2O (20 mL) was added dropwise at −50 °C a solution of Li[N(SiMe$_3$)$_2$] (20.6 mmol, 3.450 g) in *n*-hexane (40 mL). The resulting grayish suspension was slowly warmed to room temperature over a period of 2 h. Afterward the solvents were evaporated and the residues were extracted with *n*-pentane (30 mL) over a Celite-padded frit. Removal of the solvents in vacuo yielded a colorless oil as crude product, from which at −40 °C $(Me_3Si)_2NSbCl_2$ (**14**) crystallized as side product. The crude colorless mother liquor was further purified by distillation in vacuo (10^{-3} mbar; 130 °C), and 3.375 g (7.06 mmol; 71%) of (bis[*N*,*N*-bis(trimethylsilyl)amino]chlorostibane (**12**) was obtained as a colorless liquid, mp −5 °C. ^{1}H NMR (25 °C, CD_2Cl_2, 300.13 MHz) 0.31 [s, $J(^{29}Si-^1H)$ = 6.42 Hz, $J(^{13}C-^1H)$ = 118.6 Hz, 36H, Si(CH_3)$_3$]. ^{13}C{^{1}H} NMR (25 °C, CD_2Cl_2, 75.48 MHz) 6.15 [s, Si(CH_3)$_3$]. ^{29}Si INEPT NMR (25 °C, CD_2Cl_2, 49.70 MHz) 6.4 [m, $J(^1H-^{29}Si)$ = 6.5 Hz]. IR (ATR, 25 °C, 32 scans, cm^{-1}) 2950 (w), 2898 (w), 1407 (w), 1298 (w), 1249 (s), 1181 (w), 876 (s), 832 (s), 782 (s), 759 (m), 718 (m) 698 (m), 667 (s), 632 (m), 619 (m). Raman 2956 (4), 2900 (10), 2801 (1), 1409 (1), 1262 (1), 1248 (1), 893 (1), 854 (1), 794 (1), 749 (1), 716 (1), 676 (2), 635 (5), 412 (2), 361 (1), 311 (5), 274 (1), 227 (1). MS (CI, isobutene, *m*/*z*, >10%) {[(Me$_3$Si)$_2$N]$_2$Sb}$^+$ 443 (97), [(Me$_3$Si)$_2$NSbCl]$^+$ 318 (10), [H$_2$N-(SiMe$_3$)$_2$]$^+$ 162 (60).

*[(Me$_3$Si)$_2$NSbCl][(Me$_3$Si)$_2$N(GaCl$_3$)$_2$] (**5**).*[10] To a stirred solution of **12** (0.5 mmol, 0.239 g) in CH_2Cl_2 (2 mL) was added dropwise at −80 °C a solution of $GaCl_3$ (1 mmol, 0.178 g) in CH_2Cl_2 (2 mL). Upon complete addition of $GaCl_3$ the reaction mixture turned deep orange, and after being stirred for 1 h at this temperature, the mixture was concentrated to incipient crystallization. Afterward the mixture was

dx.doi.org/10.1021/ic4010104 | Inorg. Chem. 2013, 52, 7781−7790

placed in the freezer (−40 °C) for 24 h and colorless crystalline blocks of **5** were obtained, 0.350 g (0.35 mmol, 70%).

*[(Me$_3$Si)$_2$N]$_2$SbOTf (**13**).* To a stirred suspension of AgOTf (0.58 mmol, 0.150 g) in CH_2Cl_2 (2 mL) was added dropwise at −50 °C a solution of **12** (0.58 mmol, 0.276 g) in CH_2Cl_2 (8 mL). The mixture was slowly warmed to ambient temperatures over a period of 1 h and was then stirred for an additional 2 h. Afterward the solvent was removed in vacuo and the residues were extracted with *n*-hexane (10 mL). From the filtrate the *n*-hexane was removed in vacuo and 0.265 g (0.45 mmol, 78%) of bis[*N*,*N*-bis(trimethylsilyl)amino](triflato)-stibane (**13**) was obtained as a colorless crystalline powder, mp 62 °C. Anal. calcd % (found): C 26.39 (25.73); H 6.13 (5.74); N 4.74 (4.79). ^{1}H NMR (25 °C, CD_2Cl_2, 300.13 MHz) 0.34 [d, $J(^{29}Si-^1H)$ = 6.61 Hz, 36H, $Si(CH_3)_3$]. $^{13}C\{^1H\}$ NMR (25 °C, CD_2Cl_2, 75.48 MHz) 5.69 [s, $Si(CH_3)_3$]. $^{19}F\{^1H\}$ NMR (25 °C, CD_2Cl_2, 282.38 MHz) −77.56 (s, O_3SCF_3). ^{29}Si INEPT NMR (25 °C, CD_2Cl_2, 49.70 MHz) 7.42 [m, $J(^1H-^{29}Si)$ = 6.5 Hz, $Si(CH_3)_3$]. IR (ATR, 25 °C, 32 scans, cm^{-1}) 2953 (w), 2900 (w), 1428 (w), 1349 (m), 1315 (w), 1249 (s), 1231 (m), 1193 (s), 1154 (m), 1022 (w), 958 (m), 880 (m), 835 (s), 785 (m), 758 (m), 723 (m), 685 (m), 667 (m), 630 (s), 584 (m), 574 (m). Raman 2962 (2), 2901 (6), 2795 (1), 1538 (1), 1513 (1), 1414 (2), 1357 (1), 1272 (2), 1255 (2), 1232 (2), 1152 (2), 957 (2), 880 (2), 852 (2), 799 (2), 766 (7), 725 (3), 687 (4), 678 (4), 644 (10), 586 (2), 574 (2), 523 (2), 436 (9), 385 (4), 347 (2), 321 (3), 279 (3), 250 (3), 235 (4).

■ ASSOCIATED CONTENT

Supporting Information

Additional text, eight schemes, and 11 tables with experimental and computational details, crystallographic information, and synthesis and structural elucidation of compounds **8**, **9a**, **9b**, **11**, **12**, **5**, **13**, and **14** (PDF). Crystallographic datablocks and ellipsoid plots (PDF). Crystallographic files (CIF). This material is available free of charge via the Internet at http://pubs.acs.org.

■ AUTHOR INFORMATION

Corresponding Author

*E-mail axel.schulz@uni-rostock.de.

Notes

The authors declare no competing financial interest.

■ ACKNOWLEDGMENTS

Financial support by the Fonds der Chemischen Industrie (fellowship to C.H.) and the DFG (SCHU 1170/8-1) are gratefully acknowledged.

■ REFERENCES

(1) (a) Reiss, F.; Villinger, A.; Schulz, A. *Eur. J. Inorg. Chem.* **2012**, *2*, 261. (b) Hering, C.; Schulz, A.; Villinger, A. *Angew. Chem.* **2012**, *124*, 6345; *Angew. Chem., Int. Ed.* **2012**, *51*, 6241. (c) Holthausen, M. H.; Weigand, J. J. *Z. Anorg. Allg. Chem.* **2012**, *638*, 1103. (d) Brazeau, A. L.; Nikouline, A. S.; Ragogna, P. J. *Chem. Commun.* **2011**, *47*, 4817. (e) Lichtenberger, C.; Pan, F.; Spaniol, T. P.; Englert, U.; Okuda, J. *Angew. Chem.* **2012**, *124*, 13186; *Angew. Chem., Int. Ed.* **2012**, *51*, 13011. (f) Chitnis, S. S.; Burford, N.; Ferguson, M. J. *Angew. Chem., Int. Ed.* **2013**, *52*, 2042.

(2) (a) Burford, N.; Royan, B. W.; Whalen, J. M.; Richardson, J. F.; Rogers, R. D. J. *Chem. Soc., Chem. Commun.* **1990**, 1273. (b) Burford, N.; Parks, T. M.; Bakshi, P. K.; Cameron, T. S. *Angew. Chem.* **1994**, *106*, 1332; *Angew. Chem., Int. Ed. Engl.* **1994**, *33*, 5221. (c) Payastre, C.; Madaule, Y.; Wolf, J. G. *Tetrahedron Lett.* **1990**, *31*, 1145. (d) Carmalt, C. J.; Farrugia, L. J.; Norman, N. C. *J. Chem. Soc., Dalton Trans.* **1996**, 443. (e) Carmalt, C. J.; Lomeli, V.; McBurnett, B. G.; Cowley, A. H. *Chem. Commun.* **1997**, 2095.

(3) Schmidpeter, A. Multiple Bonds and Low Coordination Chemistry. In *Phosphorus Chemistry*; Regitz, M., Scherer, O., Eds.; Georg Thieme Verlag: Stuttgart, Germany, 1990; Vol. *D2*, p 149.

(4) (a) Niecke, E.; Gudat, D. *Angew. Chem.* **1991**, *103*, 251; *Angew. Chem,. Int. Ed. Engl.* **1991**, *30*, 217. (b) Weber, L. *Chem. Rev.* **1992**, *92*, 1839. (c) Davidson, J.; Weigand, J. J.; Burford, N.; Cameron, T. S.; Decken, A.; Zwanziger, W. *Chem. Commun.* **2007**, 4671. (d) Villinger, A.; Mayer, P.; Schulz, A. *Chem. Commun.* **2006**, 1236. (e) Lehmann, M.; Schulz, A.; Villinger, A. *Angew. Chem.* **2011**, *123*, 5784; *Angew. Chem., Int. Ed. Engl.* **2011**, *50*, 5221. (f) Lehmann, M.; Schulz, A.; Villinger, A. . *Angew. Chem.* **2012**, *124*, 8211; *Angew. Chem., Int. Ed. Engl.* **2012**, *51*, 8087.

(5) (a) Cowley, A. H.; Kemp, R. A. *Chem. Rev.* **1985**, *85*, 367. (b) Gudat, D. *Coord. Chem. Rev.* **1997**, *163*, 71.

(6) Payrastre, C.; Madaule, Y.; Wolf, J.-G. *Tetrahedron Lett.* **1992**, *33*, 1273.

(7) For example: (a) Porter, K. A.; Willis, A. C.; Zank, J.; Wild, S. B. *Inorg. Chem.* **2002**, *41*, 6380. (b) Kilah, N. L.; Petrie, S.; Stranger, R.; Wielandt, J. W.; Willis, A. C.; Wild, S. B. *Organometallics* **2007**, *26*, 6106. (c) Conrad, E.; Burford, N.; McDonald, R.; Ferguson, M. J. *J. Am. Chem. Soc.* **2009**, *131*, 17000. (d) Burford, N.; Ragogna, P. J.; Sharp, K. *Inorg. Chem.* **2005**, *44*, 9453.

(8) (a) Jutzi, P.; Wippermann, T.; Krüger, C.; Kraus, H.-J. *Angew. Chem.* **1983**, *95*, 244; *Angew. Chem., Int. Ed. Engl.* **1983**, *22*, 250. (b) Baxter, S. G.; Cowley, A. H.; Mehrotra, S. K. *J. Am. Chem. Soc.* **1981**, *103*, 5573.

(9) Kraft, A.; Beck, J.; Krossing, I. *Chem.—Eur. J.* **2011**, *17*, 12975.

(10) Hering, C.; Lehmann, M.; Schulz, A.; Villinger, A. *Inorg. Chem.* **2012**, *51*, 8212.

(11) Baumann, W.; Schulz, A.; Villinger, A. *Angew. Chem.* **2008**, *120*, 9672; *Angew. Chem., Int. Ed. Engl.* **2008**, *47*, 9530.

(12) Michalik, D.; Schulz, A.; Villinger, A. *Inorg. Chem.* **2008**, *47*, 11798.

(13) (a) Gynane, M. J. S.; Hudson, A.; Lappert, M. F.; Power, P. P.; Goldwhite, H. *Dalton Trans.* **1980**, 2428. (b) Olmstead, M. M.; Power, P. P.; Sigel, G. A. *Inorg Chem.* **1988**, *27*, 2045.

(14) Hering, C.; Schulz, A.; Villinger, A. *Angew. Chem.* **2012**, *124*, 6345; *Angew. Chem., Int. Ed. Engl.* **2012**, *51*, 6241.

(15) Holthausen, M. H.; Feldmann, K.-O.; Schulz, S.; Hepp, A.; Weigand, J. J. *Inorg. Chem.* **2012**, *51*, 3374.

(16) Lehmann, M.; Schulz, A.; Villinger, A. *Eur. J. Inorg. Chem.* **2010**, *35*, 5501.

(17) Niecke, E.; Bitter, W. *Synth. React. Inorg. Met.-Org. Chem.* **1975**, *5*, 231.

(18) For example: (a) Bochmann, M.; Webb, K. J.; Harman, M.; Hursthouse, M. B. *Angew. Chem.* **1990**, *102*, 703; *Angew. Chem., Int. Ed. Engl.* **1990**, *29*, 638. (b) Bochmann, M.; Webb, K. J.; Hursthouse, M. B.; Mazid, M. *J. Chem. Soc., Dalton Trans.* **1991**, 2317. (c) Bochmann, M.; Bwembya, G. C.; Grinter, R.; Powell, A. K.; Webb, K. J.; Hursthouse, M. B.; Malik, K. M. A.; Mazid, M. *Inorg. Chem.* **1994**, *33*, 2290.

(19) Spinney, H. A.; Korobkov, I.; Richeson, D. S. *Chem. Commun.* **2007**, 1647.

(20) Pyykkö, P.; Atsumi, M. *Chem.—Eur. J.* **2009**, *15*, 12770.

(21) Burford, N.; Macdonald, C. L. B.; Parks, T. M.; Wu, G.; Borecka, B.; Kwiatkowski, W.; Cameron, T. S. *Can. J. Chem.* **1996**, *74*, 2209.

(22) Mantina, M.; Chamberlin, A. C.; Valero, R.; Cramer, C. J.; Truhlar, D. G. *J. Phys. Chem. A* **2009**, *113*, 5806.

(23) Schulz, A.; Villinger, A. *Inorg. Chem.* **2009**, *48*, 7359.

(24) Burford, N.; Cameron, T. S.; Macdonald, C. L. B.; Robertson, K. N.; Schurko, R.; Walsh, D. *Inorg. Chem.* **2005**, *44*, 8058.

(25) Evans, W. J.; Rego, D. B.; Ziller, J. W. *Inorg. Chim. Acta* **2007**, *360*, 1349.

(26) Burford, N.; Macdonald, C. L. B.; LeBlanc, D. J.; Cameron, T. S. *Organometallics* **2000**, *19*, 152.

(27) Veith, M.; Bertsch, B.; Huch, V. *Z. Anorg. Allg. Chem.* **1988**, *559*, 73.

(28) Gudat, D.; Gans-Eichler, T.; Nieger, M. *Chem. Commun.* **2004**, 2434.
(29) (a) Computational details and a summary of the NBO output are given in the Supporting Information. (b) Weinhold, F.; Landis, C. *Valency and Bonding. A Natural Bond Orbital Donor-Acceptor Perspective*; Cambridge University Press: Cambridge, U.K., 2005, and references therein.
(30) Amonoo-Neizer, E. H.; Shaw, R. A.; Skovlin, D. O.; Smith, B. C.; Rosenthal, J. W.; Jolly, W. L. In *Inorganic Syntheses*; Holtzlaw, H. F., Ed.; John Wiley & Sons, Inc.: Hoboken, NJ, 2007, Vol. *8*, Chapt. 6.
(31) Whitesides, G. M.; Gutowski, F. D. *J. Org. Chem.* **1976**, *41*, 2882.
(32) Sheldrick, G. M. *SHELXS-97: Program for the Solution of Crystal Structures*; University of Göttingen, Germany, 1997.
(33) Sheldrick, G. M. *SHELXL-97: Program for the Refinement of Crystal Structures*; University of Göttingen, Germany, 1997.
(34) Sheldrick, G. M. *SADABS, version 2*; University of Göttingen, Germany, 2004.

5.5 Chlorine/methyl Exchange Reactions in Silylated Aminostibanes: A New Route to Stibinostibonium Cations

Christian Hering, Mathias Lehmann, Axel Schulz, Alexander Villinger.

Inorganic Chemistry, **2012**, *51*, 8212−8224.

DOI: 10.1021/ic300770b

In dieser Publikation wurde ein Großteil der experimentellen Arbeiten von mir durchgeführt. Der eigene Beitrag liegt bei ca. 70 %.

Inorganic Chemistry

Article

pubs.acs.org/IC

Chlorine/Methyl Exchange Reactions in Silylated Aminostibanes: A New Route To Stibinostibonium Cations

Christian Hering,[†] Mathias Lehmann,[†] Axel Schulz,*[,†,‡] and Alexander Villinger[†]

[†]Universität Rostock Institut für Chemie, Albert-Einstein-Str. 3a, 18059 Rostock

[‡]Leibniz-Institut für Katalyse e.V. an der Universität Rostock, Albert-Einstein-Str. 29a, 18059 Rostock, Germany

Supporting Information

ABSTRACT: The Lewis acid assisted triflate/methyl, azide/methyl, and chlorine/methyl exchange reactions between silicon and antimony have been studied in the reaction of $R(Me_3Si)N{-}SbCl_2$ (R = Ter) with AgOTf, AgN_3, KO*t*Bu, $GaCl_3$, and $Me_3SiN_3/GaCl_3$, resulting in the formation of different methylantimony compounds. Furthermore, $R(Me_3Si)N{-}SbCl_2$ (R = $SiMe_3$) was reacted with $GaCl_3$ at low temperatures to yield a hitherto unreported amino(chloro)stibenium cation, the proposed intermediate in methyl exchange reactions. Tetrachloridogallate salts bearing different stibinostibonium cations such as $[(Me_3Sb)SbMe_2]^+$ and $[(Me_3Sb)_2SbMe]^{2+}$ along with the $GaCl_3$ adduct of $SbMe_3$ were isolated from such $R(Me_3Si)N{-}SbCl_2/GaCl_3$ mixtures (R = $SiMe_3$) at ambient temperatures, depending on the reaction parameters.

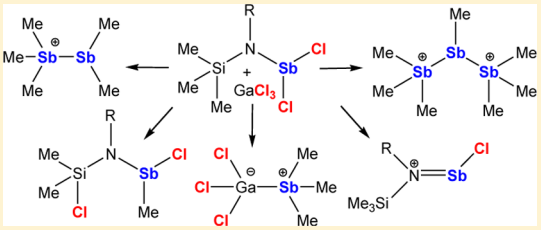

INTRODUCTION

Following our interest in low-coordinated nitrogen compounds of group 15 elements, we deal with the synthesis of binary four- and five-membered rings, especially of the heavier pnictogens (Pn) arsenic, antimony, and bismuth.[1] Silylated amino-pnictogen compounds $R(Me_3Si)N{-}PnX_2$ (R = Me_3Si, $(Me_3Si)_2N$, Mes* = supermesityl = 2,4,6-tri*tert*-butylphenyl, Ter = terphenyl = 2,6-bis(2,4,6-trimethyl-phenyl)phenyl; Pn = P, As, Sb; X = Cl, OTf = SO_3CF_3 = trifluoromethylsulfonyl) were shown to be unique starting materials for cycloaddition reactions as hidden imino-pnictogen building blocks (Schemes 1−3).[2−5] In these compounds elimination of trimethylsilyl-

Scheme 1. Synthesis of *cyclo*-Distibadiazanes via $Me_3Si{-}OTf$ Elimination[5]

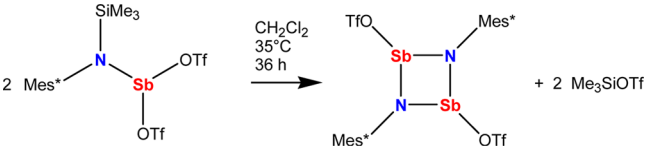

chloride $Me_3Si{-}Cl$ and -triflate $Me_3Si{-}OTf$ can occur thermally or triggered by the action of a Lewis-acid. Recently, a new synthesis of *cyclo*-distibadiazanes starting from Mes*-$(Me_3Si)N{-}Sb(OTf)_2$, which eliminates $Me_3Si{-}OTf$ at ambient temperatures (Scheme 1), was reported.[5]

Furthermore, amino-pnictogen compounds were used as hidden dipolarophiles, i.e., $R(Me_3Si)N{-}PnCl_2$ (R = Ter, Mes*; Pn = P, As), in [3 + 2] cycloaddition reactions (Scheme 2).[2−4,6] The dipolarophile, such as the reactive imino species R−N═Pn−Cl (Pn = P, As), is generated *in situ* via elimination of $Me_3Si{-}Cl$ triggered by the action of the Lewis-acid $GaCl_3$. Subsequent reaction with a 1,3-dipole-molecule such as $Me_3Si{-}N_3$ generates the neutral tetrazapnictole as $GaCl_3$ adduct (Scheme 2, eqs 1 and 2). The analogous tetrazastibole, stabilized as $B(C_6F_5)_3$ adduct, was obtained in an unusual isomerization reaction of diazido-*cyclo*-distibadiazane with $B(C_6F_5)_3$ (Scheme 2, eq 3).[7]

Also, triazadiphospholes, another class of five-membered pnictogen-nitrogen heterocycles, were prepared in a $GaCl_3$ assisted [3 + 2] cycloaddition reaction starting from *N*,*N*′,*N*′-[tris(trimethylsilyl)]hydrazino(dichloro)phosphane (Scheme 3, eq 1).[2] In this reaction 4 equiv of $Me_3Si{-}Cl$ are eliminated prior to cyclization, and the triazadiphosphole is obtained as $GaCl_3$ mono- or diadduct, which stabilizes the ring system with respect to N_2-elimination.

Astonishingly, the analogous arsenic species *N*,*N*′,*N*′-[tris-(trimethylsilyl)]hydrazino(dichloro)arsane $(Me_3Si)_2NN(SiMe_3)AsCl_2$ did not react with $GaCl_3$ to give the expected triazadiarsole, but instead both chlorine atoms attached to the arsenic atom were exchanged by a methyl group from one of the trimethylsilyl groups at the terminal nitrogen. The exchange product $[Me_2(Cl)Si]_2NN(SiMe_3)AsMe_2$ was obtained as a $GaCl_3$ adduct (Scheme 3, eq 2).[8] Removal of the Lewis acid is easily achieved by the addition of a stronger base such as 4-(dimethylamino)pyridine (DMAP).

This unusual Cl/methyl exchange reaction was further investigated and could be generalized and applied to different silylated amino(dichloro)arsane species $R(Me_3Si)N{-}AsCl_2$ (R = Me_3Si, $(Me_3Si)_2N$, Ter).[9] An initial chloride abstraction from the arsenic center by $GaCl_3$ and the intermediate formation of an cationic arsenic center triggers the exchange reaction. Due to

Received: April 13, 2012
Published: July 10, 2012

   dx.doi.org/10.1021/ic300770b | *Inorg. Chem.* 2012, 51, 8212−8224

Scheme 2. Synthesis of Tetrazapnictoles via [3 + 2] Cycloaddition Starting from Disguised Dipolarophiles $R(Me_3Si)N-PnCl_2$ (Pn = P, As; R = Ter, Mes*)

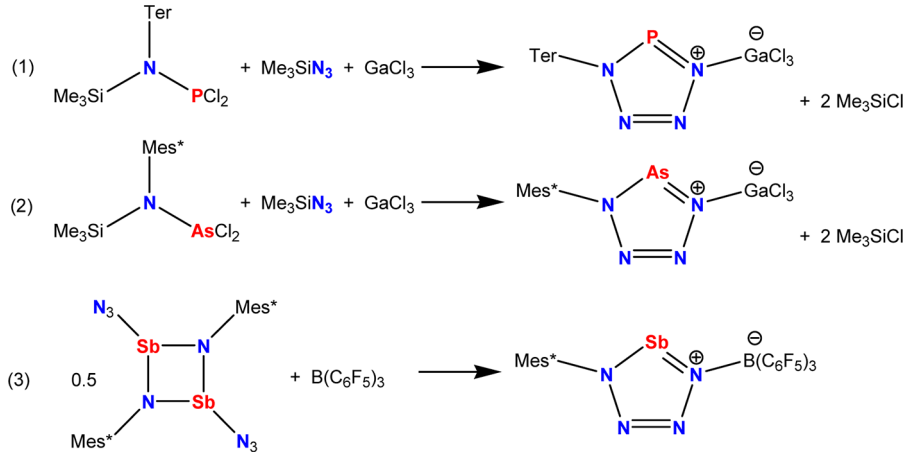

Scheme 3. Different Reaction Channels Observed for the Reaction of $GaCl_3$ and Silylated Hydrazinopnictanes $[(Me_3Si)_2N](Me_3Si)N-PnCl_2$ (Pn = P, As)[a]

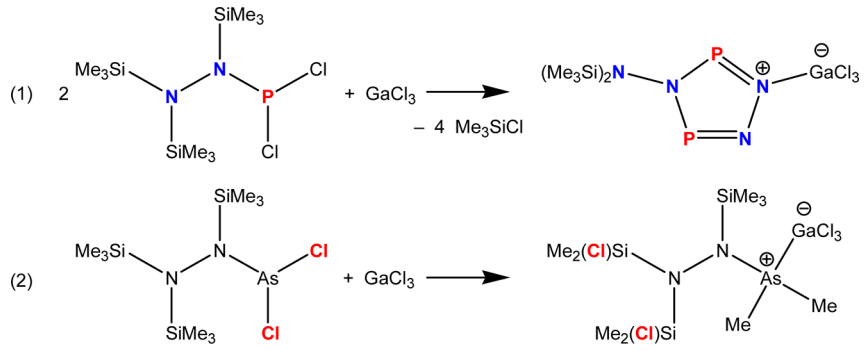

[a]Top: [3 + 2]-cycloaddition to triazadiphosphole. Bottom: methyl/chlorine-exchange.

Scheme 4. Proposed Mechanism for a Methyl/Chlorine-Exchange in Silylated Aminoarsanes

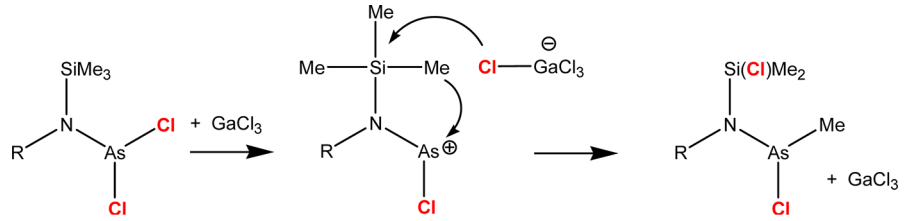

its high Lewis acidity the arsenium center stabilizes itself by abstraction of a methyl group from the Me_3Si moiety, whereas the $[Me_2Si{=}N]^+$ fragment finally abstracts a chloride from $[GaCl_4]^-$ to form the exchange product (Scheme 4).

The observation of different reaction channels for $(Me_3Si)_2N-N(SiMe_3)-PCl_2$ and $(Me_3Si)_2N-N(SiMe_3)-AsCl_2$ upon addition of a Lewis acid as well as our interest in the chemistry of the homologous silylated dichlorostibanes prompted us to study the reactions of $R(Me_3Si)N-SbCl_2$ (R = Ter, Mes*, Me_3Si) with the Lewis acids $GaCl_3$, AgOTf, AgN_3, and a mixture of $Me_3SiN_3/GaCl_3$.

RESULTS AND DISCUSSION

In a first series of experiments the synthesis and functionalization of $Ter(Me_3Si)N-SbCl_2$ was studied, followed by the reactions of $R(Me_3Si)N-SbCl_2$ (R = Ter, Mes*, Me_3Si) with $GaCl_3$.

Synthesis and Reactivity of $Ter(Me_3Si)N-SbCl_2$. $Ter(Me_3Si)N-SbCl_2$ (**1**) was prepared according to a procedure already used for the preparation of $Mes^*(Me_3Si)N-SbCl_2$ (Scheme 5).[5] The reaction of $Ter(Me_3Si)NLi$ with $SbCl_3$ in Et_2O at −78 °C afforded (after separation of LiCl) a gray crude product which was purified by sublimation at 165 °C (10^{-3} mbar), yielding 68% of pure **1**.

Starting from **1** the synthesis of the triflate derivative $Ter(Me_3Si)N-Sb(OTf)_2$ was attempted to investigate a

Scheme 5. Synthesis of $Ter(Me_3Si)N-SbCl_2$ (1)

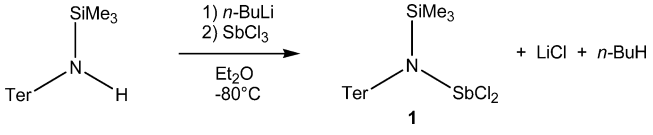

dx.doi.org/10.1021/ic300770b | Inorg. Chem. 2012, 51, 8212−8224

possible Me_3Si–OTf elimination accompanied by dimerization of the *in situ* formed imino-stibane, similar to the reaction described for Mes*$(Me_3Si)N$–$Sb(OTf)_2$ (Scheme 1).[5] However, the reaction of **1** with 2 equiv of AgOTf in CH_2Cl_2 gave the triflate/methyl exchange product, Ter$[Me_2Si(OTf)]N$–Sb(OTf)Me (**2**), in 86% yield (Scheme 6). The analogous

Scheme 6. Attempted Synthesis of Ter$(Me_3Si)N$–$Sb(OTf)_2$ Resulting in the Formation of Different Triflate/Methyl Exchange Products 2 and 3 and in O*t*Bu-Substituted Aminostibane 4

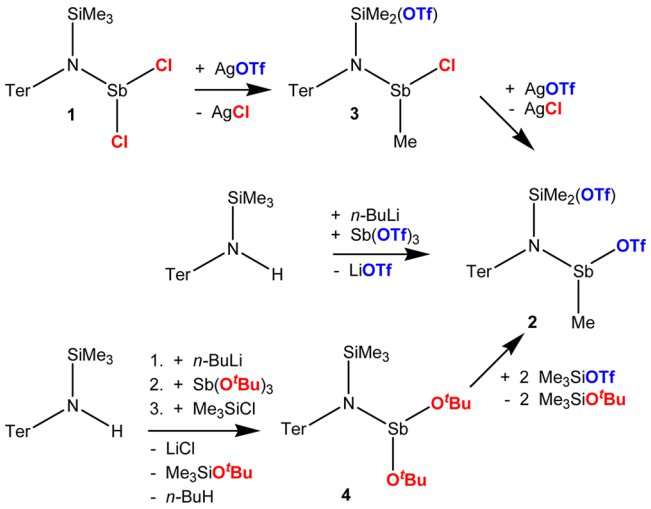

arsenic product was already observed in the reaction of Ter$(Me_3Si)N$–$AsCl_2$ with a 2-fold excess of AgOTf.[9] Presumably, the first reaction step is a triflate/methyl exchange, which was shown by reacting equimolar amounts of AgOTf with **1** in toluene, leading to the isolation of Ter$[Me_2Si(OTf)]N$–Sb(Cl)Me (**3**), in 78% yield (Scheme 6). In the second step the remaining chlorine atom at the antimony atom is substituted by a second triflate group, and **2** is obtained. Unfortunately, **2** is not suitable for thermal elimination of Me_3Si–OTf or $Me_2Si(OTf)_2$.

Since the reaction with AgOTf did not lead to the desired *cyclo*-distibadiazane, the *tert*-butoxy derivative of **1**, Ter$(Me_3Si)N$–$Sb(OtBu)_2$ (**4**), was prepared from Ter(Me_3Si)NLi, $Sb(OtBu)_3$, and Me_3SiCl in Et_2O in an overall yield of 57% (Scheme 6). Surprisingly, also this compound showed no intrinsic thermal elimination of the silylether $Me_3SiOtBu$. By addition of Me_3SiOTf to **4**, a substitution of O*t*Bu against OTf is observed, which again resulted in the formation of **2** (Scheme 6). Compound **2** was also obtained, when Ter(Me_3Si)NLi was reacted with $Sb(OTf)_3$ in an Et_2O solution at −80 °C. Conclusively these results underline the different chemistry observed for supermesityl and terphenyl substituted aminopnictanes. In contrast to the analogous silylated (supermesityl)-aminostibanes that allow substitution of chlorine atoms in Mes*$(Me_3Si)N$–$SbCl_2$ to form Mes*$(Me_3Si)N$–$Sb(OTf)_2$, which can then undergo a thermal elimination of Me_3SiOTf, in the case of the terphenyl system **1** no such direct chlorine/triflate substitution is observed and thus cannot not be applied for terphenyl substituted aminopnictanes to generate the desired terphenyl substituted *cyclo*-distibadiazane. These findings are in good agreement with the observations made for the corresponding arsenic compounds, where addition of AgOTf resulted in a triflate/methyl exchange on the arsenic center as well.

Despite the exchange reactions, we studied the reaction of **1** with $GaCl_3$ in the presence of Me_3SiN_3 (Scheme 7) to determine whether tetrazastibole formation can be observed. Interestingly, after removal of $GaCl_3$ by addition of DMAP (DMAP = 4-(dimethylamino)pyridine), Ter$[Me_2(N_3)Si]N$–Sb(Cl)Me (**5**) was isolated in 32% yield (Scheme 7), which is analogous to the formal azide/methyl exchange reaction observed for Ter$(Me_3Si)N$–$AsCl_2$ under the same reaction conditions. We also synthesized the diazide Ter$(Me_3Si)N$–$Sb(N_3)_2$ (**6a**) starting from **1** and 2 equiv of NaN_3, in 54% yield (Scheme 7). The stoichiometry can be varied, but nevertheless only the formation of **6a** is observed, indicating a favored double over a single substitution. The same result is found when **1** is treated with 1 or 2 equiv of AgN_3. It should be noted that recrystallization of **6a** from CH_2Cl_2 always resulted in a partial Cl/N_3 back-substitution depending on the crystallization time. Thus, it is recommended to use either Cl-free solvents or carry out the crystallization process very quickly. Structural data for such partial chlorine-substituted azide compounds (**6b**–**c**) are found in the Supporting Information.

In contrast to the reaction of **1** with AgOTf no azide/methyl exchange was detected. Moreover, compound **6a** showed no elimination of Me_3Si–N_3 and subsequent dimerization to the desired azido-substituted *cyclo*-distibadiazane, which would be a reasonable starting material for the synthesis of the corresponding tetrazastibole.[7] Following our interest in azidopnictanes and to see whether a chlorine substitution in **5** could give a silicon–antimony azide, **5** was reacted with

Scheme 7. Synthesis of Azido Species 5–7

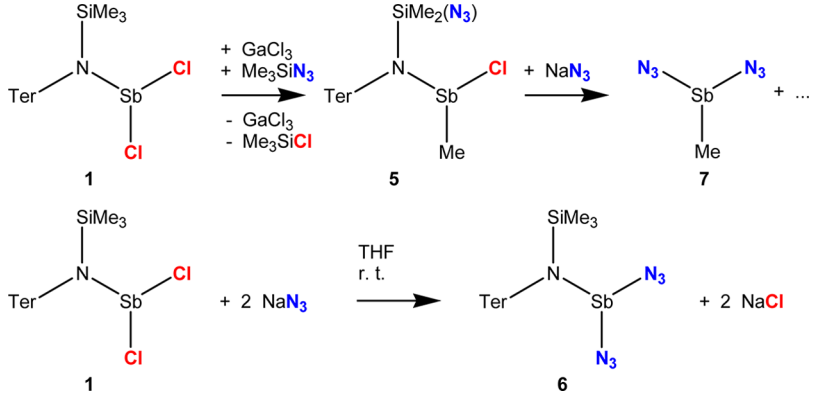

dx.doi.org/10.1021/ic300770b | *Inorg. Chem.* 2012, 51, 8212–8224

Scheme 8. Chlorine/Methyl Exchange Reactions in Silylated Aminostibane 1

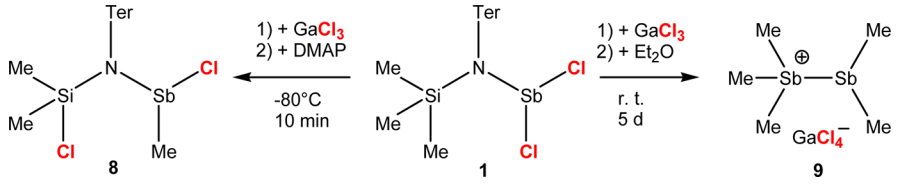

Scheme 9. Reaction of 11 with $GaCl_3$: Formation of Salts Containing Different Reactive Antimony Cations Depending on the Reaction Conditions

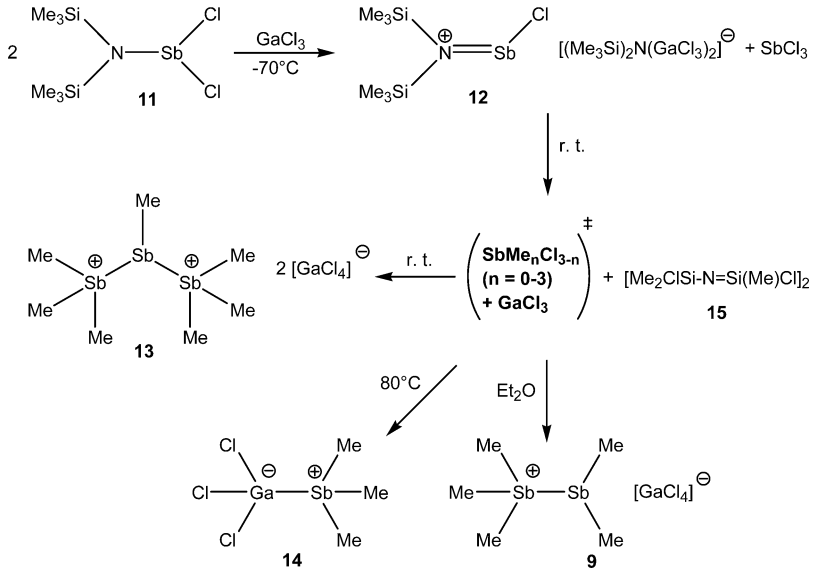

NaN_3. After workup and crystallization from toluene, among other unidentified products, only a few colorless crystals of the hitherto unreported diazido(methyl)stibane, $MeSb(N_3)_2$ (**7**), could be isolated and structurally characterized by X-ray and IR. Hence, it can be assumed that substitution can be achieved, but is immediately followed by a nitrogen antimony bond cleavage which finally results in the formation of **7** (Scheme 7).

In conclusion the reactivity of terphenyl-substituted aminopnictanes is different compared to the analogous supermesityl compounds. Neither the formation of *cyclo*-distibadiazanes nor a tetrazastibole could be observed, while similar reactions have previously been established for the lighter pnictogens phosphorus and arsenic.[5,7] However, interesting triflate- and azide/methyl exchange reactions have been found to be the main reaction in **1** in analogy to the corresponding arsenic compounds.[9] The hitherto unknown compounds **2**, **3**, **4**, **5**, and **6**, along with decomposition product **7**, could be isolated and characterized. These findings encouraged us to gain further insight in the reactivity of **1** in the presence of the Lewis acid $GaCl_3$, and to further investigate a possible extension of the $GaCl_3$ assisted chlorine/methyl exchange previously reported for hydrazinophosphanes and -arsanes, as well as for the analogous $Ter(Me_3Si)N{-}AsCl_2$.[9]

Reactivity of $R(Me_3Si)N{-}SbCl_2$ (R= Ter, Mes*, Me_3Si) toward $GaCl_3$. Different aminostibanes of the type $R(Me_3Si)N{-}SbCl_2$ (R= Ter, Mes*, Me_3Si) have been prepared and studied in the reaction with the Lewis acid $GaCl_3$. In these reactions different methyl exchange reactions were observed, and a series of products resulting from a chlorine/methyl exchange could be isolated.

When $GaCl_3$ was added to a CH_2Cl_2 solution of **1** at −80 °C and then allowed to stir for 10 min at that temperature, the product of a single chlorine/methyl exchange $Ter[Me_2(Cl)Si]N{-}Sb(Me)Cl$ (**8**) could be isolated after removal of $GaCl_3$ by adduct formation after addition of DMAP and extraction of the product with *n*-hexane (Scheme 8, left). It should be noted that, in contrast to the analogous arsenic compound for which a double chlorine/methyl exchange was observed, stirring of **1** in the presence of $GaCl_3$ at ambient temperatures led to a complex mixture of products. After five days of stirring, and addition of Et_2O, colorless crystals of $[Me_3Sb{-}SbMe_2][GaCl_4]$ (**9**) were isolated and structurally characterized (Scheme 8, right). Obviously, further methylation on the antimony center resulted in the formation of $Sb(Me)_2Cl$ and $SbMe_3$. In the presence of the chloride abstracting agent $GaCl_3$, a salt bearing the stibinostibonium cation (**9**) was formed. The stibinostibonium ion in **9** with a $[MeSbBr_3]^-$ counterion was described before by Breunig et al. in an attempt to crystallize Me_2SbBr from its melt at −28 °C.[10]

The formation of a salt containing a stibinostibonium ion prompted us to take a closer look at the analogous reaction of the supermesityl substituted species. In a previous work, the formation of $Mes^*[Me_2(N_3)Si]N{-}SbCl_2$ was reported in the reaction of $Mes^*(Me_3Si)N{-}SbCl_2$ with $GaCl_3$ and an excess of Me_3SiN_3.[7] However, when $Mes^*(Me_3Si)N{-}SbCl_2$ was reacted exclusively with $GaCl_3$ the complex reaction mixture could not be separated and only small amounts of the single chlorine/methyl exchange product $Mes^*[Me_2(Cl)Si]N{-}Sb(Me)Cl$ (**10**) in analogy to **8a** (Scheme 8, left) were obtained as a side product among other unidentified species. This shows that in the case of the supermesityl derivative such exchange reactions

dx.doi.org/10.1021/ic300770b | Inorg. Chem. 2012, 51, 8212−8224

are not favored anymore, contrary to the observations made for terphenyl species **1**.

In a next series of experiments we explored the reactivity of the *N*,*N*-bis(trimethylsilyl)amino species $(Me_3Si)_2N-SbCl_2$ toward Lewis acids. For this reason $(Me_3Si)_2N-SbCl_2$ (**11**) was prepared starting from $SbCl_3$ and $(Me_3Si)_2NLi$ in a salt elimination reaction in toluene at −50 °C. The crude product was purified by distillation *in vacuo* at 65 °C (10^{-3} mbar) affording colorless liquid **11** at ambient temperatures. Addition of $GaCl_3$ to a CH_2Cl_2 solution of **11** at −70 °C and subsequent concentration, followed by storage of the reaction mixture at −80 °C for 24 h, led to the deposition of colorless crystals, which were identified as $[(Me_3Si)_2NSbCl][(Me_3Si)_2N(GaCl_3)_2]$ (**12**) bearing a highly reactive aminostibenium cation (Scheme 9). Aminopnictenium cations have already been proposed as intermediate for chlorine/methyl exchange reaction by Schulz et al.[8,9] Compound **12** can be stored in the freezer under an argon atmosphere, but it decomposes within weeks even at −34 °C. Interestingly, $SbCl_3$ is obviously eliminated in the course of this reaction leading to the generation of the hitherto unknown complex amide anion $[(Me_3Si)_2N(GaCl_3)_2]^-$ stabilized by double $GaCl_3$ adduct formation.

Warming a mixture of **11** and $GaCl_3$ from −70 °C to ambient temperatures followed by concentration led to the formation of a black oily layer besides a reddish supernatant. After removal of the supernatant and addition of toluene to the black residue, crystals of the hitherto unknown salt $[(Me_3Sb)_2SbMe][GaCl_4]_2$ (tetragonal polymorph) (**13**) slowly grew from the oil within one week (Scheme 9). The tetragonal polymorph was studied by X-ray analysis, but the data is not sufficient to allow a detailed discussion. However, from the supernatant a monoclinic polymorph of **13** could be isolated and fully characterized. The supernatant was further concentrated, and 1,3-bis(chlorodimethylsilyl)-2,2,4,4-tetramethyl-chloro-*cyclo*-disilazane (**15**) was also isolated as crystals, which could be characterized by X-ray structure determination. In the crystal structure a partial occupancy of chlorine atoms in place of methyl groups suggests an overall molecular formula that includes about three chlorine atoms.[12] Furthermore, ^1H NMR experiments of the reaction mixture also indicate the presence of several differently substituted methyl/chloro *cyclo*-silazanes. A similar compound was already observed in the reaction of $(Me_3Si)_2N-AsCl_2$ with $GaCl_3$.[9] Such a *cyclo*-disiladiazane was first reported in the condensation reaction of dichloromethylsilane Me_2SiCl_2 with either 2,2,4,4,6,6-hexamethylcyclotrisilazane $[Me_2SiNH]_3$ or 2,2,4,4,6,6,8,8-octamethylcyclotetrasilazane $[Me_2SiNH]_4$.[13] The monoclinic polymorph of **13** was also obtained when freshly prepared **12** was stirred at ambient temperatures for 48 h.

Interestingly, when the reaction conditions were changed with respect to the thermal treatment, different products were observed. For instance, from the reaction mixture of **11** and $GaCl_3$ at 80 °C a $SbMe_3$ adduct of $GaCl_3$, $[Me_3Sb{\cdot}GaCl_3]$ (**14**), was obtained upon concentration. Compound **9** could also be prepared, when Et_2O was added to the black oily layer formed when **11** was reacted with $GaCl_3$, in an isolated yield of 5%. The crystal structure of **9** was unequivocally proven by X-ray analysis, and suitable crystals were obtained from both reaction pathways.

The formation of **12** together with the formation of the *cyclo*-disiladiazane finally proves the idea that the chlorine/methyl exchange in silylated aminostibanes is triggered by chloride abstraction upon addition of a Lewis acid such as $GaCl_3$. As a consequence, intermediate formation of an aminostibenium cation is observed, which in turn is able to abstract one methyl group from the Me_3Si moiety inducing the Cl/Me exchange reaction (Scheme 9). Conclusively, a mixture of **11** and $GaCl_3$ leads to the formation of different methylchlorostibanes of the type $SbMe_nCl_{3-n}$ (n = 0−3), which can be envisioned as a reaction medium for the generation of *catena*-antimony cations, whereas different cations are obtained depending on the temperature, concentration, or solvent.[14]

The catalytic properties of Lewis acids in reactions with Si−C bond cleavage are well described in the literature.[15] For example, in the reaction of $GaCl_3$ and $SiMe_4$, a methyl migration from silicon to gallium was found, for which an intermediate with bridging Cl and Me between Si and Ga was assumed, finally leading to the formation of Me_3SiCl and $(MeGaCl_2)_2$. Another similar reaction was reported by Carmalt et al.: The reaction of $GaCl_3$ with $(Me_3Si)_3N$ yielded, among other products, dimeric $(MeGaCl_2)_2$.[16] In that case, the product $(MeGaCl_2)_2$ is the result of monochloride substitution and transfer of a methyl ligand from the silyl group of the amine to the Ga center. A chlorine/methyl exchange is also assumed in the formation of the $GaCl_3$ diadduct of the six-membered oxadisilathiadiazine heterocycle $O(SiMe_2)(NSN)(SiMe_2)$ as hydrolysis product of the reaction of bis(trimethylsilyl)sulfur diimide and $GaCl_3$.[17] However, in these examples of chlorine/methyl exchange reactions, $GaCl_3$ is part of an intermolecular exchange reaction and stoichiometric amounts are needed, whereas in conversions of $R(Me_3Si)N-SbCl_2$ (R = Ter, Mes*, Me_3Si), the Lewis acid $GaCl_3$ only plays a catalytic role in an intramolecular Me/Cl exchange reaction.

Examples of compounds that exhibit a Pn−Pn′ backbone are rare. Burford et al. established the homoatomic coordination chemistry between neutral and cationic phosphorus centers as a high yielding and versatile synthetic route toward *catena*-phosphorus cations.[18] Only recently this concept has been successfully adapted to interpnictogen *catena*-cations displaying heteroatomic coordination chemistry between phosphorus and arsenic as well as antimony. These interpnictogen frameworks are obtained in a one pot reaction of chlorophosphane or dichlorophosphanes with arsanes (R_3As, R = Me, Et, Ph) and Ph_3Sb in the presence of a chloride ion abstracting agent ($AlCl_3$, $GaCl_3$, $Me_3SiOSO_2CF_3$) and therefore provide access to frameworks containing two, three, or four pnictogen centers. The bonding in these compounds can be viewed as interpnictogen coordination with direct As→P and Sb→P bonding.[14]

Over the past decade only a very small number of *catena*-antimony cations containing only antimony in the backbone have been isolated and fully characterized. Only three classes are known: (i) $[R_3Sb-(SbR)_n-SbR_2]^+$, (ii) $[R_2Sb-(SbR)_n-SbR_2-(SbR)_n-SbR_2]^+$, and one dicationic series (iii) $[R_3Sb-(SbR)_n-SbR_3]^{2+}$ (n = 0, 1, 2, etc.). $[Me_3Sb-SbMe_2]^+$ as $[GaCl_4]^-$ (**9**) and $[MeSbBr_3]^-$[10] salt belong to the $[R_3Sb-(SbR)_n-SbR_2]^+$ series with n = 0, while dication **13** $[R_3Sb-Sb(R)-SbR_3]^{2+}$ (n = 1) represents the next example of the series $[R_3Sb-(SbR)_n-SbR_3]^{2+}$ for which the parent species $[Me_3Sb-SbMe_3]^{2+}$ (n = 0) was isolated as $[SbF_6]^-$ salt from the reaction of Me_3Sb in the super acidic medium HF/SbF_5 by Minkwitz.[19] Furthermore, only the parent species (n = 0) of the monocationic series $[R_2Sb-(SbR)_n-SbR_2-(SbR)_n-SbR_2]^+$ has been reported which was characterized as $[Me_2Sb-SbMe_2-SbMe_2][Me_2SbBr_2]$.[20]

dx.doi.org/10.1021/ic300770b | *Inorg. Chem.* 2012, 51, 8212−8224

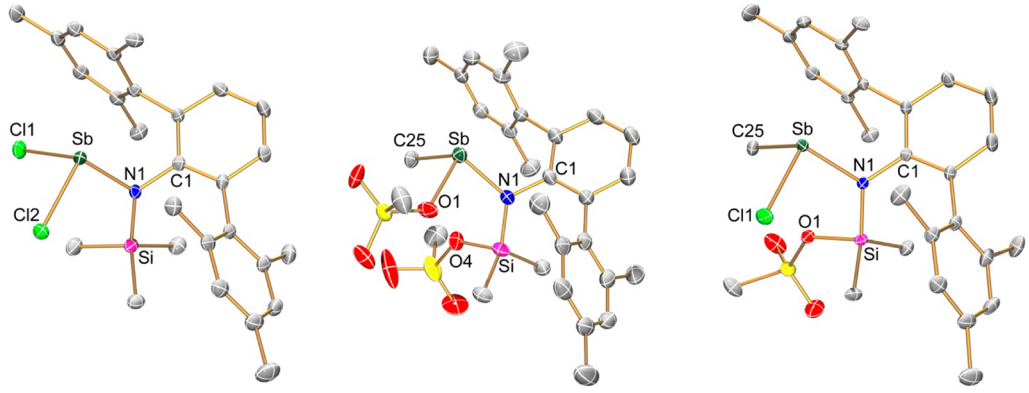

Figure 1. ORTEP drawing[11] **1** (left), **2** (middle), and **3** (right). Thermal ellipsoids with 30% probability at 173 K (hydrogen and fluorine atoms omitted for clarity). Selected bond lengths and angles are given in Table 1.

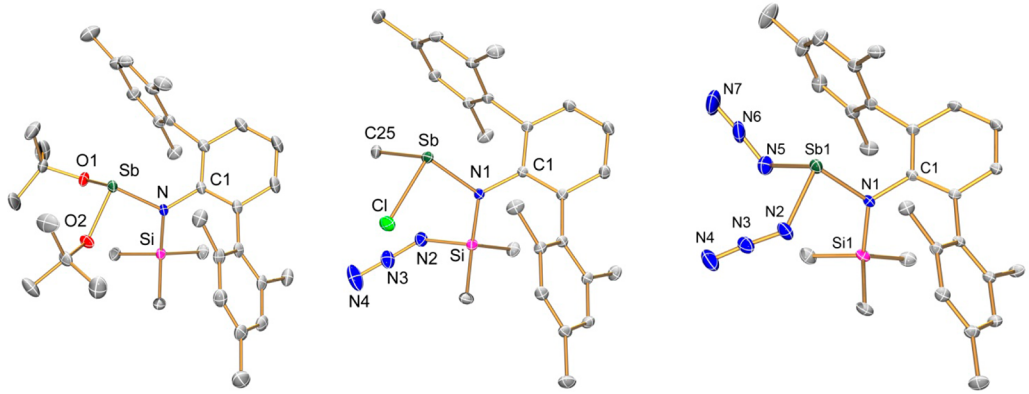

Figure 2. ORTEP drawing[11] of **4** (left), **5** (middle), and **6a** (right). Thermal ellipsoids with 30% probability at 173 K (hydrogen atoms omitted for clarity). Selected bond lengths and angles are given in Table 1.

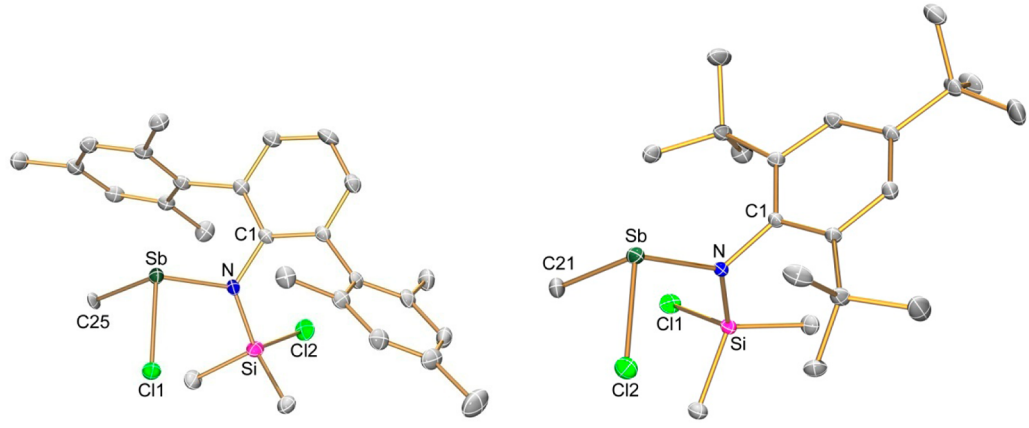

Figure 3. ORTEP drawing[11] of **8a** (left) and **10** (right). Thermal ellipsoids with 30% probability at 173 K (hydrogen atoms omitted for clarity). Selected bond lengths and angles are given in Table 1.

Spectroscopic Characterization. Compounds **2**–**6**, **8**, **11**, and **13** have been characterized by elemental analysis, differential scanning calorimetry (DSC), and vibrational and NMR spectroscopy (^{1}H, ^{13}C, ^{29}Si). For **9** and **12** as well as for adduct **14** only limited analytical data could be collected, because **9** and **14** where obtained in very small amounts and not as pure substances. Compound **12** is thermally labile and very reactive and could therefore not be characterized by Raman and NMR spectroscopy because of fast decomposition.

Terphenyl compounds **1**–**6a** and **8a**,**b** are thermally stable, indicated by high decomposition points ranging from 134 °C for **3** to 217 °C for **2**. Azides **5** and **6a** are neither heat nor shock sensitive, but should be handled with care. In contrast to azides **5** and **6a**, azide **7** detonates, e.g., when acetone is added to a small amount of **7**. $GaCl_3$ adduct **14** decomposes at 130 °C presumably initiated by dissociation of the donor–acceptor bond. Compounds **1**–**6a**, **8**, and **10** are air and moisture sensitive, but can be stored under inert gas conditions for a long period of time at ambient temperatures. They show a good solubility in aromatic solvents like benzene and toluene as well as in polar solvents such as dichloromethane.

dx.doi.org/10.1021/ic300770b | *Inorg. Chem.* 2012, 51, 8212–8224

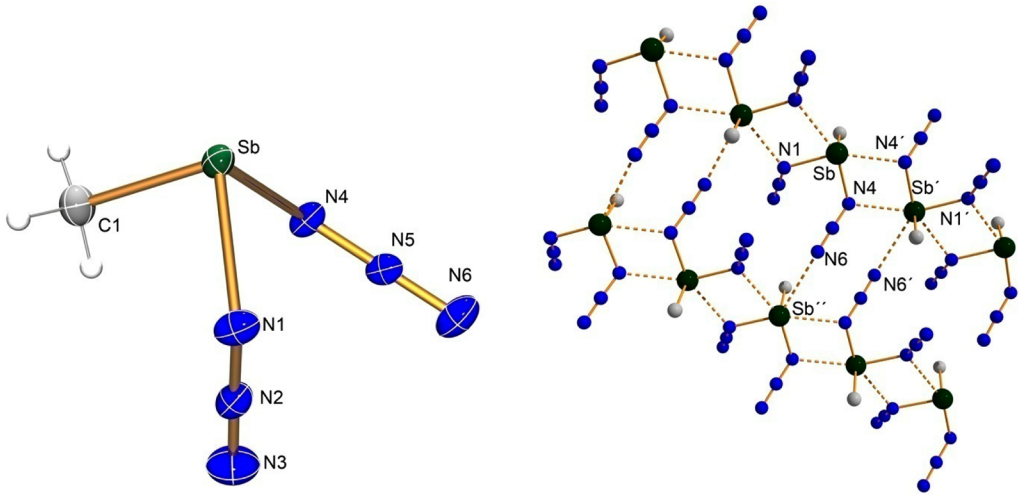

Figure 4. Left: ORTEP drawing[11] of **7**. Thermal ellipsoids with 30% probability at 173 K. Selected bond lengths (Å), and angles (deg): Sb−C1 2.128(3), Sb−N1 2.198(2), Sb−N4 2.183(2), N1−N2 1.223(3), N2−N3 1.140(3), N4−N5 1.238(3), N4−N5 1.136(4), C1−Sb−N1 91.62(11), C1−Sb−N4 91.35(11), N4−Sb−N1 85.84(9), N2−N1−Sb 117.8(2), N5−N4−Sb 118.0(2), N1−N2−N3 177.6(3), N4−N5−N6 177.7(3). Right: intermolecular interactions Sb···N1′ 2.639(2), Sb···N4′ 2.723(2), Sb″···N6 3.16 Å.

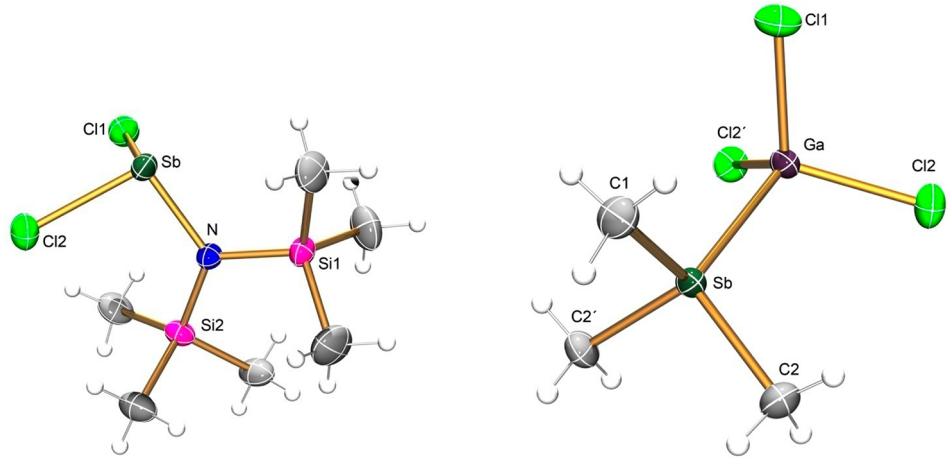

Figure 5. ORTEP drawing[11] of **11** (left) and **14** (right). Thermal ellipsoids with 50% probability at 173 K. Selected bond distances (Å) and angles (deg). **11**: Sb−N1 2.002(2), Sb−Cl1 2.3942(10), Sb−Cl2 2.3822(9), N1−Si1 1.767(3), N1−Si2 1.776(3), Cl1−Sb−N1 99.37(8), Cl2−Sb−N1 98.40(7), Cl1−Sb−Cl2 95.22(3), Si1−N1−Sb1 113.59(13), Si2−N1−Sb1 124.91(14), Si1−N1−Si2 121.37(14). **14**: Sb1−Ga1 2.6119(4), Ga(1)−Cl(1) 2.1649(8), Ga(1)−Cl(2i) 2.1791(7), Ga(1)−Cl(2) 2.1791(7), Sb(1)−C(2) 2.104(3), Sb(1)−C(2i) 2.104(3), Sb(1)−C(1) 2.111(3), C(1)−Sb(1)−Ga(1) 114.2(1), C−Sb1−C 103.7(2), 105.2(1), Cl(1)−Ga(1)−Sb(1) 111.44(3), Cl(1)−Ga(1)−Cl(2i) 110.38 (2), 108.26 (4), C1−Sb1−Ga1−Cl1 0.0.

For the chemical shifts in the ^{1}H NMR data only small differences are detected for the proton signals in the terphenyl-moieties (cf. ^{1}H NMR data for *p*-CH_3(Mes), $\delta(^{1}H)$ = 1.99−2.09; *o*-CH_3(Mes), $\delta(^{1}H)$ = 2.23 - 2.36; $C_{Aryl}H$, $\delta(^{1}H)$ = 6.80−7.27). To assign the chemical shifts in the ^{1}H NMR spectra for the protons in the methyl groups attached to the antimony atom in exchange products **2**, **3**, **5**, and **8**, COSY ($^{1}H^{13}C$) experiments were carried out. The chemical shifts of these protons lie between 0.7 and 0.8 ppm in the ^{1}H NMR spectra depending on the second substituent on the antimony center. It is interesting to note that in the exchange products **2**, **3**, and **5** all carbon atoms are chemically and magnetically non-equivalent, and therefore, 24 (**5**), 27 (**8**), 28 (**3**), and 29 (**2**) different signals are found in the ^{13}C NMR spectra.

The IR spectra of azide species **5**−**7** feature the presence of a covalently bound azido group as shown by the asymmetrical stretching mode in the range 2050−2150 cm^{-1} (**5**, $\nu_{as}(N_3)$ = 2134; **6**, 2092/2078; **7**, 2067 cm^{-1}). The splitting of this mode in **6a** into two components indicates the presence of more than one azido group, displaying an in-phase and out-of-phase coupled mode. This splitting was not observed for diazide **7** since only a broad vibrational band is observed.

Compound **13** was fully characterized in the course of this study. In the ^{1}H NMR and ^{13}C NMR spectra two different signals for the protons and carbon atoms of the stibino- and stibonium-methyl groups are detected at 2.00 ppm and 1.57 ppm, respectively, which is in good agreement for the values detected for $MeSbCl_2$ (^{1}H ($CDCl_3$) 1.90 ppm).[21]

Structural Characterization. The structures of all considered amino-stibanes (species **1**-**6**, **8**, **10**); stibanes **7**, **11**, and **14**; and the salts bearing Sb cations (**9**, **12**, and **13**) have been determined. Tables S1−S5 (see Supporting Information) present the X-ray crystallographic data. Molecular structures are shown in Figures 1−7. Table 1 summarizes selected structural parameters of the aminostibanes while for all other species selected structural data are listed along with the

dx.doi.org/10.1021/ic300770b | *Inorg. Chem.* 2012, 51, 8212−8224

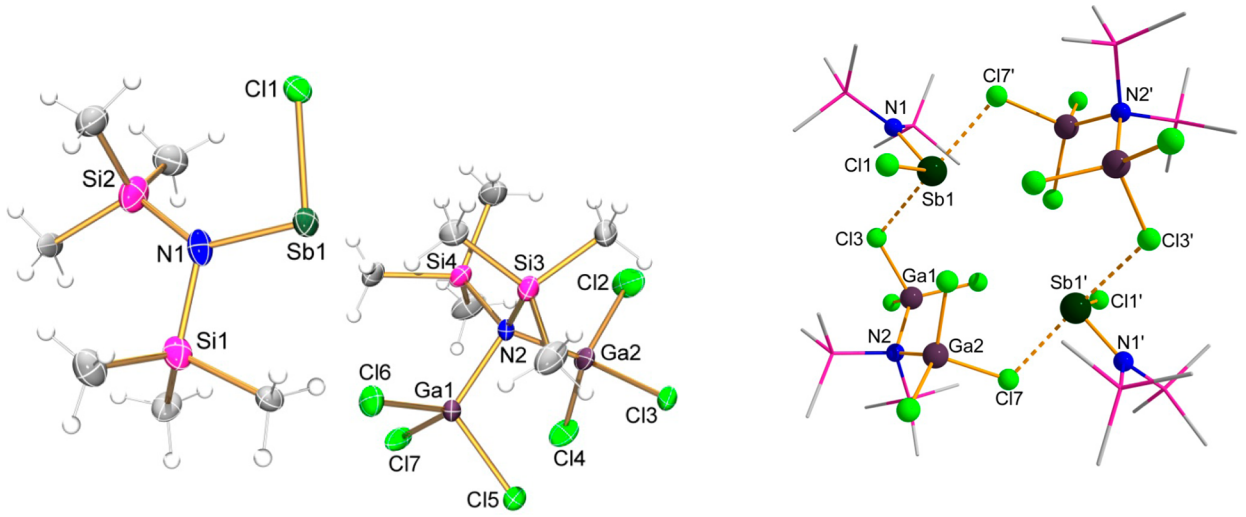

Figure 6. Left: ORTEP drawing[11] of **12**. Thermal ellipsoids with 30% probability at 173 K. Right: Ball and stick drawing of intermolecular interactions in **12**. Selected bond lengths (Å) and angles (deg): Sb−N1 1.953(5), Sb−Cl1 2.351(9), N1−Si1 1.868(7), N1−Si2 1.715(7), N2−Ga1 1.989(5), N2−Ga2 1.979(5); Cl1−Sb−N1 94.6(2), Si1−N1−Sb1 109.7(3), Si2−N1−Sb1 132.3(4), Si1−N1−Si2 118.0(3), Ga1−N2−Ga2 106.7(2); Sb1···Cl3 2.875(2), Sb1···Cl5 3.418(3), Sb1···Cl5′ 3.667(3), Sb1···Cl7′ 2.826(2).

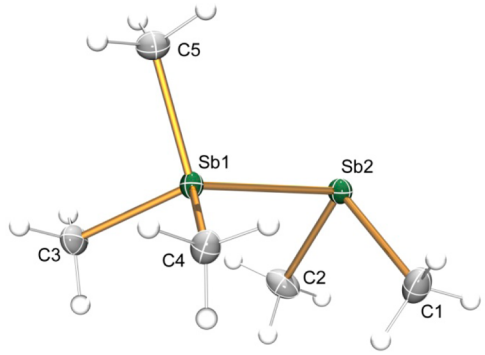

Figure 7. ORTEP drawing[11] of the stibinostibonium cation in **9** ($GaCl_4^-$ anion omitted for clarity). Thermal ellipsoids with 30% probability at 173 K. Selected bond distances (Å) and angles (deg) for **9**: Sb1−C5 2.111(4), Sb1−C3 2.113(4), Sb1−C4 2.114(3), Sb1−Sb2 2.8273(3), Sb2−C2 2.149(4), Sb2−C1 2.151(4).

figures of the molecular structure (Figures 4−7). More details are found in the Supporting Information.

In the solid state structure of compounds bearing bulky terphenyl moieties, the crystal lattice often exhibits large cavities that are accessible by solvent molecules. For example **8** could be crystallized from *n*-hexane, diethylether, benzene (**8b**), and toluene (**8a**) resulting always in solvent containing crystals. It is interesting to note that all solvate structures crystallize isotypically with exception of the different solvent molecules in the cavities. These solvent molecules are highly disordered on their positions in the crystal. The best structure could be determined for the toluene or benzene solvate. To illustrate the crystallographic problem of disordered solvent molecules in cavities of **1** and **8**, the structure refinement was carried out in two different ways: (i) refinement of solvent molecules with an appropriate disorder model (benzene, toluene) or (ii) treatment of solvent molecules as diffuse contribution to the structural factor (benzene, toluene, dichloromethane, diethyl

Table 1. Selected Bond Lengths (Å) and Bond and Torsion Angles (deg) of All Considered Aminostibanes[a]

	1[b]	2	3	4	5	6a	8a[b]	10
Sb1−N1	2.033(3)	2.023(3)	2.104(2)	2.033(1)	2.068(1)	2.013(2)	2.065(3)	2.059(2)
Sb1−X1	2.362(2)	2.179(6)	2.400(2)	1.964(1)	2.4103(4)	2.095(2)	2.4079(7)	2.3983(4)
Sb1−X2	2.396(2)	2.111(5)	2.135(3)	1.952(1)	2.181(2)	2.101(2)	2.159(5)	2.152(2)
N1−Si1	1.783(4)	1.761(7)	1.722(2)	1.770(1)	1.739(2)	1.782(2)	1.741(3)	1.732(2)
C1−N1	1.451(5)	1.441(5)	1.436(3)	1.434(2)	1.441(2)	1.445(3)	1.438(4)	1.470(2)
Si1−X3		1.733(7)	1.749(2)		1.776(1)		2.056(2)	2.110(7)
N1−Sb1−X1	106.05(1)	87.6(4)	96.42(5)	93.67(5)	97.03(3)	92.59(8)	105.5(3)	102.47(4)
N1−Sb1−X2	96.72(1)	107.6(2)	103.03(9)	94.18(5)	104.22(5)	101.80(9)	96.36(8)	101.58(6)
X1−Sb1−X2	90.34(5)	90.6(4)	93.38(8)	93.30(6)	91.63(4)	89.5(1)	90.0(2)	89.89(5)
C1−N1−Sb1	110.4(2)	111.2(2)	111.5(2)	114.91(9)	112.43(8)	112.4(1)	111.6(2)	114.84(9)
C1−N1−Si1	123.5(3)	121.0(3)	123.1(2)	123.30(9)	122.36(9)	122.5(2)	124.1(2)	119.0(1)
Sb1−N1−Si1	126.1(2)	127.5(2)	125.4(1)	121.78(6)	125.21(6)	125.1(1)	124.2(1)	126.04(7)
∑∠(N1)	360.0	359.7	360.0	360.0	360.0	360.0	359.9	359.9
C2−C1−N1−Sb1	123.0(4)	−129.5(3)	−124.9(2)	57.8(2)	54.5(2)	122.4(2)	124.6	−88.8

[a]X2 represents a carbon atom of a methyl group at antimony, and X3-, Cl-, O-, or N-atom of OTf/N_3-groups attached to the silicon atom. [b]Only one data set of the four independent molecules is listed; however, all structural parameters are within the 3σ range.

dx.doi.org/10.1021/ic300770b | *Inorg. Chem.* 2012, 51, 8212−8224

ether, n-hexane) using Platon/SQUEEZE. The latter data are listed in the Supporting Information.

The compounds **1**−**6**, **8**, and **10** show only weak intermolecular van der Waals interactions which lead to nearly isolated molecules in **1**, **4**, **5**, **8**, and **10**. However, for **2** and **6**, oxygen or nitrogen bridged dimers can be considered. An oxygen bridged chainlike structure is found for **3**. The Sb···X (X = N, O) distances vary between 3.35 and 3.96 Å indicating weak interactions (see Figures S1−S2 in the Supporting Information) comparing these distances with the sum of the van der Waals radii (Σr_{vdw}(Sb···N) = 3.8 and Σr_{vdw}(Sb···O) = 3.7 Å).

In all compounds the trivalent antimony center sits in a trigonal pyramidal environment with bond angles between 88° and 108°. Differences from the ideal pyramidal environment can be attributed to sterical effects from different substituents at the antimony atom. The amino nitrogen atom is nearly planar coordinated in all compounds, as indicated by the sum of the angles around nitrogen (Table 1). The Sb−N−Si moiety sits in a pocket formed by the bulky terphenyl group. To fit in this pocket the Si−N−Sb moiety is always twisted with respect to the central phenyl ring of the terphenyl ligand, exhibiting a torsion angle between 50° and 60°. Supermesityl species **10** shows the typical torsion angle near 90°.[5]

The Sb−N_{amino} bond lengths vary between 2.017(2) and 2.033(3) Å which are in the typical range found for Sb−N single bonds, for example d(Sb−N_{amino}) = 2.056(3) in Mes*N(SiMe$_3$)−SbCl$_2$,[5] d(Sb−N_{amino}) = 2.092(2) and d(Sb−N_{azide}) = 2.104(2) in [tBuC(iPrN)$_2$]Sb(N$_3$)$_2$,[22] and d(Sb−N_{azide}) = 2.119(4) Å in Sb(N$_3$)$_3$[23] (cf. Σr_{cov}(Sb−N) = 2.11 Å).[24] The two Sb−N_{azide} bonds in **6a** (2.125(2)/2.166(2) Å) are slightly elongated compared to the Sb−N_{amino} bonds in accord with those found for [tBuC(iPrN)$_2$]Sb(N$_3$)$_2$ and Sb(N$_3$)$_3$ (vide supra).[22,23] The azide group in **5** is covalently bound to the silicon center with a Si−N_{azide} bond length of 1.776(2) Å (cf. Σr_{cov}(Si−N) = 1.87 Å) in good agreement with the analogous arsenic compound (d(Si−N_{azide}) = 1.780(1) Å).[9,24] The Sb−Cl distances in **1** (2.362(2)/2.396(2) Å) and in **3**, **5**, **8**, and **10** (ca. 2.40 Å) are nearly identical and can be regarded as typical single bonds (cf. Σr_{cov}(Sb−Cl) = 2.39 Å).[24] The Sb−C distances are in the range 2.181(2)−2.135(3) Å) (cf. Σr_{cov}(Sb−C) = 2.15 Å).[24]

For both azide species **5** and **6a** the typical *trans*-bent structure with NNN angles of about 173−176° is observed.[25] The N_α−N_β (**5**, 1.217(2); **6a**, 1.221(3)/1.225(4) Å) and also the N_β−N_γ bond lengths (**5**, 1.130(2); **6a**, 1.126(3) /1.125(4) Å) are in the expected range of covalently bound azides.

Diazidomethylstibane **7** crystallizes in the triclinic space group $P\bar{1}$ with one molecule in the asymmetric unit. The Sb−N_{azide} distances of 2.183(2) and 2.198(2) Å are slightly elongated and in good agreement with previously reported antimony azides (cf. d(Sb−N_{azide}) = 2.125(2)/2.166(2) Å in **6**),[26,27] whereas the Sb−C distance of 2.128(3) Å is shorter than the sum of the covalent radii (cf. Σr_{cov}(Sb−C) = 2.15 Å).[24] Both azide groups are slightly *trans* bent with NNN-angles of 177.6°. In the crystal, significant intermolecular interactions are observed, as the antimony atoms are linked by the N_α atom of the azide groups, resulting in the formation of infinite zigzag chains of centrosymmetric dimers (Figure 4, right). The Sb−Sb′−Sb″angle amounts to 160°, so that the zigzag chain motif is not as obvious as in Sb(N$_3$)$_2$Cl.[26] The chain in **7** is formed due to interactions between discrete molecules with Sb···N_α distances of 2.639 and 2.723 Å. Between these chains loose interactions via the N_γ atom from an azide group of one chain and an antimony center of a neighboring chain (Sb···N_γ = 3.16 Å) are observed. This structural motif has often been observed in azidopnictanes.[27a] The overall coordination environment around antimony can be described as 3 + 3 coordination leading to a distorted pentagonal pyramide.

Compound **11** crystallizes in the trigonal space group $P3_2$ with nine molecules in the unit cell. The molecular structure is depicted Figure 5 (left). Hyperconjugative effects between σ* orbitals of the Sb−Cl bond and the p-type lone pair at the nitrogen atom can be discussed, resulting in a shortened Sb−N distance of 2.002(2) Å (cf. Σr_{cov}(Sb−N) = 2.11 Å).[28] The Sb−Cl distances are in the typical range (Sb−Cl 2.3942(10)/2.3822(9) Å) of a single bond (cf. Σr_{cov}(Sb−Cl) = 2.39 Å). The shortest distances between the antimony center and chlorine atoms of a neighboring molecule are in the range of 3.7 Å, which can be regarded as loose electrostatic interactions, resulting in nearly isolated molecules.

Furthermore, a GaCl$_3$ adduct of SbMe$_3$ (**14**) was structurally characterized (Figure 5, right), which crystallizes in the orthorhombic space group *Pnma* with four molecules in the unit cell. Compound **14** lies on a mirror plane, and the Sb−Ga bond in this adduct can be regarded as a dative bond between the donor SbMe$_3$ and the acceptor acid GaCl$_3$ with a Sb−Ga distance of 2.6119(4) Å (cf. Σr_{cov}(Sb−Ga) = 2.64 Å, cf. Sb−Ga 2.662(2)/2.659(2) Å in [Cl$_2$GaSb(tBu)$_2$]$_3$).[24,29] Molecule **14** shows an eclipsed conformation with Sb−C bonds in the range 2.104(3)-2.111(3) Å. A similar situation is found for the GaCl$_3$ unit with two slightly different bonds (2.1791(7) Å and 2.1649(8) Å).

Upon addition of GaCl$_3$ to **11** at low temperatures a salt bearing an aminostibenium cation is formed. Compound **12** crystallizes in the triclinic space group $P\bar{1}$ with one formula unit in the asymmetric unit. The whole amino(chloro)stibenium cation is disordered with the main part being populated by 51.2%. The Sb−N distances in the cation differ slightly in the two parts and are rather short with 1.953(5)/1.990(5) Å (Figure 6, cf. Σr_{cov}(Sb—N) = 2.11, Σr_{cov}(Sb═N) = 1.93 Å; Sb—N 1.966(1) Å in Mes*(Me$_3$Si)N—Sb(OTf)$_2$, 1.958(4) Å in (2-MeC$_6$H$_4$)$_3$Sb═NSO$_2$CF$_3$)[5,24,30] indicating partial SbN double bond character. Also, the Sb—Cl1 distance of 2.351(9) Å is relatively short compared to that of **11**.

The Ga−N distances of 1.978(5) and 1.989(5) Å in the anion are in the range of an elongated single bond (cf. Σr_{cov}(Ga−N) = 1.95 Å),[24] which supports the idea that the anion is a GaCl$_3$ adduct of a *N*,*N*-bis(trimethylsilyl)amide, with a tetrahedrally coordinated nitrogen center. In the solid state two close contacts between chlorine atoms Cl3 and Cl7 of the GaCl$_3$ moieties in the anion and the dicoordinated antimony are found (2.875(2) and 2.826(2) Å). In addition, two larger distances to Cl5 (3.418(3)/3.667(3) Å) are observed. The main structural motif might be regarded as a centrosymmetric dimeric ion pair with two strongly distorted octahedral coordinated antimony centers as depicted in Figure 6 (left). There are also two CH$_2$Cl$_2$ molecules in the asymmetric unit; one of them is found to be disordered.

catena-Sb cation-containing salts **9** and **13** crystallize in the monoclinic space groups $P2_1/c$ (**9**; Figure 7) and $P2_1$ (**13**; Figure 8) with four (**9**, **13**) formula units in the unit cell. For **13** an additional CH$_2$Cl$_2$ solvent molecule is present in the asymmetric unit. The Sb−Sb bonds found in the antimony backbone of both cations are nearly equidistant with 2.8273(3) in **9** and 2.811(1)/2.830(1) Å in **13** displaying a typical single

dx.doi.org/10.1021/ic300770b | Inorg. Chem. 2012, 51, 8212−8224

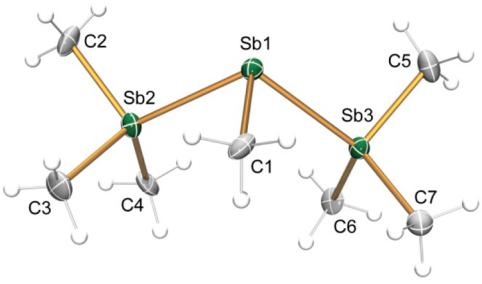

Figure 8. ORTEP drawing[11] of the cation in **13** ($GaCl_4^-$ anion omitted for clarity). Thermal ellipsoids with 30% probability at 173 K. Selected bond distances (Å) and angles (deg) for **13**: Sb1−Sb2 2.811(1); Sb1−Sb3 2.830(1); Sb1−C1 2.20(1); Sb2−C 2.05(1), 2.10(1), 2.10(1); Sb3−C 2.11(1), 2.09(1), 2.11(1); Sb2−Sb1−Sb3 100.83; C−Sb2−C 103.7(2).

bond (cf. Σr_{cov}(Sb−Sb) = 2.80 Å).[24] These Sb−Sb distances are in good agreement with those reported in $[Me_2Sb{-}SbMe_2{-}SbMe_2]^+$ (2.8203(4) Å), but are slightly shorter compared to those reported for tetramethyldistibane (Me_4Sb_2, 2.862(2) Å)[31a] and tetraphenyldistibane (Ph_4Sb_2, 2.867(1) Å).[31b] The Sb−C single bonds of the tetracoordinated (stibonium) and the tricoordinated Sb atoms (stibino centers) are observed in the expected range (2.08−2.16 Å, cf. Σr_{cov}(Sb−C) = 2.15 Å).[28] Only weak cation−anion interactions are found for **9**. For instance, four van der Waals interactions are observed for the dicoordinated Sb2 atom (Sb2···Cl distances of 3.3−3.9 Å), and three interactions for the tricoordinated antimony atoms Sb1 (3.4−3.7 Å) are observed leading to a slightly distorted $GaCl_4^-$ anion.

CONCLUSION

In summary, we report here on the successful extension of the Lewis acid assisted methyl exchange reactions to silylated aminostibanes. The methyl/chlorine exchange in the reaction of $(Me_3Si)_2N{-}SbCl_2$ **11** and $GaCl_3$ can be regarded as a valuable application of this concept for the generation of different *catena*-antimony cations, depending on the variation of either temperature or solvent.

Silylated aminostibanes of the type $Ter(Me_3Si)N{-}SbCl_2$ have been studied in the reaction with AgOTf, AgN_3, KO*t*Bu, $GaCl_3$, and $Me_3SiN_3/GaCl_3$ displaying triflate/methyl, azide/methyl, and chlorine/methyl exchange reactions. The intermediate aminopnictenium cation (**12**) could be isolated at −60 °C when $(Me_3Si)_2N{-}SbCl_2$ (**11**) was reacted with $GaCl_3$ at low temperatures. The reaction of **11** and $GaCl_3$ at ambient temperatures led to different stibinostibonium cations as tetrachloridogallates in $[(Me_3Sb)SbMe][GaCl_4]$ and $[(Me_3Sb)_2SbMe][GaCl_4]_2$ along with the $GaCl_3$ adduct of $SbMe_3$. The cations in these salts can be regarded as *catena*-antimony cations.

EXPERIMENTAL SECTION

General Information. All manipulations were carried out under oxygen- and moisture-free conditions using standard Schlenk and drybox techniques.

NMR. $^{13}C\{^1H\}$, ^{13}C DEPT, ^1H, $^{19}F\{^1H\}$, and ^{29}Si INEPT NMR spectra were obtained on a Bruker AVANCE 300 spectrometer and were referenced internally to the deuterated solvent (^{13}C, CD_2Cl_2, $\delta_{reference}$ = 54 ppm; C_6D_6, $\delta_{reference}$ = 128 ppm) or to protic impurities in the deuterated solvent (^1H, $CDHCl_2$, $\delta_{reference}$ = 5.31 ppm; C_6D_6, $\delta_{reference}$ = 7.16 ppm). CD_2Cl_2 was dried over P_4O_{10}; C_6D_6 was dried over Na/benzophenone.

IR. Nicolet 380 FT-IR with a Smart Orbit ATR device was used.

Raman. Bruker VERTEX 70 FT-IR with RAM II FT-Raman module, equipped with a Nd:YAG laser (1064 nm), was used.

CHN analyses. Analysator Flash EA 1112 from Thermo Quest, or C/H/N/S-Mikronalysator TruSpec-932 from Leco, was used.

Melting points are uncorrected (EZ-Melt, Stanford Research Systems), with heating rate 20 °C/min (clearing points are reported).

MS. Finnigan MAT 95-XP from Thermo Electron was used.

X-ray Structure Determination. X-ray quality crystals of **1**−**14** were selected in Fomblin YR-1800 perfluoroether (Alfa Aesar) (Riedel deHaen) at ambient temperatures. All samples were cooled to 173(2) K during measurement. The data were collected on a Bruker-Nonius Apex X8 and Bruker Apex Kappa-II CCD diffractometer using graphite-monochromated Mo Kα radiation (λ = 0.710 73). The structures were solved by direct methods (*SHELXS-97*)[32] and refined by full-matrix least-squares procedures (*SHELXL- 97*).[33] Semi-empirical absorption corrections were applied (SADABS).[34] All non-hydrogen atoms were refined anisotropically, and hydrogen atoms were included in the refinement at calculated positions using a riding model.

Ter(Me$_3$Si)N−SbCl$_2$ (1). To a stirred solution of *N*-(2,6-bis(2,4,6-trimethylphenyl)-phenyl)-*N*-(trimethylsilyl)-amine $TerN(H)SiMe_3$ (2.415 g, 6 mmol) in Et_2O (20 mL) is added 2.5 M *n*-butyl-lithium-solution in *n*-hexane (2.5 mL, 6.25 mmol) over a period of 10 min at ambient temperature. The resulting pale yellow solution is stirred for 1 h and then added dropwise to a solution of $SbCl_3$ (1.37 g, 6 mmol) in Et_2O (10 mL) at −80 °C. The resulting colorless suspension is allowed to warm up to RT over a period of 1 h and stirred for 30 min. The solvent is removed, and the colorless solid is dried for 2 h in vacuum. Then the residue is extracted with 30 mL benzene and filtered. The solvent is removed in vacuum, and the resulting gray solid is sublimed at 160 °C and 1 × 10^{-3} mbar, yielding 2.44 g (4.1 mmol, 68%) of $TerN(SiMe_3)SbCl_2$ (**1**) as a colorless crystalline solid. Mp = 202 °C (dec). Anal. Calcd % (Found): C 54.66 (54.62); H 5.78 (6.08); N 2.36 (2.33). ^1H NMR (25 °C, CD_2Cl_2, 300.13 MHz): −0.14 (s, 9H, $Si(CH_3)_3$), 2.09 (s, 6H, CH_3), 2.23 (s, 6H, CH_3), 2.32 (s, 6H, CH_3), 6.90−7.19 (m, 7H, C*H*). $^{13}C\{^1H\}$ NMR (25 °C, CD_2Cl_2, 75.475 MHz): 4.78 (s, 3C, $Si(CH_3)_3$), 21.33 (s, 2C, CH_3), 22.25 (s, 2C, CH_3), 22.63 (s, 2C, CH_3), 124.10 (s, 1C, CH), 129.62 (s, 2C, CH), 130.43 (s, 2C, CH), 133.12 (s, 2C, CH), 136.23 (Ar-*C*), 138.51 (Ar-*C*), 138.57 (Ar-*C*), 138.83 (Ar-*C*), 139.54 (Ar-*C*), 146.44 (Ar-*C*). ^{29}Si INEPT NMR (25 °C, CD_2Cl_2, 49.696 MHz): 16.7 ($Si(CH_3)_3$).[35]

Ter[Me$_2$(OTf)Si]N−SbMe(OTf) (2). To a stirred suspension of AgOTf (0.514 g, 2 mmol) in CH_2Cl_2 (10 mL) is added a solution of **1** (0.594 g, 1 mmol) in CH_2Cl_2 (5 mL) quickly at −80 °C. The resulting gray suspension is allowed to warm up to ambient temperature over 30 min and filtered (F4). The solution is concentrated to about 5 mL and stored at −25 °C for several hours which results in deposition of colorless crystals. The supernatant is transferred by syringe, the solvent is removed *in vacuo*, and the colorless residue is recrystallized from *n*-hexane. Drying the combined fractions yields 0.710 g (0.86 mmol, 86%) of **2** as a colorless crystalline solid. Mp = 217 °C (dec). Anal. Calcd % (Found): C 42.45 (43.13); H 4.47 (4.76); N 1.71 (1.63). ^1H NMR (25 °C, CD_2Cl_2, 300.13 MHz): −0.35 (s, 3H, Si−CH_3), 0.34 (s, 3H, Si−CH_3), 0.78 (s, 3H, Sb−CH_3), 2.09 (s, 3H, CH_3), 2.13 (s, 3H, CH_3), 2.23 (s, 3H, CH_3), 2.28 (s, 3H, CH_3), 2.33 (s, 3H, CH_3), 2. 36 (s, 3H, CH_3), 6.95−7.27 (7H, C*H*). $^{13}C\{^1H\}$ NMR (25 °C, CD_2Cl_2, 75.48 MHz): 2.01 (s, Si-CH_3), 2.36 (s, Si-CH_3), 21.22 (s, CH_3), 21.45 (s, CH_3), 21.68 (s, CH_3), 22.01 (s, CH_3), 22.45 (s, CH_3), 23.02 (s, CH_3), 26.13 (s, Sb-CH_3), 118.85 (q, $^1J(^{13}C^{19}F)$ = 318.0 Hz, CF_3), 118.97 (q, $^1J(^{13}C^{19}F)$ = 317.5 Hz, CF_3), 124.91 (CH), 129.63 (CH), 129.98 (CH), 130.69 (CH), 130.89 (CH), 131.57 (CH), 133.80 (CH), 135.39 (Ar-*C*), 136.84 (Ar-*C*), 137.76 (Ar-*C*), 138.21 (Ar-*C*), 138.27 (Ar-*C*), 138.34 (Ar-*C*), 139.21 (Ar-*C*), 142.84 (Ar-*C*), 143.26 (Ar-*C*), 143.35 (Ar-*C*), 146.04 (Ar-*C*). ^{19}F NMR (25 °C, CD_2Cl_2, 282.38 MHz): −76.94 (s, 3F, CF_3), −78.02 (s, 3F, CF_3). ^{29}Si INEPT NMR (25 °C, CD_2Cl_2, 49.70 MHz): 19.90 ($Si(CH_3)_2OTf$).[35]

Ter[Me$_2$(OTf)Si]N−Sb(Cl)Me (3). To a stirred solution of **1** (0.594 g, 1 mmol) in toluene (10 mL), a solution of AgOTf (0.257 g, 1 mmol) in toluene (5 mL) is added dropwise at −75 °C. The resulting

dx.doi.org/10.1021/ic300770b | *Inorg. Chem.* 2012, 51, 8212−8224

gray suspension is allowed to warm up to ambient temperature over 30 min and filtered (F4). The solvent is removed *in vacuo*, and the colorless residue is recystallized from *n*-hexane which yields 0.556 g (0.78 mmol, 78%) of **3** as a colorless crystalline solid. Mp = 134 °C (dec). Anal. Calcd % (Found): C 47.57 (47.95); H 4.85 (4.76); N 1.98 (1.75). ^{1}H NMR (25 °C, CD_2Cl_2, 300.13 MHz): −0.25 (s, 3H, Si−CH_3), 0.27 (s, 3H, Si−CH_3), 0.72 (s, 3H, Sb−CH_3), 2.08 (s, 3H, CH_3), 2.15 (s, 3H, CH_3), 2.17 (s, 3H, CH_3), 2.25 (s, 3H, CH_3), 2.31 (s, 3H, CH_3), 2.34 (s, 3H, CH_3), 6.92−7.22 (7H, C*H*). ^{13}C{^{1}H} NMR (25 °C, CD_2Cl_2, 75.48 MHz): 2.83 (s, Si-CH_3), 3.96 (s, Si-CH_3), 21.19 (s, CH_3), 21.34 (s, CH_3), 21.58 (s, CH_3), 22.03 (s, CH_3), 22.27 (s, Sb-CH_3), 22.53 (s, CH_3), 23.10 (s, CH_3), 118.90 (q, $^{1}J(^{13}C^{19}F)$ = 318 Hz, CF_3), 124.35 (CH), 129.45 (CH), 129.74 (CH), 129.96 (CH), 130.04 (CH), 132.15 (CH), 133.12 (CH), 135.56 (Ar-C), 136.09 (Ar-C), 137.78 (Ar-C), 138.47 (Ar-C), 138.49 (Ar-C), 138.56 (Ar-C), 138.70 (Ar-C), 140.38 (Ar-C), 140.71 (Ar-C), 140.80 (Ar-C), 146.82 (Ar-C). ^{19}F NMR (25 °C, CD_2Cl_2, 282.38 MHz): −76.95 (s, 3F, CF_3). ^{29}Si INEPT NMR (25 °C, CD_2Cl_2, 49.70 MHz): 18.83 ($Si(CH_3)_2OTf$).[35]

Ter(Me$_3$Si)N−Sb(O*t*Bu)$_2$ (4). To a stirred solution of TerN(H)-$SiMe_3$ (1.208 g, 3 mmol) in Et_2O (20 mL) is added 2.5 M *n*-butyllithium in *n*-hexane (1.2 mL, 3 mmol) over a period of 10 min at ambient temperatures. The resulting pale yellow solution is stirred for 1 h and then added dropwise to a solution of $Sb(OtBu)_3$ (1.023 g, 3 mmol) in Et_2O (10 mL) at −80 °C. The resulting colorless solution is allowed to warm up to ambient temperatures over a period of 1 h and stirred for 30 min. A solution of Me_3SiCl (0.109 g, 1 mmol) in Et_2O (3 mL) is added dropwise at 0 °C resulting in a colorless suspension which is stirred for 1 h. The solvent is removed, and the colorless solid is dried for 2 h *in vacuo*. The residue is extracted with 30 mL of *n*-hexane and filtered. The solution is concentrated to about 5 mL and stored at −25 °C for several hours which results in deposition of colorless crystals, yielding 1.140 g (1.71 mmol, 57%) of **4** as a colorless crystalline solid. Mp = 165 °C (dec). Anal. Calcd % (Found): C 62.87 (62.45); H 7.84 (8.04); N 2.09 (2.19). ^{1}H NMR (25 °C, CD_2Cl_2, 300.13 MHz): −0.16 (s, 9H, $Si(CH_3)_3$), 1.16 (s, 18H, $OC(CH_3)_3$), 1.99 (s, 6H, CH_3), 2.24 (s, 6H, CH_3), 2.29 (s, 6H, CH_3), 6.80−7.02 (7H, Ar−C*H*). ^{13}C{^{1}H} NMR (25 °C, CD_2Cl_2, 75.48 MHz): 5.65 (s, $Si(CH_3)_3$), 21.31 (s, CH_3), 22.07 (s, CH_3), 23.37 (s, CH_3), 33.68 (s, $OC(CH_3)_3$), 73.99 (s, $OC(CH_3)_3$), 122.74 (CH), 129.11 (CH) 129.79 (CH), 132.33 (CH), 137.25 (Ar-C), 138.09 (Ar-C), 138.16 (Ar-C), 139.08 (Ar-C), 140.10 (Ar-C), 148.20 (Ar-C).[35]

Ter[Me$_2$(N$_3$)Si]N−Sb(Cl)Me (5). To a stirred solution of **1** (0.475 g, 0.8 mmol) in CH_2Cl_2 (8 mL) is added Me_3SiN_3 (0.104 g, 0.9 mmol) in CH_2Cl_2 (3 mL) quickly at −70 °C. Then a solution of $GaCl_3$ (0.159 g, 0.9 mmol) in CH_2Cl_2 (3 mL) is added dropwise over a period of 15 min at this temperature. The resulting greenish solution is allowed to warm up to ambient temperature over 30 min and is stirred for 20 h. Then a solution of 4-*N*-dimethylaminopyridine (0.063 g, 0.51 mmol) is added dropwise at 0 °C resulting in a colorless solution. The solvent is removed *in vacuo*, and the colorless residue is extracted three times with 10 mL of *n*-hexane. Concentration of the colorless filtrate and storage at −25 °C for several hours yields 0.180 g (0.26 mmol, 32%) of **5** as a colorless crystalline solid. Mp = 147 °C. Anal. Calcd % (Found): C 54.06 (53.60); H 5.71 (5.68); N 9.34 (9.48). ^{1}H NMR (25 °C, CD_2Cl_2, 300.13 MHz): −0.23 (s, 3H, Si−CH_3), −0.16 (s, 3H, Si−CH_3), 0.73 (s, 3H, Sb−CH_3), 2.11 (s, 3H, CH_3), 2.15 (s, 6H, CH_3), 2.29 (s, 3H, CH_3), 2.30 (s, 3H, CH_3), 2.33 (s, 3H, CH_3), 6.89−7.14 (7H, C*H*). ^{13}C{^{1}H} NMR (25 °C, CD_2Cl_2, 75.48 MHz): 2.19 (s, Si-CH_3), 2.69 (s, Si-CH_3), 21.21 (CH_3), 21.33 (CH_3), 21.66 (CH_3), 21.82 (CH_3), 21.99 (CH_3), 22.30 (CH_3), 23.10 (CH_3), 123.57 (CH), 129.18 (CH), 129.64 (CH), 129.90 (2C, CH), 131.74 (CH), 133.15 (CH), 136.02 (Ar-C), 137.09 (Ar-C), 137.92 (Ar-C), 138.07 (Ar-C), 138.14 (Ar-C), 138.23 (Ar-C), 138.68 (Ar-C), 140.29 (Ar-C), 140.59 (Ar-C), 140.82 (Ar-C), 147.84 (Ar-C). ^{29}Si INEPT NMR (25 °C, CD_2Cl_2, 49.70 MHz): 3.7 ($Si(CH_3)_2N_3$).[35]

Ter(Me$_3$Si)N−Sb(N$_3$)$_2$ (6a). Procedure 1: NaN_3 (0.067 g, 1 mmol) is added to a stirred solution of **1** (0.297 g, 0.5 mmol) in THF at ambient temperatures, and the mixture is stirred for 20 h. Dispersed NaCl is allowed to settle, the solvent is removed *in vacuo*, and the residue is extracted with toluene. Toluene is again removed, and crystallization from *n*-hexane yields 0.165 g (0.27 mmol, 54%) of **6a** as a colorless crystalline solid. Proceedure 2: AgN_3 (0.080 g, 0.53 mmol) is added to a stirred solution of **1** (0.148 g, 0.25 mmol) in THF (5 mL) at ambient temperatures, and the mixture is allowed to stir for 8 h. The solvent is removed *in vacuo* afterward, the residues are extracted with benzene (5 mL), and concentration to 0.3 mL and storage in the freezer (−24 °C) yields 0.090 g (0.15 mmol, 60%) **6a** as colorless crystalline solid.

Mp = 148 °C. Anal. Calcd % (Found): C 53.47 (52.90); H 5.65 (5.66); N 16.17 (15.73). ^{1}H NMR (25 °C, CD_2Cl_2, 300.13 MHz): −0.24 (s, 9H, $Si(CH_3)_3$), 2.07 (s, 6H, CH_3), 2.21 (s, 6H, CH_3), 2.33 (s, 6H, CH_3), 6.92−7.16 (7H, Ar−C*H*). ^{13}C{^{1}H} NMR (25 °C, CD_2Cl_2, 75.48 MHz): 3.36 (s, $Si(CH_3)_3$), 21.41 (s, 2C, CH_3), 22.26 (s, 2C, CH_3), 22.56 (s, 2C, CH_3), 123.68 (CH) 129.56 (CH) 130.35 (CH), 132.91 (CH), 136.03 (Ar-C), 138.09 (Ar-C), 138.68 (Ar-C), 138.94 (Ar-C), 139.59 (Ar-C), 146.13 (Ar-C). ^{29}Si INEPT NMR (25 °C, CD_2Cl_2, 49.70 MHz): 13.5 ($Si(CH_3)_3$).[35]

MeSb(N$_3$)$_2$ (7). NaN_3 (0.033 g, 0.5 mmol) is added to a stirred solution of **5** (0.297 g, 0.5 mmol) in THF at ambient temperatures, and the resulting colorless solution is stirred for 24 h. Afterward the solvent is stripped off, and the residue is redissolved in toluene (0.5 mL). Within three days colorless crystals of **7** have precipitated. Only small amounts could be isolated (m < 40 mg). Mp = 120 °C, 138 °C (dec). IR (ATR, 25 °C, 32 scans, cm^{-1}): 2992 (m), 2948 (m), 2067 (s), 1608 (m), 1579 (w), 1574 (w), 1564 (w), 1494 (w), 1483 (w), 1446 (m), 1399 (m), 1396 (m), 1377 (w), 1312 (m), 1250 (m), 1199 (m), 1166 (m), 1097 (m), 1086 (m), 1029 (m), 1016 (m), 1005 (m), 986 (w), 945 (w), 914 (m), 836 (s), 796 (m), 767 (m), 749 (m), 730 (m), 720 (m), 714 (m), 694 (m), 649 (m), 594 (m), 583 (m), 552 (m), 532 (m).

Ter[Me$_2$(Cl)Si]N−Sb(Cl)Me (8). To a stirred solution of **1** (0.297 g, 0.5 mmol) in CH_2Cl_2 (5 mL) is added a solution of $GaCl_3$ (0.089 g, 0.5 mmol) in CH_2Cl_2 dropwise at −75 °C. The resulting orange solution is stirred for an additional 15 min at this temperature and allowed to warm up to 0 °C within 15 min. Then, a solution of 4-*N*-dimethylaminopyridine (0.063 g, 0.51 mmol) is added dropwise, resulting in a colorless solution. The solvent is removed *in vacuo*, and the colorless residue is extracted three times with 10 mL of *n*-hexane. Concentration of the colorless filtrate and storage at −25 °C for several hours yields 0.124 g (0.21 mmol, 42%) of **8** as a colorless crystalline solid. Prolonged drying *in vacuo* leads to complete removal of solvent molecules. Mp = 177 °C (dec). Anal. Calcd % (Found): C 54.66 (54.56); H 5.78 (5.72); N 2.36 (2.47). ^{1}H NMR (25 °C, CD_2Cl_2, 300.13 MHz): −0.09 (s, 3H, Si−CH_3), 0.04 (s, 3H, Si−CH_3), 0.71 (s, 3H, Sb−CH_3), 2.14 (s, 3H, CH_3), 2.18 (s, 3H, CH_3), 2.19 (s, 3H, CH_3), 2.29 (s, 3H, CH_3), 2.30 (s, 3H, CH_3), 2.33 (s, 3H, CH_3), 6.91−7.16 (7H, C*H*). ^{13}C{^{1}H} NMR (25 °C, CD_2Cl_2, 75.48 MHz): 7.13 (s, Si-CH_3), 8.49 (s, Si-CH_3), 21.19 (CH_3), 21.32 (CH_3), 22.05 (CH_3), 22.16 (CH_3), 22.67 (CH_3), 23.16 (CH_3), 23.56 (Sb-CH_3), 123.72 (CH), 129.06 (CH), 129.70 (CH), 129.85 (CH), 129.98 (CH), 131.74 (CH), 133.35 (CH), 136.18 (Ar-C), 137.22 (Ar-C), 137.98 (Ar-C), 138.08 (Ar-C), 138.12 (Ar-C), 138.67 (Ar-C), 139.04 (Ar-C), 140.28 (Ar-C), 140.63 (Ar-C), 140.86 (Ar-C), 148.13 (Ar-C). ^{29}Si INEPT NMR (25 °C, CD_2Cl_2, 49.70 MHz): 18.6 ($Si(CH_3)_2Cl$).[35]

[Me$_2$SbSbMe$_3$][GaCl$_4$] (9). Procedure 1: To a stirred solution of **1** (0.59 g, 1 mmol) in CH_2Cl_2 (10 mL) is added a solution of $GaCl_3$ (0.180 g, 1 mmol) in CH_2Cl_2 (3 mL) dropwise at 0 °C. The resulting orange solution is stirred for five days at ambient temperatures, the solvent is removed *in vacuo*, and the colorless residue is extracted two times with 10 mL of Et_2O. Concentration of the colorless filtrate and storage at ambient temperatures for several hours yields only a few colorless crystals of **9**. Procedure 2: To a stirred solution of **11** (1 mmol; 354 mg) in CH_2Cl_2 (3 mL) is added a solution of $GaCl_3$ (1 mmol; 177 mg) in CH_2Cl_2 (2 mL) dropwise at −60 °C. The resulting yellow solution is allowed to warm to ambient temperatures, and upon concentration to 1 mL an oily black layer deposits with a clear reddish supernatant on top. The supernatant is removed, and the black oily residue is extracted with Et_2O (5 mL). The Et_2O extract is concentrated to 2 mL and allowed to rest at ambient temperatures

dx.doi.org/10.1021/ic300770b | *Inorg. Chem.* 2012, 51, 8212−8224

for 48 h; during this time span colorless crystalline blocks of **9** have deposited (0.05 g; 5%).

^{1}H NMR (25 °C, CD_2Cl_2, 500.13 MHz): 1.60 (s, $Sb(CH_3)_3$), 1.49 (s, $Sb(CH_3)_2$). $^{13}C\{^{1}H\}$ NMR (25 °C, CD_2Cl_2, 125.76 MHz): −3.3 (s, $Sb(CH_3)_3$).

Mes*[Me$_2$(Cl)Si]N−Sb(Cl)Me (10). To a stirred solution of Mes*(Me_3Si)N−$SbCl_2$ (0.53 g, 1 mmol) in CH_2Cl_2 (10 mL) is added a solution of $GaCl_3$ (0.180 g, 1 mmol) in CH_2Cl_2 (3 mL) dropwise at 0 °C. The resulting orange solution is stirred for 48 h at ambient temperatures, and the solvent is removed *in vacuo*. THF (2 mL) and *n*-hexane (10 mL) are added, and the colorless suspension is filtered. Concentration of the colorless filtrate and storage at +5 °C for several hours yields only a few colorless crystals of **10**.

($Me_3Si)_2$N−$SbCl_2$ (11). To a stirred solution of $SbCl_3$ (6.844 g, 30 mmol) in toluene (100 mL) is added a solution of $(Me_3Si)_2NLi$ (5.020 g, 30 mmol) in toluene (50 mL) dropwise at −60 °C. The resulting colorless suspension is allowed to warm to ambient temperatures and is stirred for 10 h. The solvent is removed *in vacuo*, and the resulting colorless residue is extracted with *n*-hexane (50 mL) and filtered (F4), resulting in a colorless solution. Removal of solvent *in vacuo* gives a colorless liquid, which is distilled *in vacuo* at 75 °C, yielding **11** (5.506, 52%) as colorless liquid. Storage at −30 °C. Mp = 32 °C. Anal. Calcd % (Found): C 20.41 (19.08); H 5.14 (4.48); N 3.97 (4.08). ^{1}H NMR (25 °C, CD_2Cl_2, 500.13 MHz): 0.35 (s, $^{1}J(^{13}C^{1}H)$ = 119 Hz, $^{2}J(^{29}Si^{1}H)$ = 6.7 Hz). $^{13}C\{^{1}H\}$ NMR (25 °C, CD_2Cl_2, 125.76 MHz): 5.3 (s, $^{1}J(^{29}Si^{13}C)$ = 57 Hz). $^{29}Si\{^{1}H\}$ NMR (25 °C, CD_2Cl_2, 99.36 MHz): 9.86 (s). $^{14}N\{^{1}H\}$ NMR (25 °C, CD_2Cl_2, 36.14 MHz): −286 ($\Delta\nu_{1/2}$ = 280 Hz). IR (ATR 25 °C, cm^{-1}): 2954 (m), 2898 (w), 1404 (m), 1251 (s), 1180 (m), 1056 (m), 931 (m), 864 (s) 834 (s), 801 (s), 759 (m), 717 (m), 673 (m), 636 (m), 619 (m). Raman (75 mW, 25 °C, 500 scans, cm^{-1}): 3080 (2), 2962 (8), 2906 (10), 2780 (2), 2713 (2), 1601 (2), 1469 (2), 1446 (2), 1400 (2), 1282 (1), 1234 (1), 1176 (2), 1137 (2), 1101 (1), 1030 (1), 927 (1), 856 (1), 817 (2), 748 (1), 712 (1), 634 (1), 571 (2), 543 (1), 466 (1), 431 (1), 397 (1), 338 (5), 313 (3), 258 (2), 215 (2).

[($Me_3Si)_2$NSbCl][($Me_3Si)_2$N($GaCl_3)_2$] (12). To a stirred solution of **11** (0.354 g, 1 mmol) in CH_2Cl_2 (3 mL) is added a solution of $GaCl_3$ (0.177 g, 1 mmol) in CH_2Cl_2 (2 mL) dropwise at −60 °C. The resulting yellow solution is allowed to stir for 15 min at this temperature and is concentrated afterward. Storage at −80 °C for one week leads to the deposition of colorless crystals of **12** (yield: 0.240 g; 48%). Anal. Calcd % (Found): C 16.81 (15.95); H 4.03 (3.98); N 2.80 (3.19). IR (ATR 25 °C, cm^{-1}): 2997 (w), 2961 (w), 2901 (w), 1409 (m), 1312 (w), 1278 (m), 1257 (s), 1204 (w), 1160 (w), 1041 (m), 841 (s), 825 (s), 767 (s), 692 (m), 672 (s), 653 (s), 609 (s), 582 (s).

[MeSb(SbMe$_3$)$_2$][GaCl$_4$]$_2$ (13). Procedure 1: To a stirred solution of **11** (1 mmol; 354 mg) in CH_2Cl_2 (3 mL) is added a solution of $GaCl_3$ (1 mmol, 177 mg) in CH_2Cl_2 (2 mL) dropwise at −60 °C. The resulting yellow solution is allowed to warm to ambient temperatures, and upon concentration to 1 mL an oily black layer deposits with a clear reddish supernatant on top. The supernatant is transferred, and the black oil is washed with hexane and layered with toluene (2 mL) afterward. Within seven days colorless crystalline needles have grown from the black oil, and only a few crystals could be isolated (tetragonal polymorph). The remaining supernatant was concentrated, and colorless crystals of **13** (monoclinic configuration) grew from the solution within 7 days at 5 °C in the fridge. The supernatant was transferred again, and the crystals were washed with CH_2Cl_2 at −30 °C, yielding 100 mg (0.11 mmol; 33%) of **13**. The remaining supernatant was taken to dryness, and crystals of 1,3-bis-(chlorodimethylsilyl)-2,2,4,4-tetramethyl-*cyclo*-disilazane (**15**) were grown from a saturated CH_2Cl_2 solution. Procedure 2: A solution of **12** (0.1 mmol; 100 mg) in CH_2Cl_2 (2 mL) is stirred for 48 h at ambient temperatures, and the solution is concentrated to 1 mL afterward. Colorless crystals of **13** (monoclinic polymorph) grow within 24 h; only a few crystals could be isolated. Mp = 72 °C. Anal. Calcd % (Found): C 9.41 (9.42); H 2.36 (2.37). ^{1}H NMR (25 °C, CD_2Cl_2, 500.13 MHz): 1.58 (s, $Sb(CH_3)_3$)), 2.01 (s, $Sb(CH_3)$). $^{13}C\{^{1}H\}$ NMR (25 °C, CD_2Cl_2, 125.76 MHz): −3.5 (s, $Sb(CH_3)_3$). IR (ATR 25 °C, cm^{-1}): 3012 (w), 2959 (w), 2924 (w), 1399 (m), 1257 (m), 1232 (m), 1217 (m), 1203 (m), 844 (s), 787 (m), 739 (m), 707 (m), 552 (m). Raman (75 mW, 25 °C, 500 scans, cm^{-1}): 3012 (1), 2924 (6), 1238 (1), 1219 (1), 708 (1), 553 (5), 527 (8), 503 (2), 346 (4), 166 (10), 118 (4).

Me$_3$Sb−GaCl$_3$ (14). To a stirred solution of **11** (1 mmol; 354 mg) in CH_2Cl_2 (3 mL) is added a solution of $GaCl_3$ (1 mmol; 177 mg) in CH_2Cl_2 (2 mL) dropwise at −70 °C. The resulting solution is allowed to warm to ambient temperatures and is concentrated to 0.5 mL at 80 °C. The brownish concentrated solution is put to rest at ambient temperatures for 30 days; within this time, minimal amounts of colorless crystals form, which were identified as [Me_3Sb*$GaCl_3$]. Mp = 131 °C (dec). IR (ATR 25 °C, cm^{-1}): 2963 (m), 1407 (m), 1260 (m), 848 (s), 794 (m), 555 (s).

■ ASSOCIATED CONTENT

Ⓢ Supporting Information

Experimental details, crystallographic information, including CIF, and further experimental data of all considered species. This material is available free of charge via the Internet at http://pubs.acs.org.

■ AUTHOR INFORMATION

Corresponding Author

*E-mail: axel.schulz@uni-rostock.de.

Notes

The authors declare no competing financial interest.

■ ACKNOWLEDGMENTS

Martin Ruhmann (University Rostock) is acknowledged for the measurement of Raman spectra. Financial support by the Fond der Chemischen Industrie (scholarship for C.H.) is gratefully acknowledged. Financial support by the DFG (1170/6-1) is gratefully acknowledged.

■ REFERENCES

(1) (a) Balakrishna, M. S.; Eisler, D. J.; Chivers, T. *Chem. Soc. Rev.* **2007**, *36*, 650−664 and references therein. (b) Stahl, L. *Coord. Chem. Rev.* **2000**, *210*, 203−250 and references therein.

(2) Herler, S.; Villinger, A.; Schmedt auf der Günne, J.; Mayer, P.; Schulz, A.; Weigand, J. J. *Angew. Chem.* **2005**, *117*, 7968−7971; *Angew. Chem., Int. Ed.* **2005**, *44*, 7790−7793.

(3) Schulz, A.; Villinger, A. *Angew. Chem.* **2008**, *120*, 614−617; *Angew. Chem., Int. Ed.* **2008**, *47*, 603−606.

(4) Michalik, D.; Schulz, A.; Villinger, A.; Weding, N. *Angew. Chem.* **2008**, *120*, 6565−6568; *Angew. Chem., Int. Ed.* **2008**, *47*, 6465−6468.

(5) Lehmann, M.; Schulz, A.; Villinger, A. *Eur. J. Inorg. Chem.* **2010**, *35*, 5501−5508.

(6) Mayer, P.; Schulz, A.; Villinger, A. *Chem. Commun.* **2006**, 1236−1238.

(7) Lehmann, M.; Schulz, A.; Villinger, A. *Angew. Chem.* **2011**, *123*, 5327−5331; *Angew. Chem., Int. Ed.* **2011**, *50*, 5221−5224.

(8) Schulz, A.; Mayer, P.; Villinger, A. *Inorg. Chem.* **2007**, *46*, 8316−8322.

(9) Michalik, D.; Schulz, A.; Villinger, A. *Inorg. Chem.* **2008**, *47*, 11798−11806.

(10) Althaus, A.; Breunig, H. J.; Lork, E. *Chem. Commun.* **1999**, 1971−1972.

(11) Ortep-3 for Windows: Farrugia, L. J. *J. Appl. Crystallogr.* **1997**, *30*, 565.

(12) The methyl positions of the ring-silicon atom are found to be partly occupied by chlorine atoms in the crystal (see Supporting Information). Thus, a formula with three chlorine atoms in the disilazane can be considered, such as [$(Me_2Cl)SiNSi(Me_{1.5}Cl_{0.5})$]$_2$.

(13) (a) Geymayer, P.; Rochow, E. G. *Angew. Chem.* **1965**, *77*, 618. (b) Breed, L. W.; Elliot, R. L.; Wiley, J. C. *J. Organomet.* **1970**, *24*, 315−325.

(14) Burford, N.; Conrad, E.; McDonald, R.; Ferguson, M. *J. Am. Chem. Soc.* **2009**, *131*, 17000−17008.
(15) (a) Schmidbauer, H.; Findeiss, W. *Angew. Chem.* **1964**, *76*, 752−753. (b) Luo, B.; Young, V. G.; Gladfelter, W. L. *J. Organomet. Chem.* **2002**, 268−275.
(16) Carmalt, C.; Mileham, J. D.; White, A. J. P.; Williams, D. J.; Steed, J. W. *Inorg. Chem.* **2001**, *40*, 6035−6038.
(17) Hubrich, C.; Schulz, A.; Villinger, A. *Z. Anorg. Allg. Chem.* **2007**, *633*, 2362−2366.
(18) (a) Schmidpeter, A.; Lochschmidt, S.; Karaghiosoff, K.; Sheldrick, W. S. *Chem. Commun.* **1985**, 1447−1448. (b) Schmidpeter, A.; Lochschmidt, S.; Sheldrick, W. S. *Angew. Chem., Int. Ed.* **1985**, *24*, 226−227. (c) Burford, N.; Ragogna, P. J.; McDonald, R.; Ferguson, M. *J. Am. Chem. Soc.* **2003**, *125*, 14404−14410. (d) Dyker, C. A.; Burford, N. *Chem.—Asian J.* **2008**, *3*, 28−36. (e) Weigand, J. J.; Burford, N.; Decken, A. *Eur. J. Inorg. Chem.* **2008**, 4868−4872. (f) Dyker, C. A.; Riegel, S. D.; Burford, N.; Lumsden, M. D.; Decken, A. *J. Am. Chem. Soc.* **2007**, *129*, 7464−7474. (g) Dyker, C. A.; Burford, N.; Menard, G.; Lumsden, M. D.; Decken, A. *Inorg. Chem.* **2007**, *46*, 4277−4285. (h) Carpenter, Y.; Dyker, C. A.; Burford, N.; Lumsden, M. D.; Decken, A. *J. Am. Chem. Soc.* **2008**, *130*, 15732−15741.
(19) Minkwitz, R.; Hirsch, C. *Z. Anorg. Allg. Chem.* **1999**, *625*, 1674−1682.
(20) Breunig, H. J.; Denker, M.; Lork, E. *Angew. Chem.* **1996**, *108*, 1080−1081; *Angew. Chem., Int. Ed.* **1996**, *35*, 1005−1006.
(21) Stevens, J. G.; Trooster, J. M.; Meinema, H. A.; Noltes, J. G. *Inorg. Chem.* **1981**, *20*, 801−803.
(22) Schulz, S.; Lyhs, B.; Jansen, G.; Bläser, D.; Wölper, C. *Chem.−Eur. J.* **2011**, *17*, 4914−4920.
(23) (a) Christe, K. O.; Haiges, R.; Vij, A.; Boatz, J. A.; Schneider, S.; Schroer, T.; Gerken, M. *Chem.—Eur. J.* **2004**, *10*, 508−517. (b) Schulz, B.; Lyhs, S.; Jansen, G.; Bläser, D.; Wölper, C. *Chem. Commun.* **2011**, *47*, 3401−3403.
(24) Pyykkö, P.; Atsumi, M. *Chem.—Eur. J.* **2009**, *15*, 12770−12779.
(25) Tornieporth-Oetting, I. C.; Klapötke, T. M. *Angew. Chem.* **1995**, *107*, 559−568; *Angew. Chem., Int. Ed.* **1995**, *34*, 511−520.
(26) Klapötke, T. M.; Nöth, H.; Schütt, T.; Warchold, M. *Z. Anorg. Allg. Chem.* **2001**, *627*, 81−84.
(27) (a) Haiges, R.; Vij, A.; Boatz, J. A.; Schneider, S.; Schroer, T.; Gerken, M.; Christe, K. O. *Chem.—Eur. J.* **2004**, *10*, 508−517. (b) Klapötke, T. M.; Schulz, A.; McNamara, J. *J. Chem. Soc., Dalton Trans.* **1996**, 2985−2987.
(28) Pyykkö, P.; Atsumi, M. *Chem.—Eur. J.* **2009**, *15*, 12770−12779.
(29) Cowley, A. H.; Jones, R. A.; Kidd, K. B.; Nunn, C. M.; Westmoreland, D. L. *J. Organomet. Chem.* **1988**, *341*, C1−C5.
(30) Matano, Y.; Nomura, H.; Suzuki, H. *Inorg. Chem.* **2000**, *39*, 1340−1341.
(31) (a) Ashe, A. J.; Ludwig, E. G., Jr.; Oleksyszyn, J.; Huffman, J. C. *Organometallics* **1984**, *3*, 337−338. (b) Becker, G.; Freudenblum, H.; Witthauer, C. *Z. Anorg. Allg. Chem.* **1982**, *492*, 37.
(32) Sheldrick, G. M. *SHELXS-97: Program for the Solution of Crystal Structures*; University of Göttingen: Göttingen, Germany, 1997.
(33) Sheldrick, G. M. *SHELXL-97: Program for the Refinement of Crystal Structures*; University of Göttingen: Göttingen, Germany, 1997.
(34) Sheldrick, G. M. *SADABS. Version 2*; University of Göttingen: Göttingen, Germany, 2004.
(35) Raman and IR data can be found in the Supporting Information.

6 Anhang

6.1 Low-temperature isolation of an azidophosphenium cation

Angewandte Chemie, **2012**, *124*, 6345−6349.

Angewandte Chemie International Edition, **2012**, *51*, 6241−6245.

DOI: 10.1002/anie.201201851

In dieser Publikation wurde der Großteil der experimentellen Arbeiten von mir durchgeführt, Der eigene Beitrag liegt bei ca. 90 %.

DOI: 10.1002/anie.201201851

Phosphorus Azides

Low-Temperature Isolation of An Azidophosphenium Cation**

Christian Hering, Axel Schulz, and Alexander Villinger*

Dedicated to Professor Wolfgang Beck on the occasion of his 80th birthday

The first two-coordinate phosphorus cations, observed in so-called phosphamethine cyanines, were reported by Dimroth and Hoffmann in 1964.[1] The term phosphenium ion has been introduced to imply a high degree of positive charge accumulation at the two-coordinate phosphorus center with a formally vacant 3p orbital.[2] Phosphenium ions have some resemblance to carbenes of the type X–C–Y except that P^+ replaces the central carbon atom.[3] As is well-known, carbenes are stabilized best when X and Y are atoms or groups such as NR_2, which can serve as π-electron donors to the carbon atom. Parry et al. reported the first examples of acyclic phosphenium ions $[(Me_2N)_2P]^+$ and $[(Me_2N)(Cl)P]^+$, which were obtained by chloride abstraction from the corresponding aminochlorophosphanes by employing Lewis acids, such as ECl_3 (E = Fe, Al, Ga).[4] Structural data of acyclic aminophosphenium ions are still limited to only a few examples substituted by an amino group: $[(i\mathrm{Pr}_2\mathrm{N})_2\mathrm{P}]\mathrm{X}$ (X = $AlCl_4^-$, $GaCl_4^-$, BPh_4^-).[5,6] To the best of our knowledge, halogen- or pseudohalogen-substituted phosphenium ions of the type $[R_2N–P–X]^+$ (X = halogen or pseudohalogen) have not been isolated and structurally characterized.

Cyclo-diphosphadiazenium salts can also be regarded as phosphenium ions (Scheme 1, species **B**). Upon addition of a Lewis acid to the *cyclo*-diphosphadiazanes **A**, the corresponding cyclic cation **B** is formed, which can be regarded as binary P^{III}/N four-membered heterocyclic cation with two- and three-coordinate phosphorus atoms and a delocalized π bond within the $NP^{(+)}N$ unit. Only recently, the synthesis and full characterization of a 1-azido-*cyclo*-1,3-diphospha-2,4-diazenium salt was reported (Scheme 1, species **C**).[7] As illustrated in Scheme 1, an equilibrium between a *cyclo*-diphosphadiazane and its monomer, the corresponding iminophosphane, might be observed depending on the sterical strain of the bulky substituent R. For example, for R = terphenyl (Ter), only a stable dimer is found in the solid state and in solution but no monomeric iminophosphane R–N=P–Cl.[7b] Addition of $GaCl_3$ results in the formation of *cyclo*-diphosphadiazenium salt **B**, and in the presence of Me_3SiN_3, species **C** can be isolated. In contrast, if the bulky substituent R = supermesityl (Mes*), the monomeric species **D** is favored; thus upon addition of $GaCl_3$, an iminophosphenium ion is formed, which reacts as dipolarophile in the presence of the 1,3-dipole molecule Me_3SiN_3 to the corresponding tetrazaphosphole (Scheme 1, species **F**) in a formal [3+2] cyclization. However, no isomeric species **C** is observed.[8,9] Recently, it was shown that disguised dipolarophiles, that is, the amino-substituted dichlorophosphane $Ter(Me_3Si)N–PCl_2$ can also be used, which releases Me_3SiCl, forming the necessary highly reactive, bare dipolarophile Ter–N=P–Cl in situ. Again, addition of the 1,3-dipole Me_3SiN_3 in the presence of a Lewis acid yields the tetrazaphospole **F**.

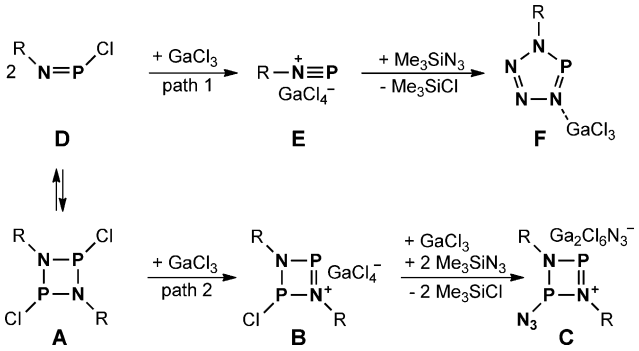

Scheme 1. Different reaction paths observed for *cyclo*-diphosphadiazanes (species **A**) depending on the sterical strain: path 1 for R = Mes*, path 2 for R = Ter.

These synthetic concepts can also be applied to the heavier analogues, but although the isolation and comprehensive characterization of tetrazapnictoles of the type $R–NE_4$ (E = N, P, As, Sb) were achieved, there are still open questions with respect to the reaction mechanism. Theoretical studies, carried out to determine the mechanism,[10] indicate that pnictenium ions are intermediates on the reaction path.[7b] Following our interest in the chemistry of compounds bearing binary NPn fragments (Pn = P,[7,8,10] As,[9] Sb,[11] and Bi[12]), we studied the reaction of the disguised dipolarophile $(Me_3Si)_2N–PCl_2$ (**1**) with the Lewis acid $GaCl_3$ by means of low-temperature techniques.[13]

We report herein on the synthesis and full characterization of the hitherto unknown, highly labile amino(azido)phosphenium salt $[(Me_3Si)_2N=P–N_3][GaCl_4]$ (**4**) utilizing a pseudohalogen/chlorine exchange reaction in aminochlorophosphenium ion $[(Me_3Si)_2N–PCl]^+$ (**2a**, Scheme 2).[14] The cation in the azide-substituted phosphenium salt **4** can formally be regarded as the first known phosphapentacenium ion $[R_2NPNNN]^+$; the parent pentacenium ion N_5^+ was described by Christe et al. in 1999.[15]

[*] C. Hering, Prof. Dr. A. Schulz, Dr. A. Villinger
Universität Rostock, Institut für Chemie
Albert-Einstein-Strasse 3a, 18059 Rostock (Germany)
and
Leibniz-Institut für Katalyse e.V. an der Universität Rostock
Albert-Einstein-Strasse 29a, 18059 Rostock (Germany)
E-mail: axel.schulz@uni-rostock.de
Homepage: http://www.chemie.uni-rostock.de/ac/schulz

[**] Financial support by the DFG is gratefully acknowledged. We thank Dr. D. Michalik for NMR spectroscopy measurements.

Supporting information for this article is available on the WWW under http://dx.doi.org/10.1002/anie.201201851.

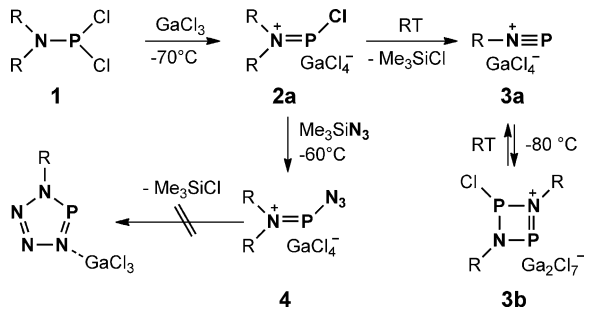

Scheme 2. Synthesis of different aminophosphenium, iminophosphenium, and *cyclo*-diphosphadiazenium salts (R = Me_3Si).

As illustrated in Scheme 2, addition of $GaCl_3$ to a solution of $(Me_3Si)_2N{-}PCl_2$ (**1**) at −70 °C resulted (according to X-ray crystallography) in the formation of a highly labile amino-chlorophosphenium ion in $[(Me_3Si)_2N{=}P{-}Cl][GaCl_4]$ (**2a**), which could be isolated as colorless crystals at −50 °C (Figure 1, right).[4] Furthermore, the synthetic approach was modified and two equivalents of $GaCl_3$ were used, resulting in

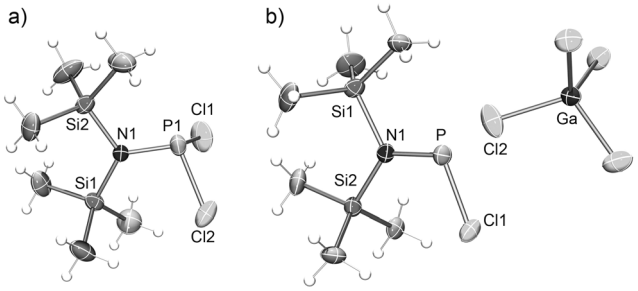

Figure 1. ORTEP view of the molecular structure of **1** (a) and **2a** (b) from signgle-crystal X-ray diffraction at 173 K. Ellipsoids are set at 50% probability. Selected bond lengths [Å] and angles [°]: **1**: P–N 1.6468(8), P–Cl2 2.0834(5), P–Cl1 2.1074(5), N–Si1 1.7940(9), N–Si2 1.7961(9); N-P-Cl2 104.37(4), N-P-Cl1 104.86(3), Cl2-P-Cl1 96.76(2), P-N-Si1 126.80(5), P-N-Si2 112.39(5), Si1-N-Si2 120.81(5). **2a**: P1A–N 1.595(2), P1B–N 1.584 (3), P–Cl1 2.019(4), Si1–N 1.847(2), Si2–N 1.841(2), P1A–Cl2A 2.871(4), P1B–Cl2B 2.811(11), Ga–Cl2 2.198(5), Ga–Cl4 2.201(8); N-P-Cl1 107.6(1), P-N-Si2 111.3 (1), P-N-Si1 126.8(1), Si2-N-Si1 121.8(1), Cl1-P-N-Si2 175.6(1).

the formation of the $[(Me_3Si)_2N{=}P{-}Cl][Ga_2Cl_7]$ (**2b**).[14] With $AlCl_3$ as Lewis acid, the isolation of $[(Me_3Si)_2N{=}P{-}Cl][AlCl_4]$ (**2c**) was achieved at temperatures below −50 °C. However, the bare cation of **2a**–**c** could not be detected in solution. This quite astonishing observation prompted us to study the temperature-dependent equilibrium chemistry of the system $(Me_3Si)_2N{-}PCl_2/GaCl_3$ by means of variable-temperature ^{31}P NMR spectroscopy (Figure 2).

If an equimolar mixture of $GaCl_3$ and **1** is allowed to warm to ambient temperature, while monitoring the process with ^{31}P NMR spectroscopy, at −80 °C only the ^{31}P NMR signal of the $GaCl_3$ adduct of starting material **1** (broad singlet at δ = 188 ppm) is observed. Between −80 °C and −15 °C a temperature-dependent downfield shift of the resonance of **1**·$GaCl_3$ from 188 ($\Delta\nu_{1/2}$ = 4000 Hz) to 285 ppm ($\Delta\nu_{1/2}$ = 370 Hz) is observed, while at the same time the signal becomes sharper,

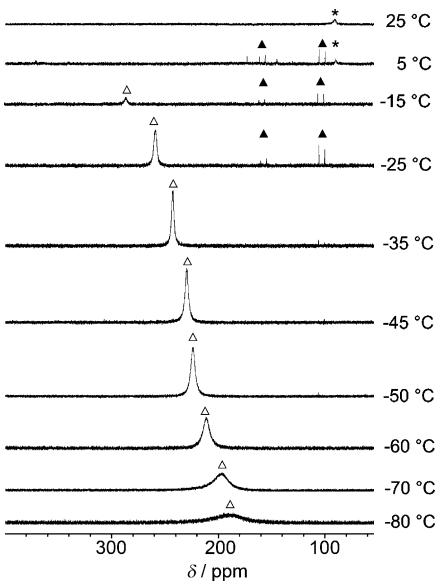

Figure 2. Temperature-dependent ^{31}P NMR study of an equimolar mixture of **1** and $GaCl_3$ between −80 °C and 25 °C. The observed species are indicated as follows: ▲ = **1**·$GaCl_3$ → **2a**, △ = $[R_2N\mathbf{P}(Cl)\cdot(Cl_2)\mathbf{P}NR_2][GaCl_4]$, ⋆ = **3a**.[14]

indicating the transition to salt formation, $[(Me_3Si)_2N(Cl)P{-}Cl{\cdots}GaCl_3]$, upon chloride abstraction by $GaCl_3$ (Figure 2). However, the most downfield-shifted signal at δ = 285 ppm (−15 °C) is still far away from the expected range for the cation of **2a** (cf. δ = 330 ppm in $[(Me_2N)(Cl)P]^+$;[4b] computed shift for **2a**: δ = 393 ppm).[14b] Obviously, species **2a** containing the amino(chloro)phosphenium ion is formed only upon crystallization, and is only stable in the solid state at temperatures below −50 °C. At −5 °C the signal for the simple adduct **1**·$GaCl_3$, $[(Me_3Si)_2N(Cl)P{-}Cl{\cdots}GaCl_3]$, has completely disappeared, while a new signal at δ = 89 ppm and an adduct of starting material **1** and the chlorophosphenium ion in **2a**, $[R_2NP(Cl)\cdot(Cl_2)PNR_2][GaCl_4]$ (R = $SiMe_3$; $^1J_{P,P}$ = 669 Hz), are observed. This large $^1J_{P,P}$ coupling constant is in good agreement with donor–acceptor adducts bearing a direct P–P linkage.[16] At room temperature, only one signal in the ^{31}P NMR spectrum remains at 89 ppm, which can be assigned to the *N*-(trimethylsilyl)iminophosphenium tetrachlorogallate, $[Me_3Si{-}N{\equiv}P][GaCl_4]$ (Scheme 2, species **3a**),[17] a yellow, viscous compound that is an ionic liquid at room temperature. If **3a** is then cooled down again (Supporting Information, Figure S2), at −80 °C compound **3a** is in an equilibrium with its cyclic dimer, a chloro-*cyclo*-diphosphadiazenium salt (**3b**), which has characteristic NMR signals for its two- and three-coordinate phosphorus centers (Scheme 2).[7a,18]

In another series of experiments, we studied the reaction of amino(chloro)phosphenium salt **2a** with 1,3-dipole molecules such as Me_3SiN_3, which can be regarded as a trimethylsilylpseudohalide.[19] Astonishingly, when a solution of Me_3SiN_3 in CH_2Cl_2 is added to **2a** at −50 °C, colorless crystals precipitate from the reaction mixture that were unequivocally identified as the highly labile amino(azido)phosphenium salt $[(Me_3Si)_2N{=}P{-}N_3][GaCl_4]$ (**4**) by low-temperature single-crystal X-ray analysis and ^{31}P NMR studies at −70 °C (cf.

$\delta_{exp} = 367$ vs. $\delta_{calc} = 354$ ppm).[14b] Compound **4** contains the first cation with an azide group attached to a two-coordinate phosphorus atom and might be regarded as constitutional isomer of a tetrazaphospholium ion with a cyclic $R_2PN_4^+$ moiety.[20] Compound **4** is a colorless crystalline solid and can be stored for at least one year under an argon atmosphere at temperatures below −30 °C, which is remarkable, because phosphorus azides are well-known for a facile release of molecular nitrogen. In contrast, **4** is stable in solution only at temperatures below −40 °C, and slowly decomposes upon further warming, releasing N_2 in a Staudinger reaction. This Staudinger reaction was studied by means of ^{31}P NMR experiments yielding a mixture of oligomeric decomposition products of the type $[R_2NP{=}NP(X)NR_2]^{2+}$ ($R = Me_3Si$; X = Cl, N_3), that could not be isolated. No indications for the formation of a tetrazaphosphole were observed. The intermediate formation of azidophosphenium ions bearing an azido substituent directly on the two-coordinate phosphorus atom has been discussed before solely on the basis of ^{31}P NMR data in the reaction of $iPr_2N{-}PCl_2$ with Me_3SiN_3 in the presence of $AlCl_3$.[21] Usually, the reaction of phosphenium ions with azides is an interesting extension of the Staudinger reaction, and so far it was impossible to isolate the azidophosphenium species. For example, it was found that only bis(dialkylamino)phosphenium ions $[(R_2N)_2P]^+$ react with azides to afford the corresponding bis(dialkylamino)-iminophosphonium ions $[(R_2N)_2P{=}NR]^+$.[22]

Aminodichlorophosphane **1** and the chlorophosphenium salts **2a**, **2b**, and **2c** crystallize in the monoclinic space group $P2_1/c$ with four formula units per cell, whereas azidophosphenium salt **4** crystallizes in the monoclinic space group $P2_1/m$ with two formula units per cell (Figure 3). A striking feature of all structures is the almost planar environment of the amino nitrogen atom (∡Si1-Si2-N-P in **1** 179.8, **2a** 176.2, **2b** 178.1, **2c** 178.1, **4** 180.0°). Thus, as shown by NBO analyses (NBO = natural bond orbital),[23] the one lone pair on the amino nitrogen atom is localized in a pure p-type atomic orbital. As expected, the three-coordinate P atom in **1** (Figure 1, left) adopts a trigonal pyramidal geometry, and a rather short $P{-}N_{amino}$ bond length of 1.6468(8) Å is found (cf. $\Sigma r_{cov}(P{-}N) = 1.82$, $\Sigma r_{cov}(P{=}N) = 1.62$ Å),[24] indicating partial double bond character owing to hyperconjugative effects of the lone pair (LP) of the amino nitrogen atom with the antibonding σ*(P−Cl) bond orbital. This p-LP(N)→σ*(P−Cl) donor–acceptor interaction accounts also for the slightly elongated P−Cl1 bond (2.1074(5) Å, cf. $\Sigma r_{cov}(P{-}Cl) = 2.04$ Å)[24] in **1**. Similar structural features with short P−N distances (1.67 ± 3 Å) have already been observed in a series of amino–iminophosphanes ($R_2N{-}P{=}N{-}R'$).[25] Even shorter $P{-}N_{amino}$ distances, ranging from 1.59 to 1.60 Å, are observed in the cations of **2a–c** and **4** (**2a** 1.595(2),[26] **2b** 1.580(2), **2c** 1.601(2), and **4** 1.597(2) Å) in accord with a typical P−N double bond (cf. $\Sigma r_{cov}(P{-}N) = 1.82$, $\Sigma r_{cov}(P{=}N) = 1.62$ Å;[24] 1.59(1) and 1.60(1) Å in $[(iPr_2N)_2P][GaCl_4]$).[6] In contrast to **1**, for **2a–c** and **4** NBO analyses display a localized N−P $p_\pi p_\pi$ double bond as expected for phosphenium ions of the type $[R_2N{=}P{-}X]^+$ (X = Cl, N_3).

As shown on numerous occasions, covalently bound azide groups display a *trans*-bent configuration (regarding the P atom, P-N1-N2-N3 180.0) with a N1-N2-N3 angle of 172.2 (2)° and a formally sp^2-hybridized N_α atom (N2-N1-P 121.1(1)°). It is interesting to note that the whole NPNNN chain, including both silicon atoms, lies in-plane (N1-P-N4-Si2 180.0°), which is obviously energetically favored. As the entire Si_2N_4P skeleton in the azido-substituted cation **4** is planar, strong in-plane and out-of-plane delocalization of π electrons is found in the MO and NBO depiction (Figure 4, top), respectively, leading among other things to a fairly short P−NNN distance of 1.673(2) Å, in accord with partial double-bond character. For comparison, the P−NNN distance in 1-azido-*cyclo*-1,3-diphospha-2,4-diazenium with 1.706(3) Å is a typical single bond (Scheme 1, species **C**).[7a]

The NBO Lewis depiction[23] of **4** shows two σ P−N bonds and one $P{-}N_{amino}$ double bond according to Lewis representation **I** in Figure 4 (bottom). However, both lone pairs localized at the N_{azide} atom are strongly delocalized, for example, into the $\pi^*(P{-}N_{amino})$ with a hyperconjugative energy of $\Delta E^{(2)} = 39$ kcal mol^{-1} corresponding to a covalent $\pi(P{-}N_{azide})$ MO bond order of 0.16 (cf. 0.46 for $\pi(P{-}N_{amino})$).

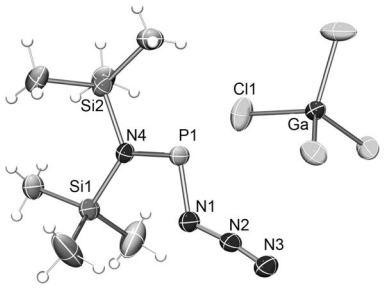

Figure 3. ORTEP view of the molecular structure of **4** from signgle-crystal X-ray diffraction at 173 K. Ellipsoids are set at 50% probability. Selected bond lengths [Å] and angles [°]: P1–N4 1.597(2), P–N1 1.673(2), N1–N2 1.254(2), N2–N3 1.113(3), N4–Si2 1.839(2), N4–Si1 1.851(2), Ga1–Cl3 2.1597(7), Ga1–Cl2 2.1688(4), Ga1–Cl1 2.1825(7), Ga–Cl4 2.1825(7), P1–Cl1 3.3923(6), P1–Cl2 3.7491(3); N4-P1-N1 101.03(9), N2-N1-P1 121.1(1), N3-N2-N1 172.2 (2), N1-P-N4-Si2 180.0, P-N1-N2-N3 180.0.

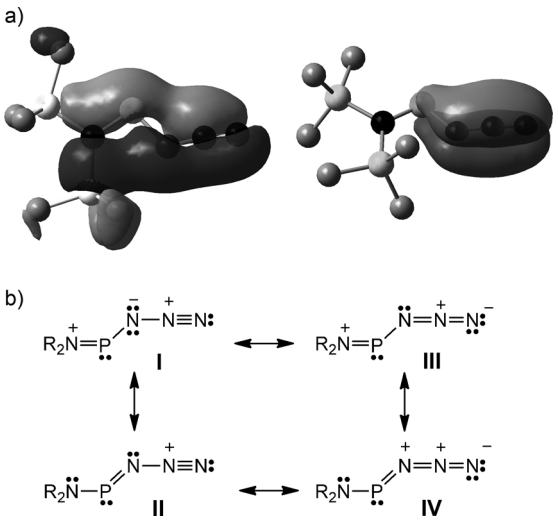

Figure 4. a) Selected molecular orbitals of the cation in **4** depicting in-plane (left) and out-of-plane π bonding (right) along the NPN_3 moiety. b) Lewis representations showing the π bonding along the NPN_3 unit.

Thus, in the VB picture the π bonding can be best described by at least four resonance structures (Figure 4, bottom). This considerable π bonding along the NPNNN unit might be one of the reasons why the Staudinger reaction occurs only at higher temperatures in solution then triggering the decomposition process. Both the σ and π P–N bonds are highly polarized (Table 1).[10] For example, only 24% of the $P{=}N_{amino}$ double bond in **4** is localized at the phosphorus atom. Similar values (23–24%) are found for the σ bonds in **1**, **2a–c**, and **4**.

Table 1: Calculated partial charges [e] and charge transfer Q_{CT}^{tot} [e] in an isolated ion pair of **1**, **2a–c**, and **4**[14b] along with partial charges of the $[(Me_3Si)_2N{=}P{-}X]^+$ ion.[a]

	1	**2a**	**2b**	**2c**	**4**
$q(P_{salt})$	1.05	1.19	1.21	1.19	1.41
$q(N_{amino,salt})$	−1.65	−1.54	−1.51	−1.52	−1.51
$q(X_{salt})$[a]	−0.31	−0.21	−0.20	−0.17	−0.33
$q(P_{cat})$	1.24	1.26	1.20	1.20	1.37
$q(N_{amino,cat})$	−1.49	−1.52	−1.46	−1.46	−1.47
$q(X_{cat})$[a]	−0.18	−0.18	−0.18	−0.17	−0.31[e]
Q_{ct}^{tot}[b]	**1**	**2a**	**2b**	**2c**	**4**

[a] Compound **1** was formally considered as the salt $[(Me_3Si)_2N{=}P{-}Cl]^+[Cl]^-$. **1** and **2a–c** X = Cl, **4** X = N_3. [b] Q_{ct}^{tot} = charge transfer with respect to the $[(Me_3Si)_2N{=}P{-}X]^{n+}$ ion (X = Cl for **1**, **2a–c** and X = N_3 for **4**), thus $Q_{cation} = 1 - Q_{CT}^{tot}$. [c] $Q_{CT}^{tot} = q(Cl^-)$. [d] $Q_{CT}^{tot} = 1 + \Sigma q(A_i)$ with the A_i atom of the anion. [e] $q(N_{azide,salt}) = -0.72$ versus $q(N_{azide,cat}) = -0.70$.

Interestingly, significant cation–anion interactions are detected in the salts **2a–c** but are only very weak in azido species **4**. The localized nonbonding electron pairs available on the $GaCl_4^-$ ion ($Ga_2Cl_7^-$ or $AlCl_4^-$) offer sites for effective electrostatic interaction with the cation and allow ion pairing, which inhibits the reactivity of the phosphenium center. The shortest P···$ClGaCl_3$ distances in **2a** amount to 2.870 and 3.021 Å, which is considerably shorter than the sum of the van der Waals radii (cf. $\Sigma r_{vdw}(P{-}Cl) = 3.70$ and $\Sigma r_{cov}(P{-}Cl) = 2.04$ Å;[24] 3.867(6), 3.976(6) and 4.020(6) Å in $[(iPr_2N)_2P][GaCl_4]$), indicating strong van der Waals interactions.[6] Similarly close contacts are found in **2b** and **2c** (2.8–3.1 Å), whereas only very weak van der Waals interactions between the ions can be assumed for **4**, with four P···Cl distances between 3.392–3.749 Å. Nevertheless, the existence of such weak cation–anion interactions is supported by a small but noticeable charge transfer from the anion to the cation (Table 1). Compound **1** can also be included into these considerations, as **1** can formally be regarded as $[(Me_3Si)_2N{=}P{-}Cl][Cl]$. The largest charge transfer is computed for **1** ($Q_{CT}^{tot} = 0.66\,e$) and decreases for **2a** (0.19 *e*) and **4** (0.07 *e*). Thus the azidophosphenium ion in **4** can be considered as an almost bare $[(Me_3Si)_2N{=}P{-}N_3]^+$ ion.

In summary, from the mixture of $(Me_3Si)_2NPCl_2$ and $GaCl_3$ at low-temperatures, for the first time an amino(chloro)phosphenium ion has been isolated in **2a**, **2b**, and **2c** and structurally characterized; however, it decomposes under release of Me_3SiCl at ambient temperatures, forming an unusual hitherto unknown ionic liquid of the type $[Me_3Si{-}N{\equiv}P][GaCl_4]$ that is stable at room temperature. Reaction of **2a** with Me_3SiN_3 affords **4** bearing an highly reactive and labile azidophosphenium ion $[(Me_3Si)_2N{=}P{-}N_3]^+$, which is the first compound with an azide group attached to a two-coordinate phosphorus center. The $[(Me_3Si)_2N{=}P{-}N_3]^+$ ion can formally be regarded as phosphapentacenium ion with a planar molecule skeleton, indicating strong delocalization of π electron density. This cation is only stable at temperatures below −40 °C. Upon a temperature increase, it does not cyclize to give a tetrazaphosphole but decomposes in a Staudinger reaction, yielding oligomeric PN compounds. It can be assumed that kinetic protection is needed to support cyclization in preference to a Staudinger reaction.

Received: March 8, 2012
Published online: May 4, 2012

Keywords: azides · NBO analysis · phosphenium ions · reactive cations · structure elucidation

[1] a) K. Dimroth, P. Hoffmann, *Angew. Chem.* **1964**, *76*, 433–434; *Angew. Chem. Int. Ed. Engl.* **1964**, *3*, 384–385; <lit b> K. Dimroth, P. Hoffmann, *Chem. Ber.* **1966**, *99*, 1325–1331.
[2] a) E. Fluck, *Top. Phosphorus Chem.* **1980**, *10*, 193–284; b) A. H. Cowley, R. A. Kemp, *Chem. Rev.* **1985**, *85*, 367–382; c) "Phosphenium Cations": M. Sanchez, M.-R. Mazieres, L. Lamande, R. Wolf in *Multiple Bond and Low Coordination in phosphorus Chemistry* (Eds.: M. Regitz, D. J. Scherer), Georg Thieme, Stuttgart, **1990**, chap. 0.1, pp. 129–148.
[3] D. Gudat, *Coord. Chem. Rev.* **1997**, *163*, 71–106.
[4] a) R. W. Kopp, A. C. Bond, R. W. Parry, *Z. Anorg. Chem.* **1976**, *15*, 3042–3046; b) C. W. Schultz, R. W. Parry, *Z. Anorg. Chem.* **1976**, *15*, 3046–3050; c) M. G. Thomas, C. W. Schultz, R. W. Parry, *Inorg. Chem.* **1977**, *16*, 994–1002.
[5] a) A. H. Cowley, M. C. Cushner, J. S. Szobota, *J. Am. Chem. Soc.* **1978**, *100*, 7784–7786; b) A. H. Cowley, C. Cushner, M. Lattman, H. L. McKee, J. S. Szobota, J. C. Wilburn, *Pure Appl. Chem.* **1980**, *52*, 789–797.
[6] N. Burford, P. Losier, C. Macdonald, V. Kyrimis, P. K. Bakshi, T. S. Cameron, *Inorg. Chem.* **1994**, *33*, 1434–1439.
[7] a) D. Michalik, A. Schulz, A. Villinger, N. Weding, *Angew. Chem.* **2008**, *120*, 6565–6568; *Angew. Chem. Int. Ed.* **2008**, *47*, 6465–6468; b) M. Lehmann, A. Schulz, A. Villinger, *Struct. Chem.* **2011**, *22*, 35–43.
[8] a) P. Mayer, A. Schulz, A. Villinger, *Chem. Commun.* **2006**, 1236–1238; b) P. Mayer, A. Schulz, A. Villinger, *J. Organomet. Chem.* **2007**, *692*, 2839–2842.
[9] A. Schulz, A. Villinger, *Angew. Chem.* **2008**, *120*, 614–617; *Angew. Chem. Int. Ed.* **2008**, *47*, 603–606.
[10] S. Herler, A. Villinger, J. Schmedt auf der Günne, J. Weigand, P. Mayer, A. Schulz, J. J. Weigand, *Angew. Chem.* **2005**, *117*, 7968–7971; *Angew. Chem. Int. Ed.* **2005**, *44*, 7790–7793.
[11] a) M. Lehmann, A. Schulz, A. Villinger, *Angew. Chem.* **2011**, *123*, 5327–5331; *Angew. Chem. Int. Ed.* **2011**, *50*, 5221–5224.
[12] a) A. Schulz, A. Villinger, *Organometallics* **2011**, *30*, 284–289; b) D. Michalik, A. Schulz, A. Villinger, *Angew. Chem.* **2010**, *122*, 7737–7740; *Angew. Chem. Int. Ed.* **2010**, *49*, 7575–7577; c) A. Villinger, A. Schulz, *Angew. Chem.* **2010**, *122*, 8190–8194; *Angew. Chem. Int. Ed.* **2010**, *49*, 8017–8020; d) W. Baumann, A. Schulz, A. Villinger, *Angew. Chem.* **2008**, *120*, 9672–9675; *Angew. Chem. Int. Ed.* **2008**, *47*, 9530–9532.
[13] O. J. Scherer, N. Kuhn, *J. Organomet. Chem.* **1974**, *82*, C3–C7.
[14] The Supporting Information includes: a) Experimental details, properties, and structural data; b) a summary of the NBO and MO study; applied level of theory is pbe1pbe/aug-cc-pVDZ.

CCDC 878830 (**1**), CCDC 878831 (**2a**), and CCDC 878834 (**4**) contain the supplementary crystallographic data for this paper. These data can be obtained free of charge from The Cambridge Crystallographic Data Centre via www.ccdc.cam.ac.uk/data_request/cif.

[15] a) K. O. Christe, W. W. Wilson, J. A. Sheehy, J. A. Boatz, *Angew. Chem.* **1999**, *111*, 2112 – 2118; *Angew. Chem. Int. Ed.* **1999**, *38*, 2004 – 2009; b) A. Vij, W. W. Wilson, F. S. Tham, G. A. Sheehy, K. O. Christe, *J. Am. Chem. Soc.* **2001**, *123*, 6308 – 6313.

[16] a) M. H. Holthausen, K. Feldmann, S. Schulz, A. Hepp, J. J. Weigand, *Inorg. Chem.* **2012**, 151, 3374 – 3387; b) Y. Carpenter, N. Burford, M. L. D. Lumsden, R. McDonald, *Inorg. Chem.* **2011**, *50*, 3342 – 3353; c) N. Burford, P. J. Ragogna, R. McDonald, M. J. Ferguson, *J. Am. Chem. Soc.* **2003**, *125*, 14404 – 14410; d) C.-W. Tsang, C. A. Rohrick, T. S. Saini, B. O. Patrick, D. P. Gates, *Organometallics* **2004**, *23*, 5913 – 5923.

[17] $[Mes^*NP]^+$ salts are known: a) E. Niecke, M. Nieger, F. Reichert, *Angew. Chem.* **1988**, *100*, 1781 – 1782; *Angew. Chem. Int. Ed. Engl.* **1988**, *27*, 1715 – 1716; b) N. Burford, J. A. C. Clyburne, P. K. Bakshi, T. S. Cameron, *J. Am. Chem. Soc.* **1993**, *115*, 8829 – 8830.

[18] A. H. Cowley, M. Lattman, J. C. Wilburn, *Inorg. Chem.* **1981**, *20*, 2916 – 2919.

[19] a) L. Birckenbach, K. Kellermann, *Ber.* **1925**, *58B*, 786 – 794; b) H. Brand, A. Schulz, A. Villinger, *Z. Anorg. Allg. Chem.* **2007**, *633*, 22 – 35.

[20] G. David, E. Niecke, M. Nieger, V. v. d. Goenna, W. Schoeller, *Chem. Ber.* **1993**, *126*, 1513 – 1517.

[21] M.-R. Mazieres, M. Sanchez, J. Bellan, R. Wolf, *Phosphorus Sulfur Relat. Elem.* **1986**, *26*, 97 – 99.

[22] a) M.-R. Marre, M. Sanchez, R. Wolf, *Phosphorus Sulfur* **1982**, *13*, 27; b) M.-R. Marre, M. Sanchez, R. J. Wolf, *Chem. Soc. Chem. Commun.* **1984**, 566 – 567.

[23] F. Weinhold, C. Landis, *Valency and Bonding. A Natural Bond Orbital Donor-Acceptor Perspective*, Cambridge University Press, **2005**, and references therein.

[24] P. Pyykkö, M. Atsumi, *Chem. Eur. J.* **2009**, *15*, 12770 – 12779.

[25] E. Niecke, D. Gudat, *Angew. Chem.* **1991**, *103*, 251 – 270; *Angew. Chem. Int. Ed. Engl.* **1991**, *30*, 217 – 237.

[26] The positions of the cation and the anion in **2a** and **2c** were found to be disordered, as is the position of one cation in **2b**. For details, see the Supporting Information.

7 Lebenslauf

Persönliche Details

Name:	Christian Hering
Geburtstag:	15. März 1986 in Güstrow
Familienstand:	ledig
Adresse:	Fritz-Reuter-Straße 9
	18057 Rostock
Email:	hering.christian@gmail.com
Telefon:	dienstl.: 0381/498-6392
	privat: 01573/4670012

Schulbildung

08/1992 -07/1996	Wilhelm-Piek-Grundschule, Güstrow.
08/1998 - 06/2005	John-Brinckman-Gymnasium, Güstrow.
	Abschluss: Allgemeine Hochschulreife (Note: 1,0).

Zivildienst

09/2005 - 06/2006	Betreuung körperlich und geistig behinderter Menschen in den Güstrower Werkstätten, Güstrow.

Studium

10/2006 - 9/2008	Chemie – Studium an der Universität Rostock. Abschluss: Vordiplom (Note 1,1).
10/2008 - 09/2011	Chemie – Studium an der Universität Rostock. Abschluss: Diplom (Note 1,0).
04/2011 - 07/2011	Chemie – Praktikum am *Massachusetts Institute of Technology* in Cambridge (USA), Arbeitsgruppe Prof. C. C. Cummins

Berufserfahrung

07/2001 - 12/2009	Übernahme von Projekten im Bereich Geologie (Erstellung digitaler Flächenmasken mit ArcGis), Biologie (Bestimmung von Makrozoobenthos), Biota Institut für ökologische Forschung und Planung, Bützow.
10/2009 - 09/2011	Studentische Hilfskraft (Administration der Institutshomepage), Universität Rostock, Institut für Chemie, Arbeitskreis Prof. Dr. A. Schulz

10/2011 – 12/2014	Wissenschaftlicher Mitarbeiter (Promotion), Universität Rostock, Institut für Chemie, Lehrstuhl für Anorg. und Elementorg. Chemie, Arbeitskreis Prof. Dr. Axel Schulz.
11/2012 - 03/2014	Wissenschaftliche Hilfskraft (Tutorien für Nebenfach Chemie), Institut für Agrarwissenschaften, Lehrstuhl für Geoinformatik.

Mitgliedschaften

03/2009 - 09/2011	Stipendiat, Studienstiftung des deutschen Volkes.
09/2009 - 04/2011	Naturwissenschaftliches Kolleg III der Studienstiftung, „Chemie an Spinzentren“, Prof. Dr. A. Gansäuer (Universität Bonn).
04/2012 - 03/2014	Stipendiat, Chemiefondstipendium für Promotions-studenten, Verband der chemischen Industrie e.V.

Auszeichnungen

10/2011	Bester Student des Jahrgangs 2011, „Fakultätspreis” der MNF der Universität Rostock.
03/2013	„Best Chairperson” und „Best Poster“ beim „10th European Workshop on Phosphorus Chemistry (EWPC-10)”, Universität Regensburg, 20.03.2013.
05/2014	Reisestipendium der Dr. Karl Wamsler-Stiftung GmbH für die Teilnahme an der 97th CSC in Vancouver.

Zusätzliche Qualifkationen

06/2003	Basketballschiedsrichterlizenz (D-Lizenz)
07/2007	Trainerschein Basketball (C-Lizenz)
10/2011	UNIcert® III Zertifikat Englisch (*Europäische Stufe C1*) (fachspezifische Fachrichtung)

Sprache: Englisch (verhandlungssicher), Latein (kleines Latinum)

Interessen

Basketball, Fotografie, Webdesign, Lesen, Reisen

Publikationen (*Peer-Review*)

1. "***Low Temperature Isolation of An Azidophosphenium Cation"***, Christian Hering, Axel Schulz, Alexander Villinger, *Angew. Chem*. **2012**, *124*, 6345−6349 (DOI: 10.1002/ange.201201851); *Angew. Chem. Int. Ed.* **2012**, *51*, 6241-6245 (DOI: 10.1002/anie.201201851).

2. "***Lewis-Acid-assisted Methyl Exchange Reactions in Silylated Aminodichlorostibanes"***, Christian Hering,Mathias Lehmann, Axel Schulz, Alexander Villinger, *Inorg. Chem.* **2012**, *51*, 8212−8224 (DOI: 10.1021/ic300770b).

3. "***On the Synthesis and Reactivity of Highly Labile Pseudohalogen Phosphenium Ions"***, Christian Hering, Axel Schulz, Alexander Villinger, *Inorg. Chem*. **2013**, *52*, 5214−5225 (DOI: 10.1021/ic4001285).

4. "***Structure and Bonding of Novel Acyclic Bisaminoarsenium Cations"***, Christian Hering, Julia Rothe, Axel Schulz, Alexander Villinger, *Inorg. Chem.* **2013**, *52*, 7781−7790 (DOI: 10.1021/ic4010104).

5. "***Diatomic PN – Trapped in a cyclo-Tetraphosphazane"***, Christian Hering, Axel Schulz, Alexander Villinger, *Chem. Sci.* **2014***, 5, 1064−1073* (DOI: 10.1039/C3SC52322E).

6. "***Azidophosphenium Ions – Versatile Reagents in Inorganic Synthesis"***, Christian Hering, Maximilian Hertrich, Axel Schulz, Alexander Villinger, *Inorg. Chem.* **2014***, 53*, 3380−3392 (DOI: 10.1021/ic500332s).

7. ***"Dimers and Trimers of Diphosphenes: A Wealth of cyclo-Phosphanes"***, Jonas Bresien,, Christian Hering, Axel Schulz, Alexander Villinger, *Chem. Eur. J.* **2014***, accepted* (DOI: 10.1002/chem.201403631).

Übersichtsartikel

8. "***The Elusive Cyano Formate Ion"***, invited highlight article**,** Christian Hering, J. v. Langermann, Axel Schulz, *Angew. Chem.* **2014**; *Angew. Chem. Intl. Ed.* . **2014***, accepted* (DOI: 10.1002/anie.201405339).

Konferenzbeiträge (Poster, Vorträge)

03/2011	***Investigation of the $GaCl_3$-assisted Trimethylsilyl-chloride elimination in N,N-Bis(trimethylsilyl-amino-dichlorophosphane - Reactive Phosphenium Cations*.**
	C. Hering, A. Schulz, A. Villinger
	8th European Workshop on Phosphorus Chemistry (EWPC-8), Universität Münster, 28.03.2011 (Vortrag)
03/2012	***Methyl Exchange Reactions as New Route to Catena-Antimony Cations*.**
	C. Hering, M. Lehmann, A. Schulz, A. Villinger
	JCF Frühjahrsymposium (14. JCF), Universität Rostock, 18.03.2012 (Vortrag)
03/2012	***Diatomic PN as Synthon in Inorganic Synthesis*.**
	C. Hering, A. Schulz, A. Villinger
	9th European Workshop on Phosphorus Chemistry (EWPC-9), Universität Rennes, Frankreich, 21.03.2012 (Poster)
07/2012	***$(Me_3Si)_2NPCl_2$ – A Molecule with a Disguised PN-Moiety*.**
	C. Hering, A. Schulz, A. Villinger
	13th International Symposium on Inorganic Ring Systems (IRIS 13), Victoria, Kanada, 29.07.2012 (Poster)
09/2012	***Phosphenium Cations as Buliding Block in Inorganic Synthesis*.**
	C. Hering, A. Schulz, A. Villinger

Norddeutsches Doktorandenkolloquim (15. NDDK), Universität Kiel, 25.09.2012 (Vortrag)

03/2013 ***Recent Advances in Phosphenium Chemistry.***

C. Hering, A. Schulz, A. Villinger

PhosSciNet Final Conference@ 10th European Workshop on Phosphorus Chemistry (EWPC-10), Universität Regensburg, 20.03.2013 (Poster)

03/2013 ***New Aspects of Diphosphene Chemistry.***

J. Bresien, C. Hering, J. Rothe, A. Schulz, A. Villinger

PhosSciNet Final Conference@ 10th European Workshop on Phosphorus Chemistry (EWPC-10), Universität Regensburg, 20.03.2013 (Poster)

09/2013 ***Synthesis and Characterization of cyclo-Tetraphosphanes.***

J. Bresien, C. Hering, J. Rothe, A. Schulz, A. Villinger

Norddeutsches Doktorandenkolloquim (16. NDDK), Universität Bremen, 19.09.2012 (Poster)

09/2013 ***Azidophosphenium Cations as building block in Inorganic Synthesis***

C. Hering, M. Hertrich, A. Schulz, A. Villinger

Norddeutsches Doktorandenkolloquim (16. NDDK), Universität Bremen, 19.09.2012 (Poster)

11/2013 ***Synthesis and Reactivity of Low-Valent N-Pn Compounds (Pn = P, As, Sb, Bi)***

C. Hering, A. Schulz, A. Villinger

Princeton Inorganic Chemistry Department, Princeton University, USA, 08.11.2013 (Einladung zum Vortrag)

01/2014 ***Synthese und Charakterisierung Niedervalenter Stickstoff-Pniktogen Verbindungen***

Life Light Matter, Projekttreffen, Universität Rostock, 24.01.2014 (Vortrag)

02/2014 ***Synthese und Charakterisierung Niedervalenter Stickstoff-Pniktogen Verbindungen***

Stipendiatentreffen FCI, Universität Berlin, 21.02.2014 (Vortrag)

03/2014 ***Azidophosphenium Ions: Versatile Reagents in Inorganic Synthesis***

C. Hering, M. Hertrich, A. Schulz, A. Villinger.

11th European Workshop on Phosphorus Chemistry (EWPC-11), Universität Sofia, Bulgarien, 24.03.2014 (Poster)

06/2014 ***Preparation and Reactivity of New Acyclic Chloropnictenium Cations***

C. Hering, M. Thomas, A. Schulz, A. Villinger.

97th Canadian Chemistry Conference and Exhibition (CSC 97), Vancouver, Kanada, 04.06.2014 (Vortrag)

07/2014 ***Recent Advances in Phosphenium Chemistry***

C. Hering, A. Schulz, A. Villinger.

20th International Conference on Phosphorus Chemistry Conference (ICPC 20), Dublin, Irland, 02.07.2014 (Poster)